CHARACTERISTICS OF SIMPLE MANUAL CONTROL SYSTEMS

by

JEROME ISAAC ELKIND

S. B. Massachusetts Institute of Technology

(1952)

S. M. Massachusetts Institute of Technology

(1952)

SUBMITTED IN PARTIAL FULFILLMENT OF THE

REQUIREMENTS FOR THE DEGREE OF

DOCTOR OF SCIENCE

at the

MASSACHUSETTS INSTITUTE OF TECHNOLOGY

June, 1956

Signature of Author ____
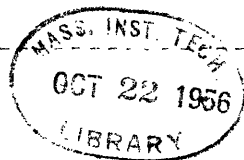
Department of Electrical Engineering, May 14, 1956

Certified by _____

Thesis Supervisor

Accepted by _____

Chairman, Departmental Committee on Graduate Students

MASSACHUSETTS INSTITUTE OF TECHNOLOGY
CAMBRIDGE 39, MASSACHUSETTS

May 8, 1956

Mr. J. I. Elkind
Lincoln C-330

Dear Mr. Elkind:

This letter is to give you permission to print additional copies of your thesis by the multilith process, and to submit to the Department of Electrical Engineering copies thus produced, in lieu of the typed copies normally required.

A copy of this letter is to be reproduced by the same process and is to be placed in each copy of the thesis immediately following its title page.

Sincerely yours,

S. H. Caldwell
for the
Department Graduate Committee

SHC:mm

CHARACTERISTICS OF SIMPLE MANUAL CONTROL SYSTEMS

by

JEROME ISAAC ELKIND

ABSTRACT

A method for measuring and describing the characteristics of manual control systems is presented. The method is applied in an experimental study of the characteristics of simple manual systems. The experimental results are discussed and analytic models are derived that approximate the measured characteristics. An analogue computer developed to implement the measurement of the system characteristics is described.

Because the human operator has many different modes, manual control systems are nonlinear and therefore require nonlinear analysis and descriptive techniques. However, a description by means of quasi-linear transfer functions is found to provide a good approximation to the characteristics of manual systems. Methods for obtaining quasi-linear approximations to the system characteristics are discussed. A complete description of system behavior in terms of quasi-linear transfer functions requires that a family of such functions corresponding to a large set of system conditions be obtained. The structure of this family and its relations to the structure of the set of system conditions if our primary interest.

The characteristics of simple pursuit and compensatory control systems were measured with a family of gaussian input signals having power-density spectra that covered a range of bandwidths, amplitudes, center frequencies and some variety of shapes. The experimental results, presented in the form of graphs, show the nature of the dependence of system characteristics upon input-signal characteristics. The superiority of pursuit systems over compensatory systems is clearly demonstrated.

Simple analytic models that approximate these measured results are derived for both systems. The compensatory model is highly developed and relations among its parameters and those of the input have been obtained. The pursuit model is not nearly so well developed and only approximated relations among its parameters and the input parameters have been found. A method for determining a more exact description of pursuit systems is suggested. The measured results and the analytic models together provide a description of manual control systems that should be useful in system design.

Thesis Supervisor: J. C. R. Licklider
Title: Associate Professor of Psychology

ACKNOWLEDGMENT

The author is indebted to many members of the staff of Massachusetts Institute of Technology and of Lincoln Laboratory for their assistance and suggestions. He is expecially indebted to Professor J. C. R. Licklider who, in supervising this thesis, has provided most valuable inspiration and encouragement and has contributed many important suggestions. The guidance provided by Professors G. C. Newton and R. C. Booton and their excellent suggestions and criticisms are greatly appreciated. The assistance and collaboration of Miss Carma Darley during most phases of the study have been invaluable. The author is grateful to R. T. Mitchell and E. Cramer for serving as subjects, J. W. Doyle for assisting in the design and construction of the electronic equipment, Miss Patricia Zartarian for assisting in the computation of the results, E. P. Brandeis for performing some of the early experiments of the study and Miss Margaret Fitzgerald for typing the manuscript.

UNCLASSIFIED

TABLE OF CONTENTS

UNCLASSIFIED

UNCLASSIFIED

UNCLASSIFIED

ILLUSTRATIONS

ILLUSTRATIONS (Continued)

ILLUSTRATIONS (Continued)

ILLUSTRATIONS (Continued)

TABLES

CHARACTERISTICS OF SIMPLE MANUAL CONTROL SYSTEMS

I. INTRODUCTION

Manual control systems have some characteristics that are highly desirable in aircraft control, missile guidance, fire control and other aiming or steering systems. The human operator's ability to adjust his characteristics to meet system requirements provides manual control systems with a degree of flexibility and "intelligence" that is difficult to achieve in wholly automatic systems.

But the human operator's adaptability and nonlinearity make it difficult to analyze and to describe mathematically the characteristics of manual control systems. The usual technique of expressing system characteristics by means of frequency-dependent linear transfer functions is not applicable to manual systems. Their characteristics can, however, be approximated with good accuracy by quasi-linear transfer functions which retain much of the inherent simplicity of linear transfer functions.

A single quasi-linear transfer function will, in general, be a satisfactory approximation for only one set of system conditions. A large group of quasi-linear transfer functions would be needed to approximate the characteristics of the control system for all possible sets of system conditions. It would be pointless to attempt to measure and to catalogue all or most of the characteristics belonging to this group. Instead, we must measure the characteristics of the human operator in several different fundamental control situations. From these measurements a family of quasi-linear transfer functions and other associated functions describing human-operator characteristics will be obtained. By studying the structure of this family and its relations to the control systems tested, basic rules for the behavior of the human operator and invariances in his characteristics can be discovered. The structure of the family of functions and the rules derived from it are of primary interest.

In this paper, measurement techniques for determining quasi-linear transfer functions for manual control systems are developed and verified. These techniques are applied in an experimental study of the influence of input-signal characteristics on the behavior of simple (no lags or filters) pursuit and compensatory control systems. From the experimental results, analytic models for the human operator's characteristics in the compensatory system have been developed, and relations among the parameters of the models and the parameters of the input signals have been derived. Models for the pursuit system are proposed, but the experimental data are not sufficient to permit the same degree of quantitative refinement in the pursuit models that was possible with the compensatory. The measured characteristics and the analytic models describe, in a certain sense, an upper bound on manual system performance. The experimental results should therefore be useful in the design of manual control systems.

A. COMPOSITION AND OPERATION OF MANUAL CONTROL SYSTEMS

A manual control system is a servo system in which a human operator has the task of detecting misalignment between system input and output and of initiating the system response necessary
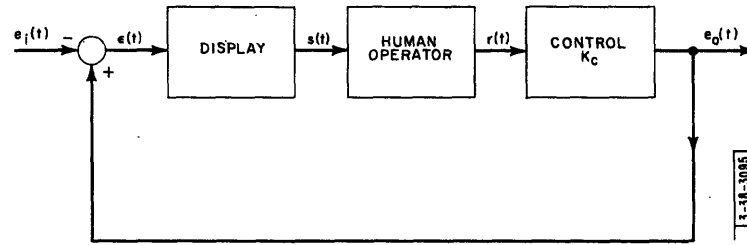
Fig.1-1. Simple compensatory control system. The subtractor is con-
nected in the way shown so that the displacement of the control and the
displacement of the indicator are in the same direction.
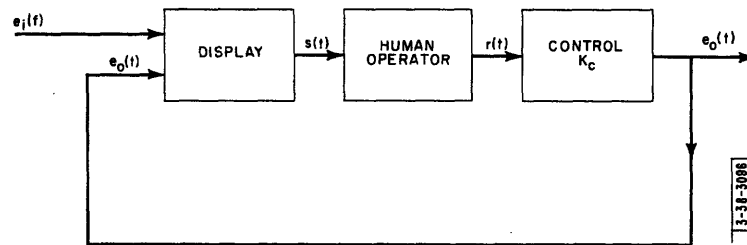
Fig.1-2. Simple pursuit control system. The display shows both $e_i(t)$ and $e_o(t)$.

(a)   (b)
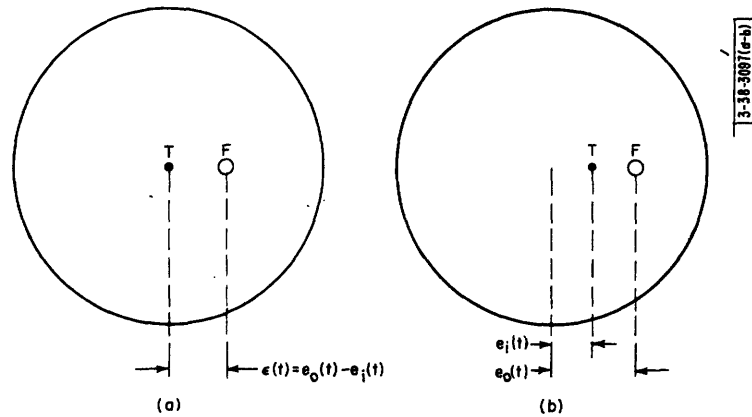
Fig.1-3. Typical displays used in (a) compensatory, and (b) pursuit systems.
T is the target and F is the follower.

2

to reduce this misalignment. This task, commonly called tracking, can be more precisely defined as the process in which the human operator tries to effect some degree of match between a controlled output quantity and an input quantity. In most manual control systems, the human operator is coupled to the rest of the system by a stimulus transducer, or display, and a response transducer, or control. The kinds of transducers used can vary widely with the system requirements as can the type of match between input and output that the human operator tries to achieve. We shall consider only simple visual-manual tracking systems in which the information displayed and the control movements are closely related to the actual input and output signals, and in which the match that the human operator tries to achieve is akin to the minimum mean-square-error criterion.

The simplest manual control systems are composed of only a display, a control and a human operator. If the control is light and frictionless, its dynamics can be neglected and it can be represented in system block diagrams by an amplifier whose gain corresponds to the scale factor transforming hand movement to system output. Block diagrams of simple forms of the two most common types of manual control systems, pursuit and compensatory, are shown in Figs. 1-1 and 1-2. In the compensatory system, only the error (the difference between input and output) is displayed. As shown in Fig. 1-3(a), the error is represented by the displacement of the follower (the circle) from the stationary reference or target (the dot) located at the center of the display. The human operator's task in this system is to compensate for, or minimize the error signal presented, by trying to keep the circle around the dot. In the pursuit system, both input and response are displayed independently [Fig. 1-3(b)]. The displacement of the target (the dot) represents the input, and the follower (the circle), the response. The human operator's task is to pursue the target with follower by trying to keep the circle around the dot.

There is considerable evidence that pursuit systems perform better than compensatory, particularly with high-frequency inputs.[1,2*] Apparently, pursuit systems are superior because the human operator can see the input directly and can predict its future in order to correct partially for phase lags and time delays present in his own characteristics and in those of other components of the system. In the compensatory system, because he sees only the error, he can not predict the input accurately and can not correct so well for lags.

B. HUMAN-OPERATOR TRACKING-RESPONSE CHARACTERISTICS

Certain features of the tracking characteristics of the human operator make him a unique element for control systems. His ability to modify his characteristics in order to match the characteristics of the control situation makes it possible for him to function effectively in many different systems and situations. Tustin, Russell and others[3,4,5,6,7] have shown that the human operator considers both the statistical characteristics of the input signal and the dynamic characteristics of the other components of the system in shaping his own response characteristics. When tracking a low-frequency sinusoid, the human operator is able to predict the future of the sinusoid and to compensate for lags present in his own characteristics and in those of other components of the system. His response is, therefore, approximately in phase with the input.[8,9] With a stochastic signal, however, prediction is necessarily imperfect, and the operator's

*Superscripts in bold face refer to references on p. 117.

response lags the input.[3,4] Russell[3] has shown that when a low-pass filter is inserted in the loop, the human operator tries to develop, in his own characteristics, terms that are the inverse of the filter in order to reduce its effects. Existing data are inadequate to indicate the range over which the human operator can modify his characteristics or to specify exactly factors he considers when making the modifications. One purpose of the experiments reported in this paper was to determine the extent of the human operator's ability to adjust to input-signal characteristics.

The most prominent features of the fine or short-time structure of human-operator responses are low bandwidth, reaction-time delay, intermittency and relatively good amplitude linearity. Both the visual and muscular systems, which are well matched to each other, are limited in their frequency response to a maximum of about 10 cycles per second. In visual-manual tasks, controlled movements cannot be made more frequently than about 2 or 3 cps.[8] Accurate tracking is obtained only with inputs whose power is concentrated in the part of the spectrum below 1 cps.

A stimulus-response latency or reaction-time delay is an inherent characteristic of the human operator. In simple discrete tracking situations, the delay is about 0.10 to 0.40 second.[10,11,12] Major sources of the delay are excitation of the retina (0.02 to 0.04 second), nerve conduction (0.01 to 0.02 second), muscle contraction (0.02 to 0.04 second) and central processes.[13] The time required for the central processes depends upon the complexity of the task and is largely responsible for the wide variation in reaction times.

There has been considerable discussion of intermittency in human-operator responses.[14,15,16,17] No experiments have been reported that show conclusively that, in a continuous tracking task, the human operator does act like an intermittent servo. Many of the arguments in favor of the intermittency hypothesis rest heavily on the observation that tracking-error curves are frequently oscillatory. But oscillations can result either from intermittency or from closed-loop instability. Merely the presence of oscillations does not prove that the human operator is intermittent. Of course, one would expect that the discrete behavior of the neural system would make tracking responses intermittent. However, the period of intermittency which has been proposed for tracking is about 0.5 second — much greater than would be predicted on the basis of neural intermittency alone. Also, a period of intermittency of 0.5 second is not consistent with the fact that the human operator is able to track well inputs having frequency components as high as 1 cps.[4] The question of whether or not the human operator acts intermittently remains to be resolved.

Human-operator characteristics are not absolutely fixed. Both the fine and the gross structures show variation with time and with repeated presentation of the same input.[18] It is likely that many of these variations result from external stimuli or represent stochastic variations in human-operator characteristics that are not related to the input signal. In most practical tracking studies, care is exercised to minimize the effects of these external stimuli. The variations in responses that do occur are treated as if they were noise.

II. ANALYSIS AND DESCRIPTIVE TECHNIQUES

From the brief review of human-operator characteristics it is apparent that the human operator is highly nonlinear in that his characteristics depend strongly upon the nature of the tracking situation. Measurements of the characteristics of the human operator in a particular tracking situation will not be sufficient to describe his characteristics in others. Rather, we must measure human-operator performance in enough different tracking situations that the structure of the family of characteristics can be ascertained. Knowing this structure and the relations between its parameters and those of the situations studied, we may be able to discover basic rules of behavior of the human operator, invariances in his characteristics that will be applicable to a wide range of different tracking situations.

Since manual control systems are similar to automatic systems in purpose and in operation, it seems reasonable to try to apply to manual systems the measurement and descriptive techniques that have been developed for automatic systems. The widely used linear methods for describing control systems in terms of invariant impulse responses and linear transfer functions are not applicable to manual systems because of the human operator's nonlinearity. However, a reasonably accurate description of manual control systems can be obtained without resorting to complicated and unwieldy nonlinear methods. By making use of the concept of quasi-linearity we can retain much of the inherent simplicity of the linear methods and still treat with good accuracy the kinds of nonlinearities peculiar to the human operator.[4]

A. QUASI-LINEARIZATION OF HUMAN-OPERATOR CHARACTERISTICS

Quasi-linearization is the process of representing the characteristics of a nonlinear device by linear transfer functions whose parameters depend upon the environment of the device, i.e., parameters of the input and of other components connected to the device.[19,20,21] These transfer functions are called quasi-linear transfer functions because they behave linearly when the set environmental parameters remain fixed and nonlinearly when these parameters are allowed to change.

Quasi-linearization is particularly suited to the kinds of nonlinearities observed in the human operator. His most significant departures from linearity occur when the input statistics or system dynamics change. Since its parameters depend upon the input and the system, a quasi-linear transfer function can handle this kind of nonlinearity. Even such nonlinearities as intermittency in response movements and amplitude distortion can sometimes be well approximated by quasi-linear transfer functions.[20]

B. SPECIFICATIONS FOR AN EXPERIMENTAL TRACKING SITUATION

In this study we are not interested in measuring the characteristics of the human operator in one particular tracking situation, but we want to obtain results that will be applicable to a wide range of tracking situations. Therefore, we must extract from actual tracking systems the most important features and incorporate them into our experimental tracking situation.

In most manual systems the input signals are low in frequency and at least partially stochastic. Often, in addition to the stochastic components, there are components that are analytic and

completely predictable. The stochastic components, however, are the most difficult to track and therefore are the ones which usually have greatest influence on human-operator characteristics. Low-frequency gaussian noise is an idealization of actual input signals. It is mathematically tractable, lends itself to precise specification, and is easy to generate. It is the natural input to use in an experimental tracking situation. Results derived from tests with low-frequency gaussian noise are likely to be more applicable to situations in which the input is aperiodic and complex than would be results derived from tests with sinusoids or step functions.

It would be too large and difficult a task to study the effects of both input signal and system dynamics. It was believed more important first to study extensively the effects of input-signal characteristics. By working with very simple pursuit and compensatory systems, it appears possible to obtain an upper bound on human-operator performance. The human operator's task is easier and his performance is probably better with a simple tracking system than with a more complicated system. Available data are not sufficient to prove this statement, but there is considerable evidence that it is largely correct. For example, it has been shown that tracking error increases as lags of the form $1/[(jf/f_n) + 1]$ are inserted in the loop.[3,22]

The simplest tracking system consists only of a display, a human operator, and a control (Figs. 1-1 and 1-2). Both the display and the control are essentially free of dynamics. The control is light, nearly frictionless, and without restoring spring forces, and can therefore be positioned without inhibiting the human operator's movement. In our experimental tracking study we used simple pursuit and compensatory systems of this kind.

C. FUNDAMENTAL QUANTITIES AND RELATIONS

The characteristics of manual control systems will be represented by quasi-linear transfer functions and other closely associated functions of frequency.[23]

To determine a quasi-linear transfer function for a manual control system we must discover for a particular set of input and system conditions the linear transfer function whose response best approximates the response of the control system to the same input. For stochastic signals it is most convenient to choose the mean-square difference criterion as the basis for selecting the best approximation. In general, the quasi-linear transfer function does not account for all the system's response. Resulting from the nonlinearities and variability in the human operator's characteristics, there are usually response components which are not linearly correlated with the input and which cannot be produced by a linear operation on the input. These uncorrelated components can be treated as noise added to the output of the quasi-linear transfer function, as shown by the model for the tracking system in Fig. 2-1. When the noise power is a small fraction of the total response power, the quasi-linear transfer function provides an adequate representation of the manual control system. If, however, the noise is a large fraction,
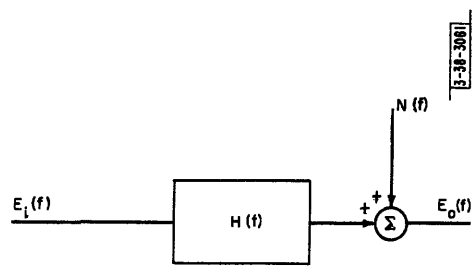
Fig. 2-1. Closed-loop block diagram for pursuit and compensatory systems.

the quasi-linear model (Fig. 2-1) may be inadequate. If the noise is nonlinearly correlated with the input, we may be forced to determine nonlinear approximations for the control system.

The model of Fig. 2-1 is a closed-loop representation for the compensatory or pursuit control systems shown in Figs. 1-1 and 1-2. It emphasizes the over-all behavior of the system and provides a basis for measurements of system performance. The characteristics of two elements of the model, $H(f)$ and $N(f)$, can be determined from measurements of input $E_i(f)$ and output $E_o(f)$ through the application of statistical techniques.[24]

A random input signal $e_i(t)$ of duration 2T has the Fourier transform

$$E_i(f) = \int_{-T}^{T} e_i(t) \, e^{-2\pi jft} \, dt \quad , \tag{2-1}$$

The power-density spectrum of the signal expressed in terms of its Fourier transform is[25]

$$\Phi_{ii}(f) = \lim_{T \to \infty} \frac{1}{T} E_i^*(f) E_i(f) \quad , \tag{2-2}$$

where $E_i^*(f)$ is the conjugate of $E_i(f)$. The cross-power-density spectrum between two signals $e_i(t)$ and $e_o(t)$ is

$$\Phi_{io}(f) = \lim_{T \to \infty} \frac{1}{T} E_i^*(f) E_o(f) \quad . \tag{2-3}$$

From these definitions, and from the fact the noise is not linearly coherent with the input $[\Phi_{in}(f)$ equals zero], the following relation for the model of Fig. 2-1 can be derived.[4]

$$\Phi_{io}(f) = H(f) \, \Phi_{ii}(f) \quad . \tag{2-4}$$

The output signal can be divided into two components: the first part being linearly coherent with the input, and the second part being not linearly coherent with the input. Therefore, the output power-density spectrum is

$$\Phi_{oo}(f) = |H(f)|^2 \, \Phi_{ii}(f) + \Phi_{nn}(f) \quad . \tag{2-5}$$

Equations (2-4) and (2-5) define the characteristics of the two elements of the model.

The fraction of the output power that is correlated with the input is a measure of the degree of the approximation to the actual control system characteristics that is provided by the quasi-linear transfer function. This fraction, which is the square of the linear correlation between input and output can be expressed in terms of the power spectrum of noise and output by the following relation:

$$\text{Linearly correlated fraction of output} = 1 - \frac{\Phi_{nn}(f)}{\Phi_{oo}(f)} \quad . \tag{2-6}$$

The power-density spectrum of the tracking error, $\Phi_{ee}(f)$, is a useful measure of the quality of system performance.

$$\Phi_{ee}(f) = \Phi_{ii}(f) + \Phi_{oo}(f) - 2 \, \text{Re} \, \Phi_{io}(f) \quad . \tag{2-7}$$

7

The mean-square tracking error relative to the mean-square input is another measure of system performance.

$$\frac{\overline{\epsilon^2(t)}}{\int_0^\infty \Phi_{ii} \, df} = 1 + \frac{\int_0^\infty \Phi_{oo} \, df - 2 \, \text{Re} \int_0^\infty \Phi_{io} \, df}{\int_0^\infty \Phi_{ii} \, df} \, . \qquad (2\text{-}8)$$

Whereas Fig. 2-1 represents the input-output relations for both pursuit and compensatory systems, the stimulus-response relations for the human operator in the compensatory system are more clearly shown in the open-loop block diagram of Fig. 2-2.
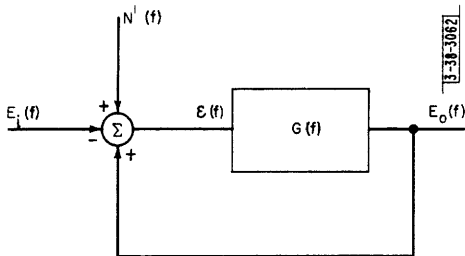
Fig. 2-2. Open-loop block diagram for compensatory system.

In compensatory systems the human operator sees only the error. The single quasi-linear transfer function $G(f)$ and the noise spectrum $\Phi_{n'n'}(f)$ suffice to describe his characteristics. The point of entry of the noise has been arbitrarily chosen to be the input. It was assumed that only visual stimuli are important and that the human operator obtains little useful proprioceptive or kinesthetic information about the position of his hand. With a light frictionless control, this assumption is probably not too drastic.

In terms of the closed-loop transfer function $H(f)$ and output-noise spectrum Φ_{nn}, the elements of the open-loop model are,

$$G(f) = \frac{H(f)}{H(f) - 1} \, , \qquad (2\text{-}9)$$

and

$$\Phi_{n'n'}(f) = \frac{\Phi_{nn}(f)}{|H(f)|^2} \, . \qquad (2\text{-}10)$$

Thus the elements of the compensatory model can be determined from measurements on system input and output, $e_i(t)$ and $e_o(t)$.

In the pursuit system the human operator sees and responds to both input and error, and a more complicated open-loop block diagram is required to represent his characteristics. If we assume again that proprioceptive feedback is not important, the block diagram of Fig. 2-3 represents the stimulus-response relations in the pursuit system. The transfer function $P_iG_1(f)$ operates on the input, and $G_2G_1(f)$ operates on the error. The noise sources are arbitrarily located at the inputs to these transfer functions. In terms of the closed-loop transfer function $H(f)$ and output noise $N(f)$, the elements of
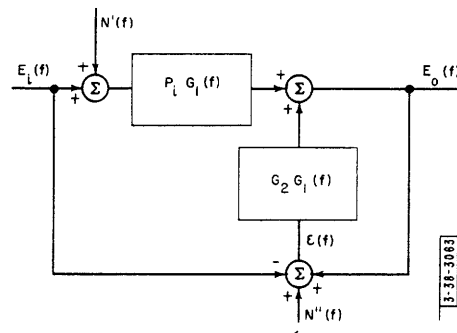
Fig. 2-3. Open-loop block diagram for pursuit system.

the open-loop pursuit model are

$$\frac{P_i G_1(f) - G_2 G_1(f)}{1 - G_2 G_1(f)} = H(f) \quad , \tag{2-11}$$

and

$$\frac{N'(f) P_i G_1(f)}{1 - G_2 G_1(f)} + \frac{N''(f) G_2 G_1(f)}{1 - G_2 G_1(f)} = N(f) \quad . \tag{2-12}$$

Thus the elements of this model cannot be determined uniquely from measurements on only $e_i(t)$ and $e_o(t)$.

By adding to the error signal a second input that is statistically independent of the primary input, we could determine $P_i G_1(f)$ and $G_2 G_1(f)$. Measurement of the power spectrum of the second input and of the cross spectrum between this input and the output would permit calculation of $G_2 G_1(f)$. ' Knowing $G_2 G_1(f)$ we could find $P_i G_1(f)$. If the second input has small amplitude and its power spectrum resembles the spectrum of the error, it is likely that the human operator's normal pursuit characteristics would not be changed by the second input. However, the additional measurements would greatly increase the complexity of data reduction.

D. SOME PROPERTIES OF QUASI-LINEAR TRANSFER FUNCTIONS

The quasi-linear transfer function $H(f)$ determined from Eqs.(2-4) and (2-5) has the following two properties: (1) Its response to the input $e_i(t)$ best approximates in the linear-mean-square difference sense the human operator's response to the same input. (2) If the input signal is a gaussian process,[26] the transfer function obtained is realizable, i.e., it operates on the past and present of the input. A proof of both properties has been given by Booton.[27] He has shown that, in general, the best mean-square difference approximation to any nonlinear device having a gaussian input will be realizable and is determined by Eq.(2-1). If the input is only approximately gaussian, we would expect that $H(f)$ would be only approximately realizable. The extent of the nonrealizability and the input conditions which produce it are not known fully.

E. MEASUREMENT OF POWER-DENSITY SPECTRA AND DETERMINATION OF TRANSFER FUNCTIONS

To determine $H(f)$ and $\Phi_{nn}(f)$ from Eqs.(2-4) and (2-5), we must compute the power-density spectra of input and output and the cross-power density spectrum between input and output. Usually these spectra have been obtained by taking the Fourier transform of the appropriate correlation functions.[24] This procedure is theoretically straightforward, but as a practical matter it is difficult because of Gibbs' phenomenon oscillations introduced by transforming only a finite portion of the correlation functions. Although methods that compensate for this effect have been developed, a long computational procedure is necessary to find the transforms.[28,29] Since we express our final results in the frequency domain, it seems more efficient to obtain the spectra without making the detour through the correlation functions. A special-purpose analogue computer, the cross-spectrum computer, which determines power-density and cross-power-density spectra directly from the time functions of two signals, has been constructed.

9

We were able to compute spectra more conveniently and in less time with the cross-spectrum computer than we could with an analogue correlator plus a digital computer to Fourier-transform the correlation functions.

A principle of operation for a cross-spectrum computer is as follows. The two signals $e_i(t)$ and $e_o(t)$ are passed through identical narrow-bandpass filters set at frequency f_c. The outputs of filters $E_i(f_c, t)$ and $E_o(f_c, t)$ represent running coefficients of amplitude spectra of the signals at frequency f_c. $E_o(f_c, t)$ is shifted in phase by 90° to obtain $\overline{E}_o(f_c, t)$. The products $E_i E_o$ and $E_i \overline{E}_o$ are formed, and the integrals of the products are obtained and plotted. The integral of $E_i E_o$ is proportional to the real part of the cross spectrum, while the integral of $E_i \overline{E}_o$ is proportional to the imaginary part of the cross spectrum. A more detailed description of the computer and a discussion of its operation and accuracy is given in Appendix B.

III. THE EXPERIMENTAL TRACKING STUDY

A. OUTLINE OF EXPERIMENT

The objectives of the experimental tracking study were: (1) to determine whether a quasi-linear transfer function provides a useful representation of manual control system characteristics and if so, under what conditions. (2) to determine the effects of input-signal characteristics on the behavior of simple manual control systems, and (3) to obtain a family of characteristics describing manual control system behavior that would be useful for system design and would represent an upper bound on human-operator performance. From this family we hope to be able to discover basic rules of behavior for the human operator, invariances in his characteristics.

To determine whether the quasi-linear transfer function is useful, we must obtain answers to the following questions. First, is H(f) [and also Φ_{nn}(f)] relatively invariant to changes of human operator and to repeated tracking runs with the same operator? Second, does a quasi-linear transfer function account for most of the output power? If not, is the noise related to the input by a nonlinear operation or is it a random disturbance that is independent of the input? If H(f) is to be a useful representation of the system characteristics, the answer to the first question must be affirmative, and that to the second question must be affirmative or we must be able to show that the noise is independent of the input. That is, we must show that the part of the human operator's characteristics that is capable of exact specification is closely approximated by the combination of a quasi-linear transfer function and a noise generator. A separate part of the experimental study was devoted to the question of variability. The results from other parts of the study have bearing on the second question.

The experiments were performed with simple pursuit and compensatory tracking systems, i.e., those having essentially no dynamics and a light frictionless control, because these systems are likely to provide results which represent an upper bound on human-operator performance. Input signals that approximate a gaussian process were used in order to obtain results that could be applied to as wide a variety of tracking situations as is possible under the restriction that the system be simple. The constrained and specifiable part of a gaussian process is completely described by its power-density spectrum. Roughly speaking, amplitude, bandwidth, center frequency, and shape describe the input spectrum. The input signals used in the experiments were approximately gaussian and covered ranges of amplitude, bandwidth, center frequency, and at least some variety of shapes.

B. EXPERIMENTAL DESIGN

A semifactorial experimental design was selected as the best way of exploring the important system characteristics. The over-all design consisted of four factorial experiments, in each of which the pursuit-compensatory dichotomy was one of the variables.

> Experiment I — Variability:— A study of variability of operator characteristics (1) in repeated runs by the same operator, and (2) from one operator to another. As a secondary outcome, the experiment yielded a preliminary determination of the extent to which quasi-linear transfer functions describe system response. The latter

indicated that the quasi-linear model was clearly useful and that, therefore, the other experiments might reasonably be undertaken.

Experiment II — Amplitude:— A study of the relation between input amplitude and system characteristics.

Experiment III — Bandwidth:— A study of the relation between input bandwidth and system characteristics.

Experiment IV — Shape:— A study of the relation between shape of input spectrum and system characteristics.

The experimental results are presented in the forms of (1) magnitude and phase of closed-loop transfer function H(f), (2) magnitude and phase of open-loop transfer function G(f) for compensatory systems only, (3) fraction of response power in the part of output that is linearly correlated with input $1 - (\Phi_{nn}/\Phi_{oo})$, (4) output noise spectrum relative to mean-square of input $\Phi_{nn}//\int_0^\infty \Phi_{ii}\,df$, (5) error spectrum relative to mean-square of input $\Phi_{ee}//\int_0^\infty \Phi_{ii}\,df$, and (6) relative mean-square tracking error $\int_0^\infty \Phi_{ee}\,df//\int_0^\infty \Phi_{ii}\,df$.

C. CONDITIONS OF EXPERIMENT

1. Input Signals

In practically all parts of the experiments, input signals were generated by summing a large number (usually between 40 and 144) of sinusoids of different frequencies and arbitrary phases. Producing the signals in this way permits very good control over the shape of the spectrum and, in particular, makes it possible to achieve a very sharp cutoff. The components of each signal were spaced uniformly in frequency. The intervals were about 0.0025 cps for the very-narrow-bandwidth signals and about 0.10 cps for the very-wide-bandwidth signals.

A signal composed of sinusoids of different frequencies and random phases approaches a gaussian process as the number of sinusoidal components becomes infinite.[30] Although 40 (the smallest number of components used frequently in these experiments) is not a very large number, it is large enough so that no periodicities in the signals are obvious. Such a signal looks quite random, as can be seen in the sample waveform shown in Fig. 3-1, and the distribution of instantaneous amplitudes is very approximately normal. In Appendix C are shown measured relative frequency and cumulative frequency distributions of amplitude for the input signal shown in Fig. 3-1. Of course, as the number of sinusoidal components increases, the approximation to a true gaussian process improves. Most of the input signals have more than 40 components and therefore should be more nearly gaussian than the one of Fig. 3-1 and Appendix C.

A signal having 40 or so components will not possess exactly the same mathematical properties that a true gaussian process does. Many theorems, such as the statement in Sec. II that H(f) will be realizable when measured with a gaussian input, are only approximately true for an input composed of sinusoids. But the mathematical properties are not so important as the psychological effects of the signal. It is highly unlikely that the human operator would be able to distinguish inputs of the kind used in these experiments from a true gaussian process. Therefore, the system characteristics obtained with our quasi-gaussian inputs are not likely to be very different from those obtained with true gaussian signals.

12

Four different types of input signals were generated. The different types of spectra are illustrated in Fig. 3-2. The actual measured spectra are shown in Appendix C. A discussion of the four types of spectra follows. (1) In idealization, the Rectangular Spectra [Fig. 3-2(a)] have infinitely sharp cutoff and are therefore particularly convenient for studies in which input bandwidth is the main variable (Experiment III). (2) The RC Filtered Spectra [Fig. 3-2(b)] simulate
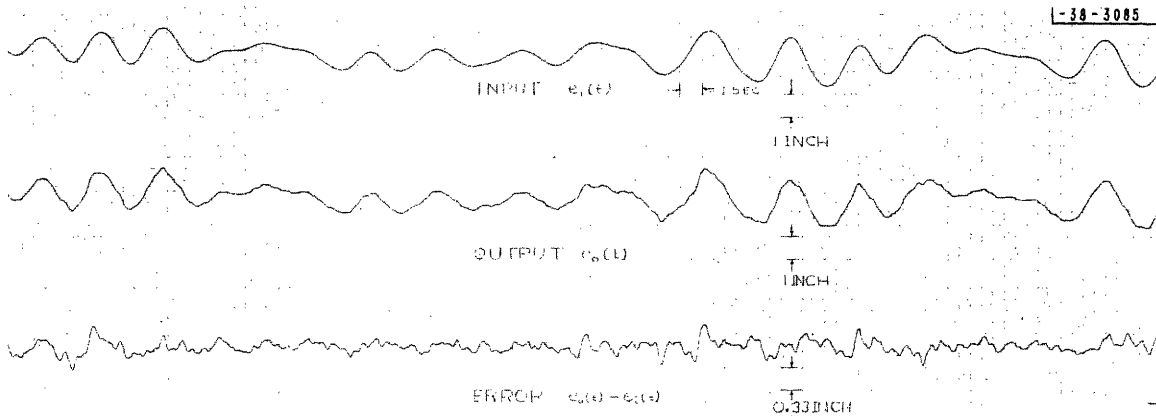

Fig.3-1. Sample waveform of Input R.40. Also shown are the output and error time functions obtained in the pursuit system.
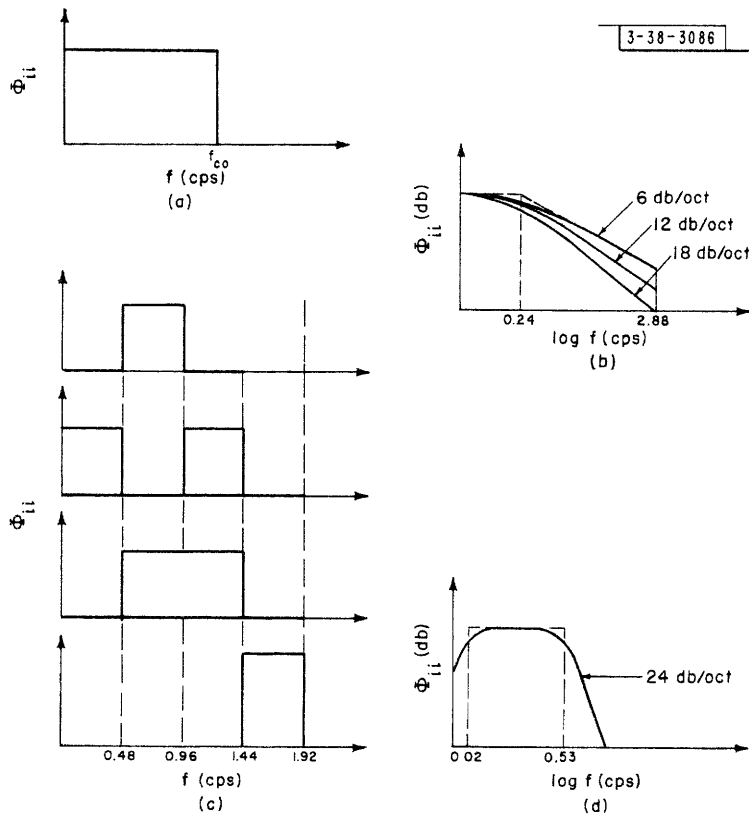

Fig.3-2. The four types of power-density spectra used in this study: (a) Rectangular, (b) RC Filtered, (c) Selected Band, and (d) Continuous.
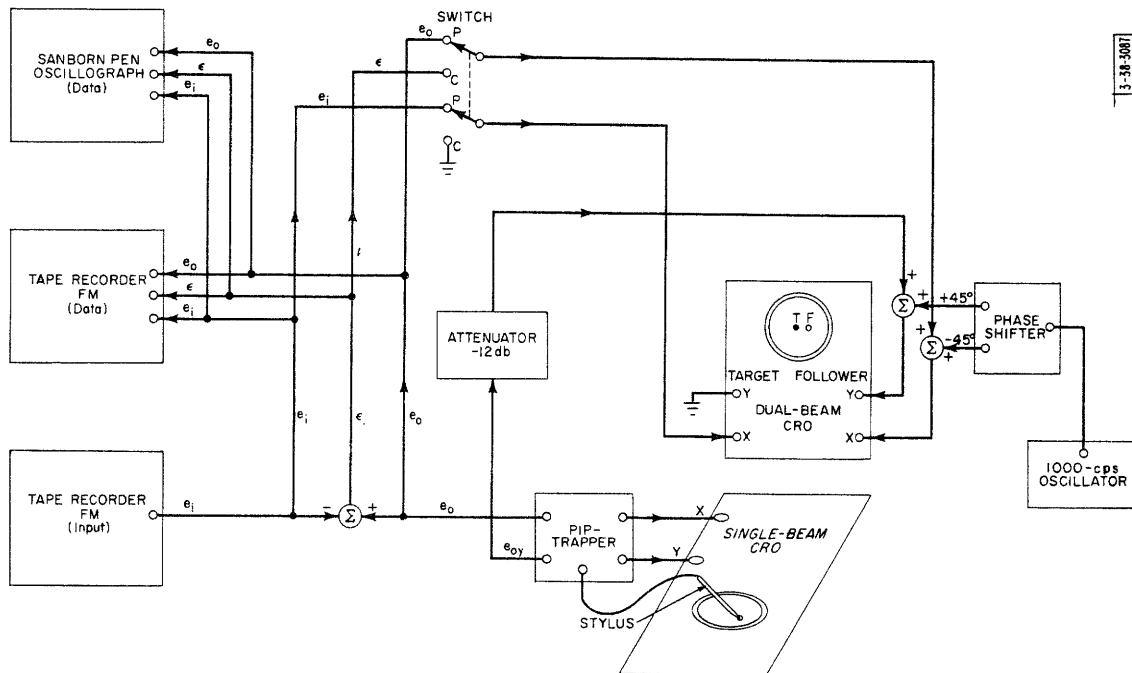
13

Fig.3-3. Tracking apparatus.

Fig.3-4. Block diagram of tracking apparatus.

14

spectral shapes encountered in actual tracking situations more closely than do the other signals. They were obtained by passing a signal, whose spectrum was rectangular with cutoff frequency of 2.88 cps, through one, two, or three cascaded low-pass RC filters. The half-power frequency of each individual RC filter was, in every case, 0.24 cps. (3) The Selected Band Spectra [Fig. 3-2(c)] were produced by combining in various ways four signals having rectangular spectra of equal bandwidth but located on the frequency scale in adjacent blocks. The Selected Band and the RC Filtered Spectra were used in Experiment IV. (4) The Continuous Spectrum [Fig. 3-2(d)] was obtained by passing a series of randomly spaced pulses through an electronic low-frequency bandpass filter (Krohn-Hite Model 330A) which had low cutoff at 0.02 cps and high cutoff at 0.53 cps. At frequencies well above the high cutoff, the attenuation increased at 24 db per octave. This input was used in the pursuit part of Experiment I.*

2. Apparatus

The tracking apparatus is illustrated in the photograph of Fig. 3-3 and in the block diagram of Fig. 3-4. One beam of the upper dual-beam cathode-ray oscilloscope (CRO) presents the target (a dot 1/16 inch in diameter); the second beam displays the follower (a circle 1/8 inch in diameter). The circle is formed by feeding to the horizontal (X) amplifiers of the follower channel a signal having a 1000-cps sinusoidal component that is shifted in phase by 90° relative to the 1000-cps component of a similar signal fed to the vertical (Y) amplifier. The cathode-ray tube of this oscilloscope has a short-persistence P-11 phosphor.

In the pursuit system, the switch is in the upper or P position and the input signal $e_i(t)$ is connected directly to the horizontal amplifier of the target channel. The vertical target amplifier is connected to ground. The target dot therefore moves back and forth only along the horizontal axis of the screen under the impetus of the input signal. The subject tries to keep the follower circle around the target dot by moving the control, a small pencil-like stylus, on the screen of the lower oscilloscope. Voltages proportional to the position of the stylus on the lower screen are generated by the electronic circuit connected to the stylus. This circuit, in combination with the stylus, is called a "pip-trapper." In the pursuit system $e_o(t)$, the voltage corresponding the stylus position along the X-axis of the lower screen, is added to the 1000-cps signal used to form the follower and controls its position. The sensitivities of the horizontal amplifiers of both oscilloscopes were adjusted so that a movement of the stylus produced a movement of the follower, equal in magnitude and in the same direction. Thus in the block diagram of the pursuit system (Fig. 1-2), the control sensitivity K_c is unity.

In the compensatory system, the switch is in the lower or C position, and the input to the horizontal target amplifier is connected to ground, making the target stationary at the center of the screen. The follower moves in proportion to the difference between the pip-trapper output and the input, $e_o(t) - e_i(t)$. This difference or error signal is added to the 1000-cps signal that forms the follower circle and controls the follower movement. As was the case in the pursuit system, a movement of the stylus produces a movement of the follower, equal in magnitude and in the same direction. The control sensitivity K_c in the block diagram of the compensatory system (Fig. 1-1) is unity.

---

*The pursuit part of Experiment I was performed before it was decided to use inputs composed of sinusoids.

Fig. 3-5. Schematic diagram of pip-trapper.

The tracking control of the pip-trapper,* the small pencil-like stylus, contains a photocell in its lower tip. A circle is generated on the screen of the lower oscilloscope by the electron beam which rotates at a 1000-cps rate. The photocell responds to this circle of light. When the tip of the stylus is centered within the circle, the photocell detects a constant light intensity. When it is off-center, the light intensity it detects varies at a 1000-cps rate. The phase of the photocell output, relative to the 1000-cps signals used to form the circle, determines the polarity of a correction voltage which, when applied to the lower oscilloscope, centers the circle about the tip of the stylus. Therefore, the circle follows the stylus as it is moved. The voltage required to make it follow corresponds to the subject's response movement. The stylus is particularly useful because it provides a tracking control that has the familiar feel of a pencil, has little friction, and is light (35 grams). A schematic diagram of the pip-trapper circuit is shown in Fig. 3-5.

The subject was seated directly in front of the upper screen and was allowed to adjust his viewing distance to whatever value he thought best (usually between 20 and 30 inches). The screen of the lower oscilloscope was located to the right of the subject as shown in Fig. 3-3. Since the motion required for tracking with a stylus control is similar to that used in writing, this location was particularly comfortable and natural. An arm rest which supported the entire forearm was provided (not shown in the figure) and the subject was allowed to use finger, wrist or forearm movements as he desired. In this way, he could adjust to different movement amplitudes by selecting the muscle group most suitable for that amplitude.

The stylus was free to move in both X- and Y-directions, but the movement in the Y-direction produced a vertical movement of the follower that was one-quarter the magnitude of the stylus movement. By allowing two degrees of freedom in the control the operator could move his hand in a free and natural fashion without external constraint. The most natural movement is an arc centered about the pivot point of the forearm, wrist or fingers. By making the vertical-control sensitivity low, the operator could move in such an arc and still not produce significant vertical movement of the follower. However, the control sensitivity was great enough so that he could correct for the slow and infrequent vertical displacements of the target or follower that appear to be unavoidable in the type of oscilloscopes available for this study [Dumont types 322 (dual-beam) and 304 (single-beam)]. Since these displacements were infrequent and of small magnitude, they were not likely to affect significantly the operator's characteristics.

The input, response, and error signals were recorded on magnetic tape by frequency modulating the signals, and on a pen oscillograph. The magnetic-tape recordings were used in computing the power spectra and cross-power spectra, from which were derived the quasi-linear transfer functions and noise spectra that describe the system characteristics.

The chief consideration in the design of the tracking apparatus was to obtain a system that would be as simple and as natural to operate as possible. The display was simple, the control natural and free-moving. The location of the display and control oscilloscope screens was carefully chosen to make the subject comfortable and to make the system convenient to operate. The tracking apparatus used in these experiments very closely approaches the ideal toward which we aimed.

---
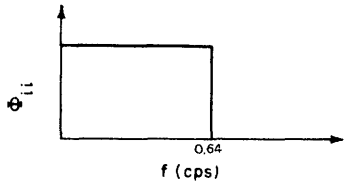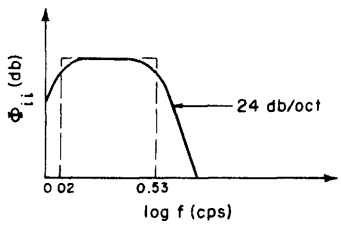
*The pip-trapper was developed by B. Waters at the M.I.T. Acoustics Laboratory.

TABLE 3-I

CONDITIONS OF EXPERIMENT I — VARIABILITY

Input Spectra	Order of Presentation		

COMPENSATORY

Input V_c

0.64
f (cps)

Φ_{ii}

Group	Members	Time from Group 1
I	V_c, V_c, V_c	
II	V_c, V_c, V_c	1 hr
III	V_c, V_c, V_c	4 hrs
IV	V_c, V_c, V_c	4 days

Rectangular Spectrum
f_{co}: 0.64 cps
rms amplitude: 1 inch
Subjects: A, B, C

PURSUIT

Input V_p

Φ_{ii} (db)

24 db/oct

0 02   0.53
log f (cps)

Group	Members	Time from Group 1
I	V_p, V_p^*, V_p	
II	V_p, V_p^*, V_p	1 hr
III	V_p, V_p^*, V_p	4 hrs
IV	V_p, V_p^*, V_p	4 days

Continuous Spectrum
Half-power frequency approximately 0.53 cps
rms amplitude: 1 inch
Subjects: D, E, F

*Signal presented backwards in time.

3. Test Conditions

The test conditions for each of the four experiments are summarized in Tables 3-I through 3-IV. Except where indicated, the same conditions were used in both pursuit and compensatory tests.

Experiment I — Variability:— Three subjects tracked four identical groups of input signals, each group containing three members. The time that elapsed between presentations of the groups was the chief variable, ranging from one hour to several days, as shown in Table 3-I. The interval between presentations of the members of a group was only a few minutes. This procedure made it possible to examine both long-time and short-time variations in the operator's characteristics. In this experiment, but only this one, the pursuit and compensatory tests are not directly comparable. In the compensatory tests, the input had a Rectangular Spectrum with cutoff frequency of 0.64 cps and 1 inch root-mean-square (rms) amplitude. The three input signals of a group were identical in all respects. In the pursuit tests, the input was the Continuous Spectrum with 1 inch rms amplitude. The three input signals of a group were identical in all respects except that the middle member was presented backwards in time.

Experiment II — Amplitude:— The inputs were three signals identical in all respects except amplitude. The spectra were rectangular with cutoff frequency of 0.64 cps. Amplitudes of 1, 0.32 and 0.10 rms inch were used (see Table 3-II).

Experiment III — Bandwidth:— The input signals had Rectangular Spectra of various cutoff frequencies. The rms amplitude was adjusted to 1 inch for each test. The range of cutoff frequencies was 0.16 to 4.0 cps (see Table 3-III). With both pursuit and compensatory systems, tracking is very easy with a cutoff frequency of 0.16 cps. With pursuit, tracking is nearly impossible with a cutoff frequency of 4.0 cps, whereas for the compensatory tests the maximum frequency that the subjects were willing to track was 2.4 cps.

Experiment IV — Shape:— Signals having RC Filtered and Selected Band Spectra were the inputs for this experiment. All signals had 1 inch rms amplitude. The rates of cutoff for the RC Filtered Spectra were 6, 12 and 18 db per octave. An input having Rectangular Spectrum with cutoff of 0.24 cps was included in the group of RC Filtered Spectra in order to connect them with the family of Rectangular Spectra used in Experiment III (see Table 3-IV). The Selected Band Spectra have shapes that are best described by Table 3-IV. Included in this group are bandpass, band-reject, and low-pass signals.

4. Subjects

One group of three subjects was used in all the experiments, except the pursuit part of Experiment I for which another group of three subjects was used. The subjects were all members of the staff of M.I.T. and were well acquainted with objectives of the experiment and the characteristics of the input signals. Before data were recorded, the subjects went through a training period of 20 hours of tracking (about thirty 4-minute tracking runs) over a period of about one week. The tracking system was simple enough to operate that the subjects achieved high proficiency during the training period.
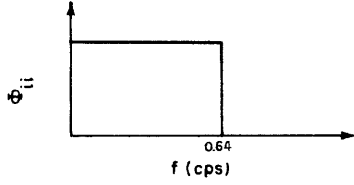
TABLE 3-II
CONDITIONS OF EXPERIMENT II – AMPLITUDE

Input Spectrum

Run	rms Amplitude
A1	1 inch
A2	0.32 inch
A3	0.1 inch

Rectangular Spectrum
f_{co}: 0.64 cps
Subjects: A, B, C

TABLE 3-III
CONDITIONS OF EXPERIMENT III – BANDWIDTH

Input Spectra	Run	f_{co} (cps)
Rectangular Spectra rms amplitude: 1 inch	R.16	0.16
	R.24	0.24
	R.40	0.40
	R.64	0.64
	R.96	0.96
	R1.6	1.60
	R2.4	2.40
	R4.0	4.00

TABLE 3-IV
CONDITIONS OF EXPERIMENT IV – SHAPE

Part I: RC Filtered Spectra

Input Spectra	Run	Spectrum	High Frequency Rate of Attenuation
RC Filtered Spectra, 1, 2 and 3 filter stages each with break frequency: 0.24 cps	F 1	6 db/oct	6
Maximum frequency: 2.88 cps	F 2	12 db/oct	12
Rectangular Spectrum f_{co}: 0.24 cps	F 3	18 db/oct	18
rms amplitude: 1 inch			
Subjects: A, B, C	F 4		∞
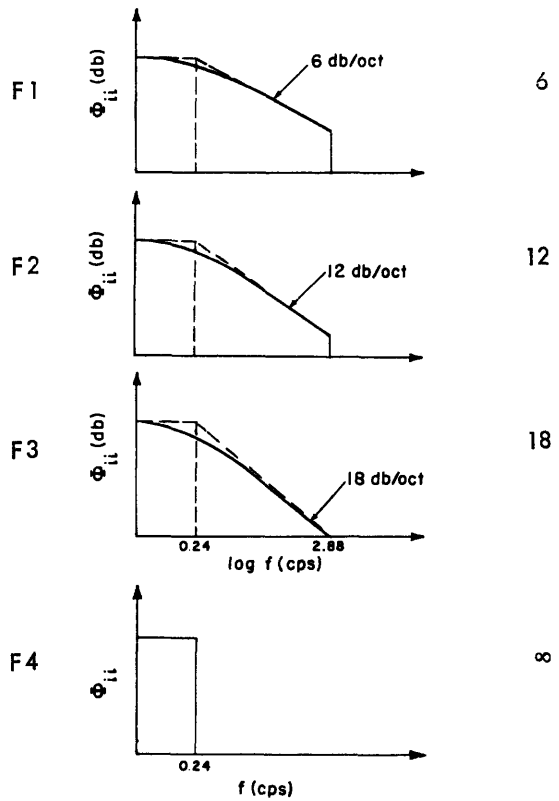
Part II: Selected Band Spectra

Input Spectra

rms amplitude: 1 inch

Subjects: A, B, C

Run: B 1   B 2   B 3
Run: B 4   B 5   B 6
Run: B 7   B 8   B 9   B 10
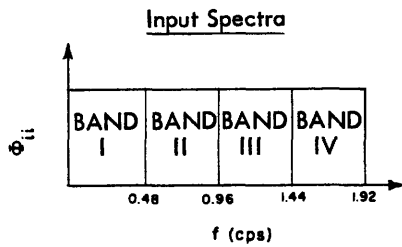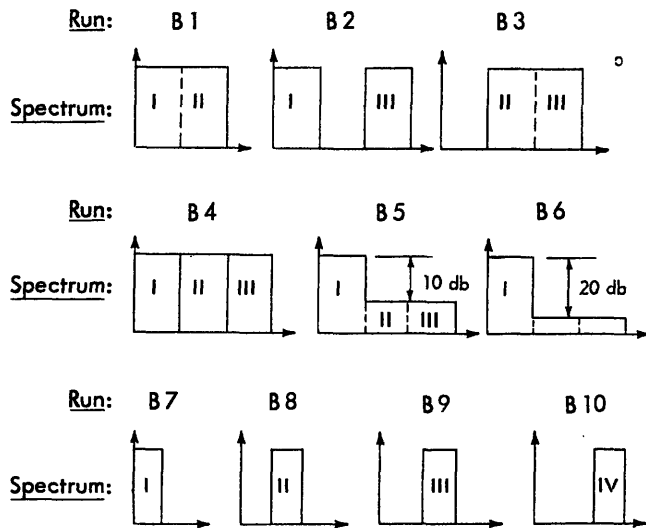
5. Procedure

All the pursuit tests were performed first, and only after they were completed were any compensatory tests begun. The reasons for following this procedure were: (1) The two situations were very different and required different tracking behavior. It did not seem wise to mix the two situations and ask the operator to change his mode frequently. (2) Pursuit tracking is more natural and required less training than compensatory. Therefore of the two systems, this was tested first.

The input signals were recorded on magnetic tape in the order shown in Tables 3-I through 3-IV and also in the reverse order. A separate tape was recorded for each set of signals. The subjects tracked each set twice — first in the forward order and then in the reverse order. The duration of each tracking run was 5 minutes. The first minute was practice, for the subject to adjust to the characteristics of the signal, and the last 4 minutes constituted the scoring run. Rest periods of about one minute were inserted between runs.

The subjects were instructed to keep the center of the follower as close as possible to the target at all times. For low-bandwidth inputs, this instruction seemed unambiguous. However, for certain high-bandwidth inputs in only the pursuit system, two different tactics were employed by the subjects. The first was to try to reproduce the input waveform as well as possible; the second was to track only the low frequency components of the input in the hope that the tracking error would be reduced. All three subjects employed the first tactic for all input signals. In the pursuit system only, two of the subjects also tracked Inputs R2.4 and R4.0, and one subject also tracked Input F1 with the second tactic. Thus for certain inputs and subjects two different tracking tactics were tested.

IV. EXPERIMENTAL RESULTS

The experimental results usually are presented in the form of graphs showing (1) magnitude and phase of H(f), (2) $1 - \Phi_{nn}/\Phi_{oo}$, (3) $\Phi_{nn}/\int_{0}^{\infty} \Phi_{ii} \, df$, (4) $\Phi_{ee}/\int_{0}^{\infty} \Phi_{ii} \, df$ (except for Selected Band Inputs), and (5) magnitude and phase of G(f) for the compensatory runs. Mean-square errors relative to the mean-square input for some of the runs were computed and are tabulated.

Too many tracking runs were performed for it to be possible to present the results of individual tests. Since the results of Experiment I showed that differences in subject characteristics are not great, only mean characteristics for each condition, obtained by averaging over subjects, are shown. However, for Experiment I – Variability, the mean characteristics for each subject obtained by averaging over replications are also presented. Standard deviations of the individual runs about the mean are indicated at several frequencies on many of the graphs of characteristics. These standard deviations provide a measure of the differences in characteristics among subjects and among different runs with the same subject.

A few runs were not included in the computation of the mean characteristics for the following reasons. Recordings of the signals obtained with one group of runs in the compensatory part of Experiment I were destroyed before they could be analyzed. Not enough time was available to carry through the analysis of all the runs; therefore, one set of runs for each of two subjects was not analyzed for the tests with the Selected Band Inputs in both pursuit and compensatory systems, for tests with the RC Filtered Spectra in the compensatory system, and for the compensatory part of Experiment II. Table 4-I shows the number of runs used to compute each set of mean characteristics.

TABLE 4-I		
NUMBER OF RUNS AVERAGED IN MEAN CHARACTERISTICS		
	Pursuit Runs	Compensatory Runs
Experiment I – Variability		
Long-Time or Group Means	9	9 (group I, only 6 runs)
Subject Means	12	12 (subject C, only 9 runs)
Experiment II – Amplitude	6	4
Experiment III – Bandwidth	6	6
Experiment IV – Shape		
RC Filtered Inputs	6	4
Selected Band Inputs	4	4

A. RESULTS OF EXPERIMENT I – VARIABILITY

The mean characteristics of each group of runs, obtained by averaging over subjects and replications within each group, are shown in Fig. 4-1 (compensatory) and Fig. 4-3 (pursuit). The mean characteristics of each subject, obtained by averaging over replications, are in Fig. 4-2 (compensatory) and Fig. 4-4 (pursuit). The differences among group means are the long-time or the
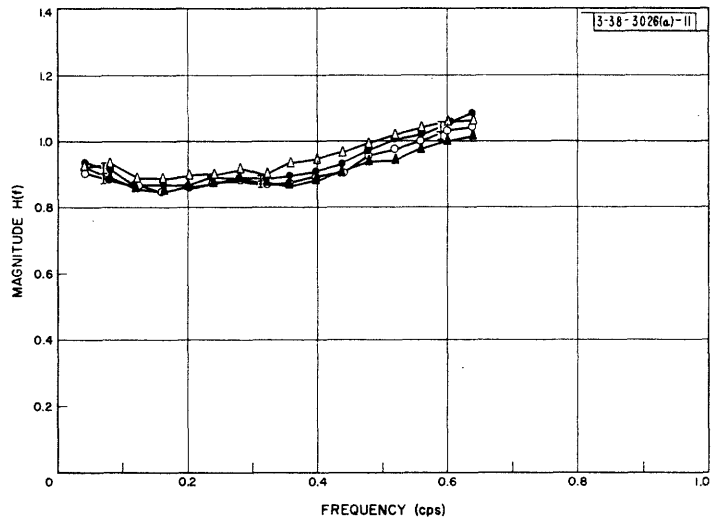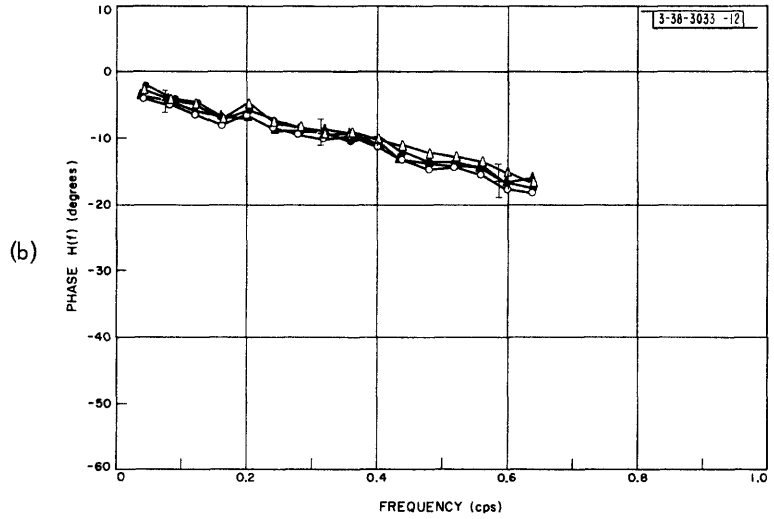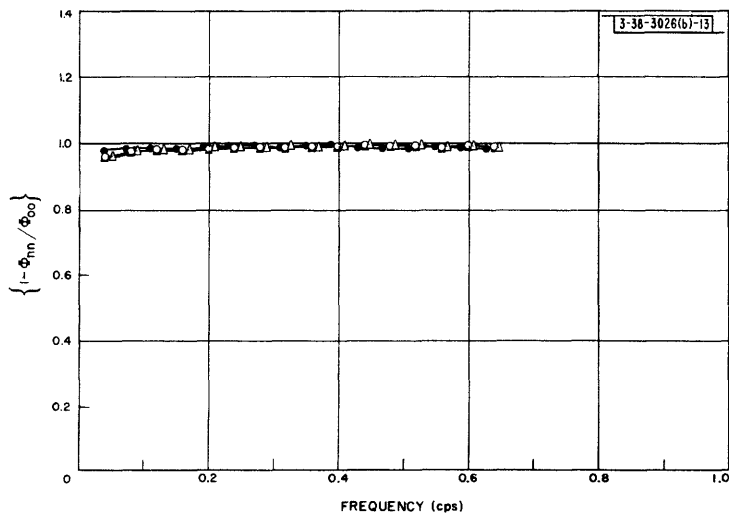
Fig. 4-1. Experiment I, compensatory — mean closed-loop characteristics of groups.

24

(d)

Group I
Group II
Group III
Group IV

(e)

Fig. 4-1 (Continued)

25
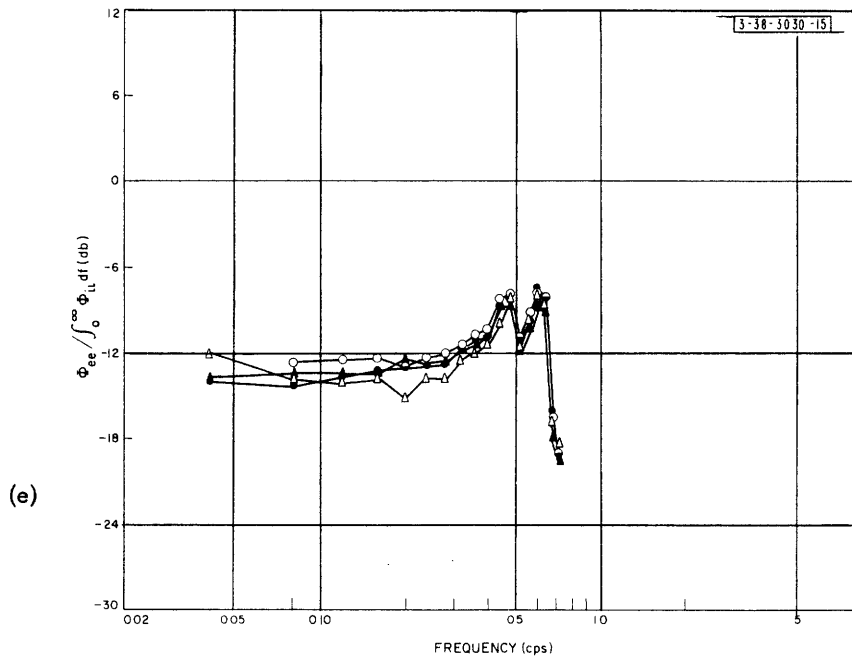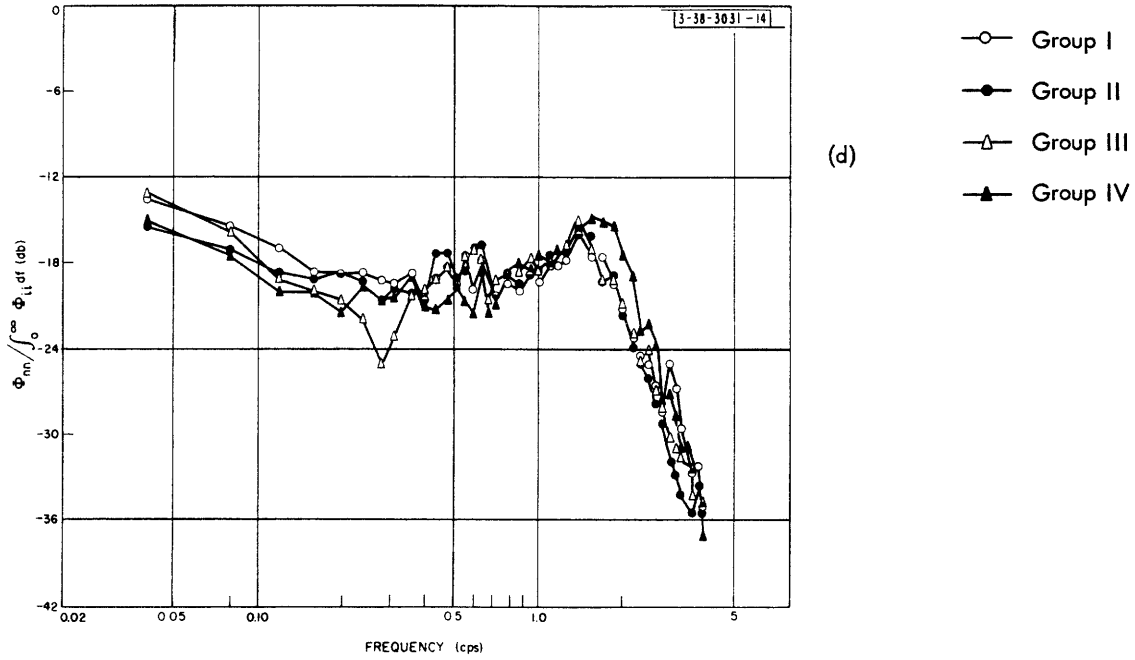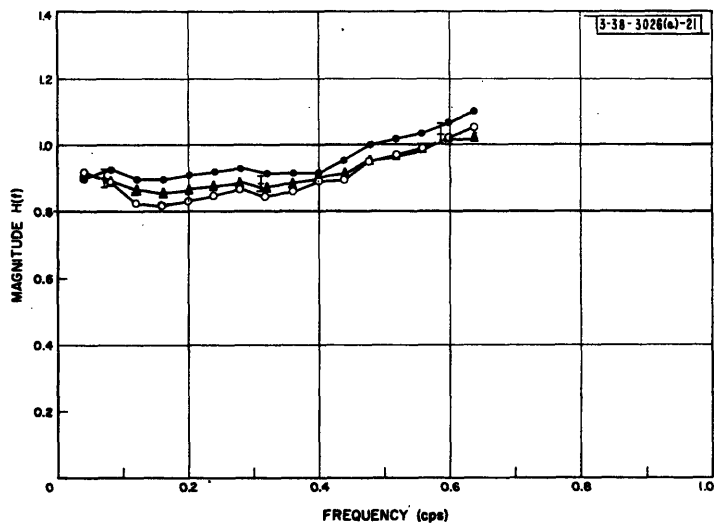
(a)
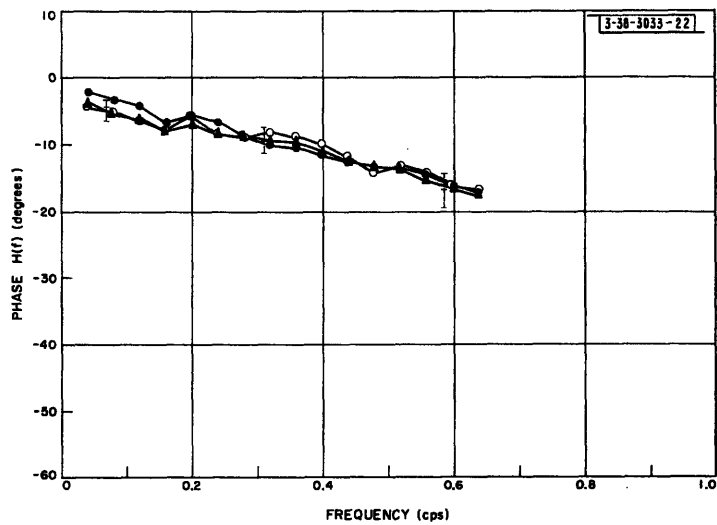
(b)
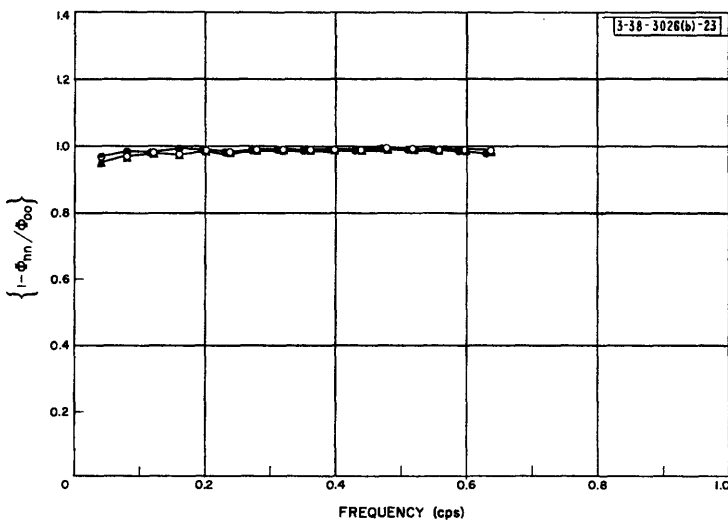
(c)

Fig.4-2. Experiment I, compensatory —
mean closed-loop characteristics of sub-
jects.
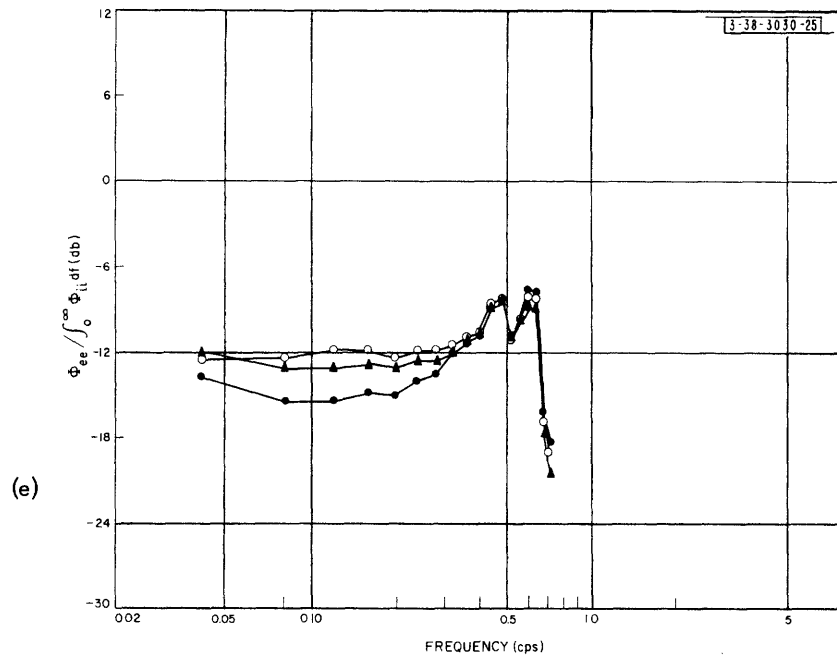
26

(d)

(e)

Fig. 4-2 (Continued)

27

Fig.4-3. Experiment I, pursuit — mean closed-loop characteristics of groups.

28

(d)

Group I
Group II
Group III
Group IV

3-38-3031-34

(e)

3-38-3030-35

Fig.4-3 (Continued)

29
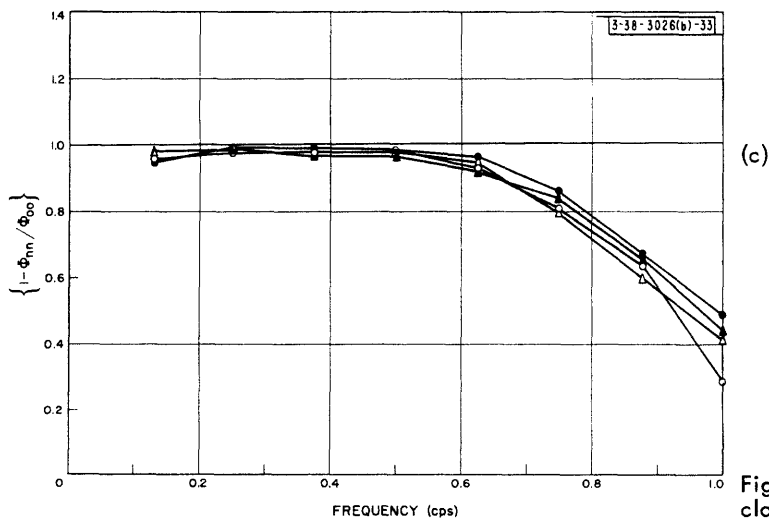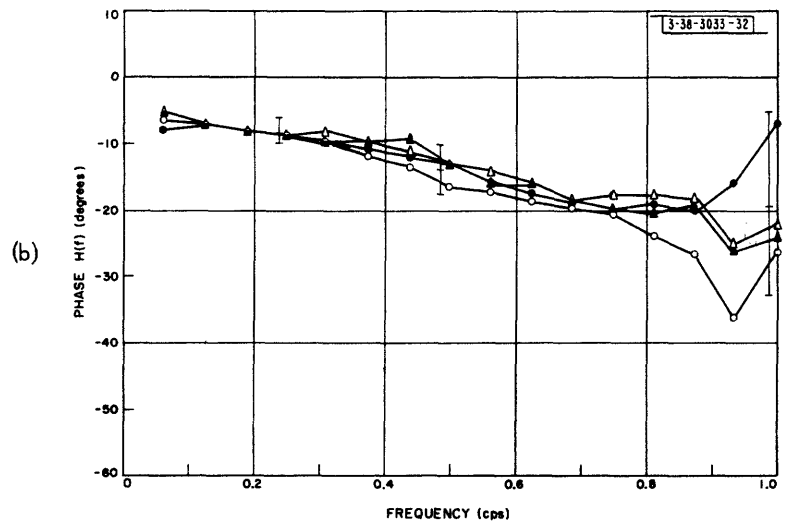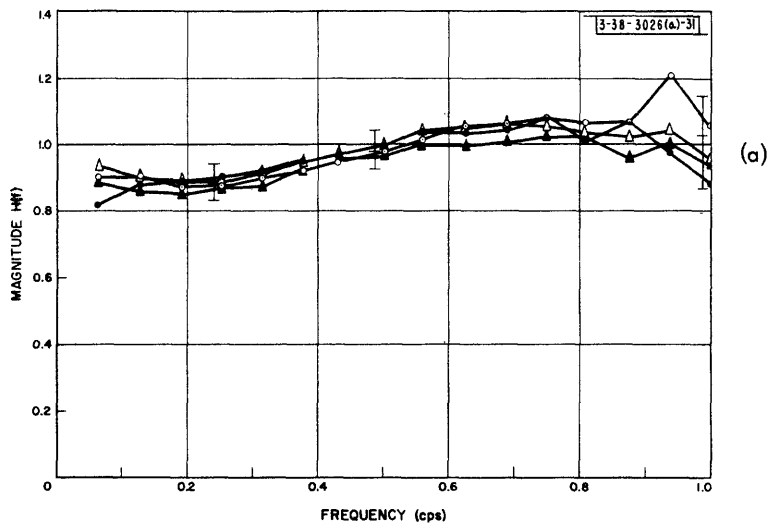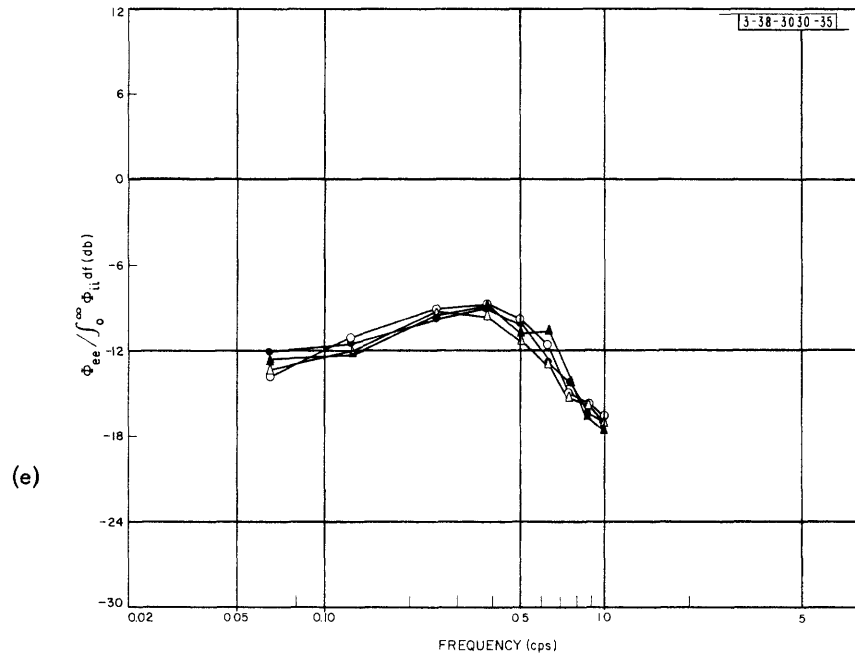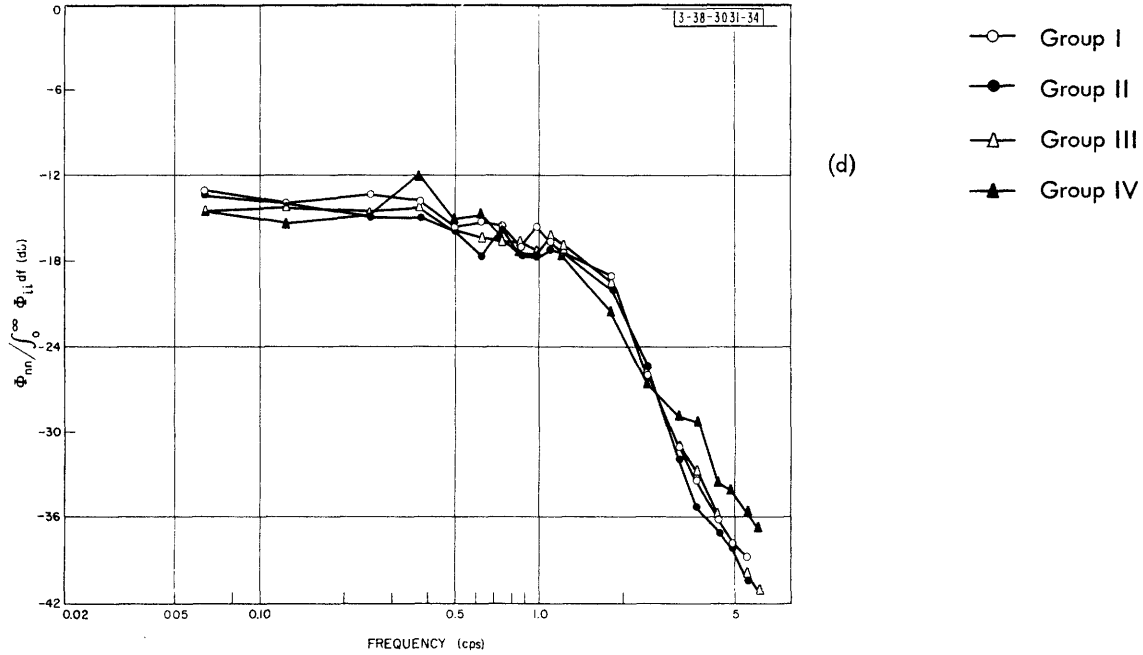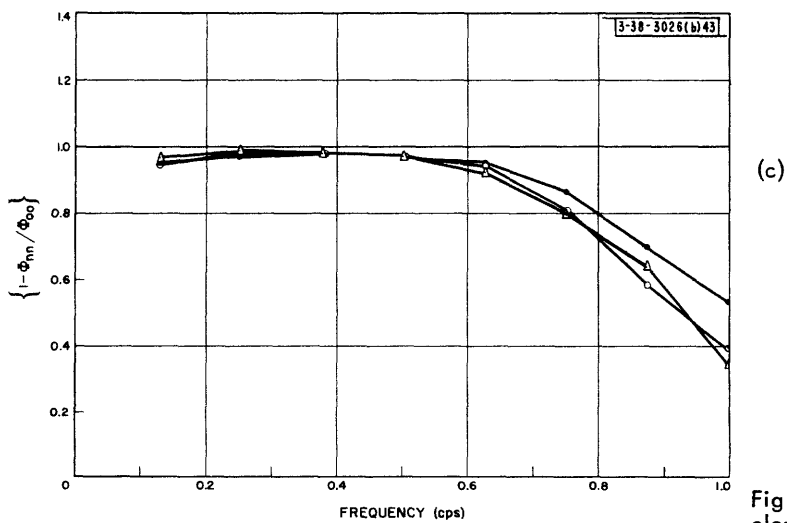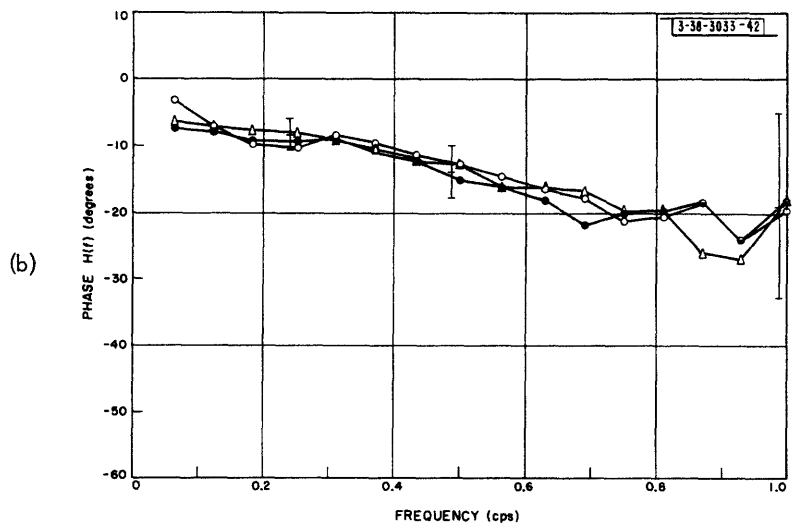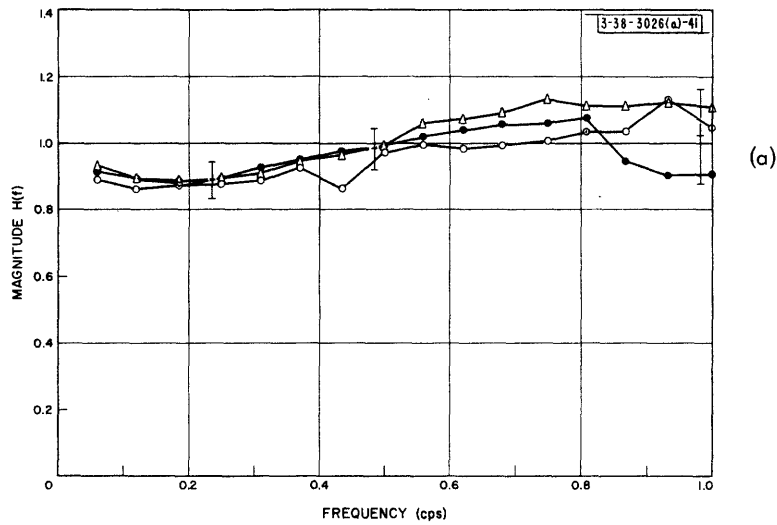
Fig.4-4. Experiment I, pursuit — mean closed-loop characteristics of subjects.

Fig. 4-4 (Continued)

31
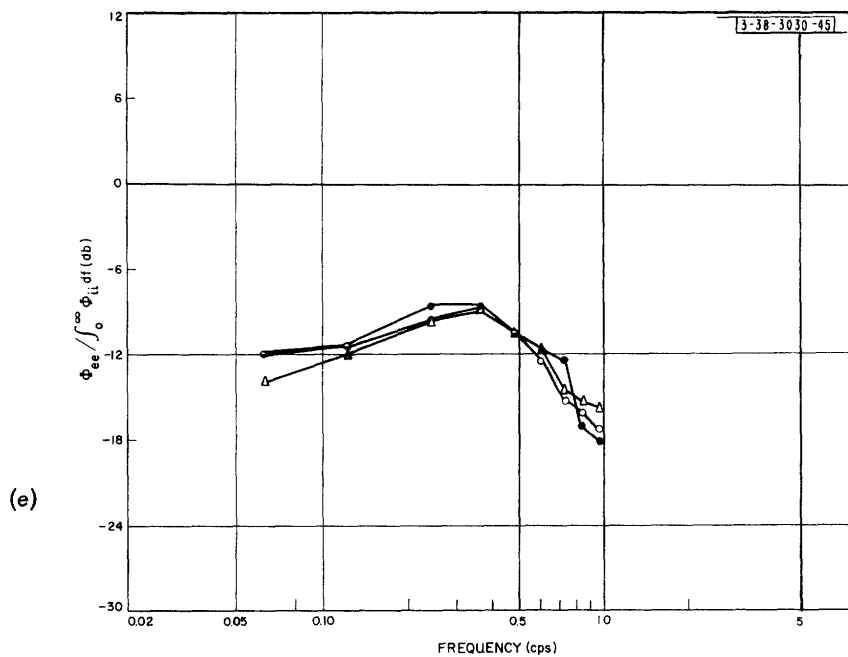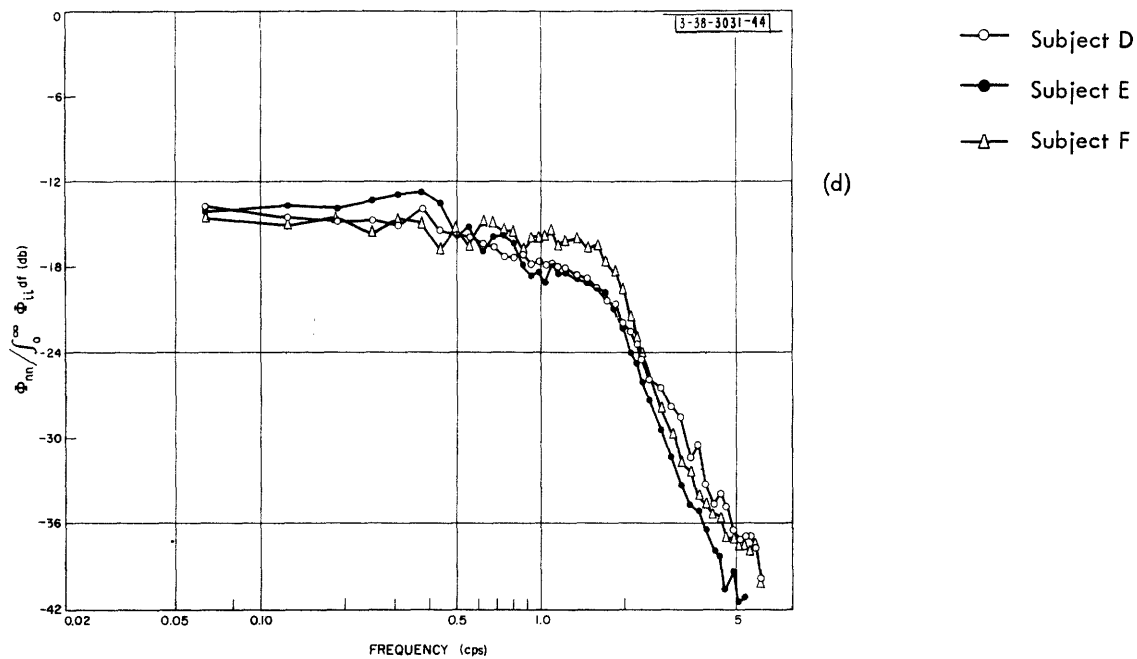
"within subject" variations in the control system characteristics, while the variations among subjects are indicated by differences among subject means. The standard deviations of all runs are shown located about the over-all mean of the characteristics. Analyses of variance of the real and imaginary parts of $H(f)$ and of $1 - \Phi_{nn}/\Phi_{oo}$ at three representative frequencies were performed in order to determine whether or not the differences in characteristics are statistically significant. The results of the analyses are shown in Tables 4-II and 4-III for the compensatory and pursuit tests, respectively.[36†]

Inspection of Figs. 4-1 through 4-4 indicates that the differences among group averages and among subject averages are small in both compensatory and pursuit systems. For the compensatory system, the standard deviation in the magnitude of $H(f)$ is about 3 per cent of the mean and the standard deviation of the phase is about 3°. For the pursuit system, the standard deviations are somewhat greater, probably because the input contained high-frequency components resulting from a gradual cutoff of the spectrum. The observed differences include the effects of inaccuracies in calibration of the recording equipment and in computation of the power-density spectra. The fact that the differences are not very much greater than would be expected from equipment calibration and computation inaccuracies alone provides further evidence that the human operator's characteristics are relatively invariant.

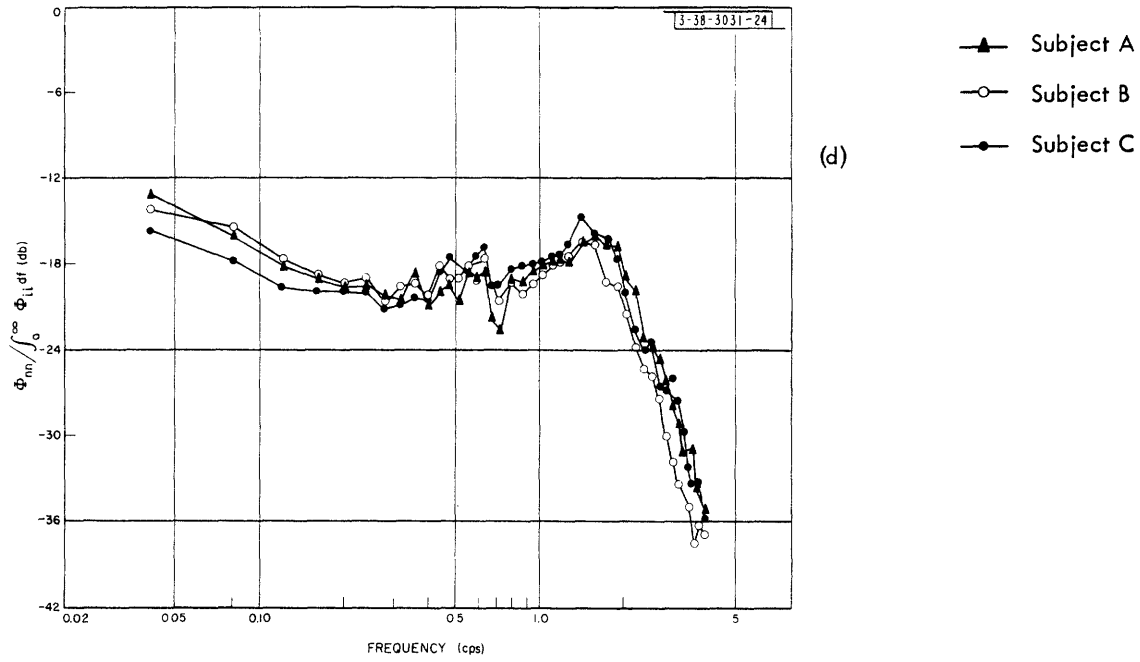|		Sources of Variance					
		Subjects	Groups (Long-Time Changes)	Members (Short-Time Changes)	Subjects × Groups	Subjects × Members	Groups × Members
Degrees of Freedom		2	3	2	5	4	6
F_c at 95% level		3.38	2.99	3.38	3.33	3.48	3.22
F_c at 99% level		5.57	4.68	5.57	5.64	5.99	5.39
Frequency	Quantity						
0.08	Imag H	3.48*	0.54	0.054	0.47	1.76	2.18
	Real H	0.56	0.10	0.05	5.30*	0.71	2.00
	$1 - \Phi_{nn}/\Phi_{oo}$	1.40	0.32	0.09	1.01	0.40	0.53
0.32	Imag H	4.51*	0.36	0.65	0.82	0.46	1.91
	Real H	1.94	0.18	0.067	1.65	2.15	1.77
	$1 - \Phi_{nn}/\Phi_{oo}$	0.32	0.53	0.21	2.51	2.27	0.85
0.60	Imag H	0.076	0.20	0.026	2.33	0.58	2.33
	Real H	2.37	1.80	0.54	4.12*	1.03	3.18
	$1 - \Phi_{nn}/\Phi_{oo}$	0.051	0.57	0.044	4.40*	2.35	2.01

TABLE 4-II
ANALYSES OF VARIANCE F VALUES FOR EXPERIMENT I, COMPENSATORY

*Significant at the 95% level.

---

†Empty cells were filled according to the standard method of least squares.[37]

The analyses of variance indicate that, statistically, the differences are not highly significant. The number of F-ratios computed in the analyses of variance is 108. The 99 per cent level of significance is reached by only one source of variance — the interaction between groups and members (long-time and short-time effects) for the real part of H(f) at 0.50 cps with the pursuit system. At the 95 per cent level, the differences among subjects for only the imaginary part of H(f) at 0.08 and 0.32 cps in the compensatory tests are significant. Seven of the F-ratios for the interactions between subjects and groups are significant at the 95 per cent level.

Half of the number of significant F-ratios can be attributed to the effects of chance alone. From a total of 108 F-ratios we would expect to find one significant ratio at the level of 99 per cent or greater, and about five at the level of 95 per cent or greater. Thus the number of significant ratios exceeds our expectations only by five. Most of the significant ratios are for the interactions of subjects and groups. This perhaps is a result of the order in which the tracking runs were performed. Each group of runs was performed as a unit. Any inaccuracies in calibration of the tracking and recording equipment would affect in the same way all the members of the group, and therefore the mean short-time characteristics would not be affected. Assuming that these inaccuracies are random, they would not tend to influence the mean characteristics of the subjects or the mean characteristics of groups (averaged over subjects). Instead, the calibration

TABLE 4-III

ANALYSES OF VARIANCE F VALUES FOR EXPERIMENT I, PURSUIT

		Sources of Variance					
		Subjects	Groups (Long-Time Changes)	Members (Short-Time Changes)	Interactions		
					Subjects × Groups	Subjects × Members	Groups × Members
Degrees of Freedom		2	3	2	6	4	6
F_c at 95% level		3.34	2.95	3.34	3.00	3.26	3.00
F_c at 99% level		5.45	4.57	5.45	4.82	5.41	4.82
Frequency	Quantity						
0.25	Imag H	1.64	0.18	1.98	0.31	0.94	0.86
	Real H	0.10	0.13	0.35	3.52*	0.93	0.94
	$1 - \Phi_{nn}/\Phi_{oo}$	0.12	0.33	0.014	0.42	0.33	1.14
0.50	Imag H	0.44	0.64	0.21	3.39*	3.11	0.89
	Real H	0.29	0.33	0.52	3.44*	1.60	4.91†
	$1 - \Phi_{nn}/\Phi_{oo}$	0.37	0.19	0.0003	2.24	0.87	0.30
0.75	Imag H	0.47	0.18	0.77	3.97*	1.40	1.18
	Real H	2.34	0.23	0.36	0.52	0.19	0.60
	$1 - \Phi_{nn}/\Phi_{oo}$	0.92	0.14	0.069	0.53	0.90	0.62

*Significant at the 95% level.

†Significant at the 99% level.

TABLE 4-IV
ANALYSES OF VARIANCE F VALUES FOR EXPERIMENT II, COMPENSATORY

		Sources of Variance		
		Subjects	Amplitude	Within Subject A
Degrees of Freedom		2	2	1
F_c at 95% level		5.14	5.14	5.99
F_c at 99% level		10.92	10.92	13.74
Frequency	Quantity			
0.12	Imag H	3.21	3.12	4.38
	Real H	1.23	0.31	2.97
	$1 - \Phi_{nn}/\Phi_{oo}$	3.33	3.13	0.34
0.36	Imag H	0.94	5.12	4.99
	Real H	8.71*	0.87	0.50
	$1 - \Phi_{nn}/\Phi_{oo}$	0.94	0.89	1.50
0.60	Imag H	1.38	1.29	2.13
	Real H	4.98	0.23	0.71
	$1 - \Phi_{nn}/\Phi_{oo}$	0.74	0.95	0.062

*Significant at the 95% level.

TABLE 4-V
ANALYSES OF VARIANCE F VALUES FOR EXPERIMENT II, PURSUIT

		Sources of Variance		
		Subjects	Amplitude	Interaction
Degrees of Freedom		2	2	4
F_c at 95% level		3.80	3.80	3.63
F_c at 99% level		6.70	6.70	6.42
Frequency	Quantity			
0.16	Imag H	1.37	3.28	1.86
	Real H	0.41	2.26	0.17
	$1 - \Phi_{nn}/\Phi_{oo}$	0.17	10.00†	0.45
0.36	Imag H	0.50	6.13*	0.85
	Real H	1.26	3.56	0.43
	$1 - \Phi_{nn}/\Phi_{oo}$	0.92	3.42	5.00*
0.60	Imag H	1.02	24.27†	1.44
	Real H	2.55	0.66	1.92
	$1 - \Phi_{nn}/\Phi_{oo}$	0.33	2.00	0.76

*Significant at 95% level.
†Significant at 99% level.

inaccuracies would tend to appear as interaction effects between subjects and groups. Thus the data reduction process is probably a major source of the significant F-ratios.

Even when the effects of data reduction are not isolated, the variations in system characteristics are not highly significant, at least for the three frequencies at which the analyses of variance were performed. However, the lack of significance does not result from a large residual variance, i.e., that variance not attributable to experimental variables, which could obscure large variations in characteristics. On the contrary, the residual is small as is indicated by the fact that the standard deviations are small. Thus not only are the variations in characteristics at the three frequencies analyzed not highly significant, but they are also relatively small in magnitude. Note that in the pursuit tests the characteristics observed for the second member of the groups, which was presented backwards in time, are not significantly different from those of the other members. Thus it appears that at least small changes in waveform do not affect system characteristics.

The characteristics at the three frequencies at which the analyses were made are representative of the system behavior as is indicated by the graphs of Figs. 4-1 through 4-4. Results obtained at other frequencies are likely to correspond closely to those obtained at these three frequencies. Thus we conclude that for the input signals tested in this experiment the characteristics of both pursuit and compensatory systems are relatively invariant.

This does not suggest, however, that the characteristics for all tracking situations will be invariant. As the difficulty of tracking becomes greater we would expect greater variations in characteristics. Conversely, as tracking situations become less difficult, the variations should be even less important. Most of the input signals in Experiments II, III and IV are not much more difficult than the ones used in this experiment. Therefore, except for very-high-speed inputs, the characteristics obtained with each of the input signals of these experiments will probably be relatively invariant.

The fraction of the output that is linearly correlated with the input, $1 - \Phi_{nn}/\Phi_{oo}$, is equal to about 0.99 for the compensatory tests and about 0.97 for the pursuit tests. For the latter, the correlated fraction of the output naturally decreases at high frequencies where the input power is low. These high correlations justify the use of quasi-linear transfer functions to describe the system characteristics observed in this experiment. For more difficult tracking situations we expect the linear correlation between input and output to decrease and the variation in characteristics to become greater. Conversely, for less difficult situations the correlation should increase and the variation decrease. Thus except for those obtained with very-high-speed inputs, the characteristics of the tracking situations considered in Experiments II, III and IV probably can be adequately described by quasi-linear models.

B. RESULTS OF EXPERIMENT II — AMPLITUDE

The characteristics of compensatory and pursuit systems are shown in Figs. 4-5 and 4-6. Analyses of variance of the real and imaginary part of H(f) and of $1 - \Phi_{nn}/\Phi_{oo}$ were performed at three representative frequencies to determine whether or not differences among characteristics are statistically significant. The results are summarized in Tables 4-IV and 4-V.
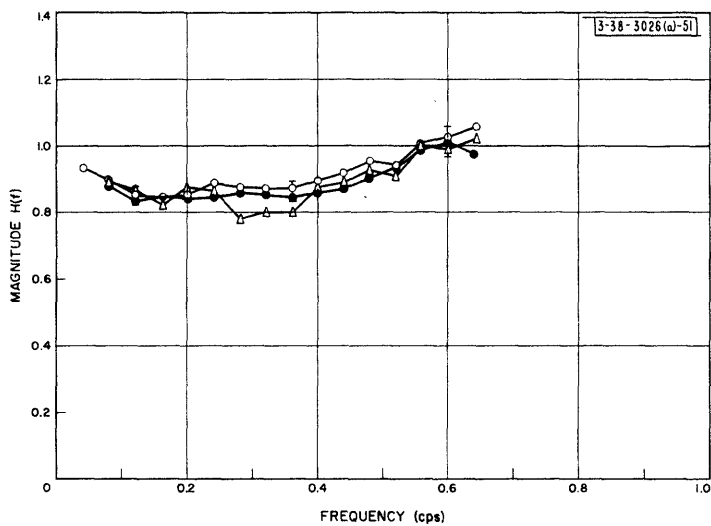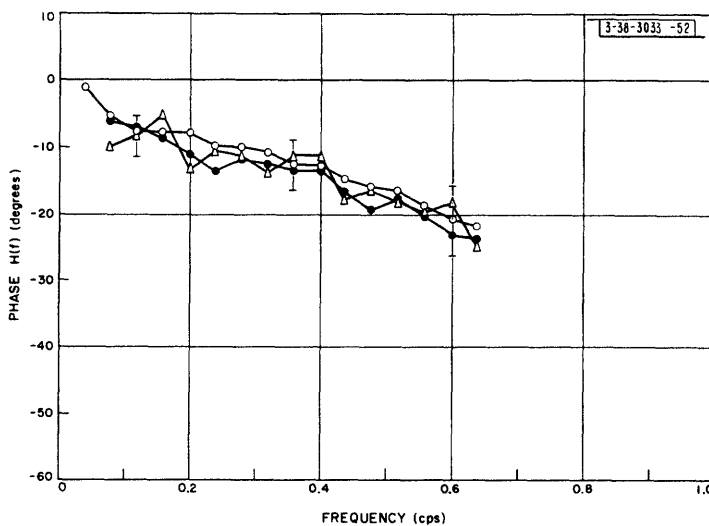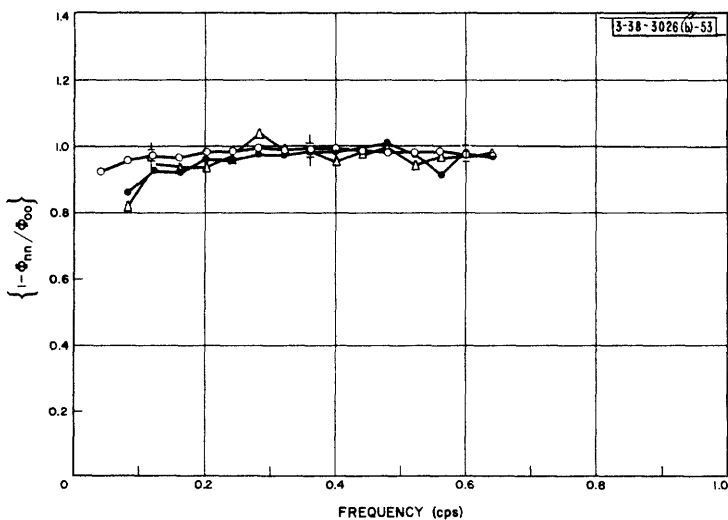
Fig.4-5. Experiment II, compensatory — mean closed-loop characteristics for each rms input amplitude.

(d)

Legend:
- A 1 (1.0" rms) — open circle
- A 2 (0.32" rms) — filled circle
- A 3 (0.1" rms) — triangle

(e)

Fig. 4-5 (Continued)

37

(a)

32

(b)

(c)
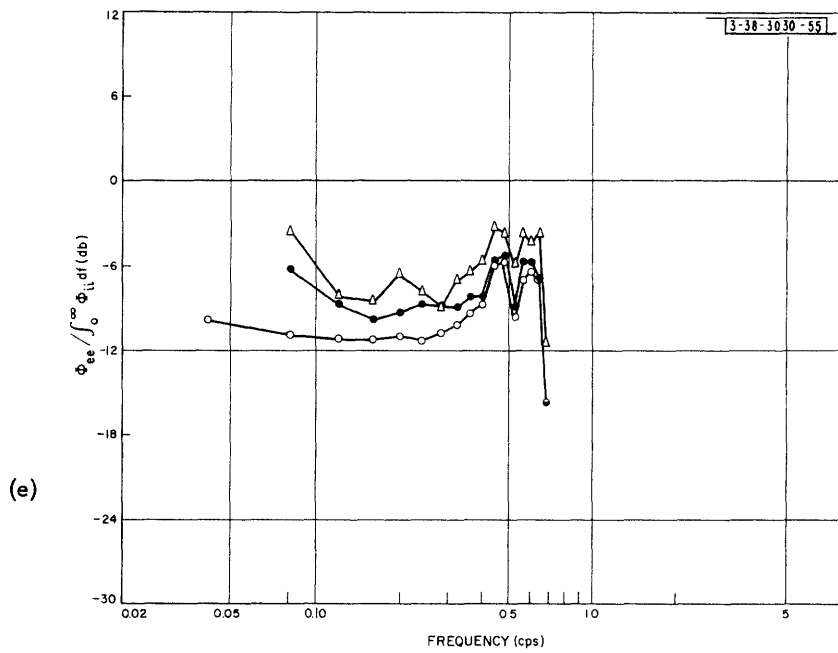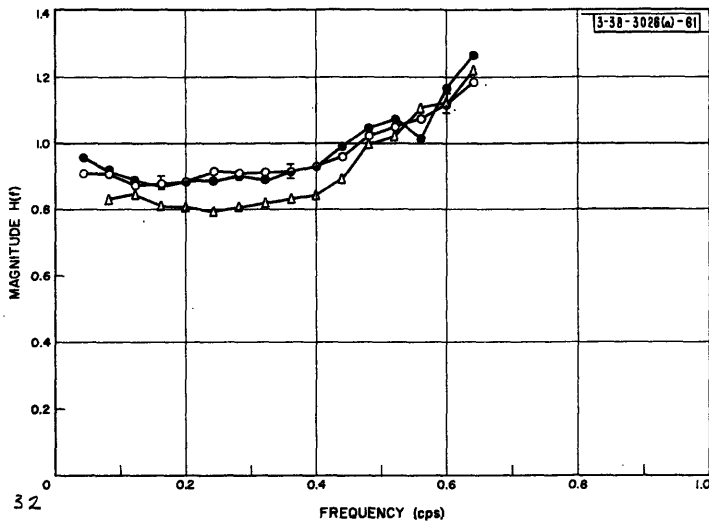
Fig.4-6.   Experiment II, pursuit — mean
closed-loop characteristics for each rms in-
put amplitude.

(d)

A 1 (1.0" rms)
A 2 (0.32" rms)
A 3 (0.1" rms)

(e)

Fig. 4-6 (Continued)

39
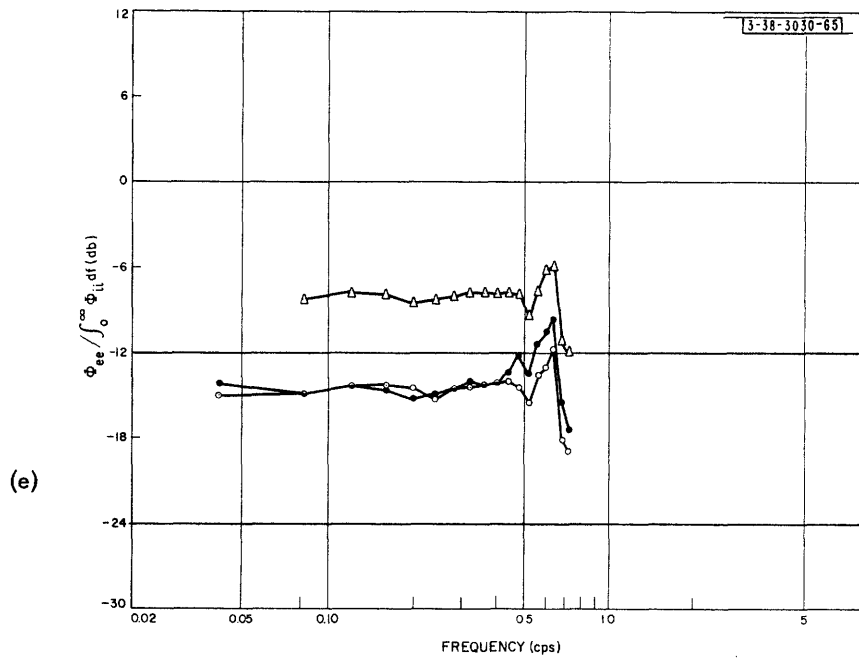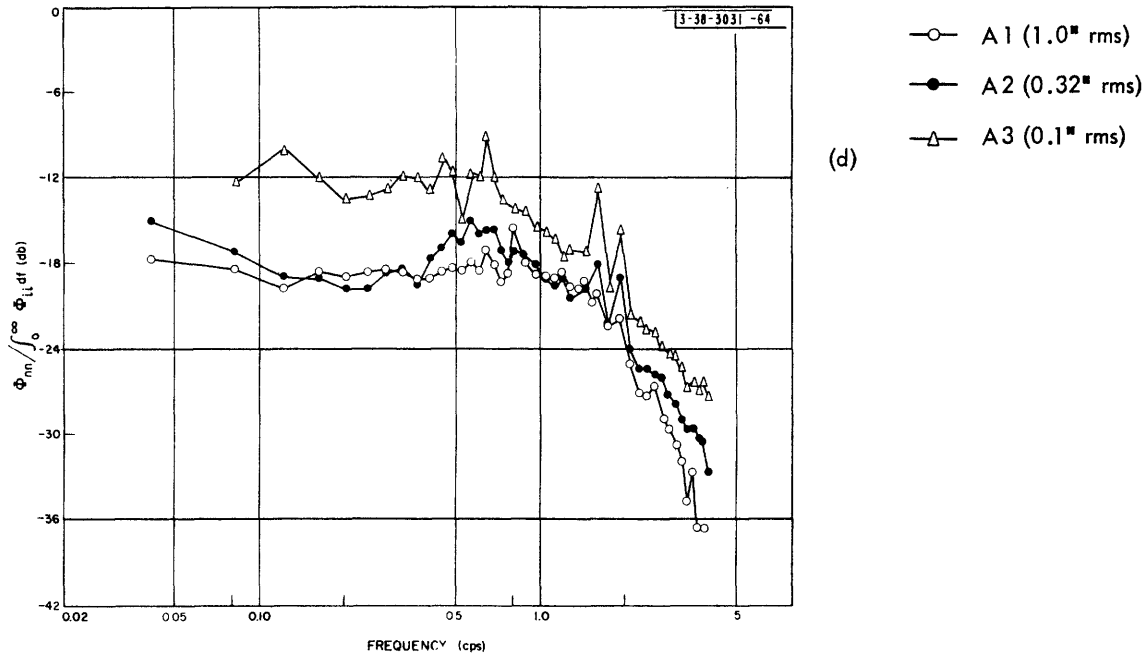
1. Compensatory Results

Figure 4-5 shows that the compensatory characteristics are largely invariant to changes in input amplitude, although there is some suggestion that, when normalized with respect to the mean-square input, the noise and error spectra tend to increase in magnitude with decreasing input amplitude. The analyses of variance (Table 4-IV) show that at three representative frequencies amplitude is not a statistically significant source of variance in $H(f)$ and in $1 - \Phi_{nn}/\Phi_{oo}$, even at the 95 per cent level. Subjects are significant at the 95 per cent level for only the real part of $H(f)$ at 0.36 cps. The number of F-ratios computed for the compensatory tests was 27, and therefore the occurrence of one significant F-ratio at the level of 95 per cent or greater can be reasonably attributed to the effects of chance. Because subjects were significant for only the real part of $H(f)$ at one frequency, we can assume that differences among subjects are not appreciable. Since $\Phi_{nn}/\int_0^\infty \Phi_{ii}\,df$ and $\Phi_{ee}/\int_0^\infty \Phi_{ii}\,df$ can be expressed in terms of $H(f)$ and $1 - \Phi_{nn}/\Phi_{o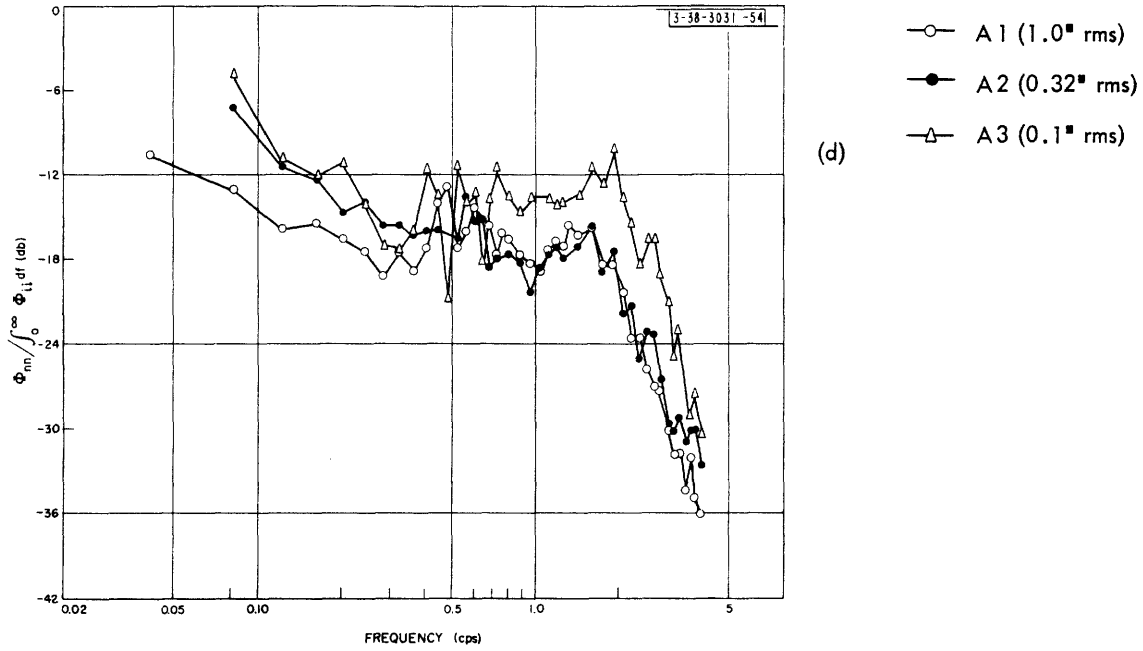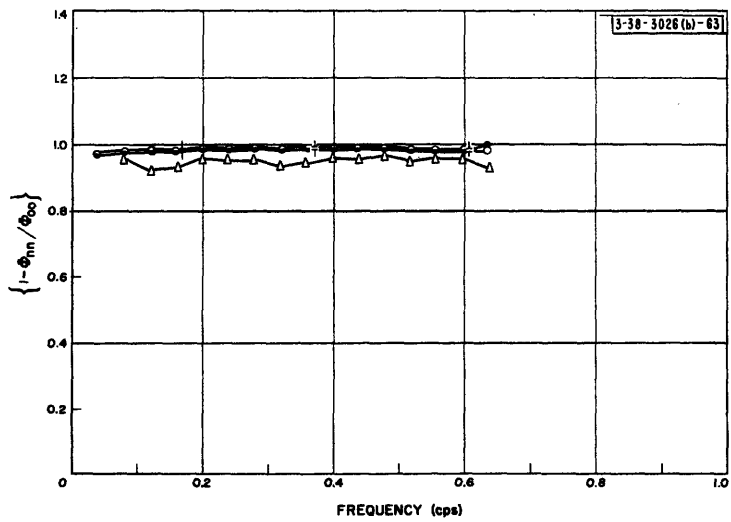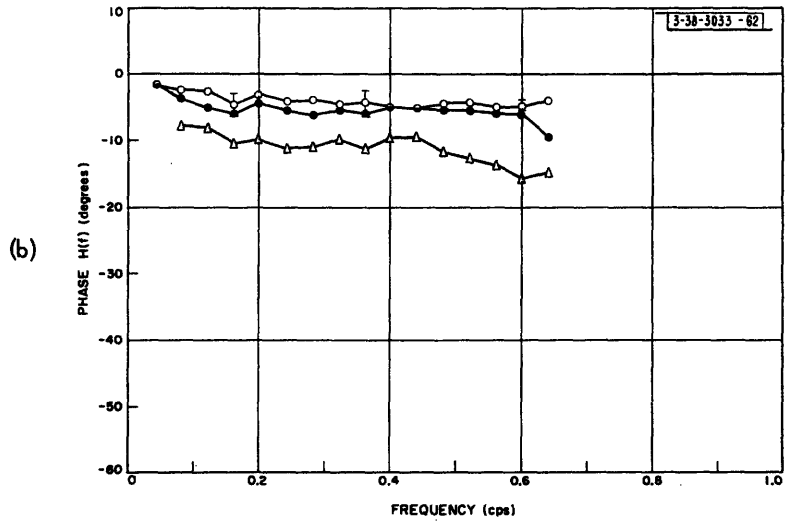o}$,* the fact that $H(f)$ and $1 - \Phi_{nn}/\Phi_{oo}$ do not change significantly implies, but does not guarantee, that within the signal band $\Phi_{nn}/\int_0^\infty \Phi_{ii}\,df$ and $\Phi_{ee}/\int_0^\infty \Phi_{ii}\,df$ also do not change significantly. No statement can be made about the significance of the spectra at frequencies beyond the input-signal cutoff. The characteristics at the frequencies chosen for analysis are representative and therefore, except for uncertainty of the significance of the differences among the high-frequency noise and error spectra, we can conclude that neither amplitude nor subjects have significant effect upon the characteristics of the compensatory system.

The results indicate that, for the compensatory system, the human-operator characteristics are invariant over the entire range of amplitudes studied in this experiment, that is, from 0.1 inch rms to 1.0 inch rms. Hence the extent of the linear amplitude range for the human operator was not determined. At the time the experiment was planned, 0.1 inch rms seemed to be about the smallest amplitude that was reasonable to use, and the dimensions of the tracking display and control oscilloscopes prevented our using larger amplitude inputs than 1.0 inch rms.

2. Pursuit Results

The characteristics of the pursuit system (Fig. 4-6) are more dependent upon input amplitude than are the compensatory. The pursuit characteristics obtained with the two greatest input amplitudes (Inputs A1 and A2) are very similar, but they are considerably different from those corresponding to the smallest amplitude (Input A3). The analyses of variance (Table 4-V) show that amplitude is a significant source of variance in the imaginary part of $H(f)$ at 0.36 cps (95 per cent level), and at 0.60 cps (99 per cent level), and of $1 - \Phi_{nn}/\Phi_{oo}$ at 0.16 cps (99 per cent level). Subjects are not a significant source of variance. On the basis of these results, we must reject the hypothesis that the characteristics of pursuit systems are invariant over the range of

---

*It is simple to derive from Eqs. (2-4) through (2-8) that

$$\Phi_{nn} = \frac{(1 - r^2)}{r^2} |H(f)|^2 \Phi_{ii} \quad ,$$

$$\Phi_{ee} = 1 + \frac{\Phi_{ii} |H(f)|^2}{r^2} - 2\Phi_{ii} \, \text{Re}\,[H(f)] \quad ,$$

where $r^2 = 1 - \Phi_{nn}/\Phi_{oo}$.

input amplitudes studied. However, Fig. 4-6 shows that most of the variance in amplitude is introduced by Input A3. Therefore, we can conclude that the range of input amplitude for which the characteristics of the pursuit system are invariant is at least from 0.3 inch rms to 1.0 inch rms. An explanation for the smaller linear range of input amplitudes of pursuit systems is given later.

3. Comparison of Pursuit and Compensatory Results

The tests with 1.0 inch rms amplitude offer the first opportunity to compare the characteristics of pursuit and compensatory systems when they are operating under equivalent and favorable conditions. The most prominent difference in the characteristics of the two systems is in the phase of H(f), which has considerably less lag for the pursuit system than for the compensatory. Naturally, the greater phase lag of the compensatory system results in greater error. The phase shift is less in the pursuit system, evidently because the human operator has direct knowledge of the input signal and can predict its values in the future of the segment currently perceived. He can therefore correct to a considerable extent for reaction-time delay and other lags present in his own characteristics. In the compensatory system, he sees only the error and hence cannot predict nearly so well. The increase in the magnitude of H(f) at high frequencies in the pursuit system is characteristic of systems that respond to input derivatives. It provides further evidence of prediction in pursuit tracking.

The compensatory results show that the motor system is capable of being adjusted to a wide range of movement amplitudes. The tracking control allowed the human operator to use finger, wrist or forearm movements to make his responses. Small, precise movements like those required for Input A3 were made with the fingers, and large, gross movements required for Input A1 were made with wrist or forearm. Since the tracking characteristics with all three inputs were the same, apparently the different muscle groups are capable of making movements of nearly equal rapidity and of about the same relative precision.

Movements made in pursuit tracking were essentially the same as those made in compensatory tracking, and therefore it is not likely that the motor system is the source of the pursuit-amplitude dependence. The only other part of the human operator's stimulus-response chain that would appear to depend heavily upon input amplitude is the visual system. For very small input amplitudes, the human operator probably has difficulty in perceiving the derivatives of the input, and he is not able to predict with the same precision. As the input amplitude becomes small, we would expect the system characteristics to suffer and to approach the characteristics observed for the compensatory system. The pursuit characteristics for 0.1 inch rms amplitude more closely resemble the compensatory characteristics than do those obtained with greater input amplitude, but the differences between pursuit and compensatory are still considerable.

Although we were not able to determine the limits of the range of input amplitudes for which human-operator characteristics would be invariant, we can make some estimates of likely values for these limits. In the compensatory system it is difficult to conceive that the lower limit of input amplitude could be much less than 0.1 inch if a unity control-displacement-to-follower-displacement ratio is retained. For smaller amplitudes, perception of error and execution of sufficiently fine control movement would be difficult. Since our results indicate that movements

41

made with fingers have about the same characteristics as movements with wrist and forearm, perhaps the upper limit approaches the human operator's reach with forearm or even with entire arm. It is not inconceivable that this limit is as much as 5 inches rms, although it is assuredly not much greater than this, because the human operator would have difficulty in reaching the large amplitude excursions of the signal. Thus the linear range of amplitudes for the compensatory system is at least 20 db but probably less than 40 db for the input signal of this experiment. Although we have no data for other signals, we expect a greater linear range for slower inputs and a smaller range for faster inputs. For fast signals the time required for movement, which increases somewhat with amplitude, would become an important factor in limiting the range of amplitude linearity.

In the pursuit system, the lower limit is about 0.3 inch rms but, as in the compensatory system, the upper limit can be greater than 1.0 inch rms. Thus the range of amplitude linearity for pursuit is at least 10 db but probably is less than 30 db.

C. RESULTS OF EXPERIMENT III – BANDWIDTH

The closed-loop characteristics obtained with each input bandwidth are shown in Figs. 4-7 and 4-8 for the compensatory system, and in Figs. 4-9 and 4-10 for the pursuit system. The average mean-square tracking errors for pursuit and compensatory tests are shown in Table 4-VI.

TABLE 4-VI RELATIVE MEAN-SQUARE ERRORS (mse)				
	Compensatory		Pursuit	
Input	Relative mse due to Noise Outside Signal Band	Total Relative mse	Relative mse due to Noise Outside Signal Band	Total Relative mse
R .16	0.0103	0.0184	0.00776	0.0116
R .24	0.0111	0.0229	0.00648	0.0102
R .40	0.0219	0.0632	0.0115	0.0242
R .64	0.0337	0.132	0.0272	0.0666
R .96	0.173	0.686	0.0644	0.238
R 1.6	0.127	1.29	0.0793	0.897
R 2.4	0.0814	1.47	0.0852	1.65
R 4.0			0.0690	1.65
R 2.4 filter			0.0852	1.34
R 4.0 filter			0.0180	1.24
F 1			0.0212	0.609
F 1 filter			0.00141	0.603

1. Correlation $1 - \Phi_{nn}/\Phi_{oo}$

The graphs of $1 - \Phi_{nn}/\Phi_{oo}$ show that, for both pursuit and compensatory systems, at least 97 per cent of the output power in the signal band is correlated with the input when the cutoff frequency is 0.64 cps or less. For the cutoff frequency of 0.96 cps, about 90 per cent of the output is correlated with the input. Higher-frequency inputs result in still lower correlations; less than half of the output power is correlated with Inputs R2.4 and R4.0. Pursuit systems tend to have slightly higher correlations than compensatory, but the differences are not great.

Because the correlations are high, we can consider the quasi-linear transfer function to be a good description of the system characteristics for rectangular inputs having a cutoff frequency less than 1 cps. For inputs whose cutoff frequency is greater than 1 cps, the quasi-linear transfer function alone does not provide a good description of the system output. However, if the noise results mostly from random variations in human-operator characteristics, $H(f)$ and $\Phi_{nn}(f)$ in combination provide as full and accurate a description as can be given.

2. Magnitude of H(f)

Except for some differences at very high and very low frequencies, the families of curves of the magnitude of $H(f)$ obtained with compensatory and pursuit systems are similar. With both systems, $H(f)$ decreases in magnitude with increasing input bandwidth. The general amplitude levels are about the same, in spite of the fact that the subjects felt that it was more difficult to track with the compensatory system. None of the subjects was willing to track the fastest input, R4.0, with the compensatory system, whereas some tracking was possible with the pursuit system.

$H(f)$ for the compensatory system is relatively constant over the input frequency range for most inputs. Extrapolation of the low-frequency part of the curves shows that for most inputs the compensatory system does not approach unity gain at zero frequency, indicating that the open-loop transfer function does not contain an integration. $H(f)$ for the pursuit system shows marked increase in magnitude at high frequencies for most inputs, probably because the human operator responds to derivatives of the input in order to predict its future. At low frequencies, the pursuit transfer functions tend to approach unity more closely than do the compensatory transfer functions.

3. Phase of H(f)

For the compensatory system, the phase is approximately a linear function of frequency with slope that increases in magnitude with input bandwidth. For the pursuit system with low-bandwidth inputs, the phase is almost constant over most of the input signal band and is much smaller than the compensatory phase lag. With certain intermediate-bandwidth inputs, like R.96 and R1.6, the low-frequency phase is nearly constant but the high-frequency phase increases linearly with frequency. The pursuit phase with very-high-bandwidth inputs is linear over all the signal band. With all inputs, the pursuit phase lag is always considerably less than the corresponding compensatory phase lag.

Pursuit phase characteristics are superior to compensatory because in the pursuit system the human operator is able to measure low order derivatives of the input signal which he can use to

43

(a)

(b)

(c)

Fig.4-7. Experiment III, compensatory —
mean closed-loop characteristics for Inputs
R .16 through R .96.

(d)

Legend:
- R.16
- R.24
- R.40
- R.64
- R.96

(e)

Fig.4-7 (Continued)

45
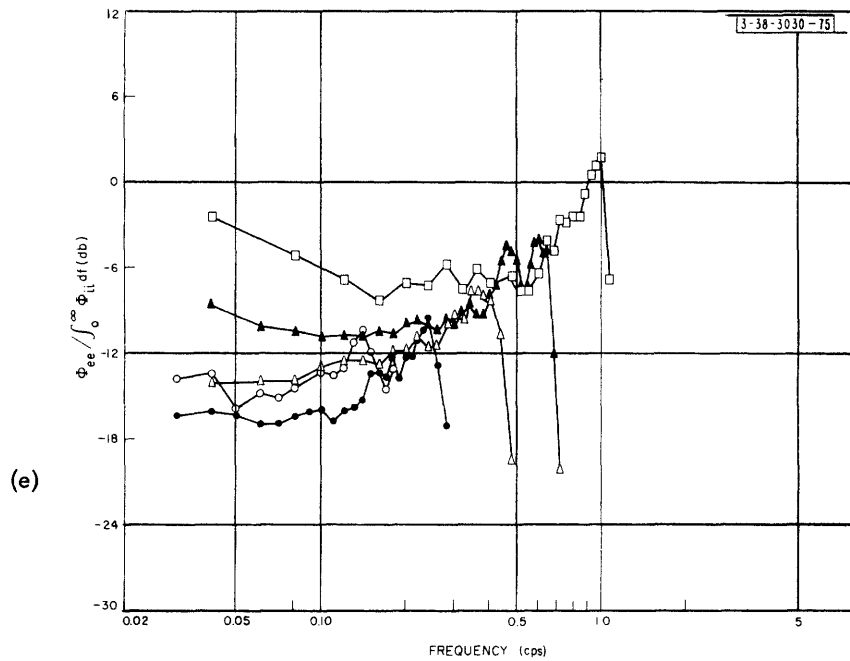
(a)

(b)

(c)

Fig.4-8. Experiment III, compensatory — mean closed-loop characteristics for Inputs R .96 through R 2.4.

3-38-3031-84

(d)

—□— R.96

—■— R1.6

—▽— R2.4

FREQUENCY (cps)

3-38-3030-85

(e)
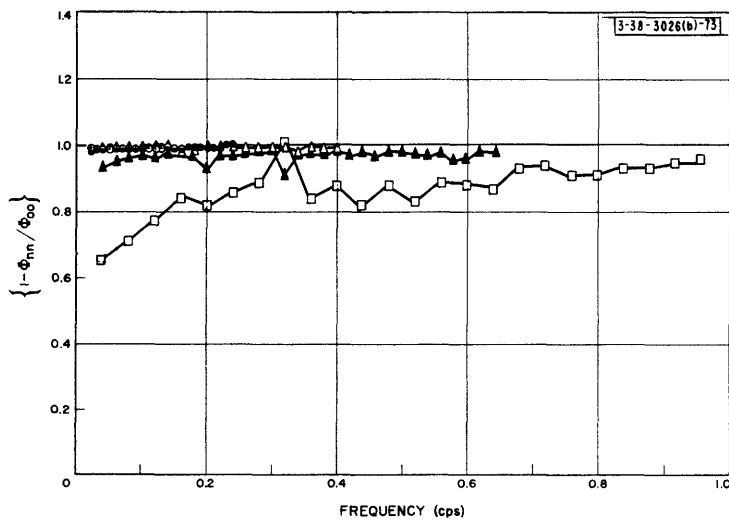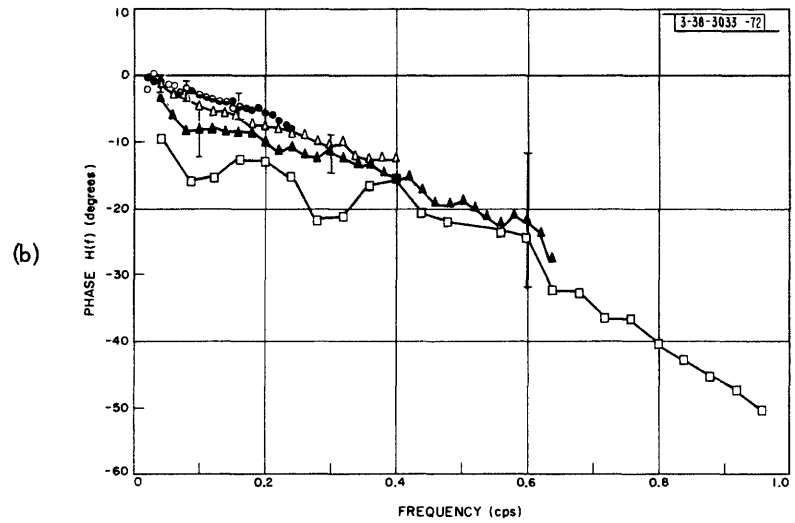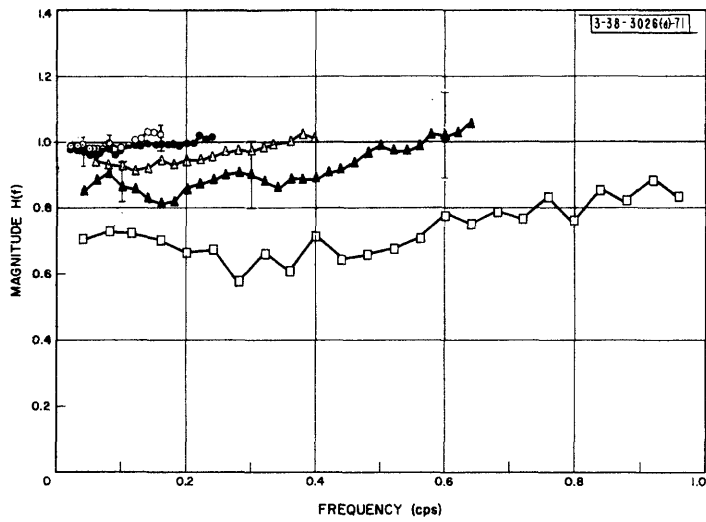
FREQUENCY (cps)

Fig.4-8 (Continued)

47
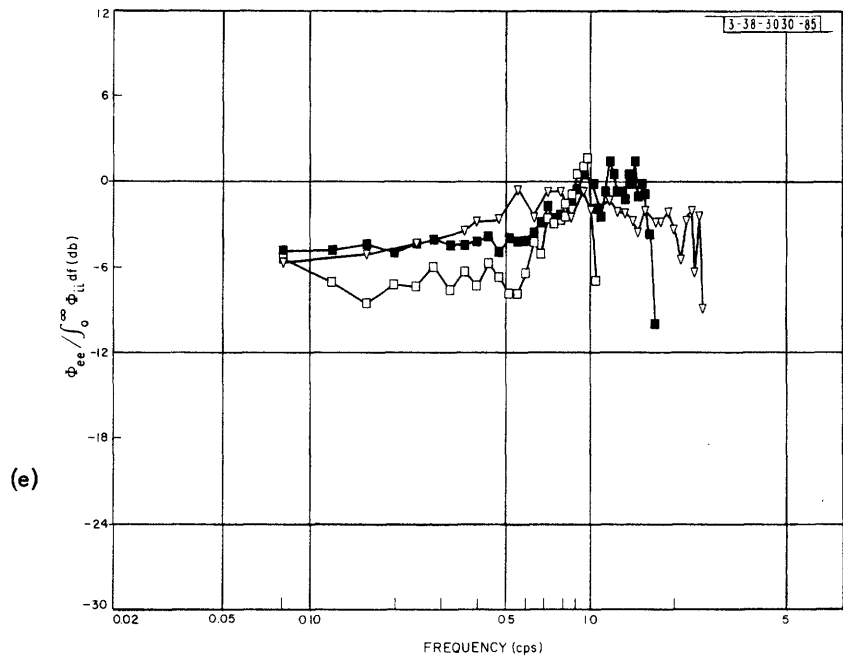
(a)

(b)

(c)

Fig.4-9.   Experiment III, pursuit — mean closed-loop characteristics for Inputs R .16 through R .96.

Fig. 4-9 (Continued)

49

(a)

(b)

(c)

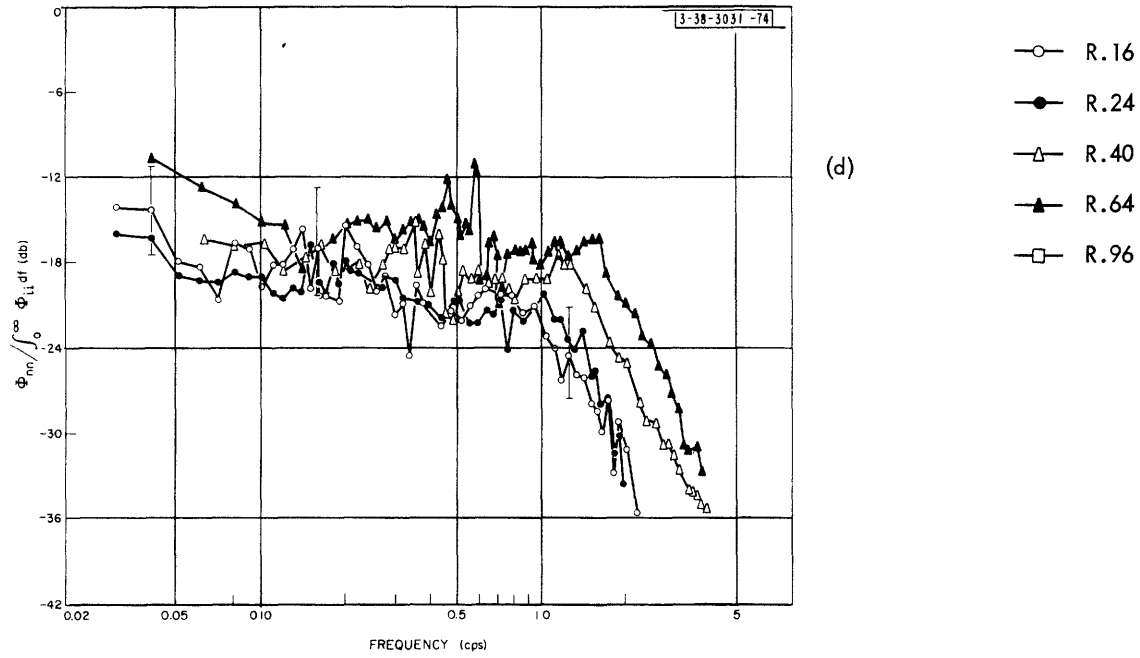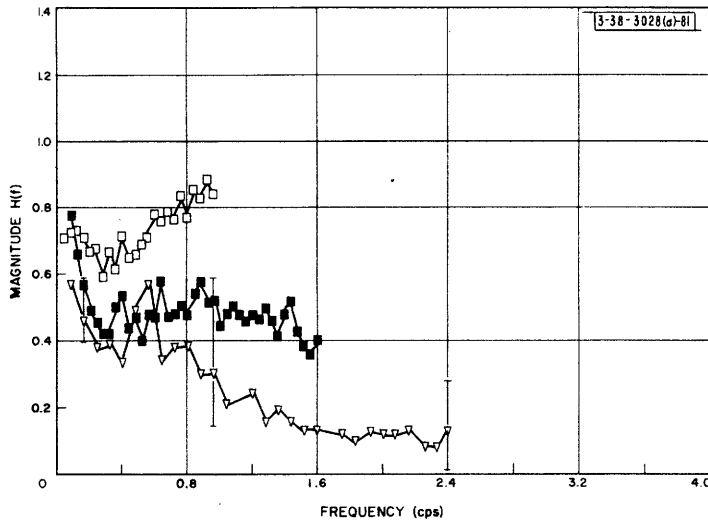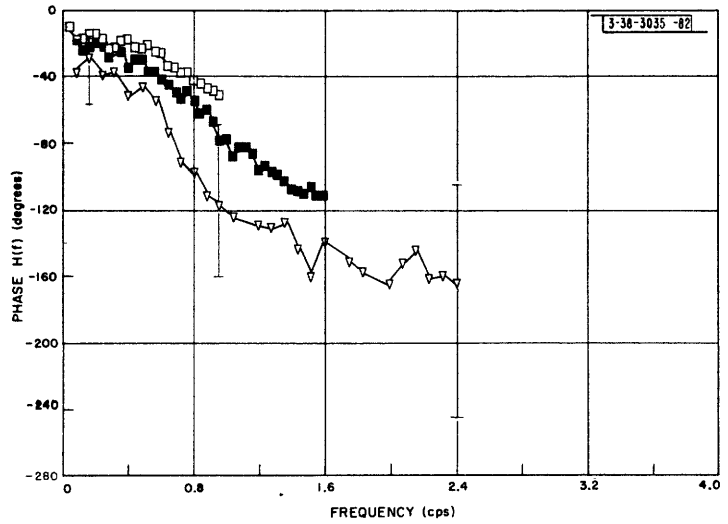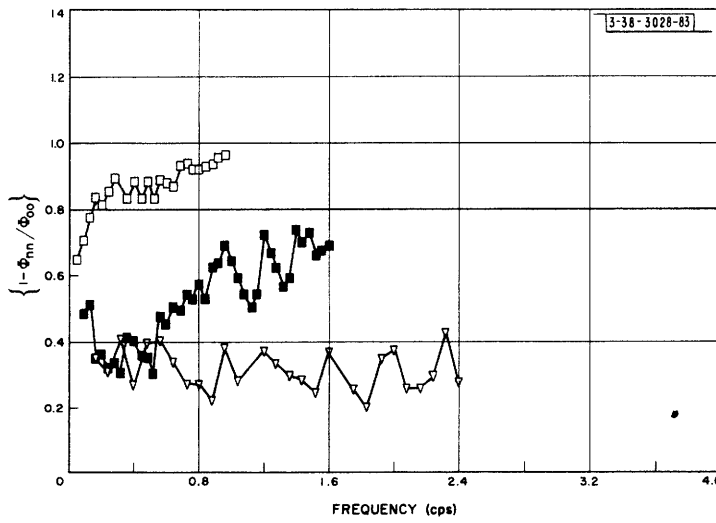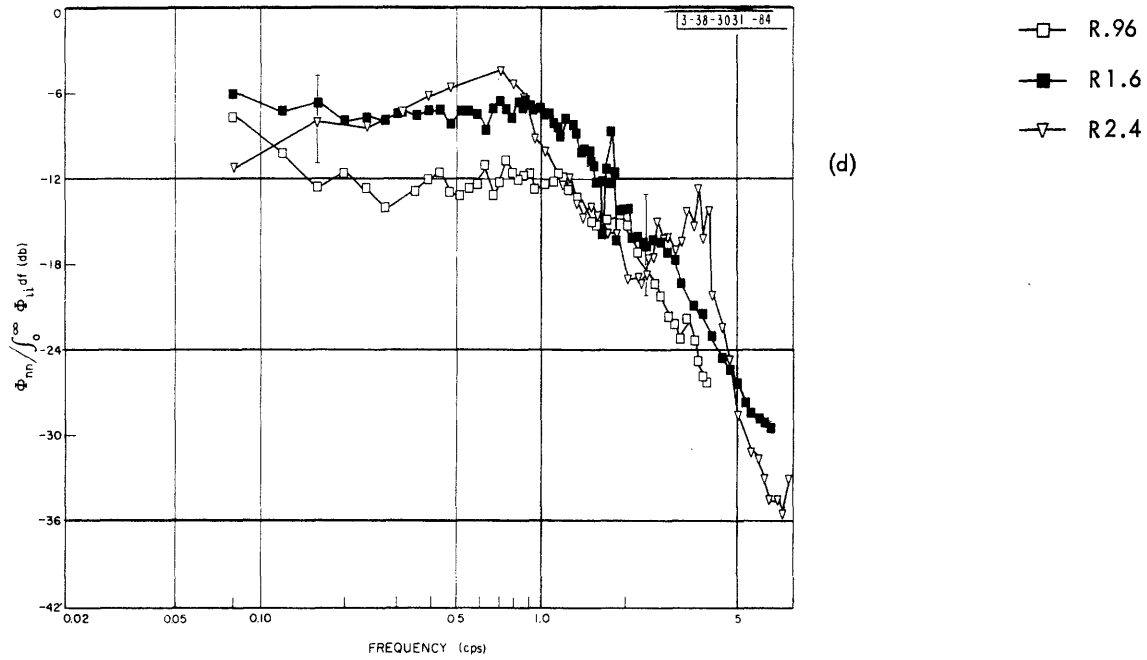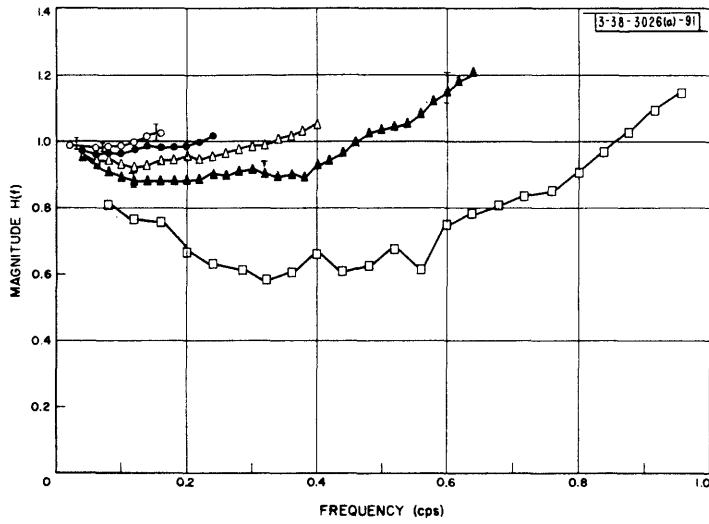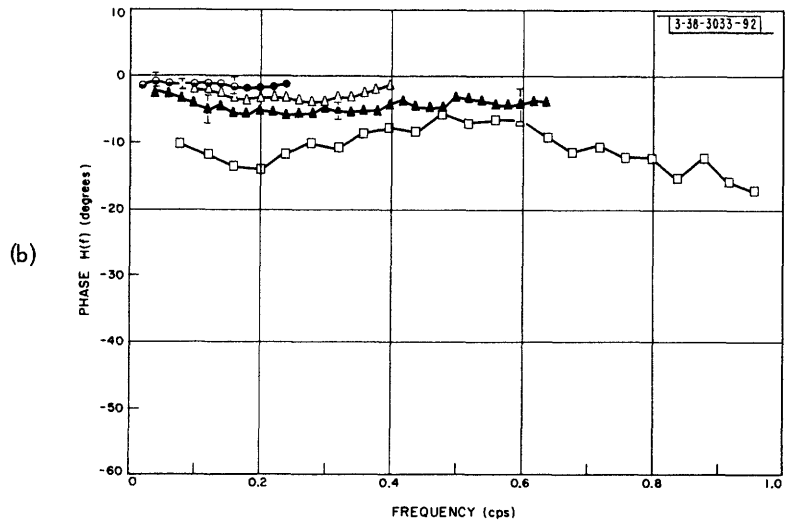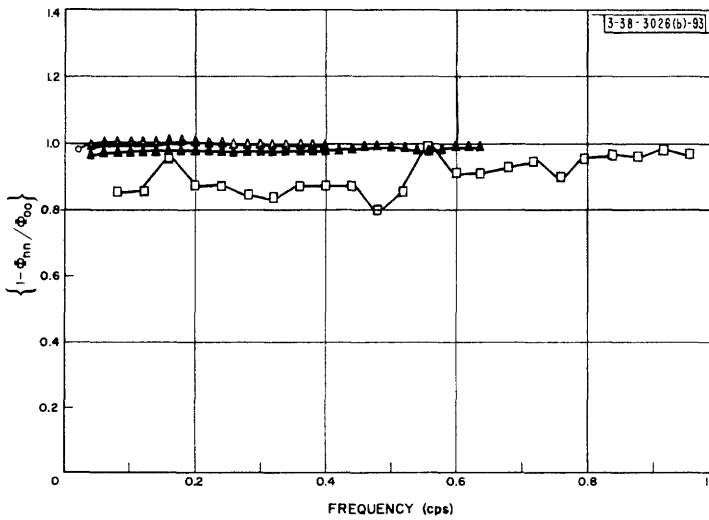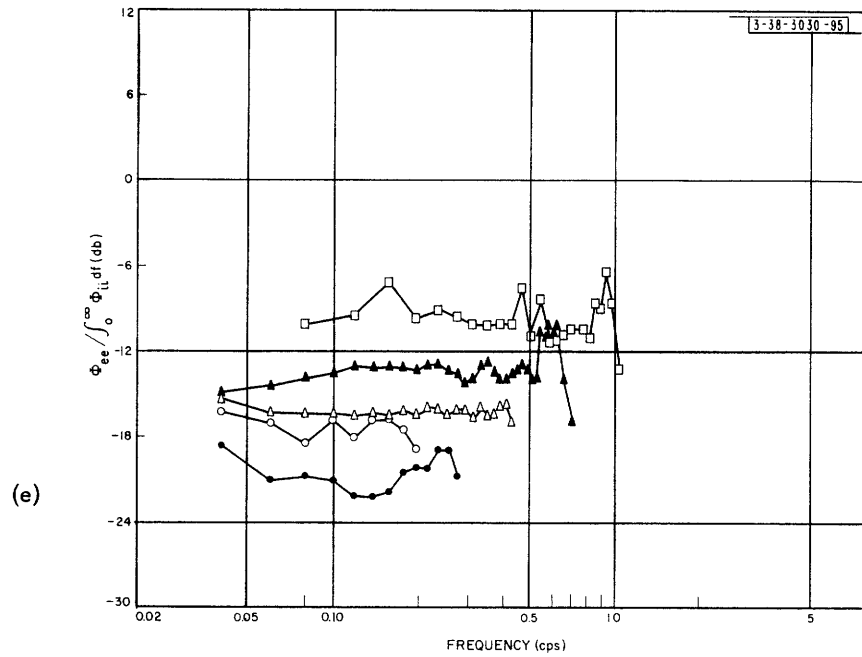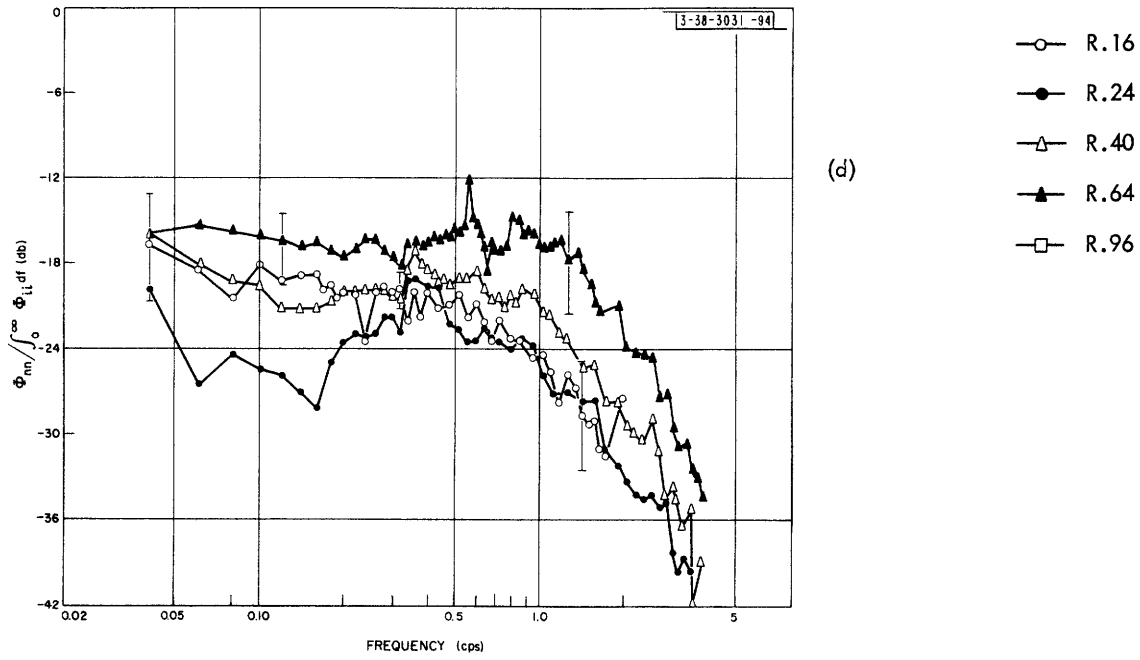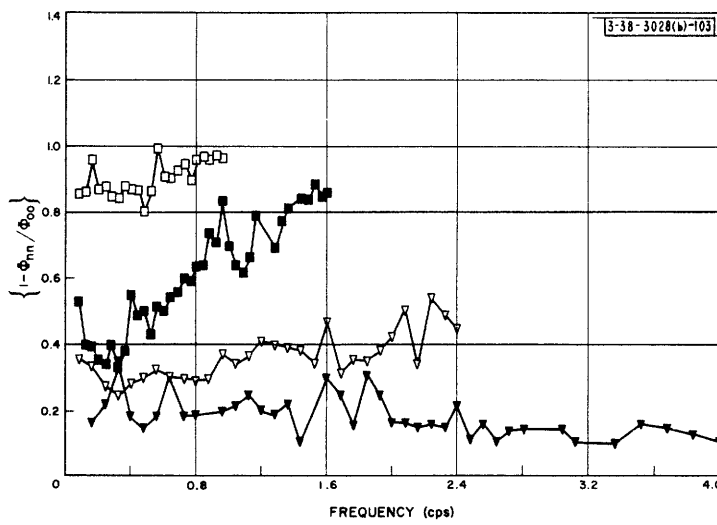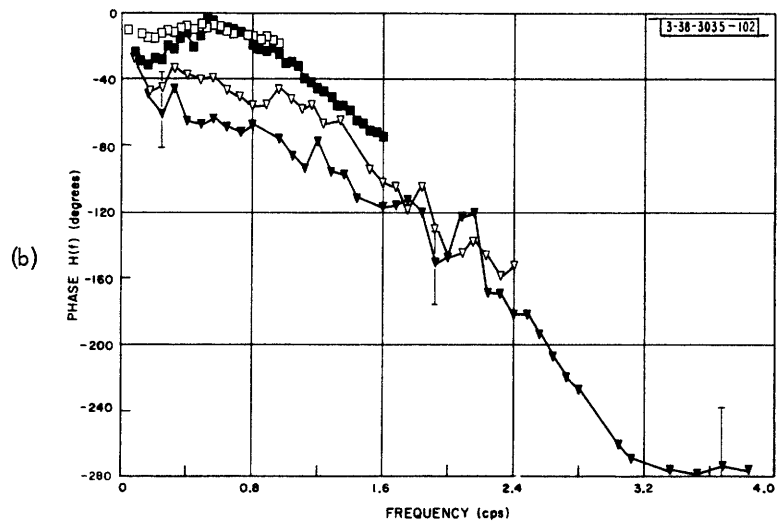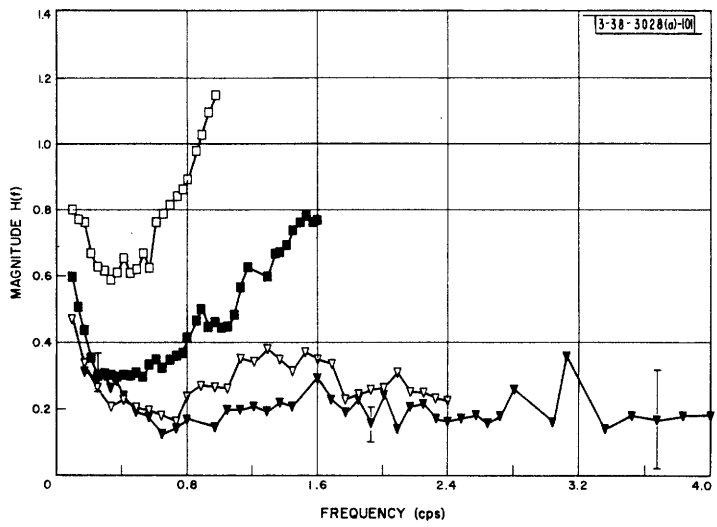Fig.4-10. Experiment III, pursuit — mean closed-loop characteristics for Inputs R .96 through R 4.0.
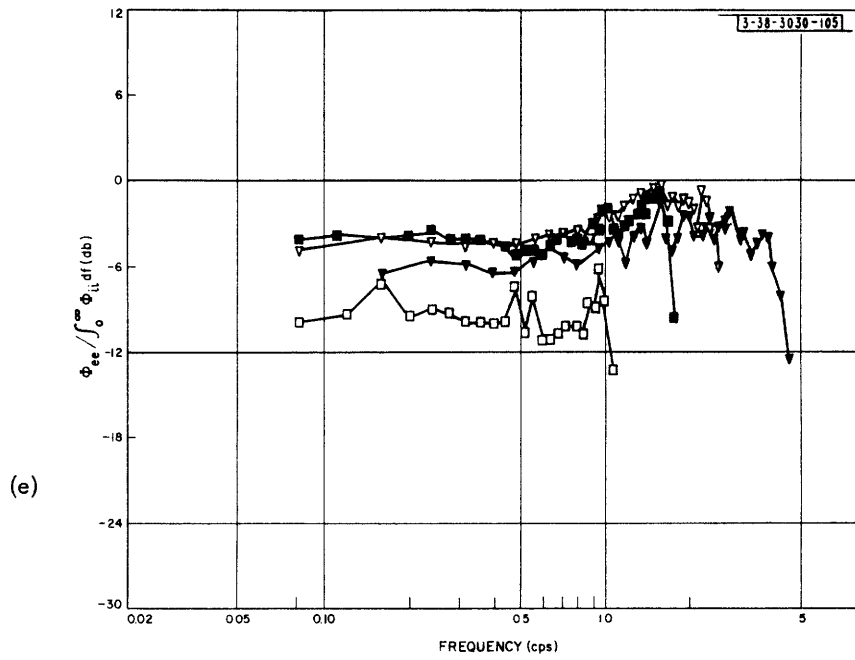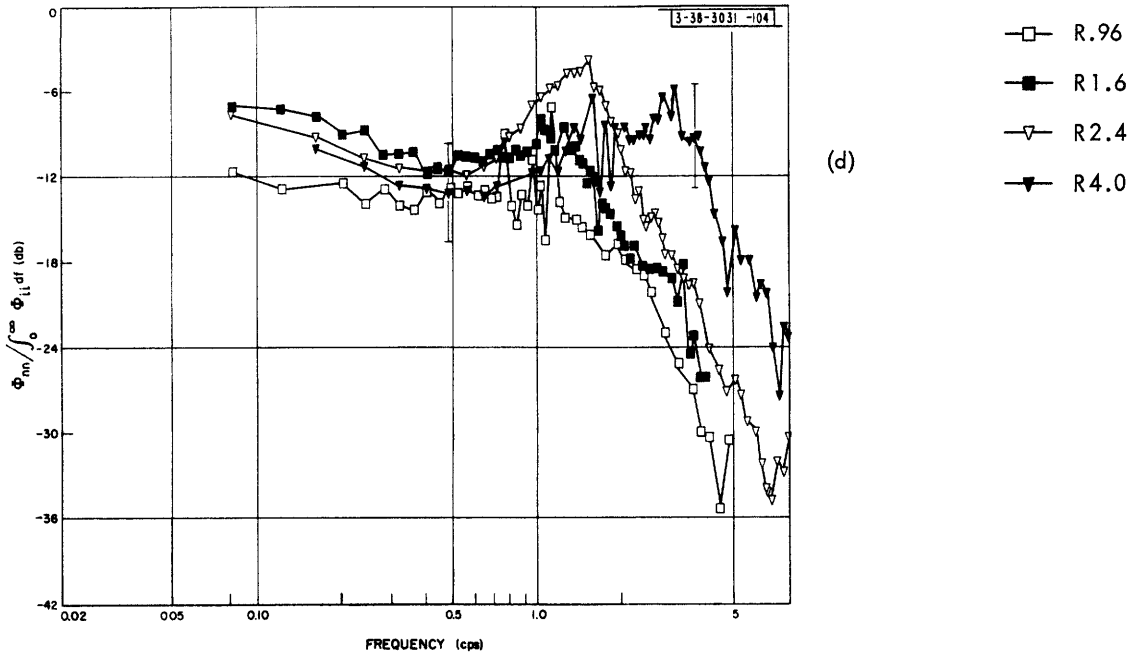
(d)

Legend:
- ☐— R.96
- ■— R1.6
- ▽— R2.4
- ▼— R4.0

(e)

Fig. 4-10 (Continued)

51

estimate the future of the input and to correct for internal delays and lags. With low-bandwidth inputs, the low order derivatives permit good prediction over the entire signal band. With inter-mediate-bandwidth inputs they permit good prediction of only the low-frequency components of the input, and therefore at high frequencies the slope of the phase curve increases. With very high-bandwidth inputs, perhaps the target moves too rapidly for the human operator to obtain good derivative information, and therefore he is not able to achieve good prediction over any of the input band.

4. Noise Power-Density Spectra

The noise power-density spectra obtained with the compensatory system are very similar to the spectra obtained with pursuit. As the input bandwidth increases, the magnitude of the noise spectra usually increases. However, the spectra obtained with very high- and very low-bandwidth inputs do not follow this trend. The magnitude decreases at high bandwidths because the ampli-tude of the human operator's responses is highly attenuated, but it is not clear why the magni-tude of the noise ceases to decrease at very low bandwidths. Perhaps with these signals, which are very easy to track, most of the noise is produced by muscle tremor rather than by variations in tracking characteristics or by system nonlinearities. We would expect that, for slowly moving targets, the amplitude of the tremor would be relatively insensitive to input bandwidth.

The shape of both the compensatory and the pursuit noise spectra corresponds closely to the shape of a quadratic function of frequency. Most of the spectra can be closely approximated by the re-lation

$$\frac{\Phi_{nn}(f)}{\int_0^\infty \Phi_{ii}\, df} = \frac{c_n^2}{\left|\left(\frac{jf}{f_n}\right)^2 + 2\zeta\,\frac{jf}{f_n} + 1\right|^2} \quad , \tag{4-1}$$

where usually the damping factor ζ is about 0.8 or 1.0, and the undamped natural frequency f_n is about 1 or 2 cps. The magnitudes of the pursuit-noise spectra are generally lower than the com-pensatory, and the pursuit damping factors are usually somewhat higher than the compensatory. However, with Inputs R2.4 and R4.0, the pursuit noise exhibits a resonant peak in the neighbor-hood of 2 cps. At frequencies near the peak, the closed-loop phase lag is about 180°, and the human operator may have difficulty in obtaining good feedback information about the accuracy of his responses. The lack of good feedback may be the reason why his responses are more noisy in this region.

Except for Inputs R2.4 and R4.0, none of the compensatory or pursuit noise spectra exhibit res-onant peaks of significant magnitude. Furthermore, there is no evidence of resonance in the noise spectra obtained from single runs (before averaging) with any of the subjects. This result is in disagreement with many statements in the literature that the noise should be highly resonant because the human operator responds intermittently.[3,15] If the human operator is able to obtain sufficient information about his responses, it seems reasonable that he will be able to adjust his characteristics to reduce errors resulting from noise in much the same way that he adjusts his characteristics to minimize errors that are correlated with input signal. Therefore, we should expect the noise to be well damped with simple pursuit and compensatory tracking systems.

UNCLASSIFIED

Although the input bandwidth varies from 0.16 to 4.0 cps, the bandwidth of the noise increases from about 1.0 cps to a maximum of only about 4.0 cps. If the noise resulted mostly from system nonlinearities, and if the nonlinearities have properties that are relatively independent of the input, then we would expect the noise bandwidth to change more nearly in proportion to input bandwidth. Since this is not the case, we must be more inclined to accept the possibility that random variations in human-operator characteristics are a more important source of noise than nonlinearities. In fact, oscillograms of response indicate that, as the tracking task becomes more difficult, the human operator's responses tend to become more erratic and variable. This effect would surely account for the increase in noise power that accompanies an increase in the bandwidth of the input and could account for the relatively small changes in noise bandwidth. However, the likelihood is that both nonlinearities and random variations are important. We do not have sufficient data to determine what fraction of the noise is truly independent of input and what fraction is nonlinearly related to the input.

5. Error Power-Density Spectra

The error power-density spectra are considerably smaller in magnitude with the pursuit system than with the compensatory. The pursuit error spectra are relatively constant over the signal band, whereas the compensatory spectra increase with frequency. These effects are a result of the facts that the phase lags are smaller and less dependent on frequency in the pursuit system than in the compensatory system. Because with increasing bandwidth the magnitude of H(f) decreases and the phase lag increases, the error spectrum also increases in magnitude. For very-high-input bandwidths (R1.6 and R2.4 for compensatory and R2.4 and R4.0 for pursuit), the magnitudes of the error spectra tend to remain constant or even to decrease slightly. Two effects are important causes of this. (1) As bandwidth increases, the error tends to become larger because the human operator's closed-loop phase lag and noise increase. (2) The amplitude of the responses with high bandwidths is low, and most of the error is contributed by the input. As input bandwidth increases, the magnitude of the input power-density spectrum decreases (because mean-square input is constant), and therefore the magnitude of the error spectrum decreases. These two effects oppose each other and explain the observed results.

The anomalous inversion of the error spectra for inputs R.16 and R.24 probably results from the fact that the input power, and therefore the output power, is distributed over a wider bandwidth for R.24 than for R.16, and since H(f) and the noise spectra are about the same in both cases, the error power-density will be lower for R.24 than for R.16.

6. Mean-Square Errors

The magnitudes of the total relative mean-square error and of that part of the error due to noise located outside the signal band are shown in Table 4-VI.

The behavior of the mean-square errors is consistent with that of the error power-density spectra. The pursuit errors are very much smaller than the compensatory. Except at very low and very high bandwidths, the error tends to increase with increasing bandwidth. The fact that the errors for the two lowest bandwidths are nearly equal suggests that at these bandwidths the human operator's tracking accuracy is limited by factors other than target speed, e.g., muscle

53

UNCLASSIFIED

tremor. For these signals, the noise outside the signal band contributes the major fraction of the error, and therefore reduction of error probably could be achieved if the high-frequency noise were removed by filtering. For the very-high-bandwidth inputs, the errors are greater than unity, which means that better tracking, in the mean-square-error sense, could have been achieved if the subjects stopped responding. In the pursuit system, two subjects tried to filter out the high-frequency components and to track only the lows. The errors with this tactic are lower than when the subjects responded normally and attempted to reproduce the waveform. However, the difference between the two types of response characteristics is not great and, even in the filter mode, the error is greater than unity. Hence the subjects were not very effective at filtering the high frequencies.

7. Open-Loop Transfer Function G(f)

Magnitudes and phases of G(f), the open-loop transfer function for the compensatory system, are shown in Figs. 4-11 and 4-12. As would be expected from the behavior of the closed-loop transfer functions, the magnitude of G(f) decreases with increasing input bandwidth. The phase lag, which is roughly linear with frequency, decreases with increasing input bandwidth, whereas the closed-loop phase lag increases with input bandwidth. The closed-loop phase is determined by both the open-loop gain and the open-loop phase. With low-bandwidth inputs, the open-loop gain is high, and therefore the closed-loop phase lag is small. With high-bandwidth inputs, the magnitude of G(f) is low and the closed-loop phase is similar to the open-loop phase.

Note that G(f) does not appear to behave like a pure integration of the form $1/2\pi jf$. The magnitude of G(f) at low frequencies generally does not go to infinity and the phase does not approach 90°. From physical considerations alone, it is clear that the human operator cannot have a term like $1/2\pi jf$ in his transfer function. His visual and muscular systems do not have infinite resolution at zero frequency. The reason for stressing this point is that many models for the human operator proposed in the literature do contain an integration.[3,5,6,25] Strictly speaking, such models are incorrect. Analytic models, which more correctly approximate human-operator characteristics and which describe quantitatively much of the behavior of G(f), are discussed in Sec. V.

D. RESULTS OF EXPERIMENT IV – SHAPE

The mean closed-loop characteristics derived from the tests with the RC Filtered Spectra, obtained by averaging over subjects, are shown in Fig. 4-13 for the compensatory system and in Fig. 4-14 for the pursuit system. The open-loop characteristics of the compensatory system are in Fig. 4-16. The characteristics obtained with the Selected Band Spectra are in Figs. 4-17, 4-18 and 4-19 (closed-loop compensatory), Figs. 4-20, 4-21 and 4-22 (closed-loop pursuit), and Figs. 4-23, 4-24 and 4-25 (open-loop compensatory).

1. Results with RC Filtered Spectra

Consider first the results obtained with the set of RC Filtered Spectra. The closed-loop characteristics of the compensatory system are similar to those of the pursuit system. As the slope of the high-frequency portion of the input spectrum increases, the magnitude of H(f) and the

correlation increase, while the phase lag, the magnitude of the error, and the magnitude of the noise spectra all decrease. However, the pursuit phase lags and error spectra are generally smaller in magnitude than the compensatory. In neither system are resonant peaks observed in the noise spectra. These results agree with those obtained in Experiment III, in which the input signals had Rectangular Spectra.

The characteristics obtained with Input F3 (three RC filters with break frequency of 0.24 cps) are nearly equivalent to those obtained with Input F4 (Rectangular Spectrum with cutoff frequency of 0.24 cps). The spectrum of F3 is considerably attenuated in the neighborhood of 0.24 cps, and the attenuation increases rapidly at higher frequencies. Apparently, the presence of even small amounts of high-frequency power compensates for the attenuation near and below the break frequency (0.24 cps). In terms of the system characteristics produced, it appears that at least an 18 db per octave attenuation rate is required before an RC Filtered Spectrum will be equivalent to a Rectangular Spectrum.

Input F1 has the appearance of a low-frequency random signal on which a high-frequency noise has been superimposed. In the pursuit tests, one of the subjects felt that his tracking performance would be improved if he tracked only the low-frequency components of F1 and filtered out the high frequencies. This subject also tracked F1 in the normal way in which he tried to follow or reproduce all the target motion. The characteristics resulting from the two modes are shown in Fig. 4-15. The mean-square tracking error (Table 4-VI) for the normal (follow) mode is 0.609, and the mean-square error for the filter mode is 0.603. The effects of the filtering action are apparent in the magnitude of H(f) and in the phase of H(f). By filtering the highs, the human operator is able to maintain somewhat greater gain at low frequencies at the expense of greater phase lag. However, he does not alter his tracking error appreciably.

In most respects, the open-loop characteristics G(f) for the RC Filtered Inputs are similar to those obtained with the Rectangular Spectra of Experiment III. The gain and the phase lag increase as the input signal becomes easier to track. Note the way in which the human operator adjusts his phase margin as the high-frequency content of the input is reduced. For Input F1, which has considerable power at high frequencies, the phase margin is about 70°. For Input F3, the phase margin is only 35° and the closed-loop characteristics are more resonant. Smaller phase margin permits the operator to have higher gain and therefore better low-frequency tracking performance. In terms of over-all system performance, these changes in phase margin and gain make sense and illustrate the human operator's ability to match his characteristics to those of the input.

2. Results with Selected Band Spectra

In the first group of Selected Band Inputs (Figs. 4-17 and 4-20) are two Rectangular Spectra — B1 (cutoff of 0.96 cps) and B4 (cutoff of 1.44 cps) — a band-reject spectrum B2 (no power in the center band of frequencies), and a bandpass spectrum B3 (no power in the lowest band). The characteristics obtained with inputs B2 and B3 more closely correspond to those obtained with B4 than with B1. Except for the phase of B3, the characteristics of both B2 and B3 are approximately the same or somewhat inferior to those of B4. The human operator's characteristics,

particularly the magnitude of H(f) and the correlation, appear to be determined more by the high-frequency components of the input signal than by the total bandwidth or predictability of the signal. Note that the presence of the high frequencies degrades the characteristics, even at low frequencies.

The results obtained with the second group of signals, B4 through B7 (Figs. 4-18 and 4-21), illustrate in another way the influence of high-frequency components on the response characteristics. As the power in the two highest frequency bands is reduced, H(f) increases in magnitude at all frequencies, and the correlation increases sharply in the lowest band of input frequencies. The phase lag at low frequency decreases, but the high-frequency phase lag increases somewhat. The characteristics obtained with Input B6 (high-frequency power down 20 db) are nearly equivalent to those obtained with B7 (no power in the two highest bands). It therefore appears that high-frequency components of the input must be attenuated by at least 20 db before they will cease to have a significant effect on the system characteristics at low frequencies.

The results obtained with the group of bandpass signals, B7 through B10 (Figs. 4-19 and 4-22), illustrate the human operator's ability to take advantage of the predictability of the input in order to improve system performance. Bandpass random signals closely resemble a carrier modulated in amplitude and in phase by random noise. With the pursuit system, the human operator sees the input signal and is able to keep his response closely synchronized with it. The phase lags at the mid-band frequencies are very nearly zero for the three bandpass inputs. At frequencies below the mid-frequency, the response leads the input, and at high frequencies it lags the input. With the compensatory system, the human operator does not have good information about the input and cannot achieve the same degree of phase correction.

The superior phase characteristics of the pursuit system are accompanied by greater closed-loop gain and with higher correlation than were obtained with the compensatory system. However, with both systems, the magnitudes of H(f) and correlations are approximately equal to those obtained with rectangular spectra having cutoff frequencies equal to the high cutoff of the bandpass spectra. Compare the results of Inputs B8 and B9 with those of B1 and B4.

The noise power spectra for Inputs B9 and B10 are peaked in the bandpass region perhaps because much of the noise results from phase or frequency modulation of the responses. None of the other noise spectra have resonant peaks.

The compensatory open-loop characteristics (Figs. 4-23, 4-24 and 4-25) for the Selected Band Inputs are similar to those obtained for Rectangular and RC Filtered Spectra. In particular, note that the phase margin obtained with B4, B5 and B6 decreases as power at high frequencies decreases. The open-loop transfer functions for the bandpass signals (B3, B8, B9 and B10) were translated down the frequency scale so that the lowest frequency of those inputs corresponded to the origin on the new frequency scale. The translated transfer functions are somewhat similar to those associated with normal low-pass inputs. When confronted with a bandpass input, to a certain extent, the human operator appears to be able to shift his low-pass characteristics up the frequency scale like a single-sideband modulator. When he makes these transitions, however, his gain is reduced and his phase lag is considerably increased. For B10, G(f) appears to have

the amplitude characteristics of a high-pass filter instead of the usual low-pass characteristics. The reason for this is not clear from the data.

E. SUMMARY OF EXPERIMENTAL RESULTS

The characteristics of compensatory and pursuit systems are invariant to changes of human operator and to repeated runs with the same operator, at least for inputs having a bandwidth less than 0.64 cps. The characteristics of compensatory systems are also invariant to input amplitude changes over a range extending at least from 0.1 inch to 1.0 inch rms. The linear amplitude range for pursuit systems is at least from 0.3 inch to 1.0 inch. Although measurements could not be made with rms amplitudes greater than 1.0 inch, we would expect that the upper limit of the linear amplitude range can be extended for both systems.

For inputs having most of their power concentrated at frequencies below 0.64 cps, the fraction of the output power that is linearly correlated with the input is greater than 0.97, and therefore the quasi-linear transfer function H(f) provides a good description of the system characteristics. For higher-frequency inputs, the correlation is much lower, but there are indications that a large fraction of the noise may result from random variations in characteristics rather than from non-linearities. If this is the case, the transfer function together with the noise power-density spectrum Φ_{nn} (f) provide a good description of the actual characteristics of the system.

In the pursuit system, the human operator can see the target motion and can estimate its future in order to correct his inherent lags and delays. The pursuit phase lag is therefore very much less than the compensatory. Superior phase response results in error spectra and mean-square errors that are considerably smaller for the pursuit than for the compensatory system. Knowledge of the input is a particular advantage with high-bandwidth inputs and with inputs having band-pass spectra.

The results clearly show that the human operator is very nonlinear with respect to changes in the input spectrum. Increasing the bandwidth of the input degrades the quality of system characteristics at all frequencies. Even the presence of small-amplitude, high-frequency components adversely affects the low-frequency characteristics. The human operator can, however, take advantage of the predictability of the input to improve system performance, provided sufficient information is presented to him. This nonlinear behavior results from the human operator's ability to adapt to new situations, and represents the greatest advantage that manual systems have over automatic systems.
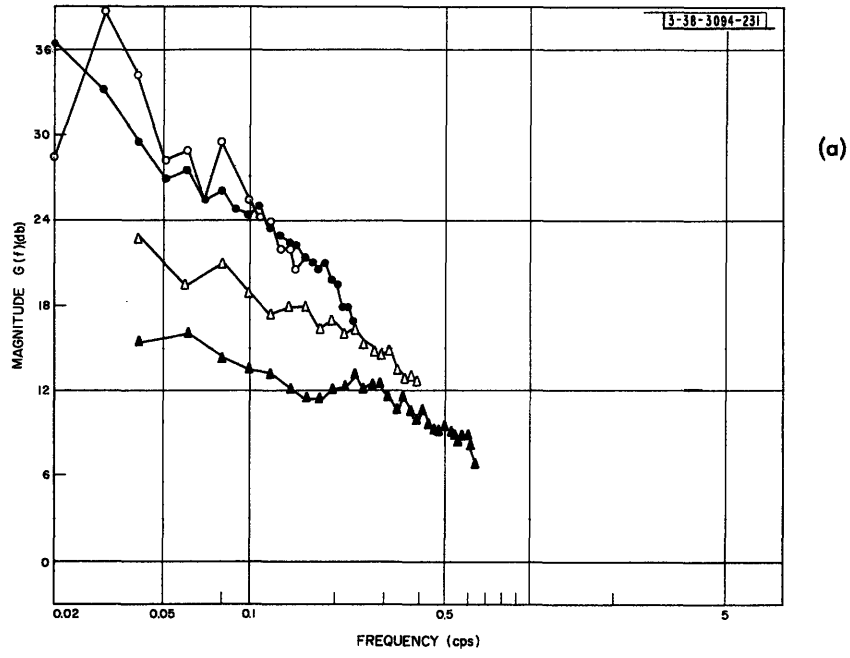
Fig.4-11. Experiment III, compensatory — mean open-loop characteristics for Inputs R.16 through R.96.
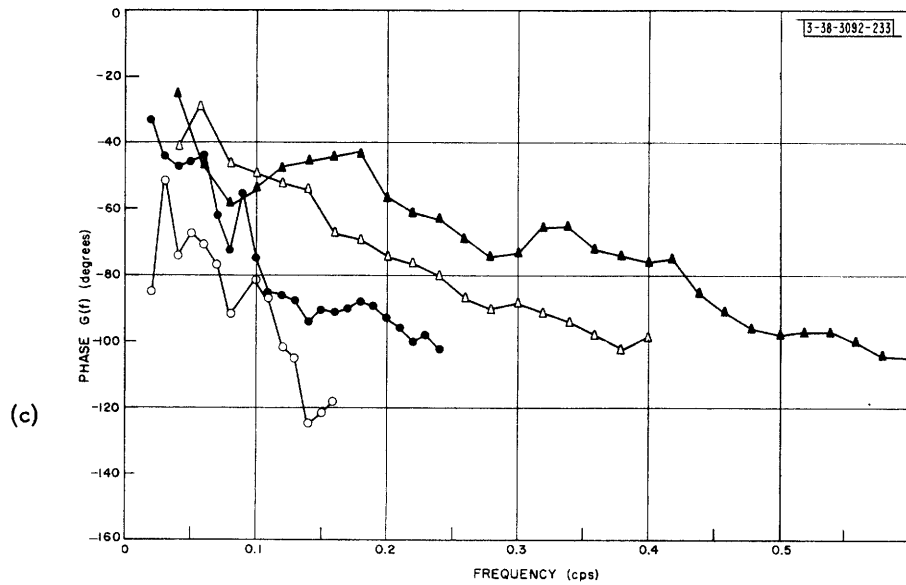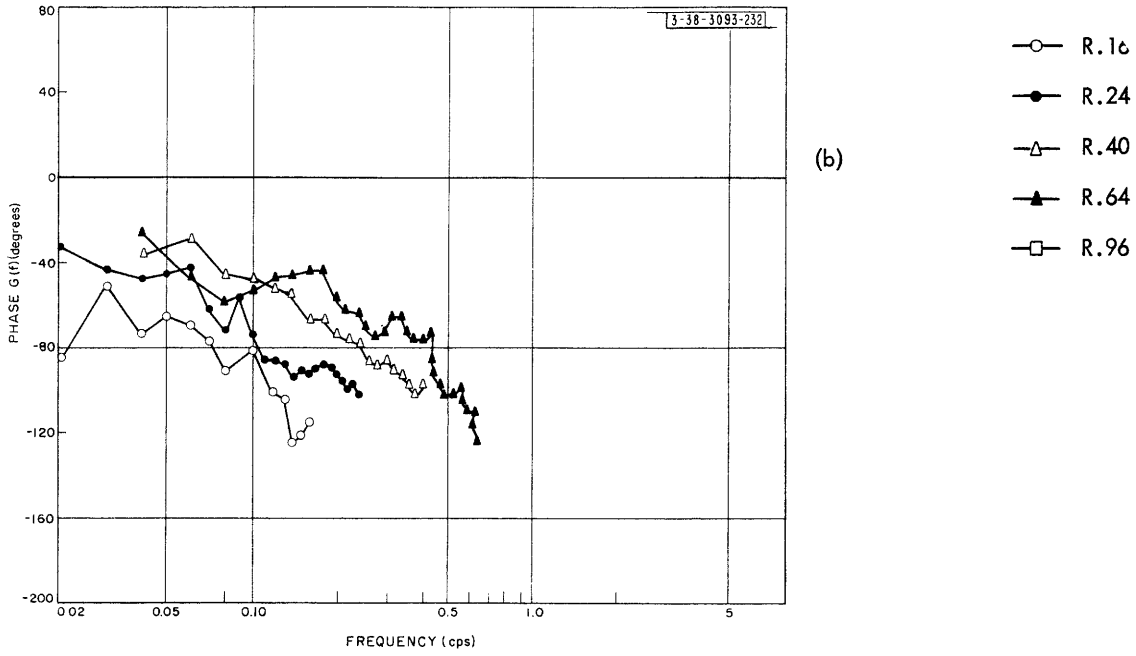
(b)

(c)

Fig.4-11 (Continued)

59
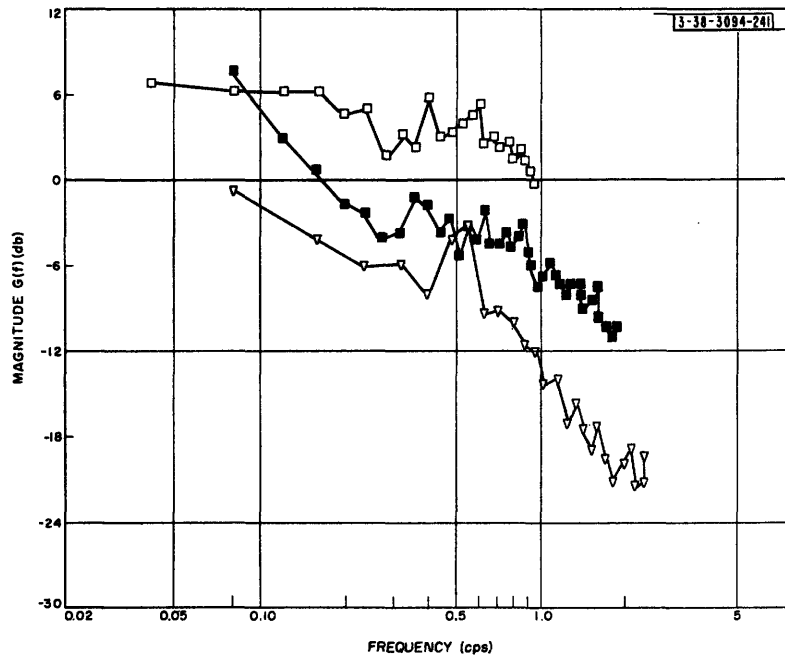
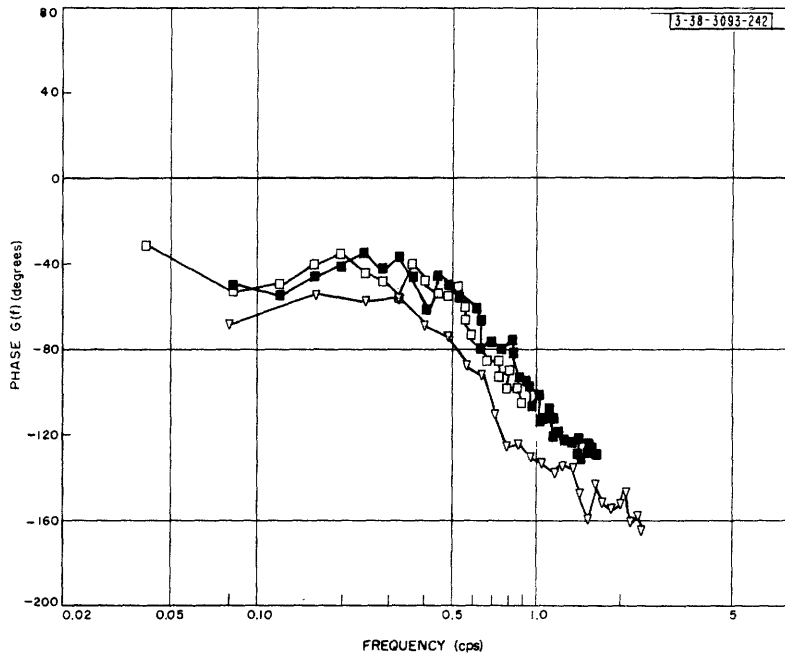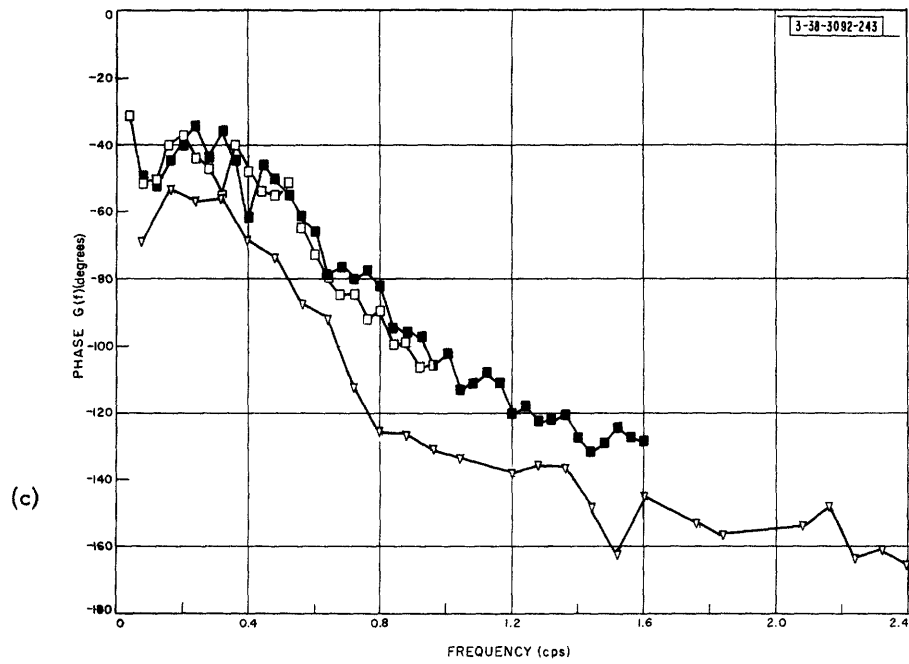Fig.4-12. Experiment III, compensatory — mean open-loop characteristics for Inputs R.96 through R.2.4.

Fig. 4-12 (Continued)

61

Fig.4-13. Experiment IV, compensatory — mean closed-loop characteristics for RC Filtered Inputs.

62

(d)

(e)

Fig. 4-13 (Continued)

63

(a)

(b)

(c)
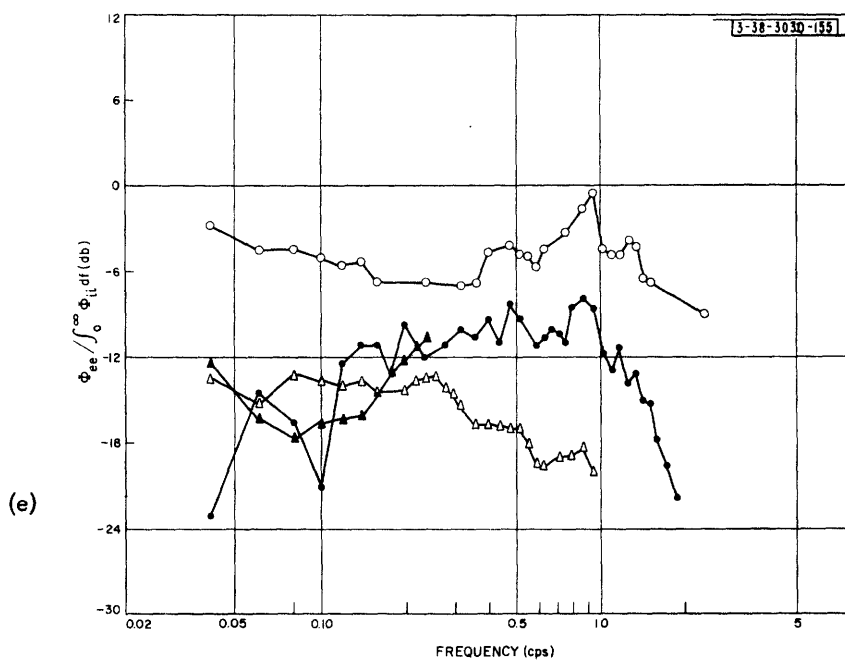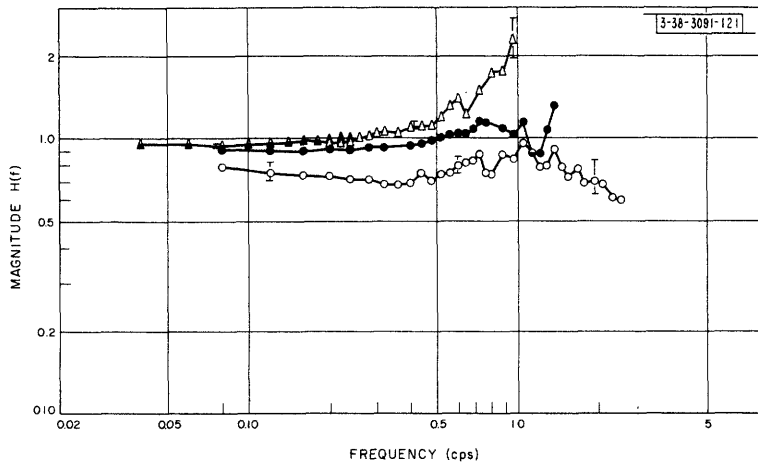
Fig. 4-14. Experiment IV, pursuit —
mean closed-loop characteristics for
RC Filtered Inputs.

64

(d)

Legend:
- —O— F 1
- —●— F 2
- —△— F 3
- —▲— F 4

(e)

Fig.4-14 (Continued)

65
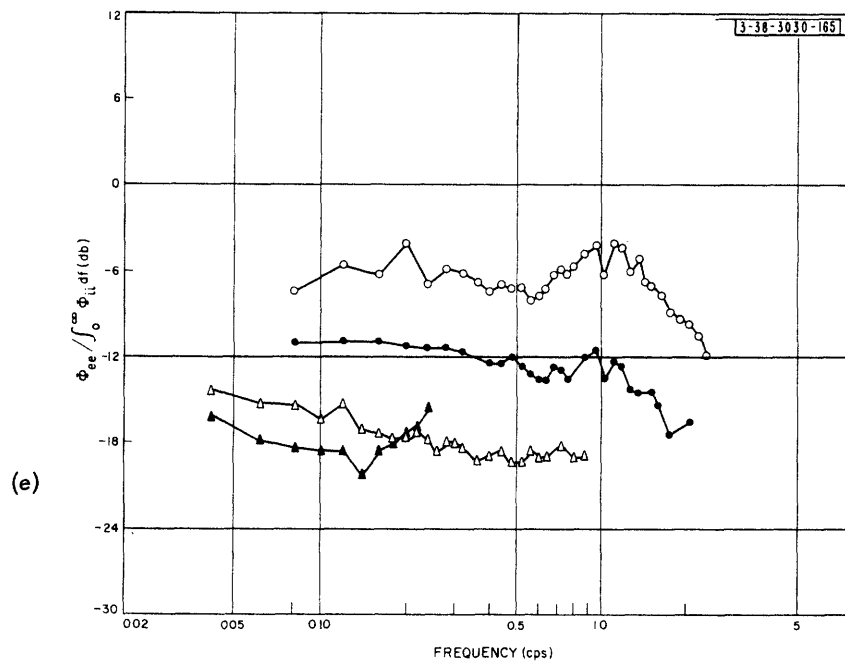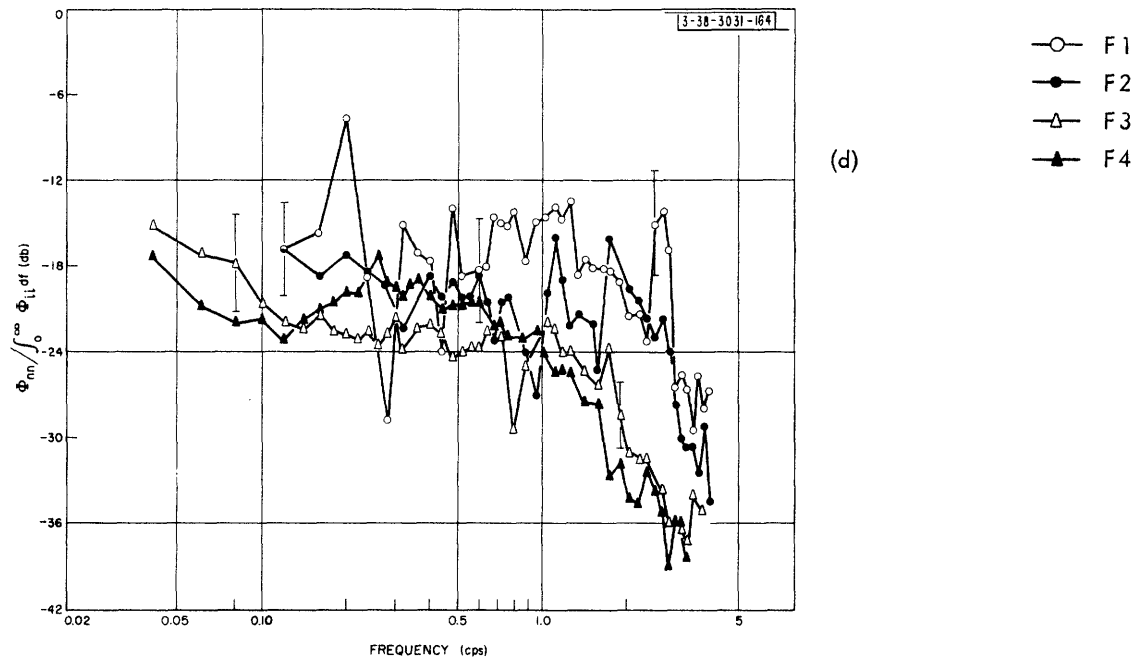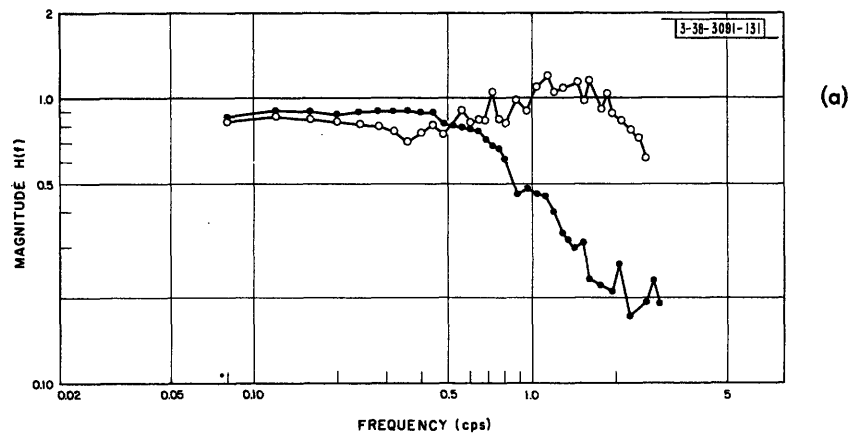
Fig.4-15. Experiment IV, pursuit — mean closed-loop characteristics obtained with Input F1 for one subject operating in the normal mode and in the filter mode.
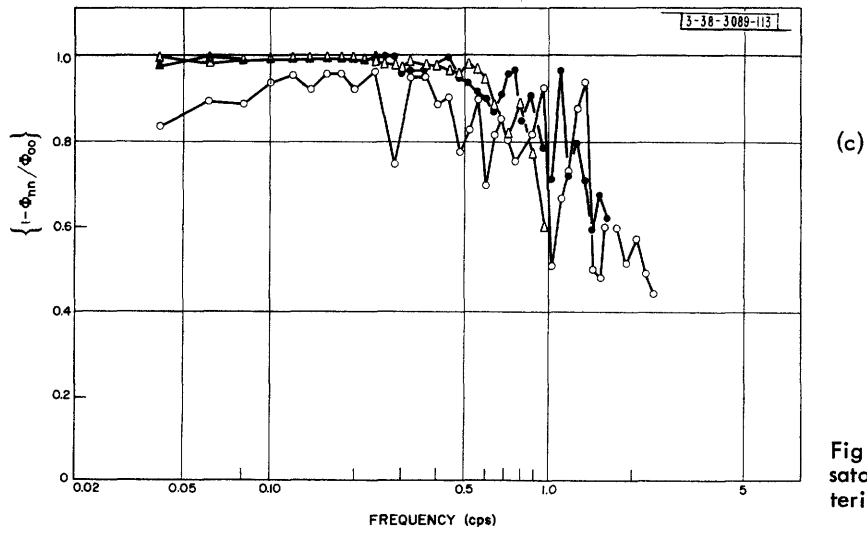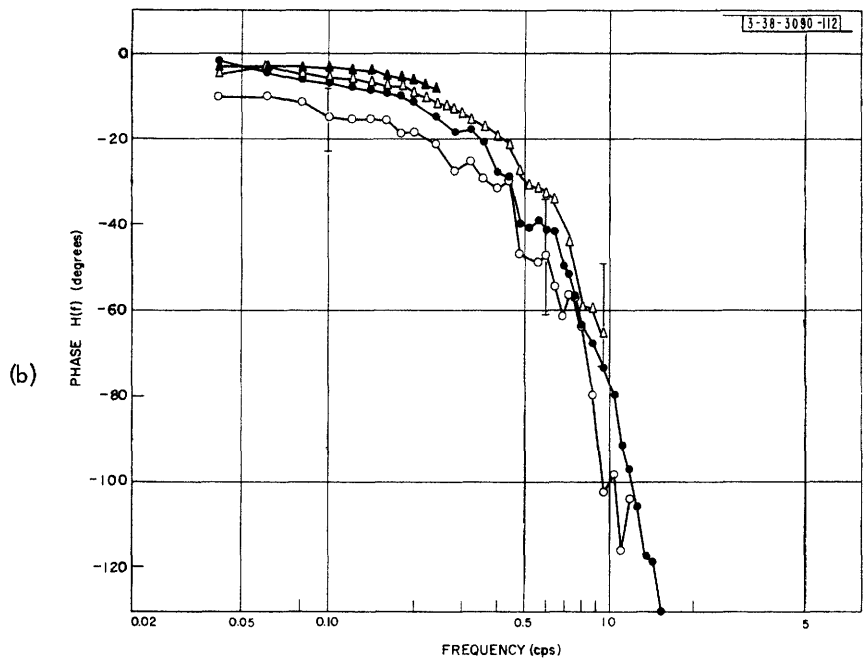
(b)
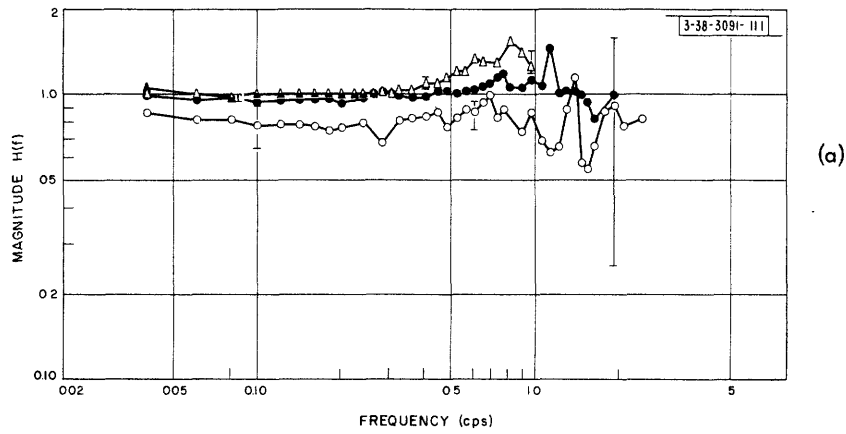
(c)

Fig.4-15 (Continued)

67
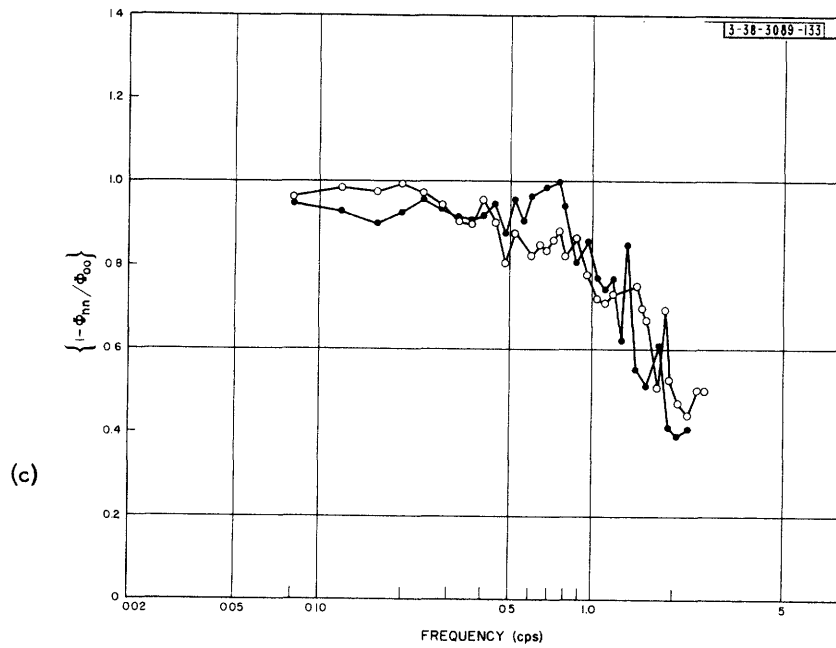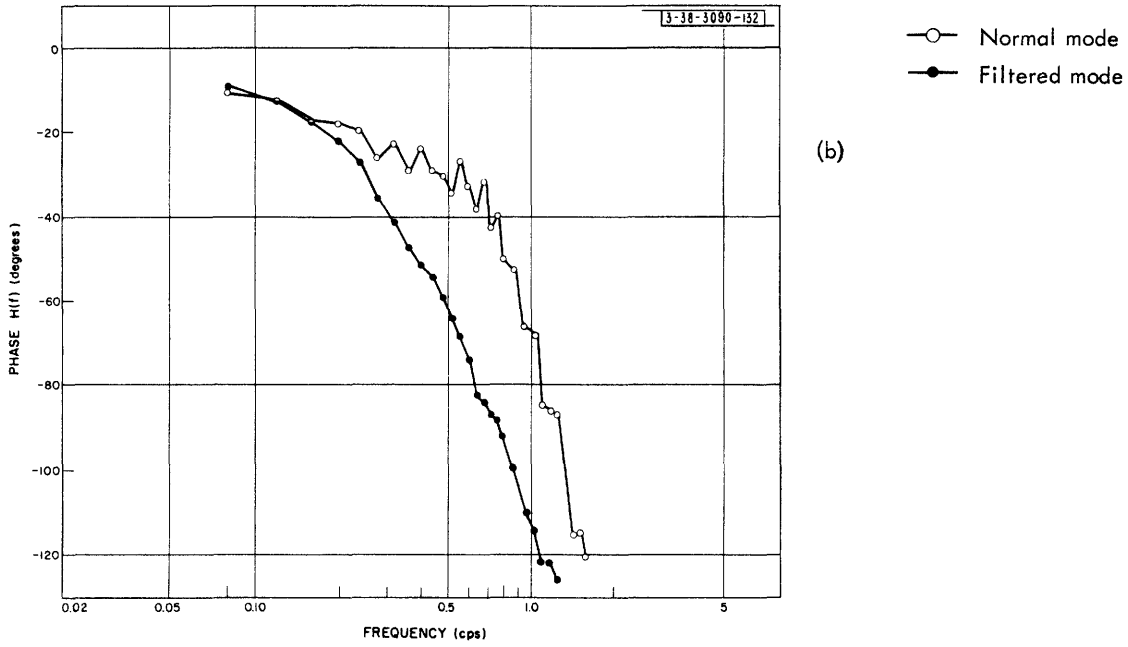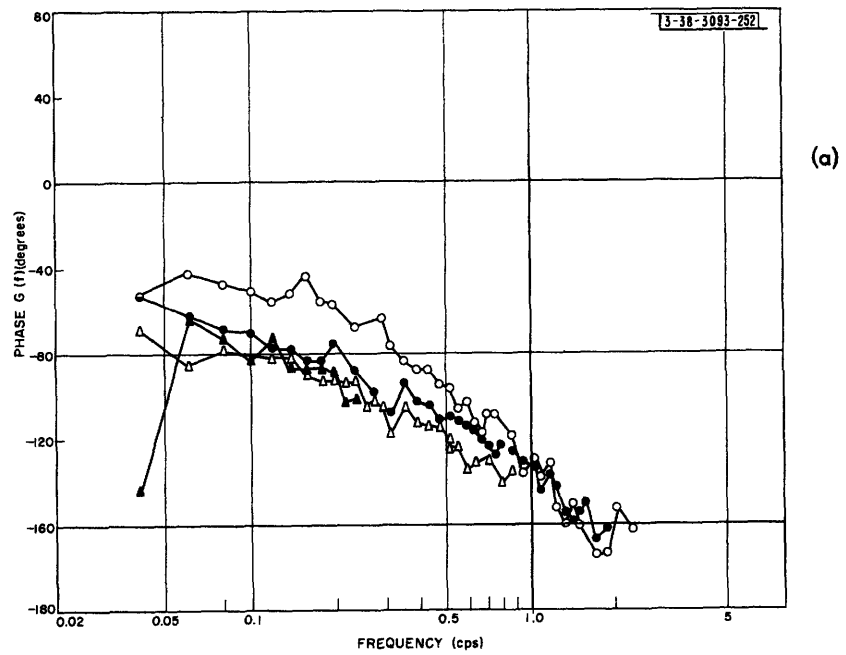
Fig.4-16. Experiment IV, compensatory — mean open-loop characteristics for RC Filtered Inputs.
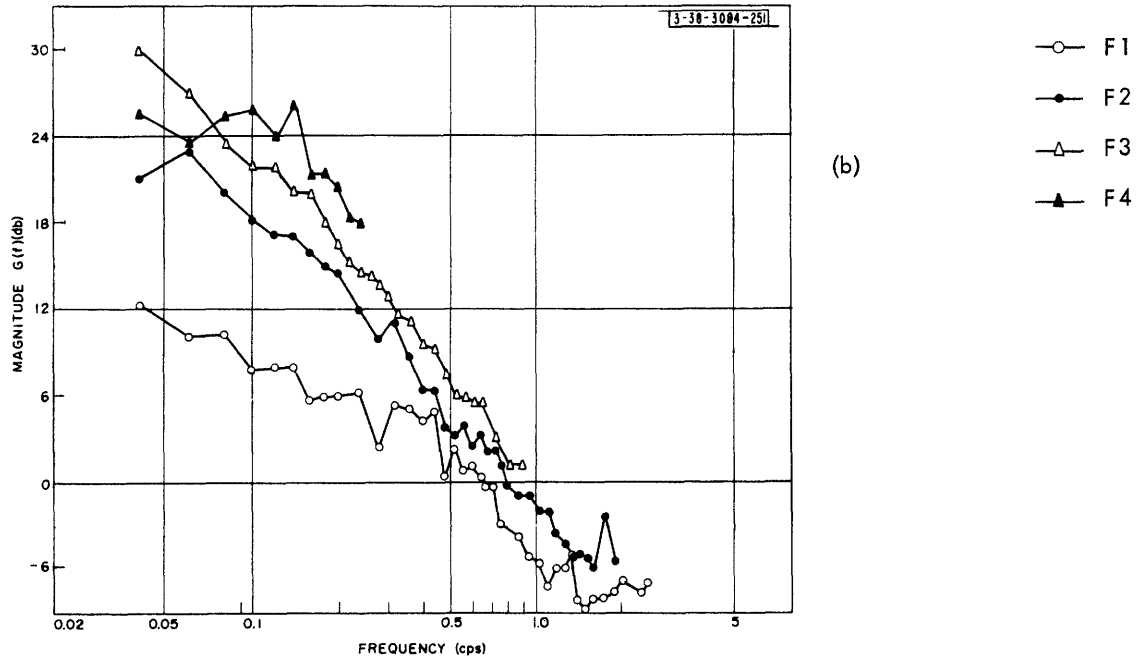
(b)
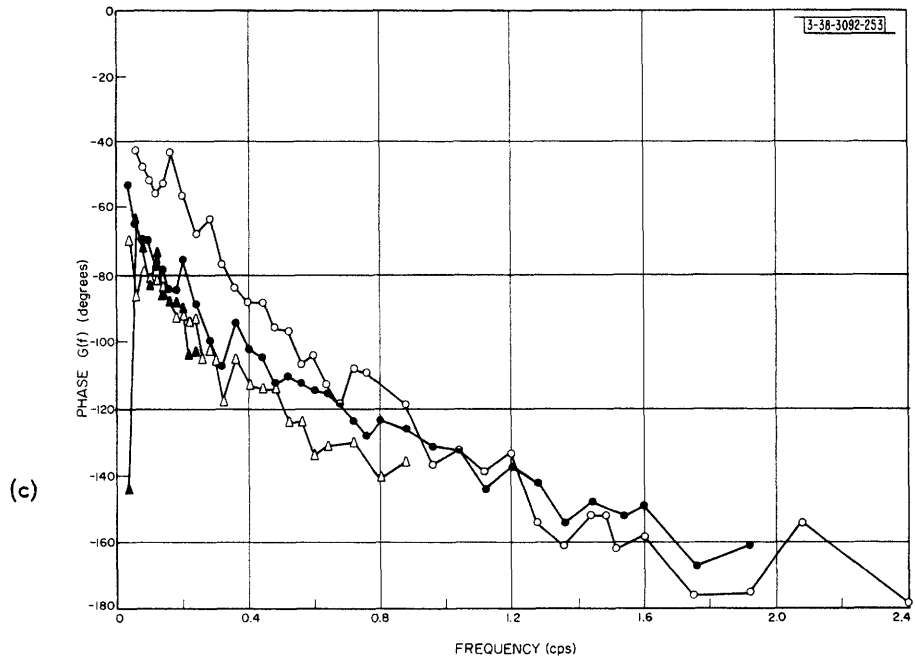
(c)

Fig.4-16 (Continued)
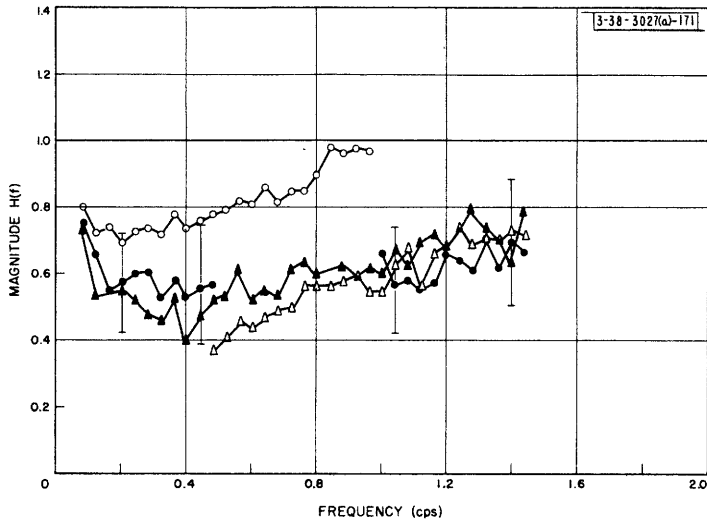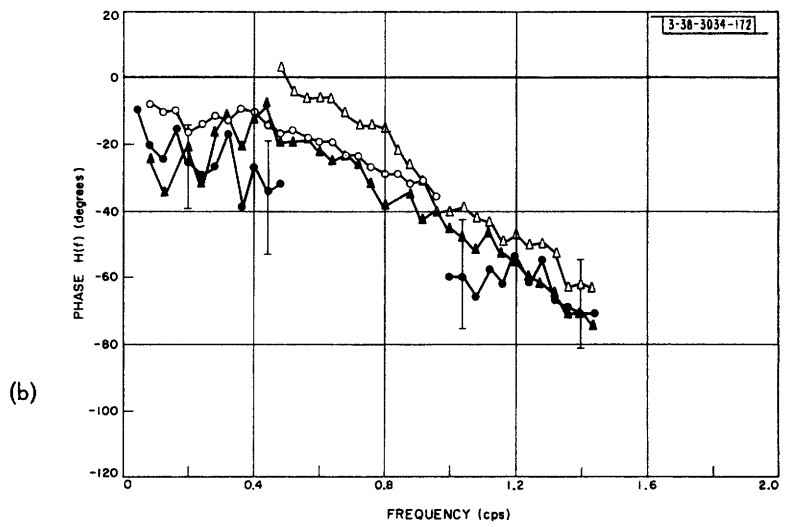
Fig.4-17. Experiment IV, compensatory — mean closed-loop characteristics for Selected Band Inputs B 1 through B 4.

(c)

Legend:
- B 1 (open circle)
- B 2 (filled circle)
- B 3 (open triangle)
- B 4 (filled triangle)

(d)
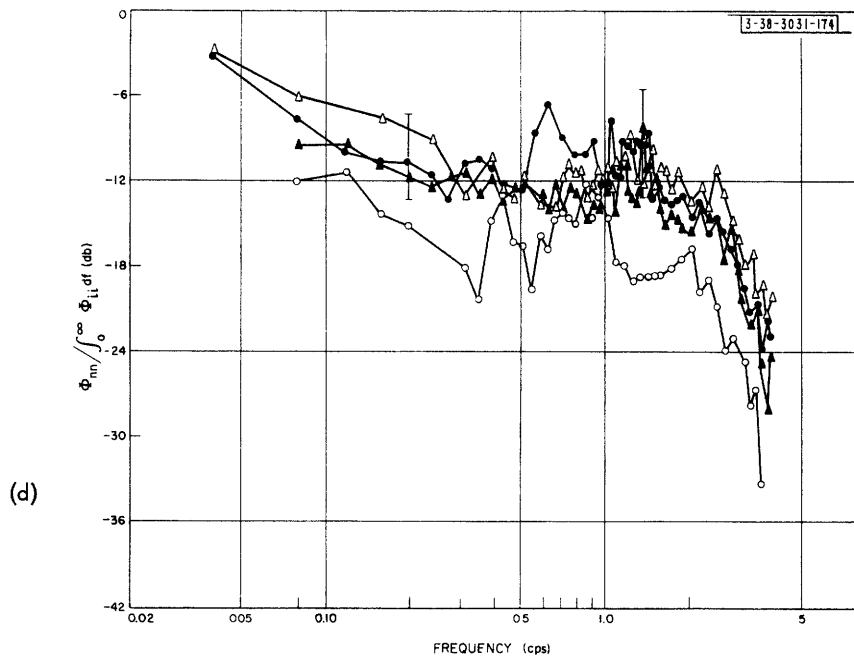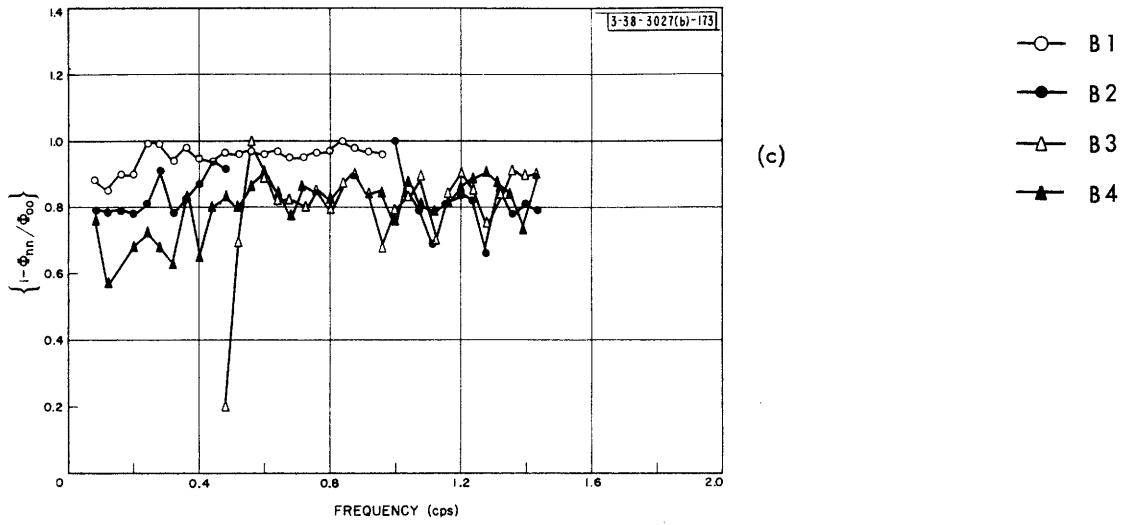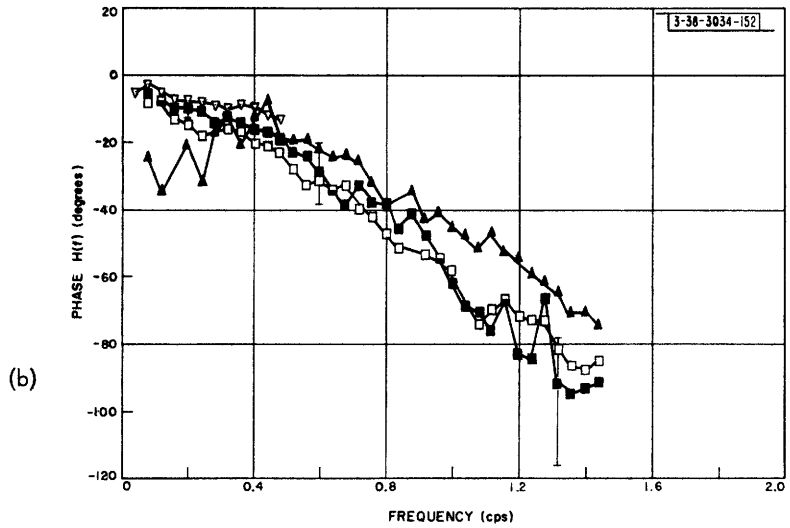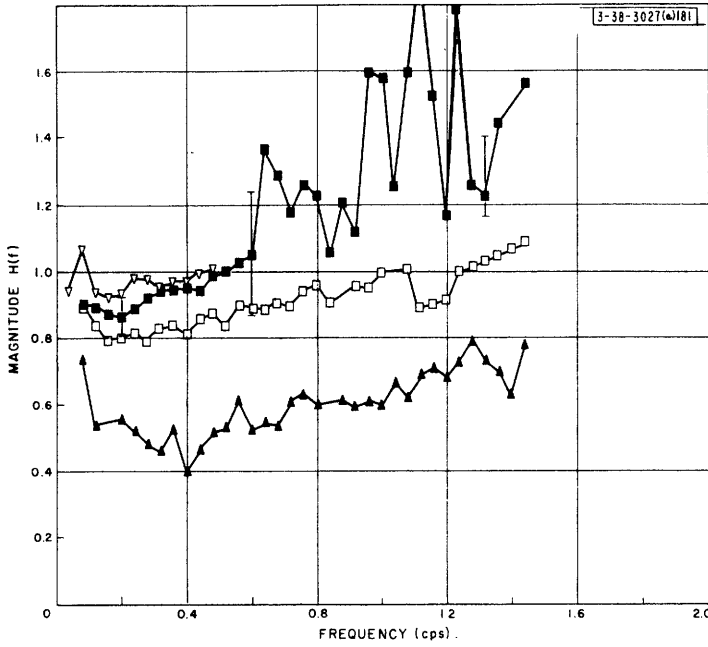
Fig. 4-17 (Continued)

Fig.4-18. Experiment IV, compensatory — mean closed-loop characteristics for Selected Band Inputs B 4 through B 7.

(c)

B 4
B 5
B 6
B 7

(d)

Fig.4-18 (Continued)

73
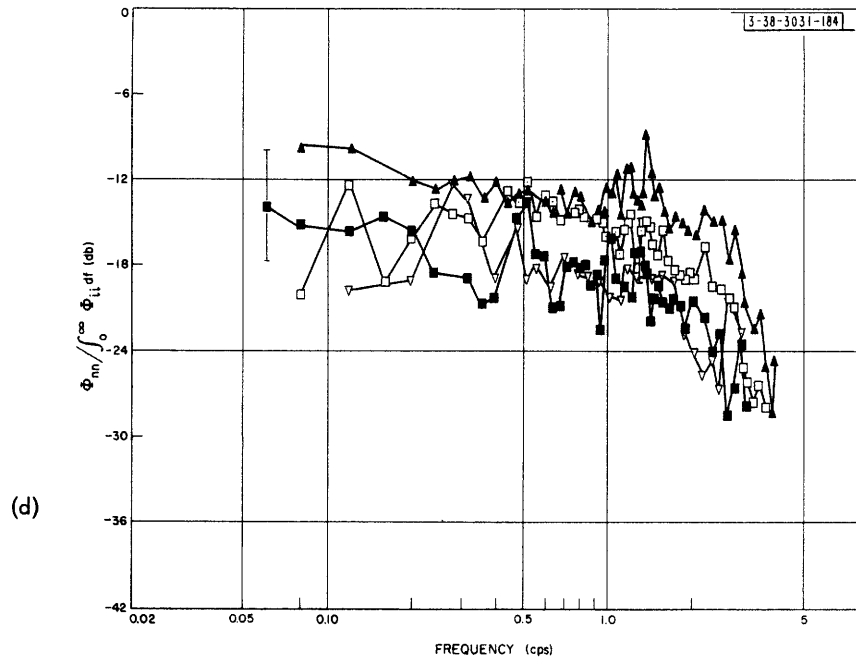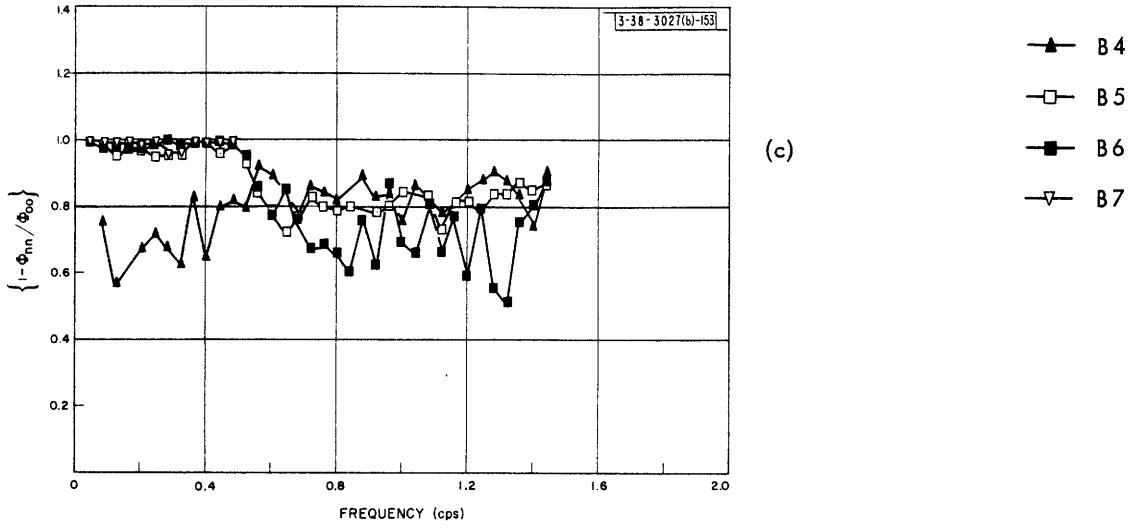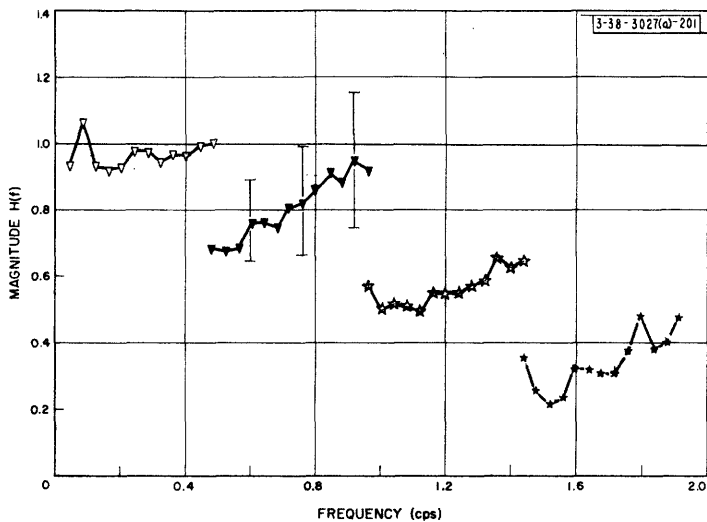
(a)
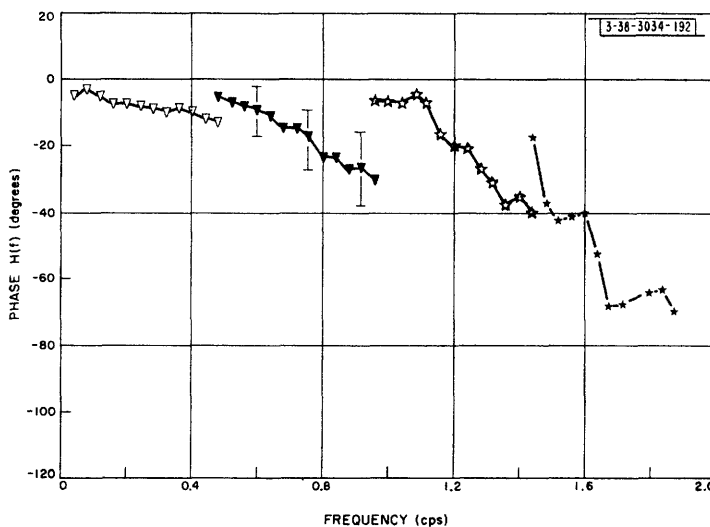
(b)

Fig.4-19. Experiment IV, compensatory — mean closed-loop
characteristics for Selected Band Inputs B7 through B10.

(c)

(d)
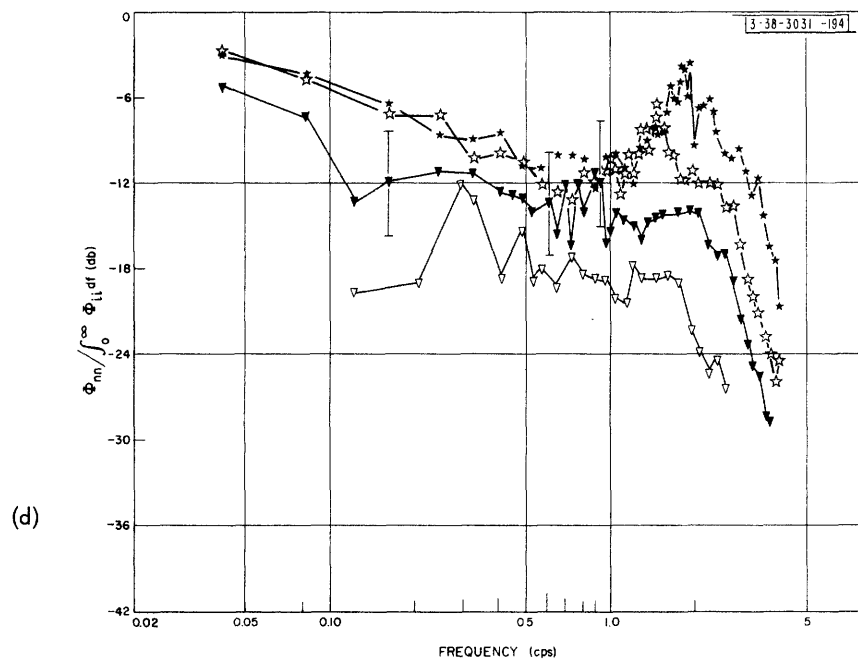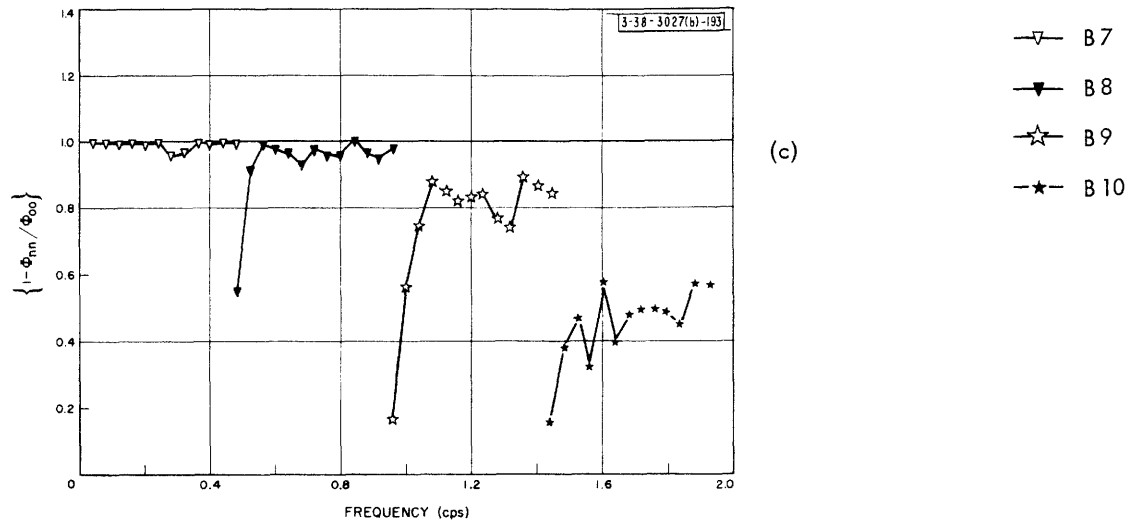
Fig. 4-19 (Continued)
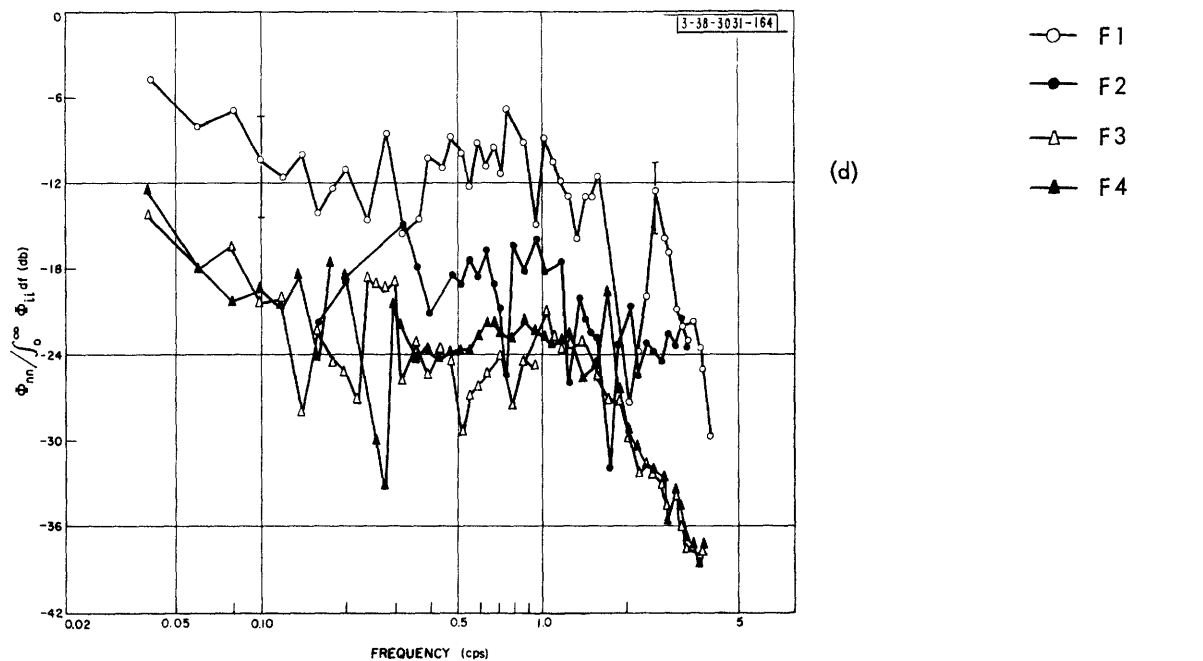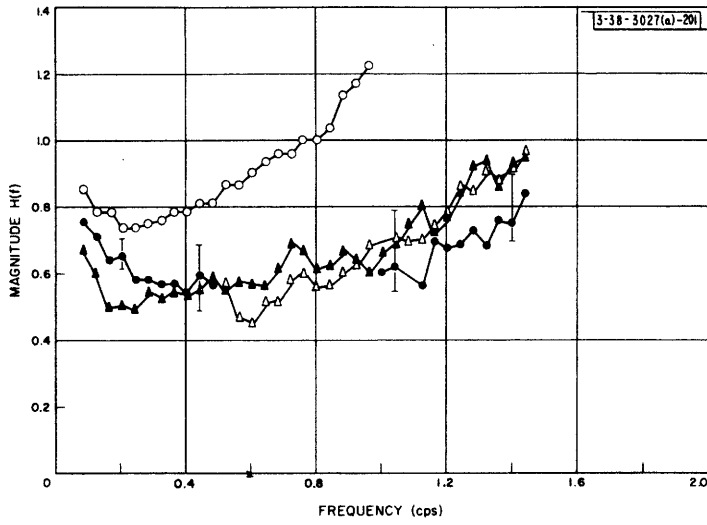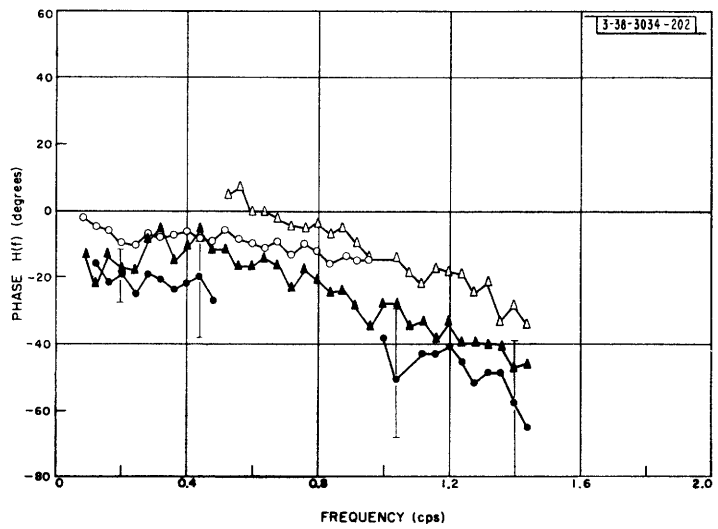
Fig. 4-20. Experiment IV, pursuit — mean closed-loop characteristics for Selected Band Inputs B 1 through B 4.
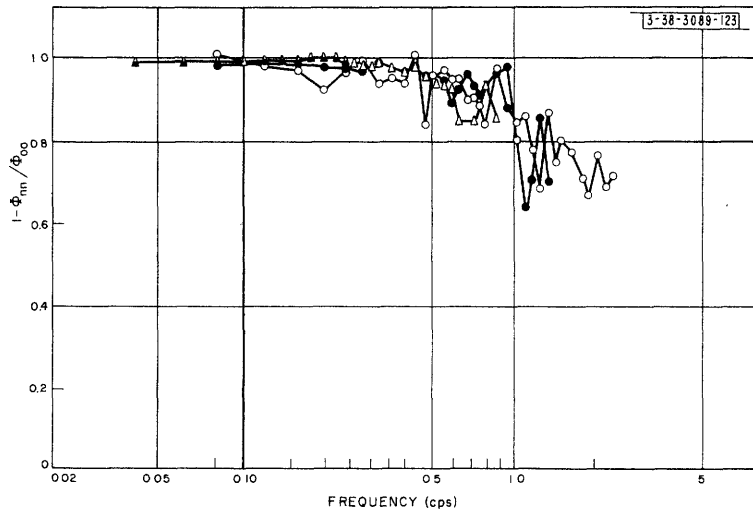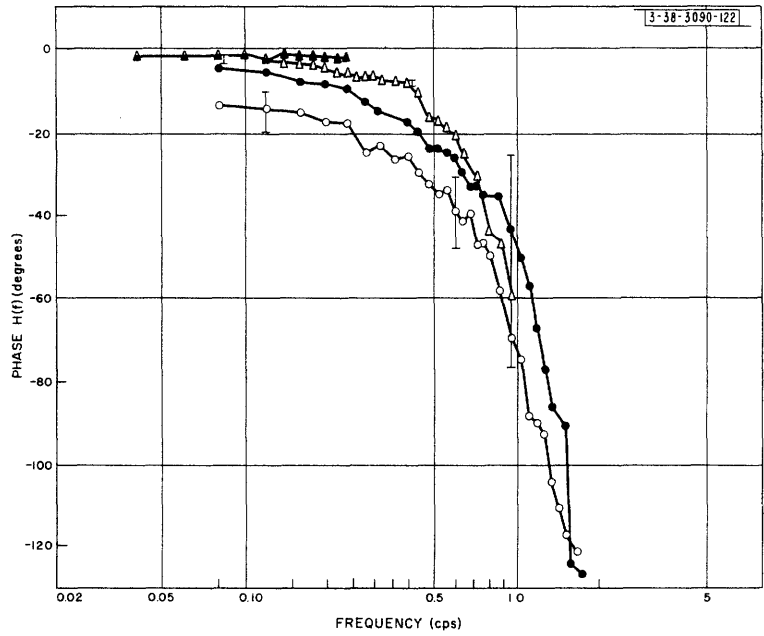
(c)

(d)

Fig. 4-20 (Continued)

77
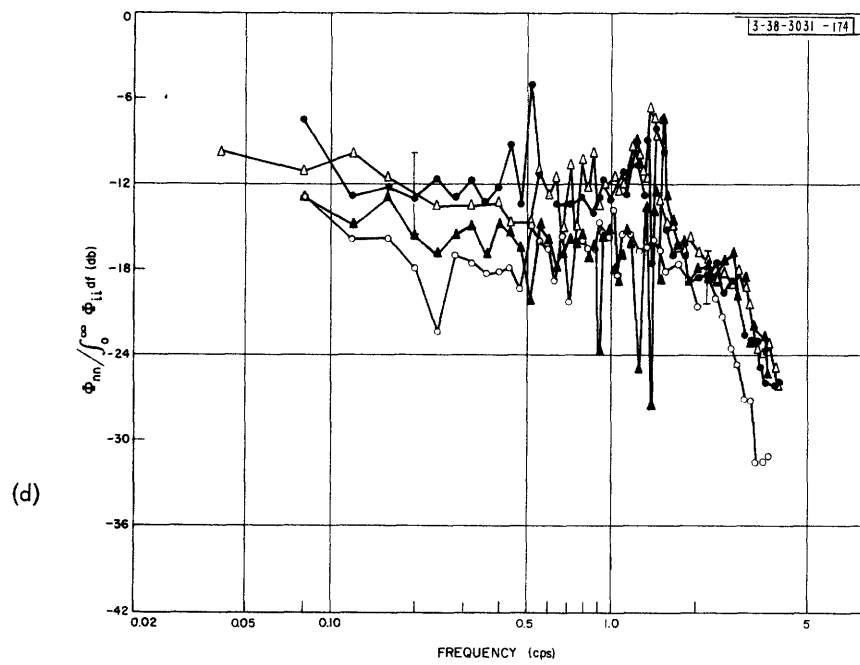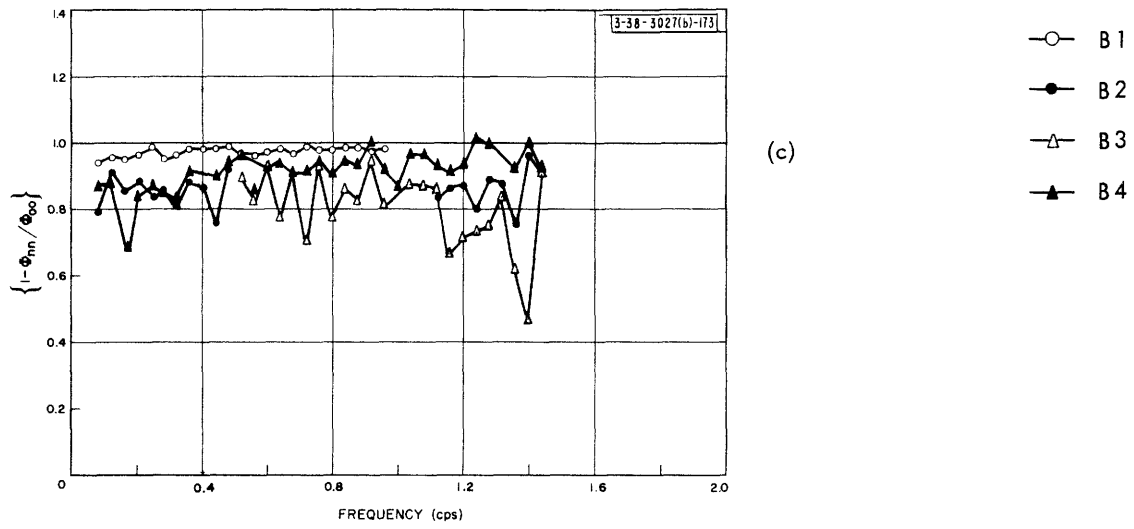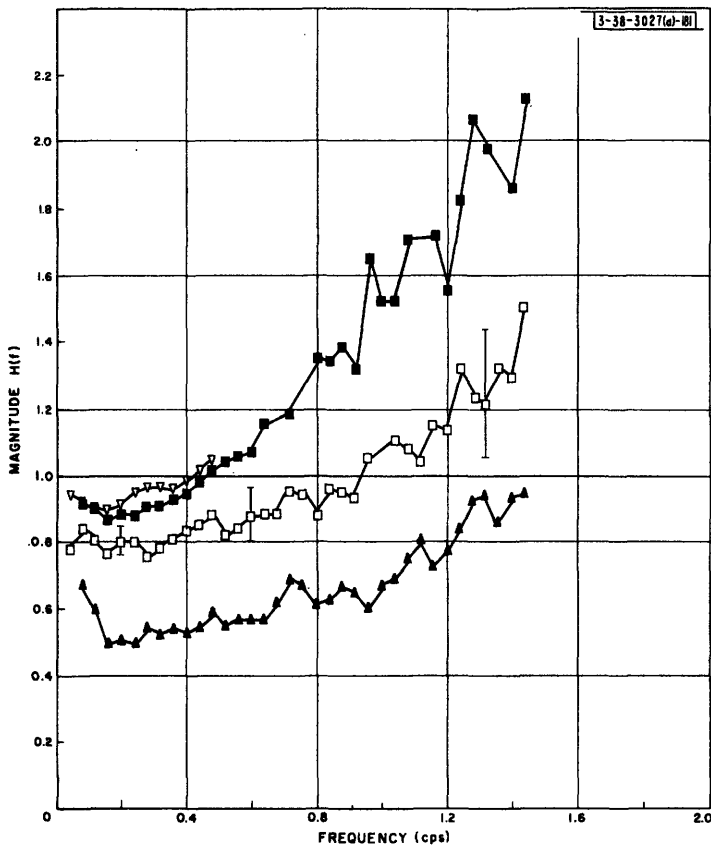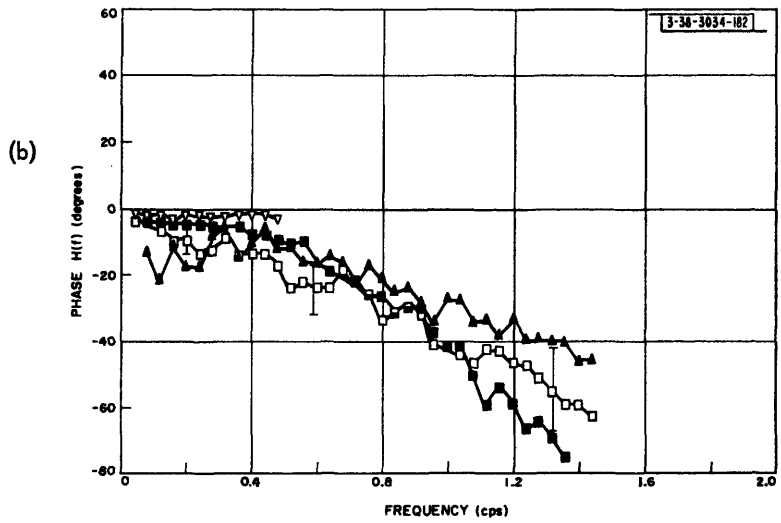
Fig.4-21. Experiment IV, pursuit — mean closed-loop characteristics for Selected Band Inputs B4 through B7.

78

(c)

(d)
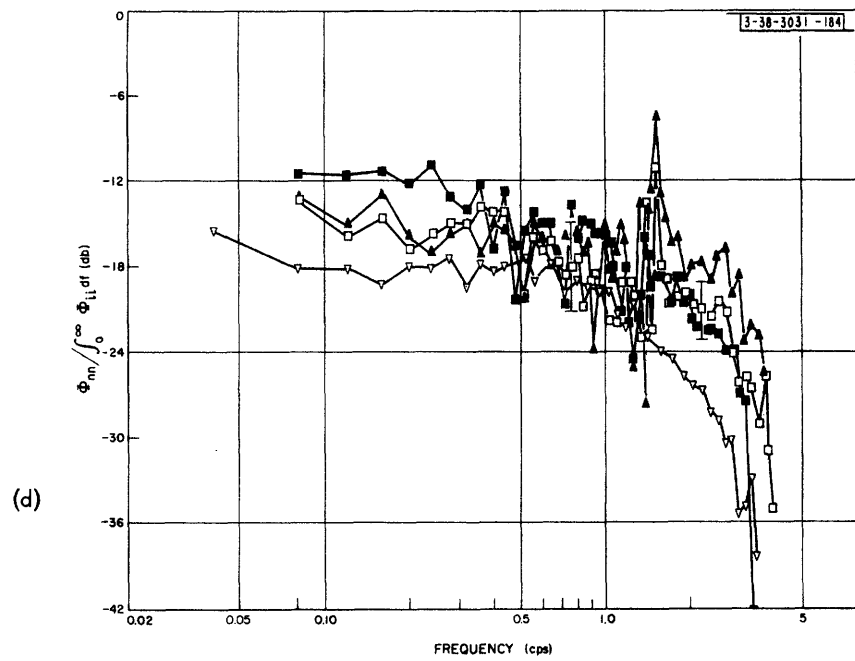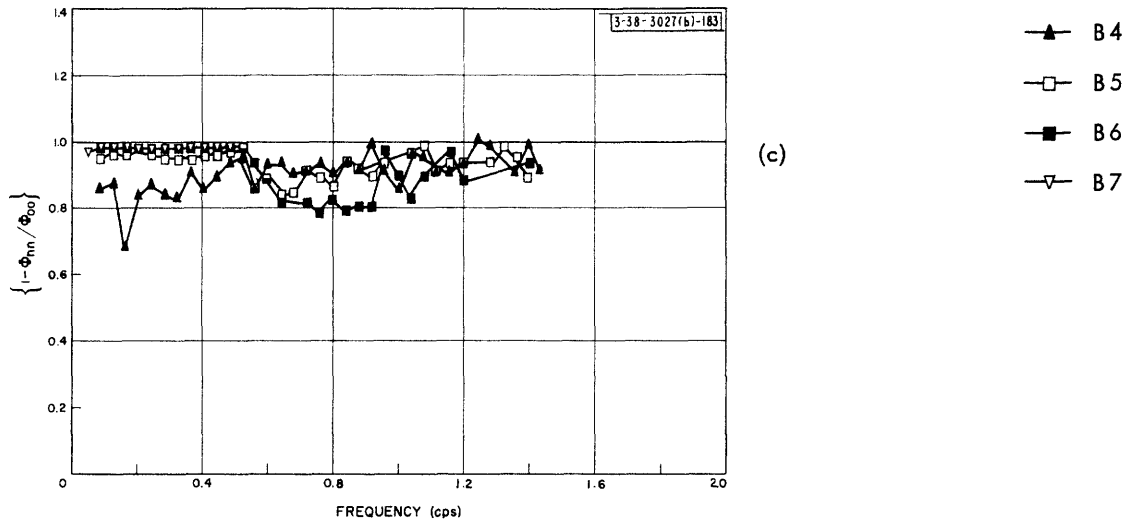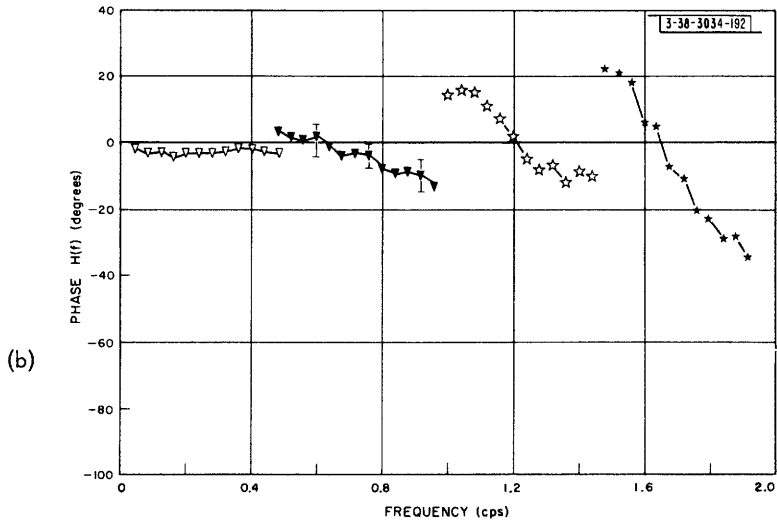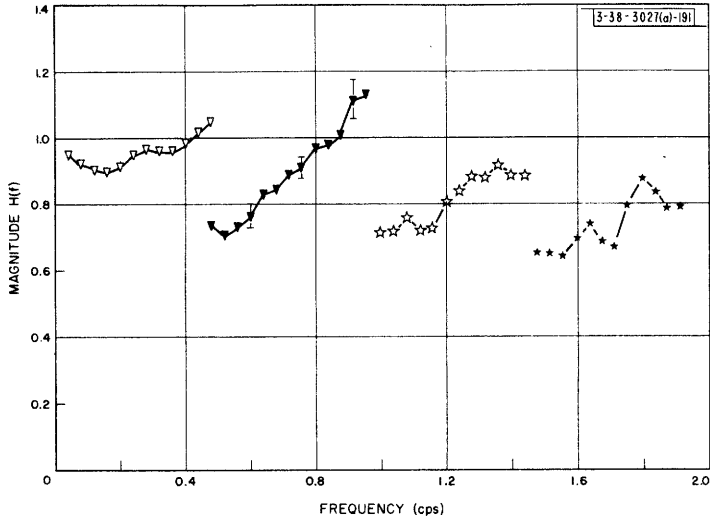
Fig. 4-21 (Continued)

Fig.4-22. Experiment IV, pursuit — mean closed-loop characteristics for Selected Band Inputs B 7 through B 10.

(c)

(d)

Fig. 4-22 (Continued)

81
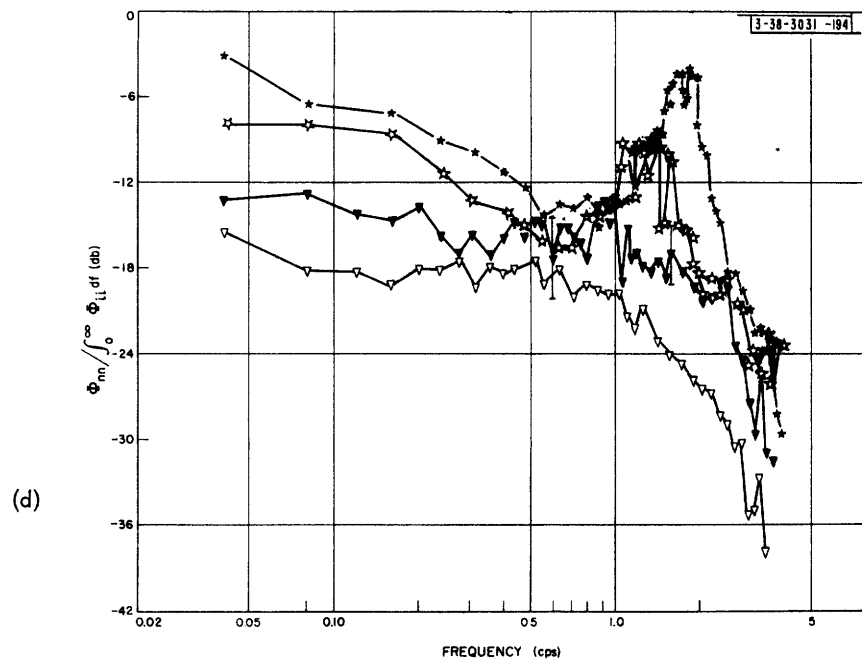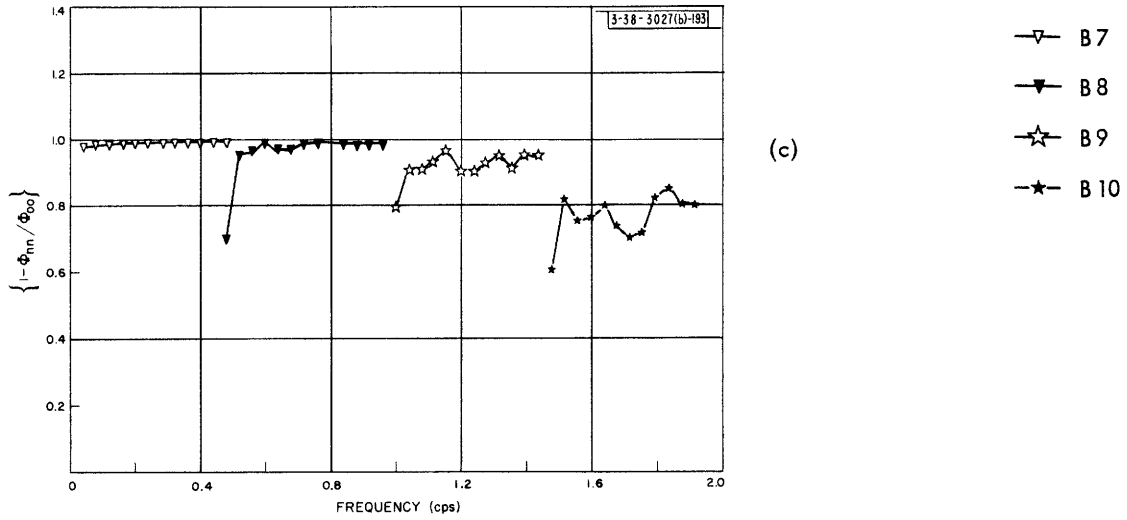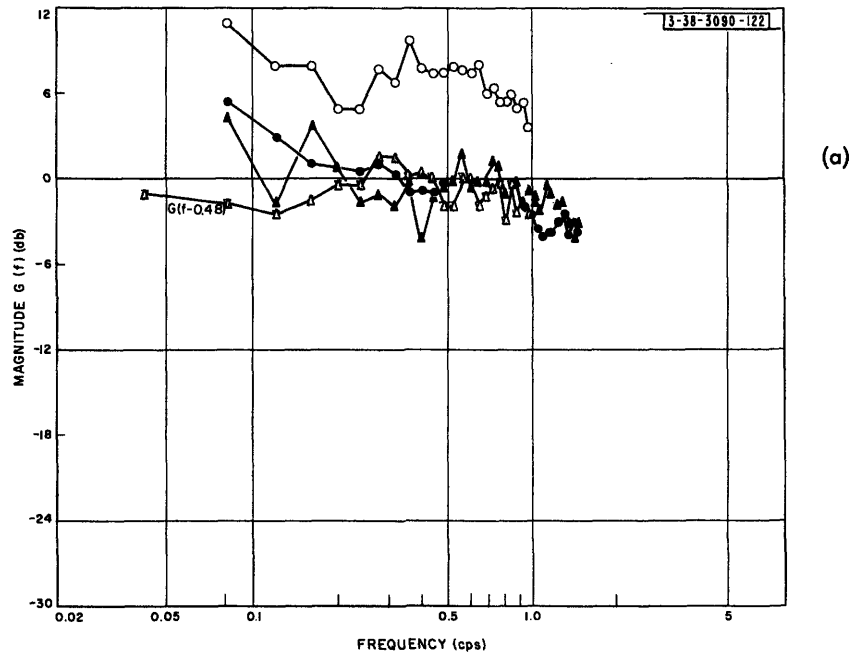
Fig.4-23. Experiment IV, compensatory — mean open-loop characteristics for Selected Band Inputs B 1 through B 4.

(b)

	B 1
	B 2
	B 3
	B 4

(c)
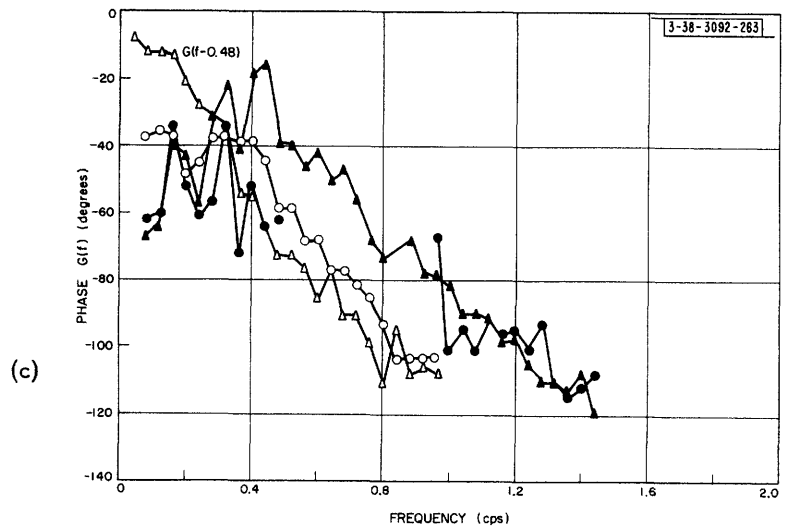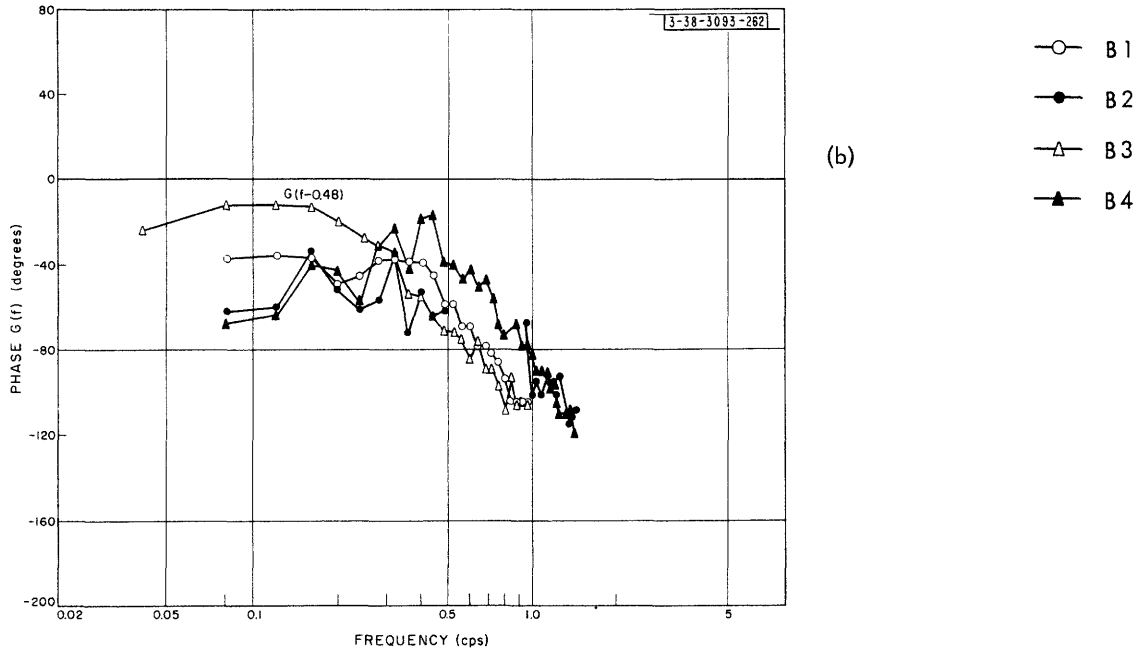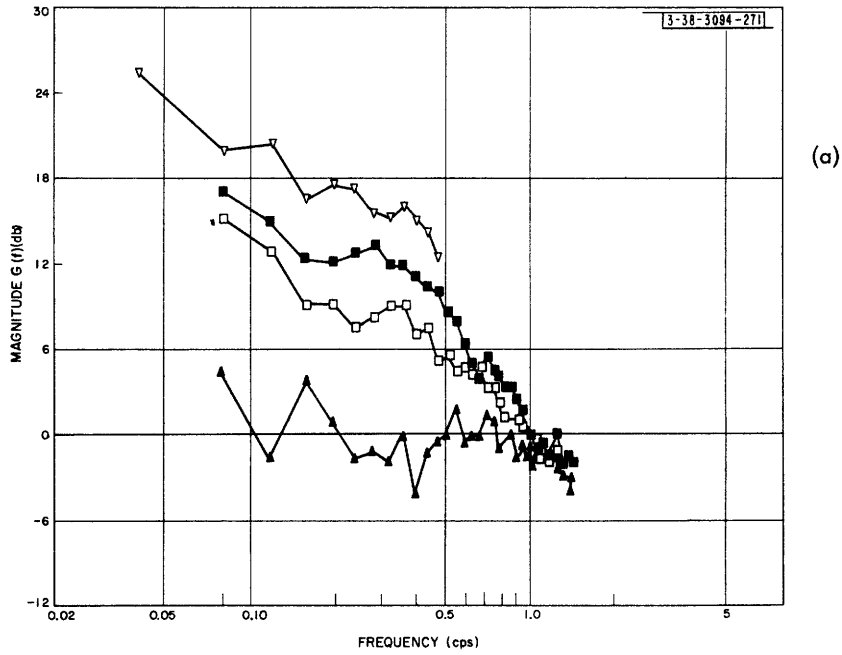
Fig. 4-23 (Continued)

Fig.4-24. Experiment IV, compensatory – mean open-loop characteristics for Selected Band Inputs B 4 through B 7.

(b)

(c)

Fig. 4-24 (Continued)

85
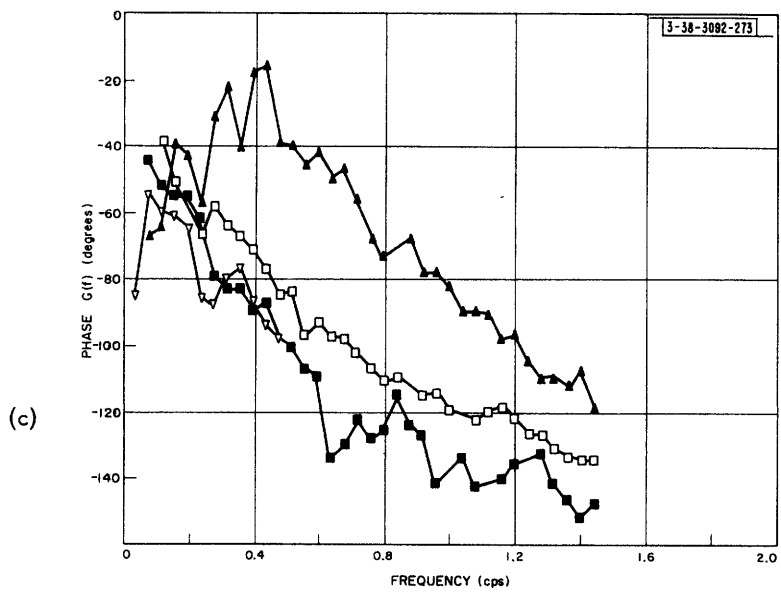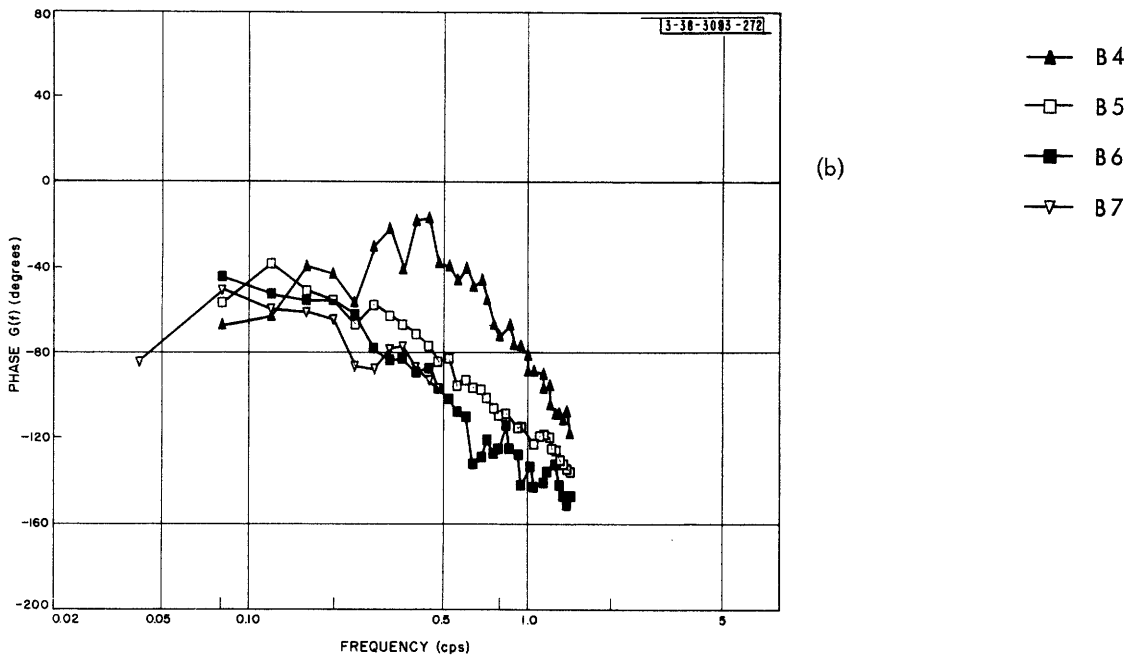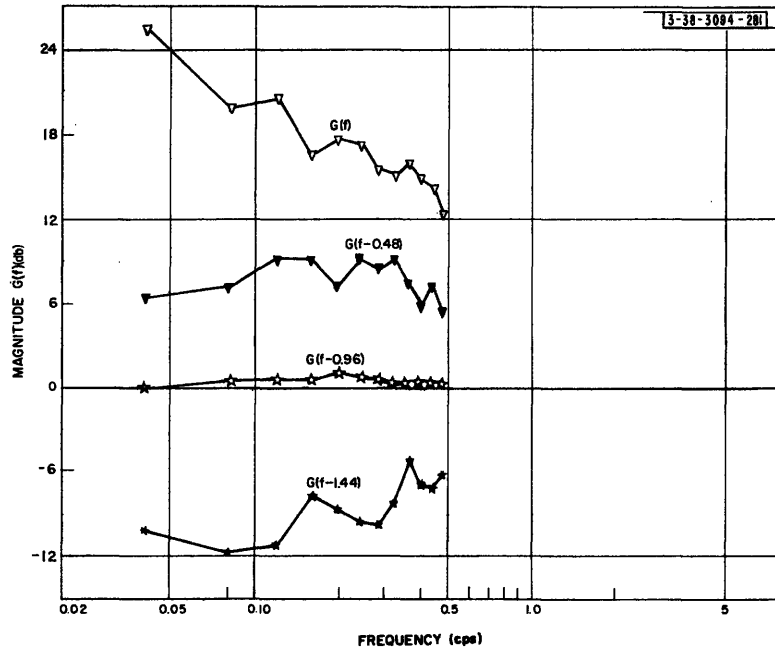
Fig.4-25. Experiment IV, compensatory – mean open-loop characteristics for Selected Band Inputs B 7 through B 10.

(b)

(c)

Fig. 4-25 (Continued)

87
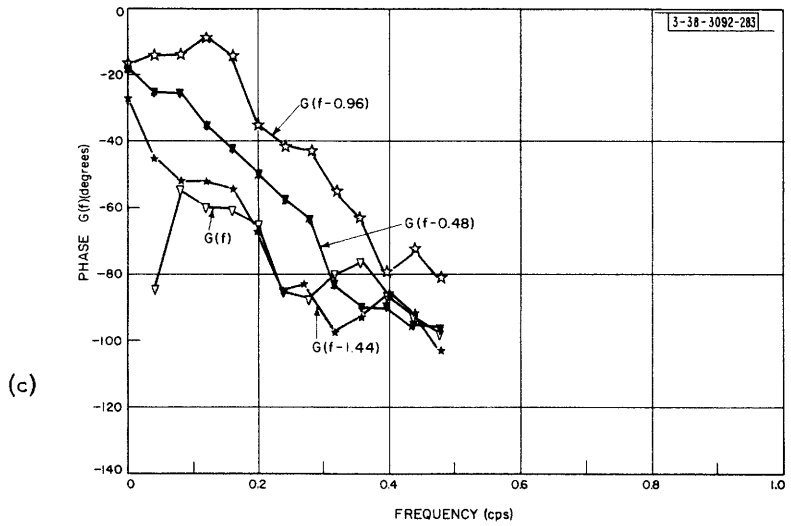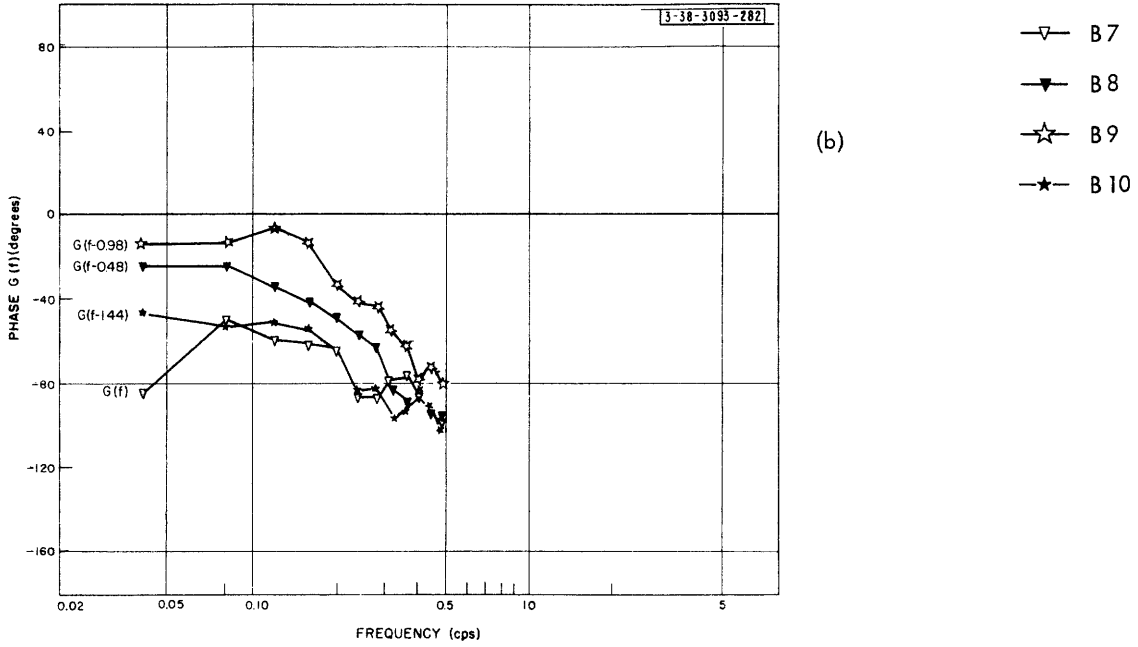
V. ANALYTIC MODELS FOR THE HUMAN OPERATOR

Although the graphical results presented in the previous section show how human-operator characteristics depend upon input signal parameters, they do not present the relation analytically. There is too much detail in the graphs for us to be able to see clearly the relations among the families of system and input characteristics. To determine the system-input relations, one must try to isolate a few parameters that describe the system characteristics, and to study their relations to the parameters that describe the input signals.

One way to obtain a set of parameters describing system behavior is to fit analytic functions to the measured characteristics. If these functions are simple and if their parameters can be related to the input, the functions — taken together as a complex or family — define a quasi-linear model of the control system. It should be a useful vehicle for exploring the behavior of the human operator. Simple analytic functions which approximate the open-loop transfer functions $G(f)$ and of the output-noise spectra $\Phi_{nn}(f)$ have been derived for the compensatory system. Quantitative relations among the parameters of these functions and the input-signal parameters have also been obtained. With the pursuit system, we do not have the proper data from which to derive rigorously a satisfactory analytic model. However, with physical reasoning to support the experimental results, a semiquantitative model has been developed. It provides fair approximation to the measured system characteristics.

In this section, only adaptive quasi-linear models, i.e., models whose components have parameters that change as a function of the parameters of input, are discussed. It may also be possible to find nonlinear models of fixed parameters which have the same quasi-linear behavior as the models presented here. However, an extensive attempt to develop nonlinear models was not made because quasi-linear adaptive models describe the results well and the data did not seem sufficient for development of nonlinear models.

A. MODELS FOR THE COMPENSATORY SYSTEM

1. Models for Open-Loop Transfer Functions

Measured open-loop transfer functions $G(f)$ for compensatory systems can be approximated with reasonable accuracy by simple analytic functions of frequency having only a few parameters. The form of the analytic functions used to approximate $G(f)$ was suggested by the experimental results and by certain basic characteristics of visual-manual responses. (1) The human operator is fundamentally a low-pass device; his open-loop gain at high frequencies must go to zero. (2) For low-bandwidth inputs, his low-frequency gain can be very high but must remain finite because of physical limitations of the visual and motor systems. Thus, although the human operator can act as a low-pass filter with high gain, he cannot act as an integrator. (3) Any approximation to $G(f)$ must contain a delay which is analogous to the reaction-time delay or stimulus-response latency of the human operator in a discrete tracking task.

a. First Analytic Function $G'_a(f)$

The simplest transfer function that satisfies these requirements has the form

$$G'_a(f) = \frac{K\,e^{-2\pi jf\alpha'}}{\left(\dfrac{jf}{f_o} + 1\right)} \quad , \tag{5-1}$$

where K is the low-frequency gain, α' is the delay in seconds, and f_o is the bandwidth in cps. The symbol $G'_a(f)$ is used to represent the analytic approximation to the measured open-loop transfer function $G(f)$.

The process of fitting (5-1) to the measured characteristics to determine the values of the parameters of $G'_a(f)$ is illustrated in Fig. 5-1, which shows the measured open-loop characteristics obtained with the RC Filtered Input F1. A good fit between $G(f)$ and $G'_a(f)$ must be accomplished simultaneously in magnitude and phase. It may be necessary to shuttle back and forth between magnitude and phase and adjust the parameters of $G'_a(f)$ in order to obtain the compromise that gives the best fit. The delay $e^{-2\pi jf\alpha'}$ does not affect the amplitude characteristics of $G'_a(f)$, and therefore the magnitude of $G(f)$ can be fitted by the function

$$\left|G'_a(f)\right| = \left|\frac{K}{\dfrac{jf}{f_o} + 1}\right| \quad . \tag{5-2}$$
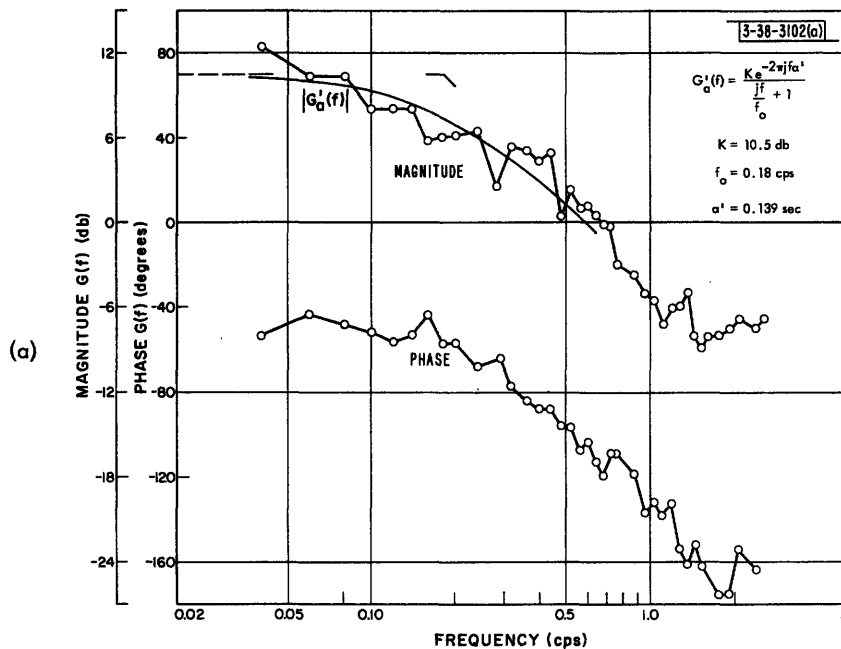
Fig. 5-1. Measured open-loop characteristics of the compensatory system obtained with RC Filtered Spectrum F 1. The smooth curves in (a) and (b) are the magnitude of $G'_a(f)$ and the phase shift associated with $|G'_a(f)|$. The residual phase is approximated by the delay exp $[-2\pi jf\alpha']$, the straight line. The parameters of $G'_a(f)$ listed in (a) provide a good visual fit to both magnitude and phase.

(b)

(c)

Fig. 5-1 (Continued)

91
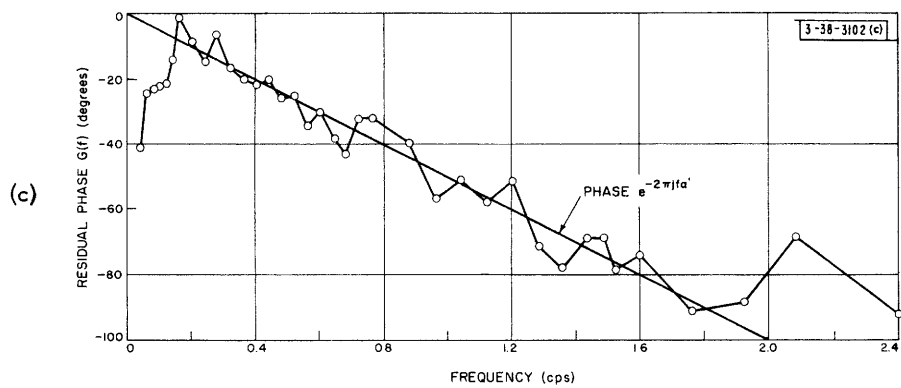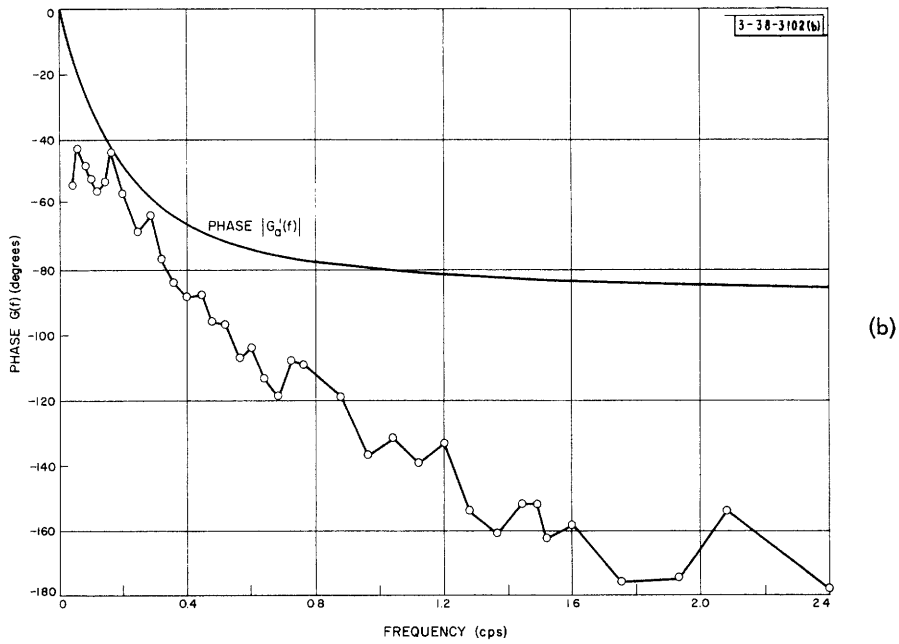
The particular $G_a'(f)$ having K equal to 10.5 db and f_o equal to 0.18 cps, represented in Fig. 5-1(a) by the smooth curve provides a fairly good fit to the magnitude of the G(f) represented by the datum points.

Associated with this function $G_a'(f)$ is a phase lag [smooth curve in Fig. 5-1(b)] which, when added to the phase lag of $e^{-2\pi jf a'}$, must approximate the phase of G(f). In other words, the residue, obtained by subtracting from the measured phase the phase associated with $G_a'(f)$, should be linear with frequency with a slope equal to the delay a'. For Input F1, the residual phase [Fig. 5-1(c)] is approximately linear and has a slope equal to 0.130 second. If the residue had not been linear, it would have been necessary to select another $G_a'(f)$, having different K and f_o, to obtain a more linear residue.

With certain low-bandwidth inputs, the parameters determined by fitting (5-1) to the measured open-loop characteristics yield a $G_a'(f)$ that is unstable in the closed loop. The delay is too large and makes the phase greater than 180° when the magnitude of $G_a'(f)$ is 0 db. Since the actual control system was stable, the analytic transfer functions determined from (5-1) must be incorrect. However, in all cases the frequency at which $G_a'(f)$ oscillates is much greater than the input bandwidth and lies outside the region in which G(f) can be measured. The difficulty is that the approximation to the low-frequency portion of G(f) is not valid at high frequencies.

b. Second Analytic Function $G_a(f)$

We cannot determine the high-frequency behavior of G(f) from only low-frequency measurements, but we can postulate new analytic transfer functions that are stable and have the same low-frequency characteristics as the first approximation (5-1). We suppose that for very-low-bandwidth inputs the high frequencies are not important. The human operator should therefore attenuate the high-frequency part of his responses more than is indicated by (5-1). It is well known that a low-pass filter with high critical frequencies produces nearly linear phase lag and almost no attenuation at very low frequencies.[31] If the human operator, working with very-low-bandwidth inputs, introduces more attenuation of the high frequencies than predicted by (5-1), his phase characteristics at low frequencies would contain an additional lag that would be nearly linear with frequency. The low-frequency characteristics that result from this high-frequency attenuation can be approximated by simple RC low-pass filters. Thus a second analytic model for G(f) is

$$G_a(f) = \frac{K e^{-2\pi jf a}}{\left(\dfrac{jf}{f_o} + 1\right)\left(\dfrac{jf}{f_1} + 1\right)} \ . \tag{5-3}$$

where f_1 is much greater than f_o and a is a new value for the delay. The low-frequency linear phase lag produced by the second lag term has a slope $1/2\pi f_1$ seconds. The residual phase lag approximated by $e^{-2\pi jf a}$ in (5-3) is reduced by the lag associated with f_1 and therefore a is less than a' in (5-1). Hence by proper choice of parameters $G_a(f)$ can be stabilized.

The parameters K and f_o of $G_a(f)$ in (5-3) have the same values as K and f_o of $G_a'(f)$ in (5-1) since f_1 is much higher than f_o. The sum a plus $1/2\pi f_1$ of (5-3) is equal to the delay a' of (5-1), but we cannot find unique values for a and for f_1 of (5-3) from only the low-frequency part of G(f). However, we can find maximum values for these two parameters which satisfy the requirement that

$G_a(f)$ leads to a stable system. These maximum values, denoted by the symbols α_{max} and f_{max}, are the values of α and f_1 corresponding to a $G_a(f)$ which has zero phase margin, i.e., 180° phase lag when $G_a(f)$ is 0 db. Since the results of Experiment IV show that the human operator reduces his phase margin when the high-frequency content of the input is reduced, it is likely that the actual phase margin, if it could be measured, would be close to zero. Thus the parameters α_{max} and f_{max} are reasonable ones to use for describing the measured characteristics.

Analytic functions of the forms (5-1) and (5-3) were fitted to the mean open-loop characteristics of the compensatory system for all the runs of Experiments III and IV. Before the fitting was done, the bandpass characteristics (B3, B8, B9 and B10) were translated down the frequency scale, the low-frequency cutoffs being set at zero. Values obtained for the parameters of $G_a'(f)$ and $G_a(f)$ are shown in Table 5-I. In Appendix A the analytic functions are shown superimposed on the graphs of the measured functions $G(f)$.

The accuracy with which the parameters of Table 5-I are determined can be estimated from the graphs of Appendix A. The analytic functions were fitted visually to the measured characteristics by the author and were checked by another person. In many cases, the best compromise to make between the approximations to the measured magnitude and to the measured phase of $G(f)$ were not obvious. Some uncertainty in the choices of parameters therefore exists. However, the author believes that the values chosen for the parameters are probably correct to within the following tolerances: ± 3 db for K, $\pm 0.2 f_o$ cps for f_o, and ± 0.022 second for α_{max}. The limit for α_{max} is the standard deviation of the values obtained with all the low-pass inputs. The other limits were estimated from the curves of Appendix A.

2. Behavior of the Parameters of the Models

a. Delay α_{max}

The mean value of the delay α_{max} (Table V-I) obtained with low-pass input signals (all inputs except Selected Band signals B3, B8, B9 and B10) is 0.13 second. The standard deviation of the values of α_{max} is 0.022 second. No consistent pattern of variation that can be related to input-signal characteristics is apparent. We shall therefore treat the delay α_{max} as a constant equal to the mean, 0.13 second.

The values for α_{max} obtained with bandpass inputs (B3, B8, B9 and B10) are very much larger than any of the delays obtained with low-pass inputs, but with bandpass inputs the human operator's mode is very different from the mode he uses with low-pass signals. In a sense, he has to translate his characteristics in frequency in order to track both center frequency and envelope. The added complexity of the task and the process of frequency translation or modulation may be causes of long delay. Therefore, to include the bandpass delays in the computation of the mean α_{max} does not seem justified. A more representative value is obtained by using only the low-pass results. However, the band-reject input has been included in the mean because the transfer functions show that the human operator apparently responds to it as he would to a low-pass signal.

The mean delay α_{max} (0.13 second) is, in a sense, analogous to the reaction-time delay inherent in human-operator responses to a discrete stimulus. It would be questionable, however, to use

93

<div align="center">

TABLE 5-1

SUMMARY OF PARAMETERS OF $G_a'(f)$ AND $G_a(f)$

</div>

Input	α_{max} (second)	f_{max} (cps)	a' (second)	f_o (cps)	Kf_o (cps)	K (measured) (db)	K_c $\left(=\dfrac{0.39}{\sigma_f \bar{f}}\right)$ (db)	K'_c $\left(=\dfrac{3.8}{\sigma_f\, e^{\bar{f}/0.38}}\right)$ (db)
R .16	0.110	0.300	0.64	0.035	1.86	34.5	38.8	35.04
R .24	0.104	0.99	0.264	0.050	1.88	31.5	30.72	30.36
R .40	0.133	1.96	0.214	0.125	1.67	22.5	22.76	24.36
R .64	0.150	4.83	0.183	0.275	1.54	15.0	15.68	14.30
R .96	0.139	∞	0.139	0.58	1.22	6.5	6.48	8.08
R 1.6	0.122	∞	0.122	0.6	0.56	−0.6	−0.36	−2.09
R 2.4	0.116	∞	0.116	0.3	0.213	−3.0	−7.56	−14.79
F 1	0.139	∞	0.139	0.18	0.604	10.5	6.56	9.14
F 2	0.126	∞	0.126	0.05	0.89	25.0	21.4	21.92
F 3	0.178	∞	0.178	0.03	1.34	33.0	31.2	29.28
F 4	0.102	0.78	0.306	0.056	1.96	31.0	30.6	30.30
B 1	0.153	∞	0.153	0.76	2.13	9.0	8.0	10.20
B 2	0.107	∞	0.107	0.8	0.95	1.5	0.58	0.85
B 3	0.278	∞	0.278	2.0	1.78	−1.0	3.45	−0.38
B 4	0.150	∞	0.150	2.0	1.94	−0.3	0.76	0.32
B 5	0.128	∞	0.128	0.30	1.07	11.1	10.4	13.10
B 6	0.149	∞	0.149	0.16	1.23	17.7	16.8	19.28
B 7	0.100	2.84	0.156	0.14	2.02	23.2	18.28	20.72
B 8	0.219	1.00	0.388	0.5	1.41	9.0	11.48	11.68
B 9	0.390*	∞	0.390*	2.0*	2.09*	0.4	6.42	−0.72
B 10	1.14*	∞	1.14*	0.45†		−11.0	3.24	−11.74

*Approximate

†Lead

the term "reaction-time delay" for a_{max} since reaction time usually implies the existence of a period of delay following presentation of a stimulus during which no response is made. In a continuous task, stimuli are presented and responses made continuously and the response to a single stimulus perhaps cannot be identified.

Nevertheless, a close relation exists between the delay in a continuous task and the reaction-time delay. The mean value for a_{max} obtained in this study is slightly lower than reaction times obtained with discrete visual stimuli. For the discrete case, a delay of about 0.17 second is representative.[13] In a continuous task we would expect a shorter delay, since the time at which a response will have to be made is less uncertain than it is in most discrete reactions. Because of this difference in experimental conditions, a value of 0.13 second does not seem unreasonable for the delay. However, a_{max} represents an upper limit to a in (5-3), and the value for a may be lower than 0.13 second.

    b.   Gain-Bandwidth Product Kf_o

Table V-I shows that f_o, the bandwidth of $G_a(f)$, is roughly inversely proportional to the gain K, i.e., the gain-bandwidth product Kf_o is approximately constant, over a wide range of input-signal characteristics. In Fig. 5-2 are plotted measured values of K in db vs log f_o. Except for inputs having significant power at high frequencies (F1 and R2.4), the approximate relation between K and f_o is

$$K = \frac{1.5}{f_o} \quad . \tag{5-4}$$
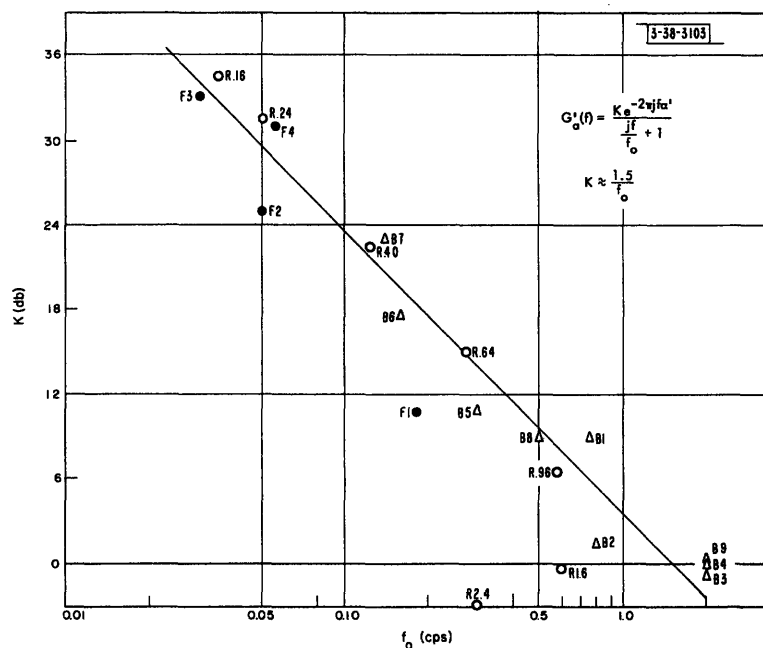
Fig. 5-2. Gain vs bandwidth of $G'_a(f)$, the analytic approximation to measured $G(f)$. B10 is not plotted because its characteristics are not low-pass and cannot be approximated by $G'_a(f)$.

95

Therefore, the gain-bandwidth product equals about 1.5 cps on the average. For low-bandwidth inputs, the gain-bandwidth product is generally greater than 1.5 cps but seems to have a maximum of about 2.0 cps (Table V-I). For inputs with high-frequency components, the gain-bandwidth product is usually lower than the average.

The gain-bandwidth product is an important figure of merit of system performance. For systems having open-loop transfer functions of the form

$$\frac{K}{\dfrac{jf}{f_o} + 1} \quad , \qquad\qquad (5\text{-}5)$$

Kf_o is the frequency at which the magnitude of the transfer function is unity (if K is greater than unity) and is approximately equal to the closed-loop bandwidth (if K is large). At the frequency Kf_o, the open-loop phase shift must be less than $180°$ if the closed-loop system is to be stable.

With a delay of 0.13 second, the gain-bandwidth product of the transfer function (5-3) must be less than about 2.0 cps. At this frequency the delay contributes $94°$ phase shift, and, provided f_o is small, the first lag of (5-3) adds nearly $90°$ more, for a total of about $180°$. The fact that the observed maximum Kf_o is only slightly greater than 2.0 cps is confirmation of the validity of our measurements for the delay a_{max}. If the input contains significant power at high frequencies, good tracking performance requires that the stability be good within the signal band, and therefore the phase margin must be fairly large. Table V-I shows that, for wide-bandwidth inputs, Kf_o is considerably less than 2.0 cps, indicating large phase margin. This result implies that the human operator adjusts Kf_o in accordance with the requirement for phase margin and with the distribution of input power in frequency.

c. <u>Frequency of Second Lag, f_{max}</u>

The values for f_{max} in Table V-I are, with one exception, 10 to 20 times as great as the low-bandwidth break frequency f_o. Usually f_{max} is considerably greater than the input bandwidth. Thus the second lag does not affect $|G_a(f)|$ at low frequencies.

With bandpass input B8, f_{max} is only twice f_o, but the fact that the input is bandpass appears to be responsible for the low value of f_{max}. The delay a' obtained by fitting (5-1) to the B8 results is larger than that obtained with low-pass inputs. Therefore, f_{max} must be low in order to make the system stable.

With wide-band inputs or with inputs containing high-frequency components, the system is stable without the second lag. For these inputs, $G'_a(f)$ of (5-1) provides adequate approximations to the experimental transfer functions. Thus the delay a_{max} is equal to the delay a' obtained with (5-1), and f_{max} is infinite. It must be kept in mind that f_{max} is the upper limit to f_1, and that f_1 was introduced to stabilize $G'_a(f)$. $G_a(f)$ therefore approximates the low-frequency, and probably not the high-frequency, part of the operator's characteristics. We should not attach much physical significance to f_{max}.

d. Gain K

The gain K is the most important parameter of the open-loop models of (5-1) and (5-3). It is also the parameter that is related most directly to the parameters of the input signal. We have been able to develop expressions relating K to certain functions of the input power-density spectrum which describe the predictability of the input and its location on the frequency scale. We shall discuss these relations and some of the steps leading to their development.

The family of Rectangular Spectra of Experiment III provides the most effective vehicle for determining the nature of the relation between K and input characteristics. Since results of Experiment II — Variability showed that input amplitude does not markedly affect the characteristics of compensatory systems, the only significant parameter of the Rectangular Spectra is the cutoff frequency f_{co}. A plot of K vs f_{co} should reveal the relation between gain and input characteristics. Figure 5-3 shows that K is very nearly inversely proportional to the square of the cutoff frequency. Only at extreme values of f_{co} does K depart significantly from this relation. The approximate relation between K and f_{co} in Fig. 5-3 is

$$K = \frac{2.2}{f_{co}^2} \ .$$

(5-6)
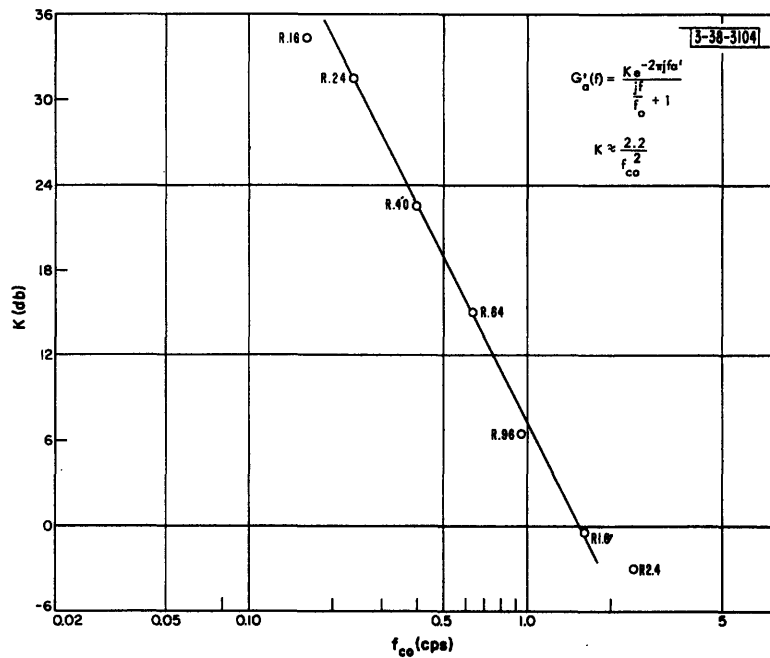
Fig. 5-3. Gain of $G_a'(f)$ vs cutoff frequency of Rectangular Spectra.

The RC Filtered and the Selected Band Spectra are more complex than the Rectangular and cannot be described simply by a cutoff frequency. We must look therefore, for more fundamental measures of input-signal characteristics which apply equally well to all the input spectra. Two factors seem to have the most important influence on the gain K: the predictability of the input, and its

Fig.5-4. Gain of $G_a^!(f)$ vs measured values of $1/\sigma_f \bar{f}$ for Rectangular Spectra.

$$G_a^!(f) = \frac{K e^{-2\pi j f a^!}}{\frac{jf}{f_o} + 1}$$

$$K \approx \frac{0.39}{\sigma_f \bar{f}}$$

$$K_c = \frac{0.39}{\sigma_f \bar{f}}$$

Fig.5-5. Measured gain K of $G_a^!(f)$ vs computed gain K_c for all input spectra. Measured values of σ_f and $\bar{f}$ were used to determine K_c.

98

location on the frequency scale. Clearly, K will be larger for a predictable input than for an unpredictable input. Translating a signal in frequency does not affect its predictability. Since the results with the bandpass inputs (B7, B8, B9 and B10) show that the gain decreases as the input band is moved up the frequency scale, it is evident that the factor of location in frequency (center frequency) comes into play.

Many different quantities describe in a general way the location and predictability of an input signal. Expressions involving several of the most likely quantities were compared with the experimental results. It was found that one particular pair produced the best match to all the measured values of K. The members of the pair are $\bar{f}$, the mean frequency, and σ_f, the standard deviation of the spectrum. The mean frequency $\bar{f}$ is the first moment of the input power-density spectrum normalized with respect to the mean-square input power. The standard deviation σ_f is the square root of the second moment of the spectrum about its mean, also normalized with respect to the mean-square input power. In terms of the spectrum $\Phi_{ii}(f)$,

$$\bar{f} = \frac{\int_0^\infty f \, \Phi_{ii} \, df}{\int_0^\infty \Phi_{ii} \, df} \quad , \tag{5-7}$$

and

$$\sigma_f = \left[\frac{\int_0^\infty f^2 \, \Phi_{ii} \, df}{\int_0^\infty \Phi_{ii} \, df} - (\bar{f})^2 \right]^{1/2} \quad . \tag{5-8}$$

Normalization with respect to input power eliminates the effect of rms input amplitude. The quantity $\bar{f}$ is a measure of location. The quantity σ_f, which is related to the width of the spectrum, is a measure of predictability. The product $\sigma_f \bar{f}$ has the dimensions of frequency squared. For rectangular spectra it is directly proportional to the square of the cutoff frequency f_{co}.

Since the actual input spectra differ somewhat from the nominal spectra, σ_f and $\bar{f}$ were computed from measurements on the actual spectra (see Appendix C). Figure 5-4 is a plot of K from $G_a'(f)$ against measured values of $1/\sigma_f \bar{f}$. A good fit (obtained visually) to the plotted points is provided by the relation

$$K = \frac{0.39}{\sigma_f \bar{f}} \quad . \tag{5-9}$$

Equation (5-9) can be used to compute values for the gain from measured values of σ_f and $\bar{f}$ for RC Filtered and Selected Band Inputs. We shall let K_c denote the computed values obtained from (5-9). In Fig. 5-5, K is plotted against K_c for all the inputs. The measured gain K was obtained by fitting $G_a'(f)$ to the measured functions $G(f)$. Both K and K_c are in decibels. The agreement between measured and computed values is good for low-pass inputs, but it is not very good for bandpass inputs. The latter, B3, B8, B9 and B10, are connected by the dash-lines. The points for low-pass inputs are nicely distributed about the line of unity slope passing through the origin.

99

Fig. 5-6. Measured values of $K\sigma_f$ vs measured $\bar{f}$ for the bandpass spectra.

Fig. 5-7. Measured gain K of $G_a'(f)$ vs computed gain K_c' for all input spectra. Measured values of σ_f and $\bar{f}$ were used to determine K_c'.
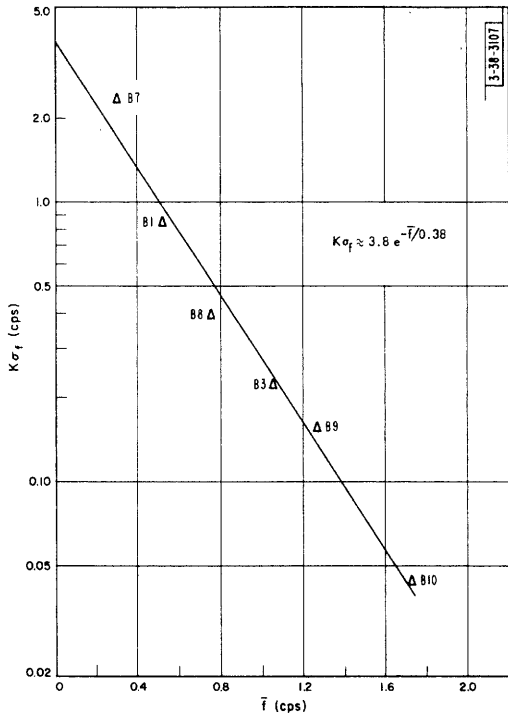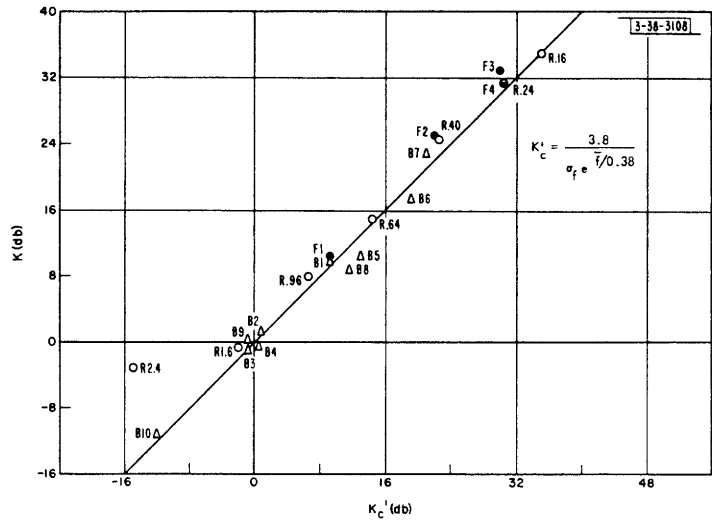
For the low-pass inputs, the correlation between K and K_c (in db) is 0.986. Thus, if we omit the bandpass data, Eq.(5-9) accounts for most of the variance in K.

As the mean frequency $\bar{f}$ of the bandpass inputs becomes greater, the difference between K and K_c increases. Since Inputs B7 through B10 all have the same σ_f, it is evident that (5-9) does not weight $\bar{f}$ heavily enough. By plotting measured values of the product $K\sigma_f$ against $\bar{f}$, we can isolate the effect of $\bar{f}$. Figure 5-6 is a semilogarithmic plot of $K\sigma_f$ vs $\bar{f}$ for two sets of bandpass inputs, B7 through B10, and B1 and B3. Although the values of σ_f for the two sets are different, σ_f is constant within each set, and only $\bar{f}$ changes. The least squares fit to the plotted points is provided by the relation

$$K\sigma_f = \frac{3.8}{e^{\bar{f}/0.38}} \qquad (5-10)$$

or

$$K = \frac{3.8}{\sigma_f\, e^{\bar{f}/0.38}} . \qquad (5-11)$$

With the aid of (5-11), values for the gain can be computed for all the other inputs from measured values of σ_f and $\bar{f}$. We shall let K'_c denote the computed values obtained from (5-11). Figure 5-7 is a plot of measured gain K in db vs K'_c in db. It shows that, except for the case of Input R2.4, K'_c is a good approximation to the measured gain. The points are close to the line of unity slope passing through the origin. The correlation between K and K'_c (in db) is 0.976. This indicates that, for the entire set of input signals, Eq.(5-11) accounts for most of the variance in K.

The exponential weighting of $\bar{f}$ in K'_c has advantages. As the mean frequency goes to zero, the exponential approaches unity, and the gain remains finite (if σ_f is nonzero). As $\bar{f}$ becomes large, the exponential increases rapidly and forces the gain to zero. This behavior of the exponential corresponds closely to the human operator's tracking behavior. He cannot have infinite gain even at zero frequency, and he cannot track input frequencies much above 3 or 4 cps, i.e., his gain goes to zero. Perhaps the exponential weighting is too strong, but it seems more appropriate than weighting the gain inversely to only $\bar{f}$ as in (5-9). The fit to the low-pass data is about as good with (5-9) as with (5-11), but the fit to the bandpass data is much better with (5-11).

Although relations (5-9) and (5-11) for K_c and K'_c approximate with good accuracy the measured values of gain, we cannot assume that these relations will be valid for inputs whose characteristics lie outside the range of those studied in these experiments. It is possible to find signals for which these relations will not be valid. For example, a sinusoid has a σ_f of zero which, according to both (5-9) and (5-11), leads to a computed open-loop gain of infinity — an impossibility for the human operator. There are several ways in which this inconsistency can be corrected, but the results of our experiments do not provide sufficient information for us to know exactly what modifications should be made in the relations to account for this and other inconsistencies.

We cannot be sure that, with respect to the human operator's gain, the quantities σ_f and $\bar{f}$ are the most fundamental parameters of the input signals. However, these quantities do provide far better approximations to the measured gain obtained with most of the inputs than do many more obvious quantities like the root-mean-square velocity, half-power frequency, etc. Note that although

the constant of proportionality in the expression of K_c was determined from results with only the Rectangular Spectra, the values of K_c determined from (5-9) closely approximate the measured gains for all low-pass inputs. Also, although the constants in the expression for K_c' were determined from the results with only the bandpass inputs, the values of K_c' determined from (5-11) closely approximate the measured gains for all inputs except R2.4. The fact that these two expressions provided very good approximations to nearly all the results supports the belief that σ_f and $\bar{f}$ are useful parameters.

3. Models for Compensatory Noise

An analytic expression has been developed which accounts for most of the variance in the magnitudes of the noise spectra obtained with the various input signals. The output-noise spectra obtained in the compensatory system can be approximated by the quadratic function:

$$\frac{\Phi_{nn}}{\int_0^\infty \Phi_{ii}\, df} = \frac{c_n^2}{\left|\left(\frac{jf}{f_n}\right)^2 + 2\zeta\left(\frac{jf}{f_n}\right) + 1\right|^2} \qquad (5\text{-}12)$$

where the parameters f_n (undamped natural frequency), ζ (damping factor), and c_n^2 (magnitude) change with input signal. With most inputs, f_n is between 1 and 2 cps, and ζ is between 0.8 and 1.0. The greatest variation is shown by c_n^2, which lies between 0.01 and 0.25 $(\text{cps})^{-1}$. It therefore merits the greatest attention in our development of analytic models.

In order to derive the relation between c_n^2 and input characteristics, certain simplifying assumptions must be made. The human operator's response movements can be approximated by a series of discrete step functions spaced T seconds apart. Assume that each step has two components: one part, Δe_o, that is related to the input signal and the other part that is not related to the input, but represents random error or noise in the operator's responses. Assume that the random or noise component of each step is independent of all other steps. Assume also that, over all, the mean-square noise is proportional to the mean-square value of Δe_o, the part of the step responses that is related to the input:

$$\overline{n^2} \propto \overline{(\Delta e_o)^2} \quad . \qquad (5\text{-}13)$$

To a first approximation,

$$\overline{(\Delta e_o)^2} \propto \overline{(v_i\, H_\ell\, T)^2} \quad , \qquad (5\text{-}14)$$

where v_i is the velocity of the input, T is length of the interval, and H_ℓ is the average magnitude in the low-frequency region of the closed-loop transfer function. In (5-14), $v_i H_\ell$ is approximately the velocity of the actual output of the system. If this velocity is fairly constant within the interval T, $(v_i H_\ell T)$ is approximately proportional to the incremental amplitude of the output in the interval. Thus relation (5-14) is approximately true.

The mean-square velocity of the input is related to the input spectrum,

$$\overline{v_i^2} = (2\pi)^2 \int_0^\infty f^2 \, \Phi_{ii} \, df \quad . \tag{5-15}$$

Since the noise was assumed to be composed of step functions of random and independent amplitudes spaced T seconds apart, the spectrum of the noise will have the form $(\sin x/x)^2$, with the first zero at $1/2T$ cps. For simplicity assume that the noise has a rectangular spectrum with cutoff frequency of $1/2T$ cps. The power-density spectrum of the noise has the following relation to the mean-square noise:

$$\Phi_{nn}(f) = 2T \, \overline{n^2} \quad . \tag{5-16}$$

Combining Eqs. (5-13) through (5-16) and normalizing the noise spectrum with respect to the mean-square input, we obtain

$$\frac{\Phi_{nn}}{\displaystyle\int_0^\infty \Phi_{ii} \, df} \propto 2T \, H_\ell^2 \, \frac{\displaystyle\int_0^\infty f^2 \, \Phi_{ii} \, df}{\displaystyle\int_0^\infty \Phi_{ii} \, df} \quad , \quad \text{for} \quad f < \frac{1}{2T} \text{ cps} \quad . \tag{5-17}$$

For convenience, represent

$$H_\ell^2 \, \frac{\displaystyle\int_0^\infty f^2 \, \Phi_{ii} \, df}{\displaystyle\int_0^\infty \Phi_{ii} \, df}$$

by the symbol c_1^2. If our assumptions are correct, the measured magnitude of the noise spectrum, c_n^2, should be proportional to c_1^2.

We can determine the extent to which (5-17) accounts for variations in the magnitude of the noise spectrum by plotting, as in Fig. 5-8, measured values of c_n^2 against values of c_1^2. The computations of c_1^2 are summarized in Appendix A. Most of the points lie near the line of unity slope, indicating that the measured magnitude of the noise spectrum, c_n^2, is approximately proportional to c_1^2. The correlation between values of c_n^2 and c_1^2 in db is 0.87. Therefore, it appears that Eq. (5-17) has approximately the proper form and accounts for most of the variance in c_n^2.

A slightly better approximation to c_n^2 can be obtained if we take into account the fact that the noise bandwidth actually increases with increasing input bandwidth. With one assumption added to the list — that the noise bandwidth is equal to the undamped natural frequency f_n — we can derive the following relation:

$$\frac{\Phi_{nn}}{\displaystyle\int_0^\infty \Phi_{ii} \, df} \propto \frac{H_\ell^2}{f_n} \, \frac{\displaystyle\int_0^\infty f^2 \, \Phi_{ii} \, df}{\displaystyle\int_0^\infty \Phi_{ii} \, df} \quad . \tag{5-18}$$

Fig. 5-8. c_n^2, measured magnitude of noise power density spectrum, vs c_1^2, $H_\ell^2 \left(\int_0^\infty f^2 \Phi_{ii} \, df \middle/ \int_0^\infty \Phi_{ii} \, df \right)$, for all compensatory results.
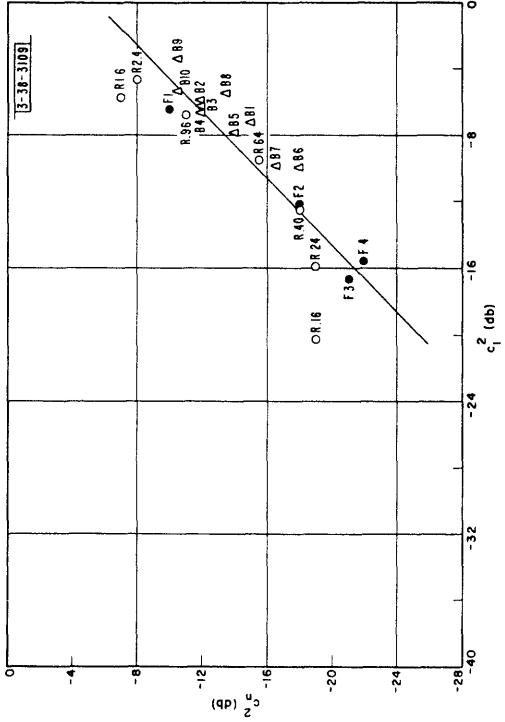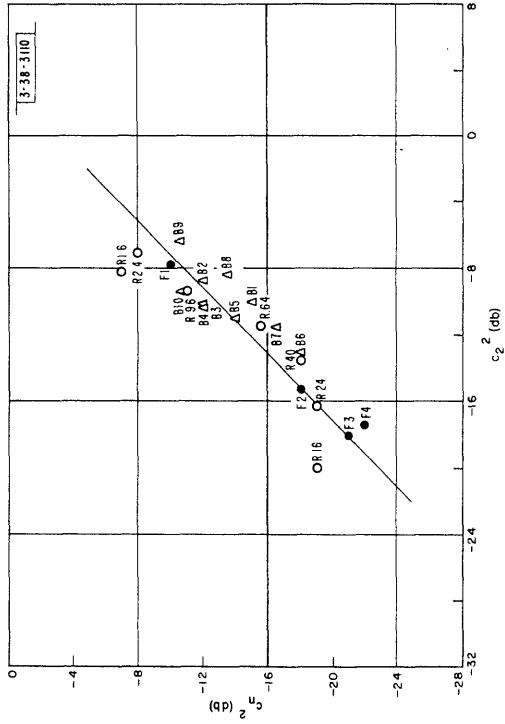
Fig. 5-9. c_n^2, measured magnitude of noise power density spectrum, vs c_2^2, $(H_\ell^2 / f_n) \left(\int_0^\infty f^2 \Phi_{ii} \, df \middle/ \int_0^\infty \Phi_{ii} \, df \right)$, for all compensatory results.
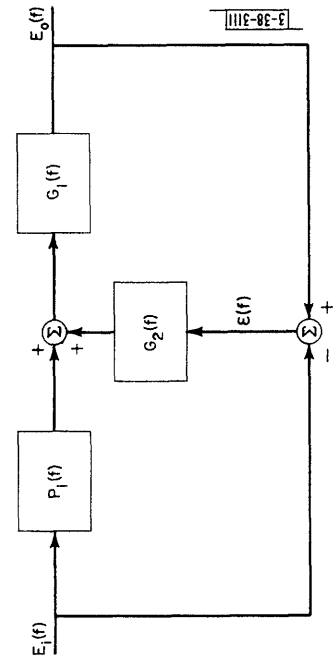

Fig. 5-10. Alternative block diagram for pursuit system. The noise sources of Fig. 2-3 are not represented.

104

For convenience, represent

$$\frac{H_{\ell}^2 \int_0^{\infty} f^2 \, \Phi_{ii} \, df}{f_n \int_0^{\infty} \Phi_{ii} \, df}$$

by the symbol c_2^2.

In Fig. 5-9, measured values of c_n^2 in db are plotted against values of c_2^2 in db. The computations are summarized in Appendix A. Most of the points lie near the line of unity slope. The correlation between values of c_n^2 and c_2^2 is 0.90. Hence, (5-18) is slightly superior to (5-17).

From fairly simple assumptions we have been able to derive relations that have approximately the correct form and account for most of the variance in the measured values of c_n^2. The basic assumption in the derivation was that the noise spectrum $\Phi_{nn}(f)$ is a result of a random disturbance and not a result of system nonlinearities. The fact that such an assumption leads to an effective model suggests that at least a large fraction of the noise may actually result from random disturbances in the operator's responses.

B. MODELS FOR THE PURSUIT SYSTEM

The human operator's characteristics in a pursuit system can not be represented properly by a single open-loop transfer function operating only on error. As shown in Fig. 2-3, two transfer functions are required: $P_i \, G_1(f)$ operates on the input, and $G_2 \, G_1(f)$ operates on the error. However, these two transfer functions can not be determined from measurements of only input and output. A second input signal added to the error and additional measurements, such as those outlined in Sec. II, would be required to determine the transfer functions.

At the time the experimental part of this study was being planned, our major interest was to obtain results that would allow direct comparison of pursuit and compensatory systems. We could not be sure that the addition of a second input would not affect the human operator's characteristics in the pursuit system. Also we did not know at that time that we would be so successful in deriving open-loop models for the compensatory system, and we could not anticipate that similar models could be derived for the pursuit system had we measured $P_i \, G_1(f)$ and $G_2 \, G_1(f)$. Rather than risk altering the characteristics, the decision was made to limit the experiments to ordinary pursuit systems, i.e., only one input signal.

As a result, we cannot develop analytic models for the human operator in the pursuit system that are as complete as those developed for the compensatory system. However, from the closed-loop characteristics and from some auxiliary measurements, we have been able to postulate models, which provide fair approximation to the system characteristics, and to establish bounds on the characteristics of some of the elements of these models.

1. Model for Closed-Loop Transfer Functions

The block diagram of Fig. 2-3 can be put into the equivalent form shown in Fig. 5-10. $G_1(f)$ represents certain limiting or inherent characteristics, which ultimately restrict the human operator's
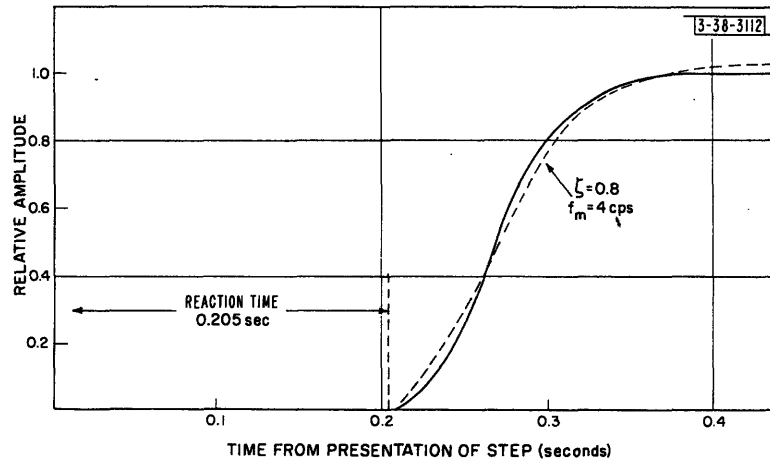
Fig. 5-11. Step function response of pursuit system. The approximation by Eq.(5-19) is shown by the dash lines.
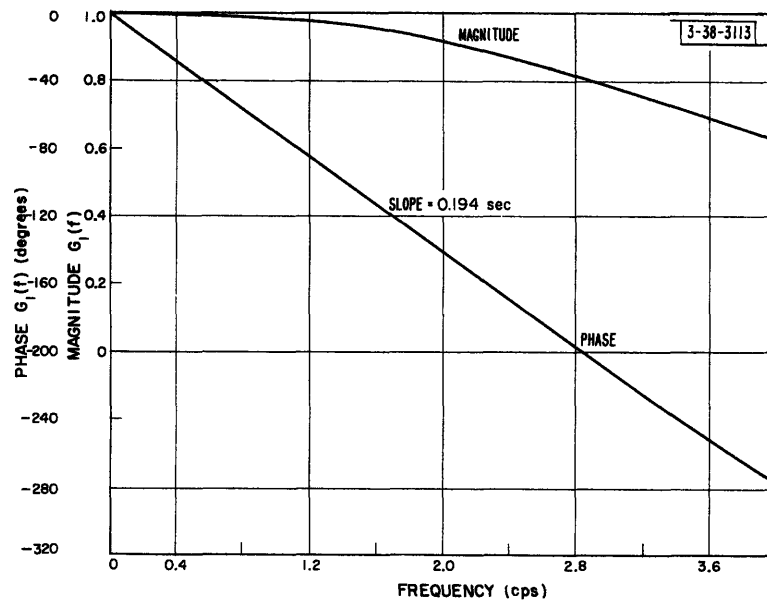

Fig. 5-12. Magnitude and phase $G_1(f)$ determined from step response.

106

tracking performance, such as his delay and the maximum bandwidth of the visual and motor systems. $P_i(f)$ is a predictor whose function is to estimate the future of the input in order to correct for the lags and delays introduced by $G_1(f)$. The purpose of $G_2(f)$ is similar to that of the open-loop transfer function of the compensatory system; that is, to provide feedback and reduce noise and error. Note that if $P_i G_1(f) = 1$, the signal part of the error is zero. In this case $G_2(f)$ operates only on the noise and does not affect the signal.[32]

a. Inherent Characteristics $G_1(f)$

We can obtain an estimate of $G_1(f)$ by measuring the human operator's response to an input step displacement of known amplitude but unknown time of initiation. By instructing the human operator to respond as fast as possible we can obtain an upper bound on his response characteristics. Once the input displacement has occurred, the signal is completely predictable and the initial response movement essentially is determined by G_1 which represents the human operator's ability to make the quickest response possible. A fast response to a step usually consists of several discrete movements, each of which apparently is completed before the next one is begun.[33] The initial movement seems to be triggered off as a unit and is not altered very much while it is being made. A measurement of only the initial movement of the operator's step response does not include most of the effects of feedback, and therefore should provide an estimate of $G_1(f)$.

Figure 5-11 shows the average response to a step of 1.5 inch amplitude obtained from seven trials with one of the subjects in the pursuit system. A fairly good approximation to the measured response is provided by the time function whose Fourier transform is

$$\frac{G_1(f)}{2\pi jf} = \frac{e^{-2\pi jf\alpha}}{2\pi jf} \frac{1}{\left(\frac{jf}{f_m}\right)^2 + 2\zeta\left(\frac{jf}{f_m}\right) + 1} \quad , \tag{5-19}$$

where α is 0.205 second, f_m is 4.0 cps and ζ is 0.8. The magnitude and phase of $G_1(f)$ is plotted in Fig. 5-12, and the time function corresponding to (5-19) is shown by the dash-line in Fig. 5-11. Actually, the constant of proportionality in the numerator of (5-19) is indeterminate because $G_1(f)$ represents the transformation of some internal signal, i.e., neural impulse, to human-operator hand movement. The composite transfer function $P_i G_1(f)$, of course, has determinate gain which tends to be close to unity. For convenience, we have taken the proportionality constant of (5-19) to be equal to unity.

The delay determined in this experiment probably is not a good value for the delay in a continuous tracking situation. For a discrete stimulus, the delay is likely to be longer than for a continuous stimulus. Since the human operator's tasks in pursuit and compensatory systems are similar, we can use the value determined for the compensatory delay, 0.13 second, in the pursuit model. Doing this, we have the following relation for $G_1(f)$:

$$G_1(f) = \frac{e^{-2\pi jf(0.13)}}{\left(\frac{jf}{4}\right)^2 + 1.6\left(\frac{jf}{4}\right) + 1} \quad . \tag{5-20}$$

Figure 5-12 shows that at low frequencies the quadratic of (5-20) acts like a delay of 0.064 second. Therefore, $G_1(f)$ is essentially a delay of 0.194 second at low frequencies.

b. Feedback $G_2(f)$

We do not have sufficient data to make very precise statements about $G_2(f)$. However, since the function of $G_2(f)$ is similar to that of the open-loop transfer function of the compensatory system, both are likely to have similar properties and to be approximated by analytic functions of the same form. The delay has been included in $G_1(f)$, and therefore $G_2(f)$ can probably be approximated by the following function:

$$G_2(f) = \frac{K}{\left(\frac{jf}{f_o} + 1\right)\left(\frac{jf}{f_1} + 1\right)} \quad . \tag{5-21}$$

Because there are two channels for signal flow in the pursuit system, the requirements on $G_2(f)$ are less stringent than those on the open-loop transfer function for the compensatory system. We would expect the gain and bandwidth of $G_2(f)$ to be lower than in the compensatory system, but we do not know what values these quantities have.

c. Predictor $P_i(f)$

The characteristics of $P_i(f)$ depend upon $G_1(f)$, the noise generated by the human operator, and the statistical characteristics of the input signal. We can assume that, subject to the restrictions imposed by these factors, the human operator tries to adjust $P_i(f)$ so as to minimize his tracking error. The error criterion that the human operator uses to adjust $P_i(f)$ depends upon the instructions that he is given and upon the nature of the task. The form of $P_i(f)$ and its ability to act as an optimum predictor are limited by the human operator's capacity for perceiving high derivatives of the input and by the very limited bandwidth of the visual system.

A first approximation to $P_i(f)$ can be obtained if we make the assumptions that (1) the human operator adjusts $P_i(f)$ so that it best corrects for the lags and delays introduced by $G_1(f)$ with minimum mean-square error; (2) the human operator makes use of only input displacement and velocity to predict the input; (3) the human operator does not consider his own noise when establishing the optimum $P_i(f)$; and (4) $G_2(f)$ can be neglected when computing the optimum $P_i(f)$. These assumptions were made for the following reasons. In a simple tracking task, the mean-square error criterion is probably a close approximation to the human operator's actual-error criterion, and it is the most tractable criterion to use with random signals. The visual system can perceive displacement with good accuracy and velocity with fair accuracy, but is not well suited to measuring acceleration or higher derivatives. The noise is neglected to simplify the computation of the optimum $P_i(f)$. If the magnitude of Φ_{nn} is small, we probably will not introduce important errors by making this simplification.

Neglecting $G_2(f)$ simplifies the calculations for $P_i(f)$. If $P_i G_1(f)$ is approximately unity, $G_2(f)$ does not affect greatly the system's response to the input, and the computed $P_i(f)$ should not be affected very much.

Under these assumptions, the low-frequency part of $P_i(f)$ can be approximated by the relation

$$P_i(f) = b_0 + b_i(2\pi jf) \quad , \tag{5-22}$$

where b_0 and b_i are adjusted for minimum mean-square error between system input and output with a particular combination of input signal and transfer function $G_1(f)$. At high frequencies where the visual process loses its ability to perceive target motion, $P_i(f)$ must go to zero. However, because there are no terms involving $2\pi jf$ in the denominator, (5-22) does not go to zero. As long as we consider only low frequencies, this inconsistency in (5-22) is not important, and it is not necessary to complicate the calculations for $P_i(f)$ by including terms in the denominator.

2. Comparison of Pursuit Model and Measured Closed-Loop Transfer Functions

The parameters of the optimum $P_i(f)$, (5-22), have been computed (Appendix A) for the RC Filtered Spectra and for the Rectangular Spectra. $G_1(f)$ was approximated by a pure delay of 0.194 second in these calculations. Knowing $P_i(f)$ and $G_1(f)$, we can compute an approximate closed-loop transfer function $P_i G_1(f)$ and compare it with the measured closed-loop characteristics $H(f)$.

Comparison of the computed transfer functions of Figs. 5-13 and 5-14 with the corresponding measured functions of Figs. 4-9 and 4-14 shows that for Rectangular Inputs, the agreement between measured and computed is fair for low bandwidths but deteriorates for high-bandwidth inputs. For bandwidths greater than 0.96 cps the agreement is very poor. This is to be expected, since the calculations for $P_i(f)$ were based on the assumptions that the tracking task was simple and that the error and noise were small. These assumptions are not valid for inputs having bandwidths greater than 0.96 cps, and therefore the calculated transfer functions have not been plotted.

The agreement between measured and calculated transfer functions is better for the RC Filtered Inputs and, in particular, for Input F1. The optimum $P_i(f)$ for F1 is simply an attenuation (see Appendix A). If the human operator is acting in the optimum fashion, the closed-loop phase lag will be linear with frequency. In Fig. 5-15 are shown measured and computed phase for F1 plotted against linear frequency. Note that the measured phase shift is very nearly linear with a slope of 0.210 second. The fact that this delay is almost equal to that produced by $G_1(f)$ (0.194 second), which was obtained from step-response tests and from the compensatory results, provides some confirmation of the validity of the analytic expression for $G_1(f)$.

Almost always, the phase of $P_i G_1(f)$ is considerably less than the measured phase of $H(f)$, indicating that the prediction obtained by the human operator does not approach the optimum very closely. Probably his estimate of input displacement and velocity is degraded by noise or errors introduced by the visual process. Since the best agreement between measured and computed results was obtained with Input F1, which does not require velocity information for prediction, it is likely that the human operator's estimate of displacement is fairly accurate but that his estimate of velocity and higher input derivatives is inaccurate. If we were to take into account the measurement noise introduced by the visual system, a better approximation to the measured characteristics could probably be made. However, we do not know the magnitude or the spectrum of the visual noise. Until measurements are made which provide this information and which reveal more completely the characteristics of $P_i(f)$, $G_1(f)$ and $G_2(f)$, we cannot hope to derive more accurate analytic models for the pursuit system.
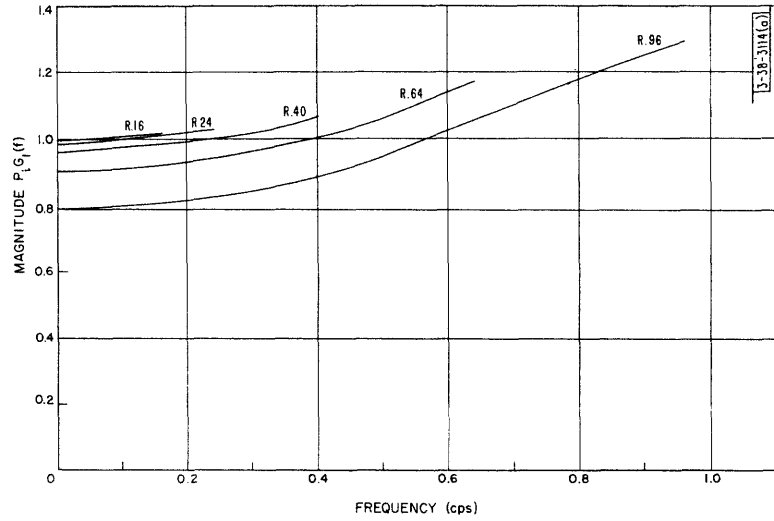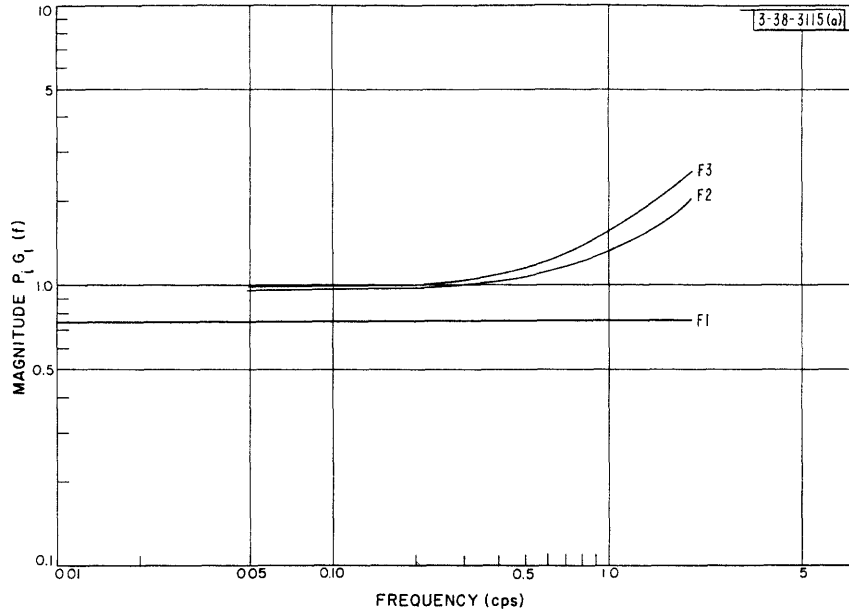
(a)
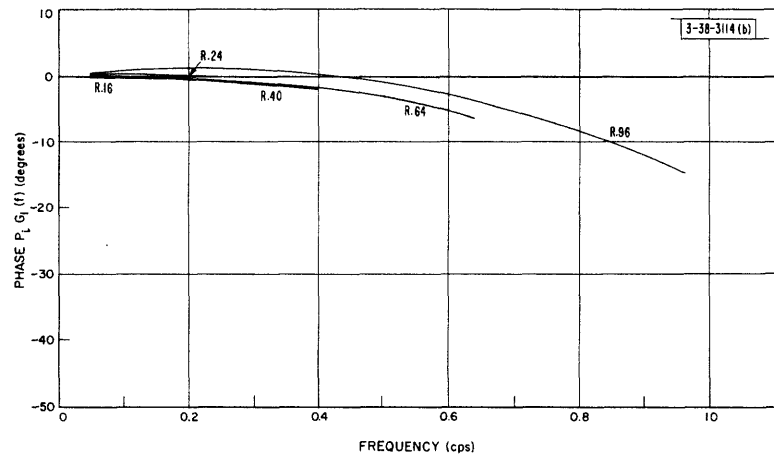
(b)

Fig. 5-13. Calculated magnitude (a) and phase (b) of $P_i G_1(f)$ for Rectangular Spectra.
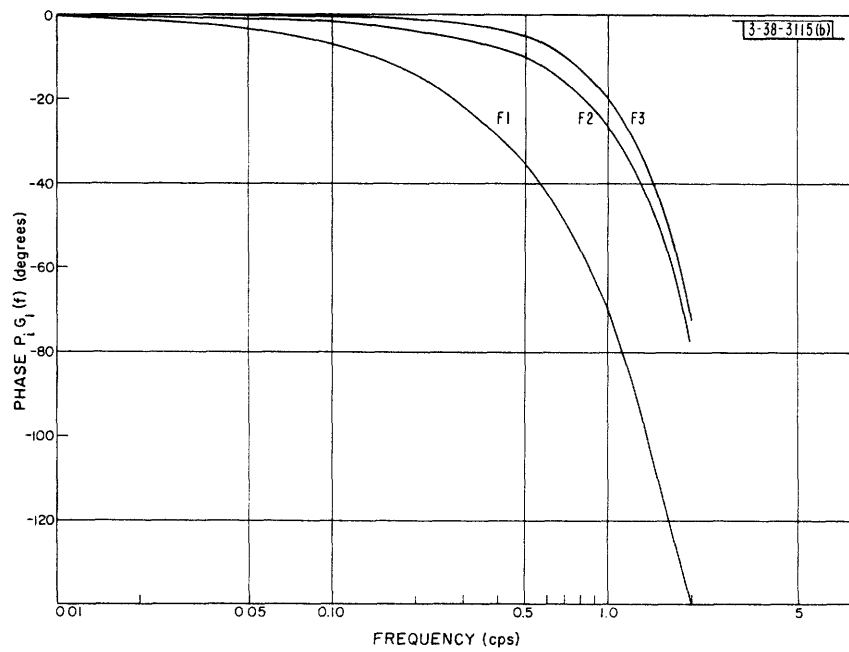
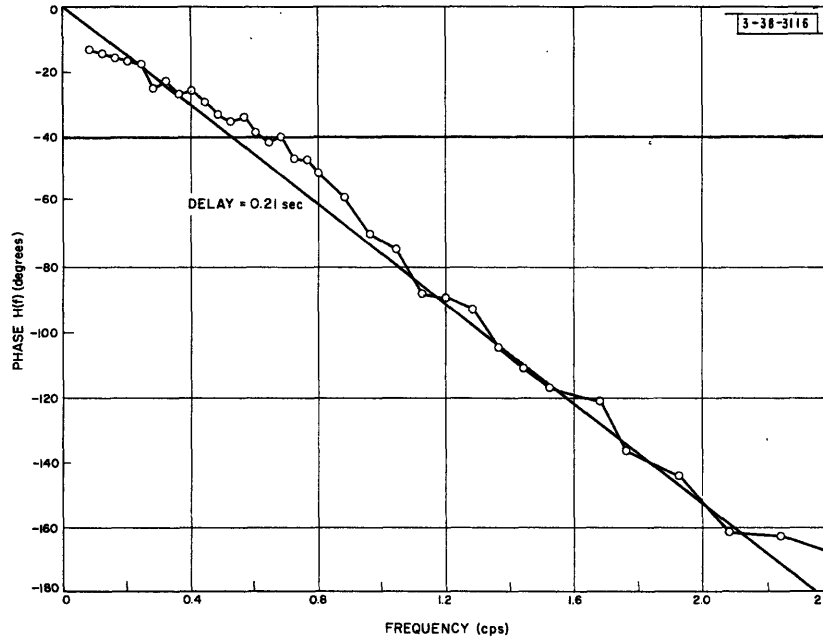Fig. 5-14. Calculated magnitude (a) and phase (b) of $P_i\, G_1(f)$ for RC Filtered Spectra.

111

Fig. 5-15. Measured phase of H(f) obtained with Input F1 in the pursuit system.
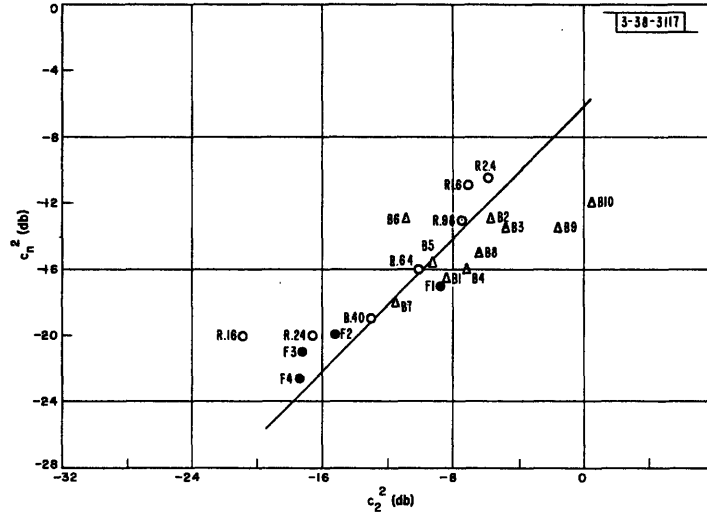

Fig. 5-16. c_n^2, measured magnitude of noise power spectrum, vs c_2^2,

$$(H_\ell^2/f_n)\left(\int_0^\infty f^2 \Phi_{ii}\, df \middle/ \int_0^\infty \Phi_{ii}\, df\right), \text{for all pursuit results.}$$

3. <u>Model for Pursuit Noise</u>

The expression (5-18) derived for the magnitude of the noise spectrum in the compensatory system can be applied to the pursuit system. The assumptions made in the derivation can also be made for the pursuit system as well as for the compensatory. In Fig. 5-16 are plotted measured values for the magnitude of the noise spectrum, c_n^2, against computed values, c_2^2 (5-18). The computations are summarized in Appendix A.

Except for bandpass Inputs B9 and B10 and Rectangular Input R.16 the plotted points are fairly well distributed about the line of unity slope. The correlation of all the points is 0.843, which indicates that (5-18) accounts for more than half the variance in the measured magnitude of the noise spectrum. It would not be unreasonable to disregard the points corresponding to Inputs B8 and B9, since the noise spectra for these signals are highly peaked in the neighborhood of the bandpass region. Probably much of this noise is phase- or frequency-modulation noise resulting from the human operator's attempts to track the center frequency of the input.

The assumptions used in deriving (5-18) therefore do not apply to this part of the noise of B9 and B10, and we should not expect good agreement. The fact that the same relation for the noise approximates reasonably well both pursuit and compensatory systems provides some confirmation that the expression is a valid one.

VI. CONCLUSIONS

The experimental results show that for a wide variety of input signals a good description of the characteristics of simple manual control systems is provided by quasi-linear transfer functions. Except for high-speed inputs, these functions account for a very large fraction of the power in the system output and appear to be an invariant and stable description of the system. The family of quasi-linear transfer and other associated functions obtained from the experiments provides a fairly complete description of the system characteristics over the range of input-signal characteristics studied. Since simple systems were used in these tests, the characteristics obtained represent, in a certain sense, an upper bound on human-operator performance. As such, they should be useful in the design of manual control systems.

The analytic models, particularly those derived for the compensatory system, probably constitute the most important contribution of this study. For the compensatory system, the models are simple and highly developed. They provide a good description of the system characteristics in terms of only a few parameters. These parameters are simply related to parameters of the input signal which describe its predictability and the location of its power spectrum on the frequency scale. For the pursuit system, only a very approximate model has been developed. The experimental results were not sufficient to reveal accurately the nature of the components of the model. Therefore, it was not possible to derive accurate relations among the parameters of the model and of the input.

The fact that the parameters of the compensatory system were related to the input parameters indicates that the structure of the family of system characteristics is well defined. This suggests that the human operator's characteristics in the pursuit system, and even in more complicated manual control systems, are likely also to have a structure that can be determined. Future work in the field of tracking could profitably be directed toward discovering the structure of the human operator's characteristics in such systems.

On the basis of the results obtained with simple systems, certain general statements about the performance of manual systems can be made. Pursuit systems are superior to compensatory systems because the human operator has more complete information about the input signal. In simple systems, the human operator's characteristics contain a delay that is closely related to the reaction-time delay observed in responses to discrete stimuli. In pursuit systems, when the input is predictable, the human operator is able to correct for much of this delay more completely than in compensatory. Furthermore, the presence of high-frequency components in the input degrades the performance of both systems at all frequencies.

General rules for applying the results and models obtained in this study to the design of actual control systems are difficult to formulate. The reason is that many important features of an actual control situation are likely not to correspond to those of our experimental situations. The display, control, system dynamics, input signals, ability of the human operator, etc., may differ in certain important respects from those in our systems. As a consequence, we can not expect to be able to predict with high accuracy the absolute performance of systems that are different. However, we would expect that if we perform a few tests on the actual system in order to obtain

a calibration between the behavior of the experimental system and the behavior of the actual system, we could predict with good accuracy the effects upon system characteristics of modifications in the actual tracking situation. We can be fairly confident that changes in the actual situation would affect system performance in much the same manner that corresponding changes affected the performance of our experimental situation. Of course, as the differences between experimental and actual situations become greater, the range of conditions for which the calibration between the two systems would be useful is diminished, and more tests with the actual system under various conditions would be required to predict its performance over the range of conditions of interest. Thus, although we may not be able to predict well the absolute performance of actual systems, we can predict better their relative performance. As more data are obtained that reveal the interactions between system behavior and the characteristics of other elements of the control situation, such as the control, system dynamics, etc., we should be able to predict performance of actual systems over a much wider range of conditions than is possible at present.

REFERENCES

1. J.W. Senders and M. Cruzen, "Tracking Performance on Combined Compensatory and Pursuit Tasks," Technical Report 52-39, Wright Air Force Base, Ohio (February 1952).

2. E.C. Poulton, "Perceptual Anticipation in Tracking with Two-pointer and One-pointer Displays," Brit. Jour. Psychol. 43, 222 (1952).

3. L. Russell, "Characteristics of the Human as a Linear Servo-Element," Master's Thesis, Electrical Engineering Department, M.I.T. (June 1951).

4. J.I. Elkind, "Tracking Response Characteristics of the Human Operator," Memorandum 40, Human Factors Operations Research Laboratories, Air Research and Development Command, USAF, Washington, D.C. (September 1953).

5. A. Tustin, "The Nature of the Operator's Response in Manual Control and Its Implications for Controller Design," Jour. Inst. Elec. Engrs. (London) 94, Part IIA, 190 (1947).

6. C. E. Walston and C.E. Warren, "A Mathematical Analysis of the Human Operator in a Closed-loop Control System," Research Bulletin, AFPTRC-TR-54-96, Air Force Personnel and Training Research Center, Lackland Air Force Base, San Antonio, Texas (1954).

7. E.S. Krendel and G.H. Barnes, "Interim Report on Human Frequency Response Studies," Technical Report 54-370, Air Materiel Command, USAF, Wright Air Development Center, Ohio (June 1954).

8. D.G. Ellson and F. Gray, "Frequency Response of the Human Operators Following a Sine Wave Input," Memorandum Report MCREXD 694-2H, Air Materiel Command, USAF, Wright Field, Ohio (22 December 1948).

9. R. Mayne, "Some Engineering Aspects of the Mechanism of Body Control," Electrical Engineering 70, 207 (March 1951).

10. R. Chernikoff and F.V. Taylor, "Reaction Time to Kinesthetic Stimulation Resulting from Sudden Arm Displacement," NRL Report 3887, Naval Research Laboratory, Washington, D.C. (19 November 1951).

11. W.E. Hick, "Man as an Element in a Control System," Research 4, 112 (1951).

12. D.G. Ellson and L. Wheeler, "The Range Effect," Technical Report 5813, Air Materiel Command, USAF, Wright-Patterson Air Force Base, Ohio (May 1949).

13. R.S. Woodworth and H. Schlosberg, Experimental Psychology (Holt, New York, 1954), pp. 8-42.

14. W.E. Hick, "The Discontinuous Functioning of the Human Operator in Pursuit Tasks," Quart. Jour. Exptl. Psychol. 1, 38 (1948).

15. K.J.W. Craik, "Theory of the Human Operator in Control Systems: I. The Operator as an Engineering System," Brit. Jour. Psychol. 38, 56 (1947).

16. M.A. Vince, "The Intermittency of Control Movements and the Psychological Refractory Period," Brit. Jour. Psychol. 38, 149 (1948).

17. J.A.V. Bates, "Some Characteristics of the Human Operator," Jour. Inst. Elec. Engrs. (London) 94, Part IIA, 298 (1947).

18. J.D. North, "The Human Transfer Function in Servo Systems," Automatic and Manual Control (Butterworths Scientific Publications, London, 1952), pp. 473-501.

19. K. Chen, "Quasi-Linearization Techniques for Transient Study of Nonlinear Feedback Control Systems," Trans. A.I.E.E., Applications and Industry 22, 354 (1956).

20. M.V. Mathews, "A Method for Evaluating Nonlinear Servomechanisms," Trans. A.I.E.E., Applications and Industry 74, 114 (1955).

21. R.C. Booton, "Nonlinear Servomechanisms with Random Inputs," Technical Report No. 70, Dynamic Analysis and Control Laboratory, M.I.T. (August 1953).

22. M. Levine, "Tracking Performance as a Function of Exponential Delay Between Control and Display," Technical Report 53-23, Wright Air Development Center, Wright-Patterson Air Force Base, Ohio (October 1953).

23. W.H. Huggins, "Memo on the Experimental Determination of Transfer Functions of Human Operators and Machines," Memorandum E-4070, Cambridge Field Station, Air Materiel Command, Cambridge, Mass. (1949).

24. Y.W. Lee, "Applications of Statistical Methods to Communication Problems," Technical Report No. 181, Research Laboratory of Electronics, M.I.T. (1950).

25. H.M. James, N.B. Nichols and R.S. Phillips, Theory of Servomechanisms (McGraw-Hill, New York, 1947), pp. 262-368.

26. M.S. Bartlett, Stochastic Processes (University Press, Cambridge, 1955), pp. 1-14.

27. R.C. Booton, personal communication (1956).

28. J.W. Tukey, "The Sample Theory of Power Spectrum Estimates," Symposium on Applications of Autocorrelation Analysis to Physical Problems, ONR Publication NAVEXOS-P-735 (1949).

29. D.T. Ross, "Improved Computational Techniques for Fourier Transformation," Report 7138-R-5 Servomechanisms Laboratory, M.I.T. (25 June 1954).

30. S.O. Rice, "Mathematical Analysis of Random Noise," Bell System Tech. Jour. 24, 1 (1945).

31. H.W. Bode, Network Analysis and Feedback Amplifier Design (Van Nostrand, New York, 1945), pp. 303-336.

32. G. Lang and J.M. Ham, "Conditional Feedback Systems: A New Approach to Feedback Control," Trans. A.I.E.E., Applications and Industry 74, 152 (1955).

33. W.E. Hick and J.A.V. Bates, "The Human Operator of Control Mechanisms," Permanent Records of Research and Development No. 17.204, British Ministry of Supply (May 1950).

34. F.B. Smith, "Analog Equipment for Processing Randomly Fluctuating Data," Preprint No. 545, Institute of Aeronautical Science (January 1955).

35. W.B. Davenport, Jr., R.A. Johnson and D. Middleton, "Statistical Errors in Measurements on Random Time Functions," Jour. Appl. Phys. 23, 377 (1952).

36. H.M. Walker and J. Lev, Statistical Inference (Holt, New York, 1953).

37. W.G. Cochran and G. Cox, Experimental Designs (Wiley, New York, 1950), pp. 72-74.

UNCLASSIFIED

APPENDIX A
CALCULATION OF MODEL PARAMETERS

I.   COMPENSATORY OPEN-LOOP TRANSFER FUNCTIONS

In Figs. A-1, A-2 and A-3 are shown the magnitude of the open-loop transfer function G(f) and residual phase lag obtained by subtracting from the total phase of G(f) the lag associated with

$$|G_a'(f)| = \left| \frac{K}{\frac{jf}{f_o} + 1} \right| \quad .$$

(A-1)

On each plot of $|G(f)|$ is shown the function $|G_a'(f)|$ which provides the best (visual) approximation to the measured G(f). On each graph of the residual phase is plotted the phase produced by the delay $e^{-2\pi jf a'}$ where a' is chosen to obtain the best (visual) approximation to the measured points. By obtaining a good fit simultaneously in magnitude and phase, to the experimental results, values can be obtained for the three parameters of $G_a'(f)$, the analytic approximation to the measured characteristics.

$$G_a'(f) = \frac{K\, e^{-2\pi jf a'}}{\frac{jf}{f_o} + 1} \quad .$$

(A-2)

The values for the parameters are shown in the graphs of $|G(f)|$.

For the bandpass inputs B3, B8, B9 and B10, the measured characteristics of G(f) were translated down the frequency scale so that the low-cutoff frequency of the pass band was at zero frequency. This procedure enabled us to fit the measured characteristics with functions of the form given in Eq. (A-2).

As explained in Sec. V, with certain low-bandwidth inputs it is necessary to approximate the measured results with the functions $G_a(f)$ in order to obtain a model that will be stable in the closed loop.

$$G_a(f) = \frac{K\, e^{-2\pi jf a}}{\left(\frac{jf}{f_o} + 1\right)\left(\frac{jf}{f_1} + 1\right)} \quad .$$

(A-3)

Only a_{max} and f_{max}, the maximum values for a and f_1, can be obtained from the measured results.

The procedure for finding these maximum values will be illustrated for results obtained with Input R.16. The parameters obtained by fitting $G_a'(f)$ to the measured characteristics are: K equal to 34.5 db, f_o equal to 0.035 cps, and a' equal to 0.64 second. The transfer function $G_a'(f)$ having these parameters would have unstable closed-loop performance. To find the maximum values of a and f_1 of (A-3), we must choose f_1 so that the phase margin of $G_a(f)$ is zero. The necessary value of f_1 can be determined by a cut-and-try procedure in which we select a value of f_1 and see if it leads to zero phase margin.
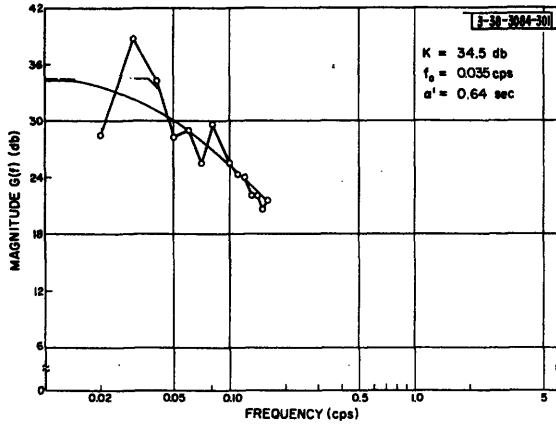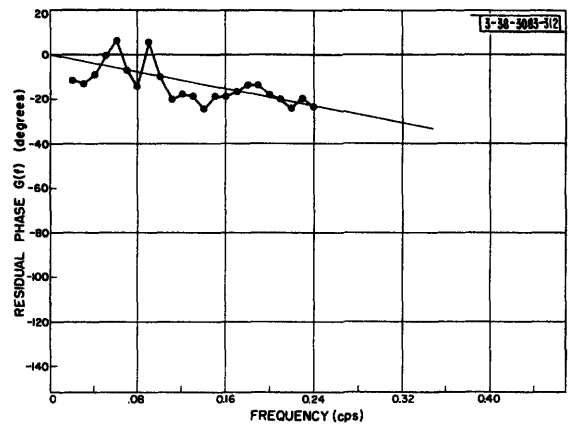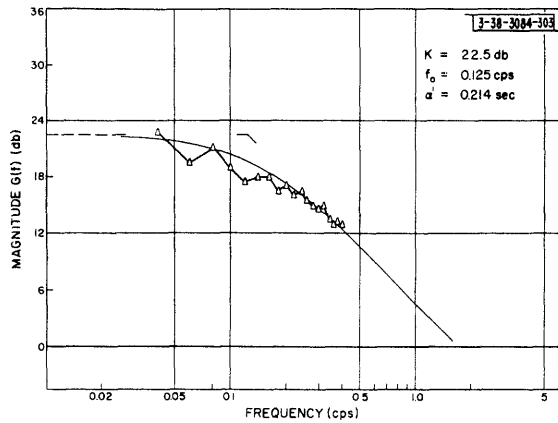
(a) R.16
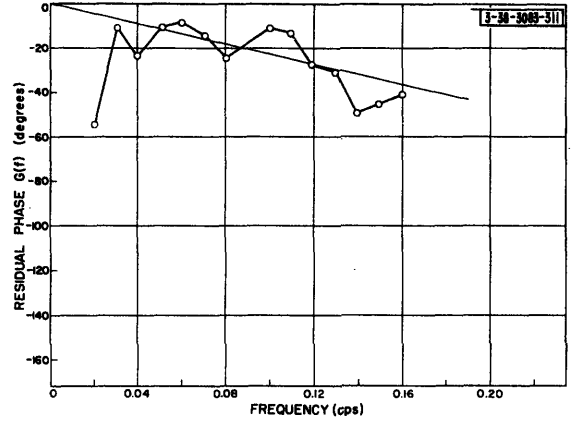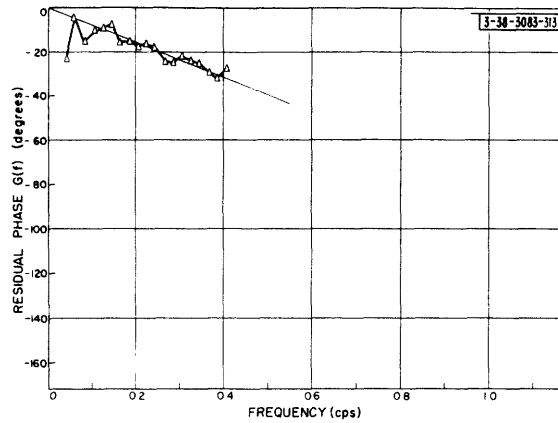
(b) R.16
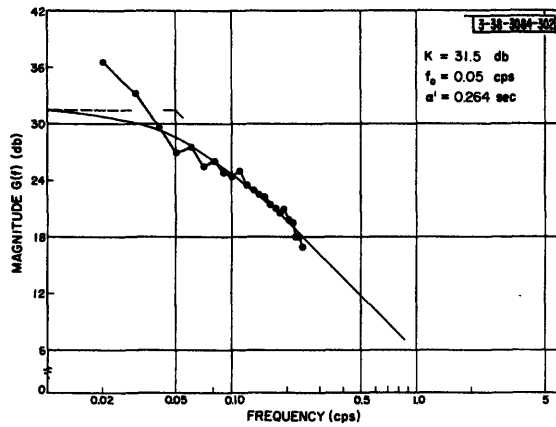
(c) R.24

(d) R.24

Fig.A-1. Magnitude and residual phase of G(f) obtained with Rectangular Spectra. The smooth curves represent the analytic function G'_a (f) which approximates both magnitude and phase of G(f) best.

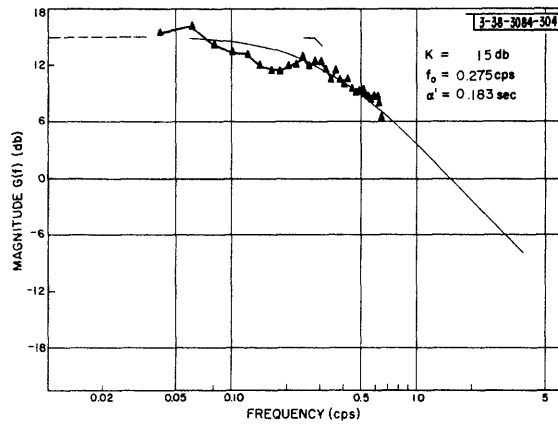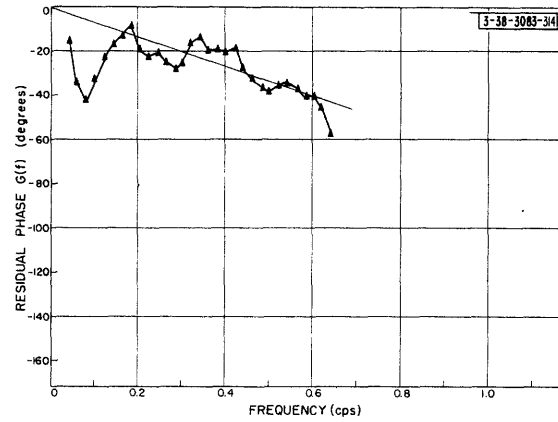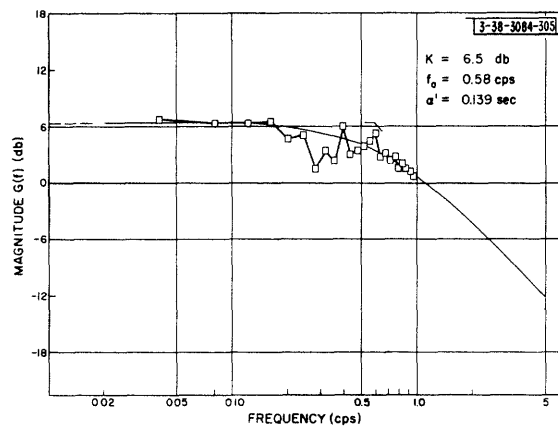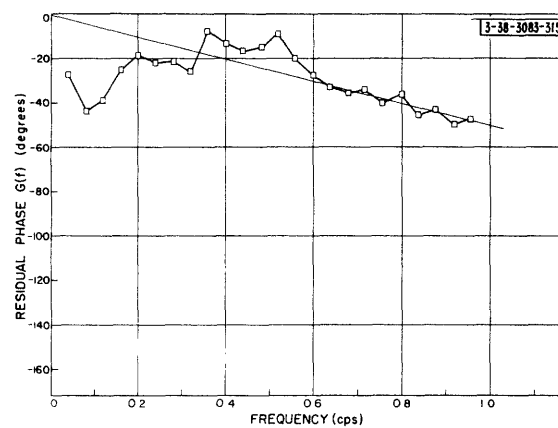$$G'_a (f) = \frac{K \, e^{-2\pi j f a'}}{\left(\dfrac{jf}{f_o} + 1\right)}$$
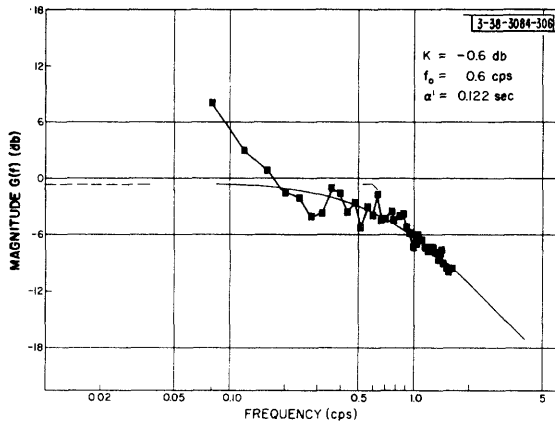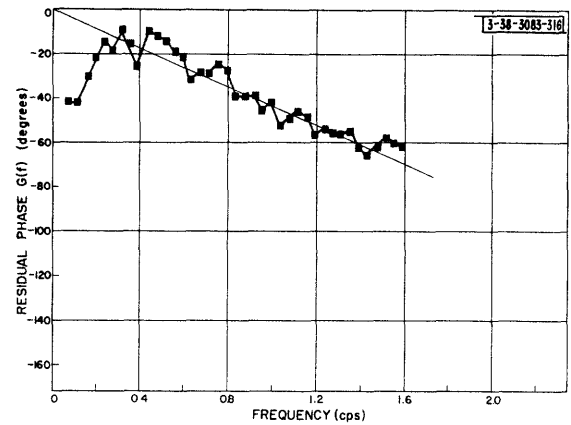
120
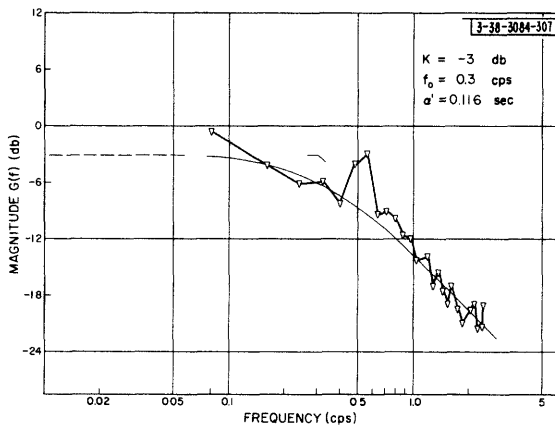
(e) R.40

(f) R.40

(g) R.64
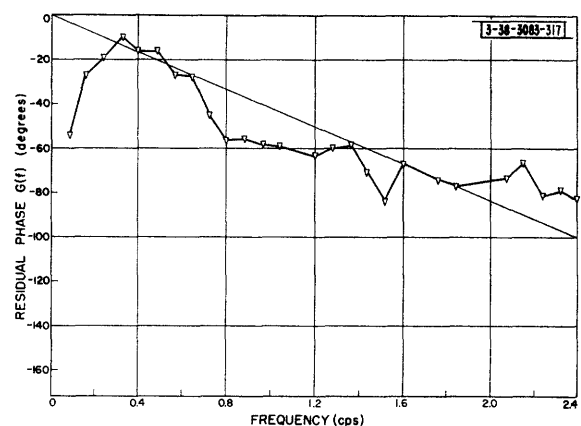
(h) R.64

(i) R.96

(j) R.96

Fig.A-1 (Continued)

121

(k) R 1.6

(l) R 1.6

(m) R 2.4

(n) R 2.4

Fig. A-1 (Continued)

122
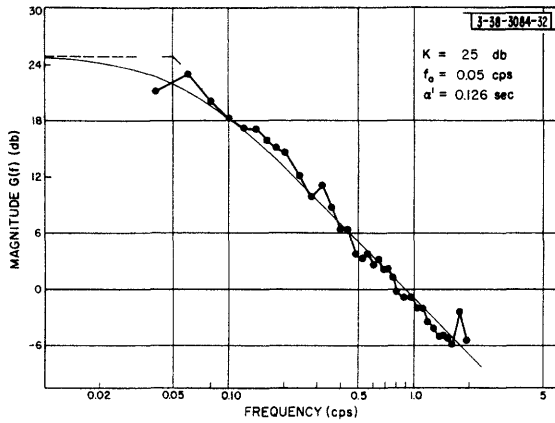
(a) F 2
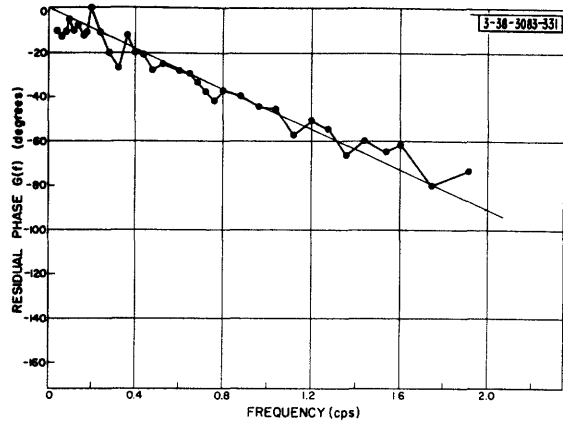
(b) F 2
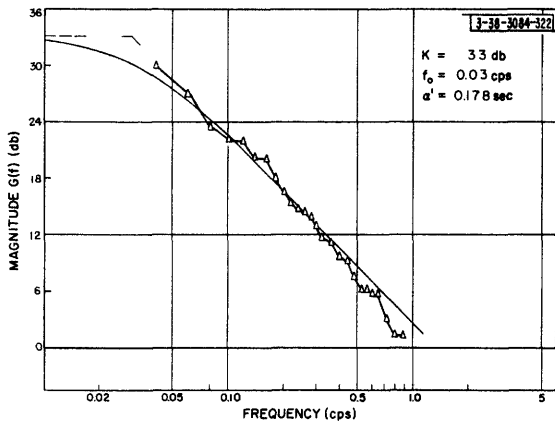
(c) F 3
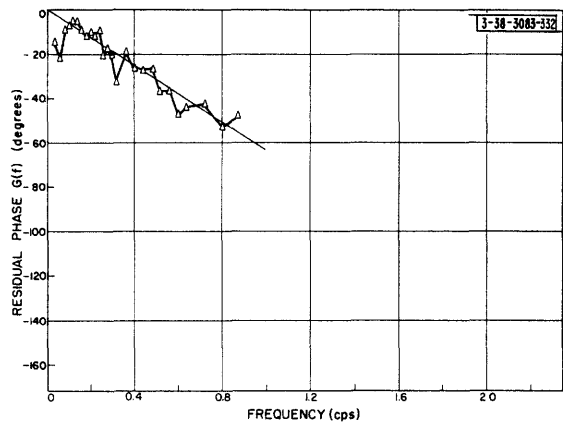
(d) F 3
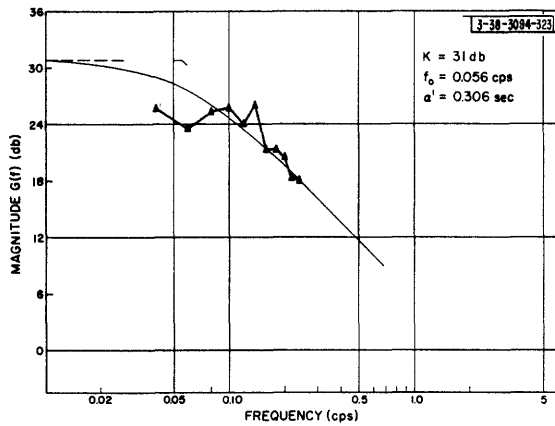
(e) F 4
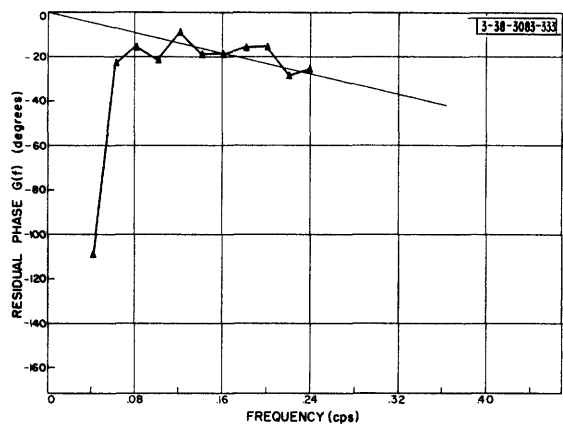
(f) F 4

Fig. A-2. Magnitude and residual phase of G(f) obtained with RC Filtered Spectra. The smooth curves represent the analytic function $G_a'(f)$ which approximates both magnitude and phase of G(f) best.

$$G_a'(f) = \frac{K\, e^{-2\pi j f a'}}{\left(\dfrac{j f}{f_o} + 1\right)}$$

123
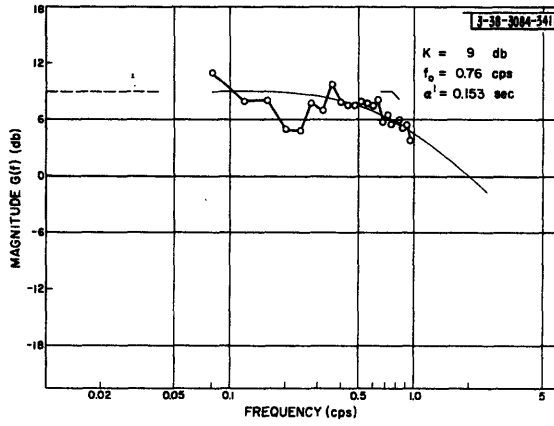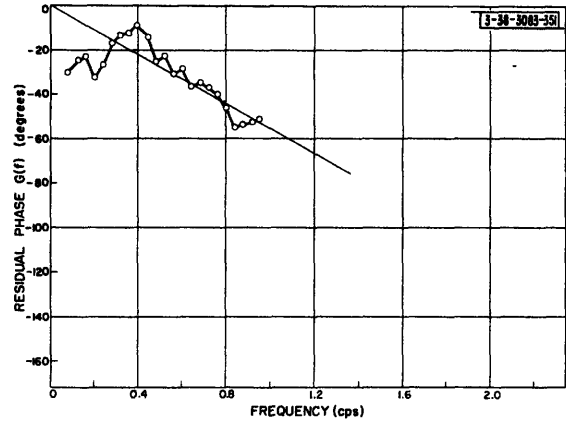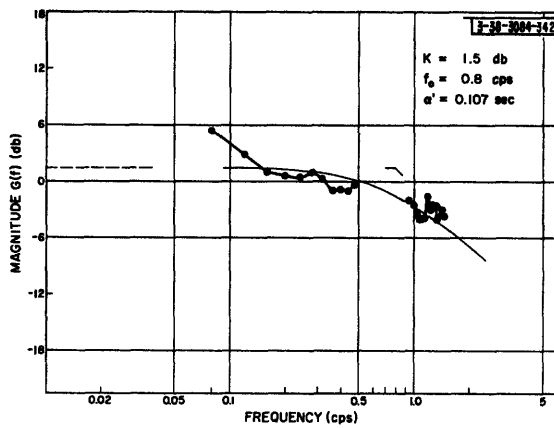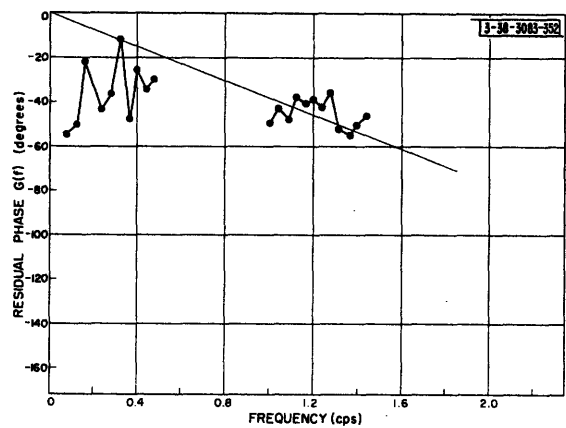
Fig. A-3. Magnitude and residual phase of G(f) obtained with Selected Band Spectra. The smooth curves represent the analytic function G'_a (f) which approximates both magnitude and phase of G(f) best.

$$G'_a (f) = \frac{K e^{-2\pi j f a'}}{\left(\frac{jf}{f_o} + 1\right)}$$

124
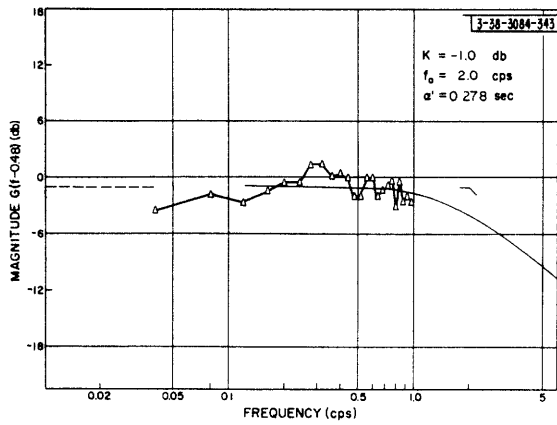
(e) B3
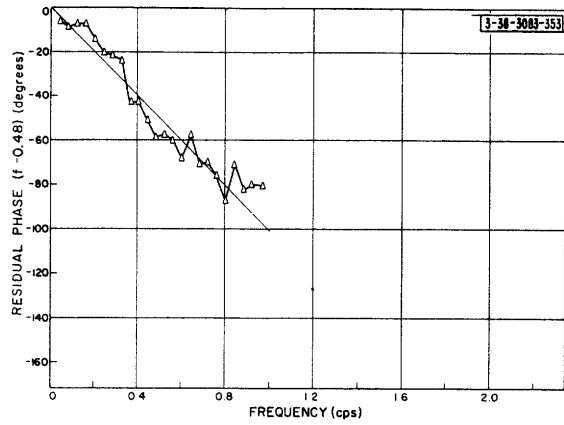
(f) B3
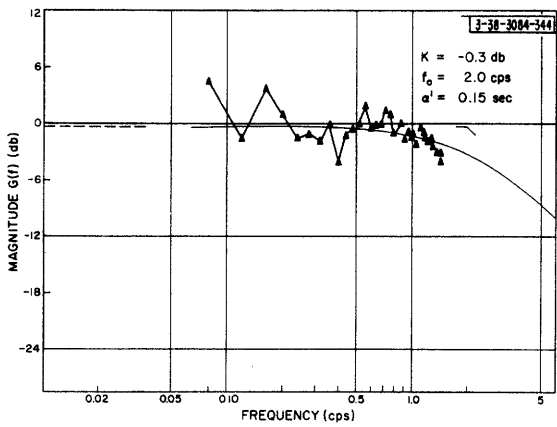
(g) B4
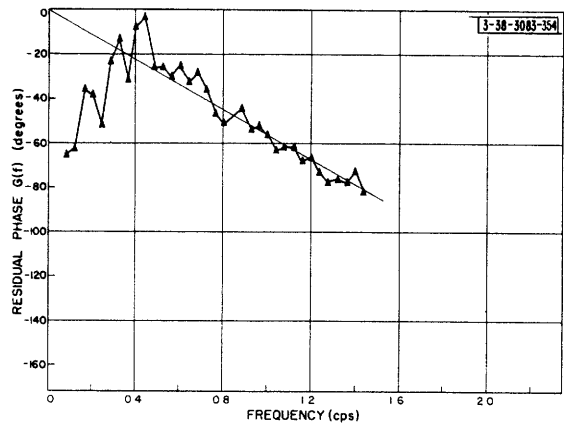
(h) B4
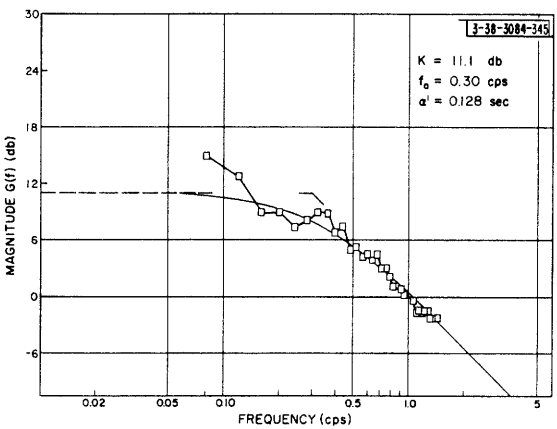
(i) B5
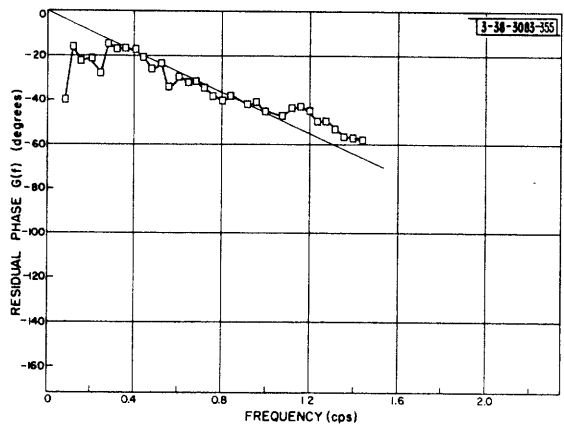
(j) B5

Fig. A-3 (Continued)

125
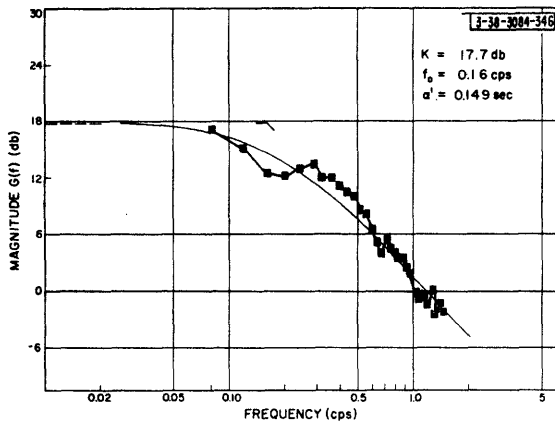
(k) B 6
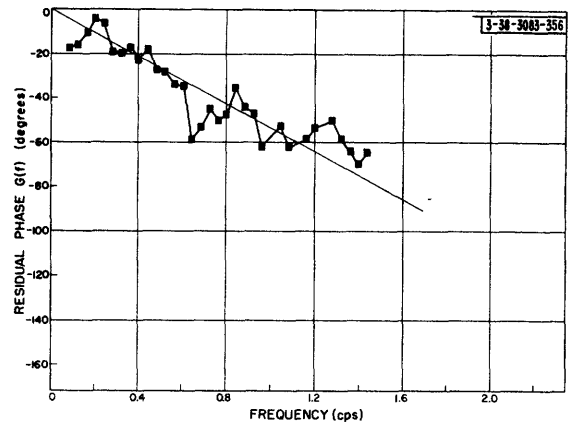
(l) B 6
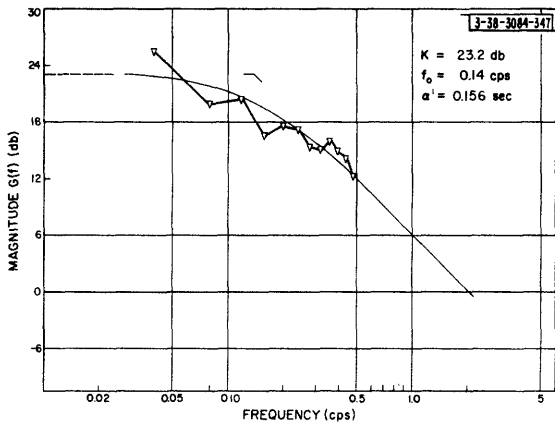
(m) B 7
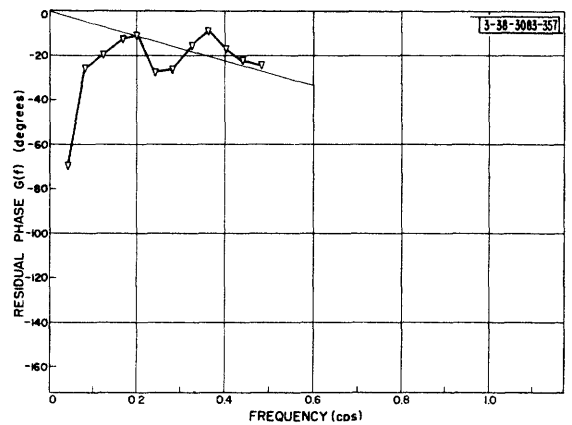
(n) B 7
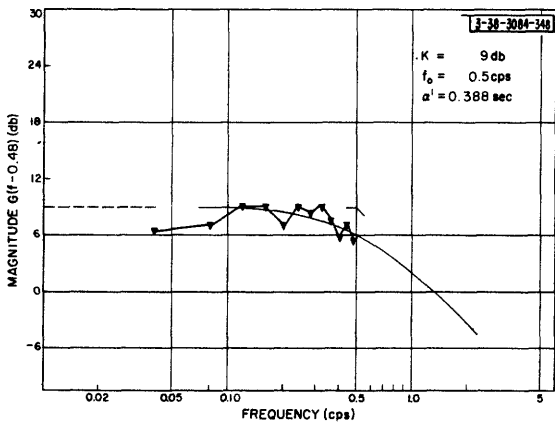
(o) B 8
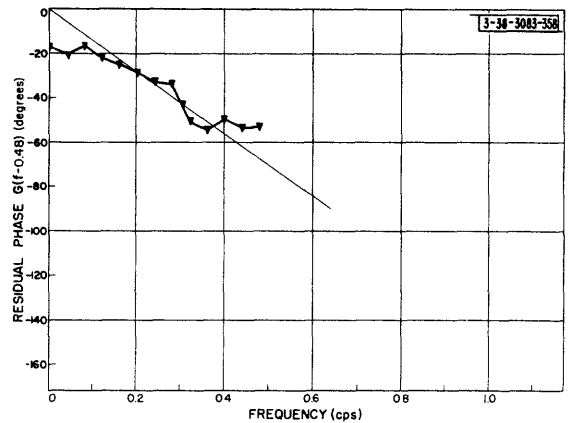
(p) B 8

Fig. A-3 (Continued)

126
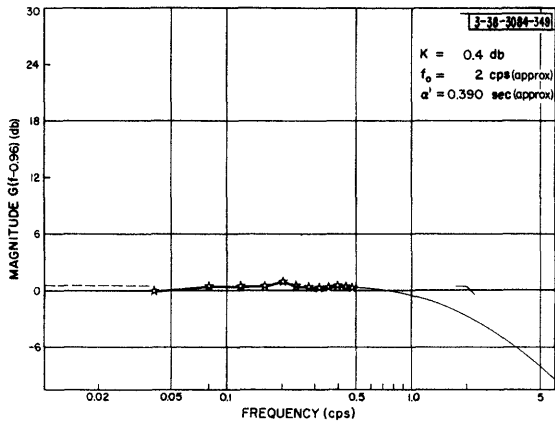
(q) B 9
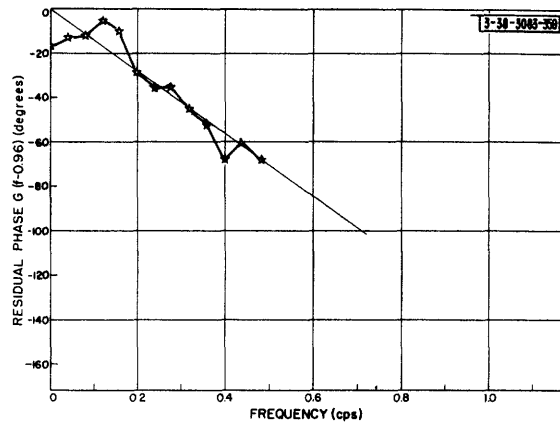
(r) B 9
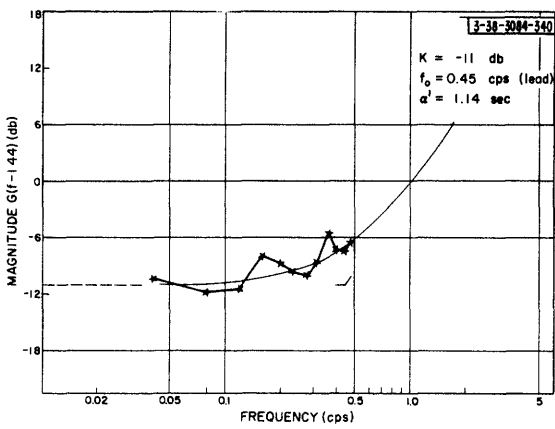
(s) B 10
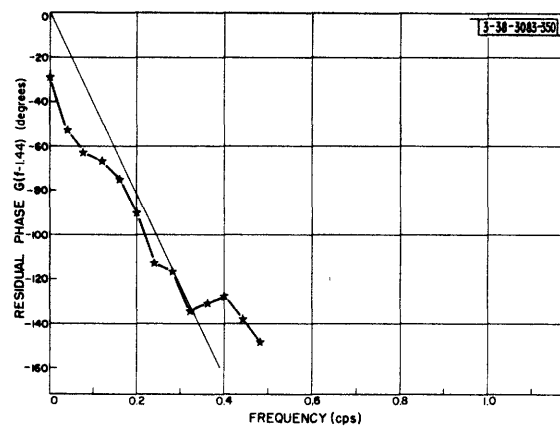
(t) B 10

Fig. A-3 (Continued)

127

The relations used to find a_{max} and f_{max} are

$$a' = a + \frac{1}{2\pi f_1} \quad .$$

(A-4)

$$180 = 360 \, f_c \, a_{max} + \tan^{-1} \frac{f_c}{f_o} + \tan^{-1} \frac{f_c}{f_{max}} \quad ,$$

(A-5)

where f_c is the frequency at which $|G_a(f)|$ equals unity. The first relation results from the fact that the low-frequency phase lag of both (A-2) and (A-3) must be equal. The second is a statement of the zero phase margin requirement.

If f_1 is chosen to be 0.30 cps, a is equal to 0.110 second. By graphical techniques we find that f_c is approximately 0.68 cps. Substituting these values into (A-5), we find that they result in a phase lag at f_c that is very nearly 180°, thereby satisfying the requirement of zero phase margin. Hence a_{max} is 0.110 second and f_{max} is 0.30 cps.

II. NOISE MODELS

Computations for the pursuit and compensatory noise models are summarized in Table A-I. Values for H_l, f_n and c_n^2 were obtained from the measured closed-loop characteristics. The ratio a_2/a_o is

$$\frac{a_2}{a_o} = \frac{\int_o^\infty f^2 \, \Phi_{ii} \, df}{\int_o^\infty \Phi_{ii} \, df} \quad .$$

(A-6)

The values for a_2/a_o were obtained from Table C-II and were computed from measurements on the actual input spectra.

III. PURSUIT PREDICTOR $P_i(f)$

The predictor $P_i(f)$ has the form

$$P_i(f) = b_o + 2\pi j f b_1 \quad ,$$

(A-7)

where b_o and b_1 are chosen to minimize the mean-square error, $\overline{[e_o'(t) - e_i(t)]^2}$. The simplified version of the pursuit model assumed for the calculation of $P_i(f)$ is shown in Fig. A-4. The output and the input of the model are $e_o'(t)$ and $e_i(t)$, respectively. $G_1(f)$ is approximated by a pure delay a equal to 0.194 second.
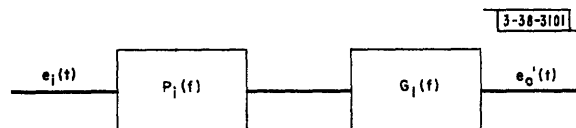
Fig. A-4. Simplified block diagram of pursuit system for use in computation of $P_i(f)$.

	Compensatory					Pursuit		
			c_1^2 $H_\ell^2(a_2/a_o)$	c_2^2 $(H^2/f_n)(a_2/a_o)$	$\dfrac{c_n^2 \, \Phi_{nn}}{\int_0^\infty \Phi_{ii}\,df}$			c_2^2 $(H_\ell^2/f_n)(a_2/a_o)$	$\dfrac{c_n^2 \, \Phi_{nn}}{\int_0^\infty \Phi_{ii}\,df}$
Input	H_ℓ	f_n (cps)	(db)	(db)	(db)	H_ℓ	f_n (cps)	(db)	(db)
R.16	.997	.96	−20.13	−19.94	−19	.99	1.19	−20.93	−19.5
R.24	.985	1.11	−15.85	−16.32	−19	.98	1.19	−16.58	−19.5
R.40	.93	1.27	−12.45	−13.51	−18	.95	1.27	−13.11	−19
R.64	.86	1.59	− 9.42	−11.44	−15.5	.90	1.43	−10.12	−16
R.96	.67	1.75	− 6.85	− 9.29	−11	.65	1.67	− 7.48	−13
R 1.6	.50	1.75	− 5.88	− 8.32	− 7	.30	1.59	− 7.13	−11
R 2.4	.40	1.75	−4.64	− 7.07	− 8	.23	1.91	− 5.89	−10.5
R 4.0						.19	1.82	− 5.24	−12
F 1	.78	1.36	− 6.41	− 7.74	−10	.72	1.99	− 8.77	−17
F 2	.95	1.99	−12.22	−15.22	−18	.92	2.07	−15.30	−19.5
F 3	.99	1.36	−16.74	−18.06	−21	.97	1.11	−17.26	−21
F 4	.998	1.51	−15.72	−17.52	−22	.97	1.43	−17.42	−22.5
B 1	.72	1.91	− 7.31	−10.11	−15	.75	1.91	− 8.52	−16.5
B 2	.57	1.99	− 5.91	− 8.90	−12	.60	1.75	− 5.68	−13
B 3	.45	2.55	− 6.28	−10.34	−12	.55	1.91	− 4.76	−13.5
B 4	.52	2.08	− 6.45	−10.38	−12	.55	2.39	− 7.16	−16
B 5	.82	2.08	− 7.90	−11.06	−14	.80	1.67	− 9.37	−15.5
B 6	.90	2.08	− 9.86	−13.02	−18	.90	1.51	−11.21	−13
B 7	.95	1.51	− 9.82	−11.60	−16.5	.92	1.51	−11.55	−18
B 8	.70	1.91	− 5.51	− 8.34	−13.5	.75	1.91	− 6.48	−15
B 9	.53	1.91	− 3.41	− 6.40	−10.5	.75	1.75	− 1.59	−13.5
B 10	.28	2.08	− 6.30	− 9.46	−10.5	.70	1.91	+ .40	−12

TABLE A-I

SUMMARY OF CALCULATIONS FOR NOISE MODELS

In terms of the power density spectra, the mean-square error is

$$\overline{\epsilon^2} = \int_0^\infty \Phi_{ii} [1 + |P_i G_1|^2 - 2 \, \mathrm{Re} \, (P_i G_1)] \, df \quad . \tag{A-8}$$

Substituting $e^{-2\pi j f a}$ for $G_1(f)$ and (A-7) for $P_i(f)$, we obtain

$$\overline{\epsilon^2} = \int_0^\infty \Phi_{ii} \left\{ 1 + |b_0 + 2\pi j f b_1|^2 - 2 \, \mathrm{Re} \, [e^{-2\pi j f a} \, (b_0 + 2\pi j f b_1)] \right\} df \quad . \tag{A-9}$$

To find the values of b_0 and b_1 that minimize $\overline{\epsilon^2}$, differentiate (A-9) with respect to b_0 and b_1 and set equal to zero. The desired values for b_0 and b_1 are

$$b_0 = \frac{\int_0^\infty \Phi_{ii} \cos 2\pi f a \, df}{\int_0^\infty \Phi_{ii} \, df} \quad , \tag{A-10}$$

and

$$b_1 = \frac{\int_0^\infty 2\pi f \, \Phi_{ii} \sin 2\pi f a \, df}{\int_0^\infty (2\pi f)^2 \, \Phi_{ii} \, df} \quad . \tag{A-11}$$

Values for b_0 and b_1 have been computed, using nominal values for the input spectra, from (A-10) and (A-11) for the Rectangular and RC Filtered Spectra. The results are in Table A-II.

TABLE A-II
PARAMETERS OF $P_i(f)$

Run	b_0	b_1
R.16	0.9935	0.1916
R.24	0.9856	0.1962
R.40	0.9616	0.1918
R.64	0.9016	0.1766
R.96	0.7869	0.1687
R1.6	0.4763	0.3130
R2.4	0.3415	0.2607
R4.0	−0.3326	0.1601
F1	0.7461	0
F2	0.9647	0.1448
F3	0.9860	0.1872

APPENDIX B
CROSS-SPECTRAL ANALYSIS AND A CROSS-SPECTRUM COMPUTER

Cross-spectral analysis is a technique for measuring or approximating the characteristics of linear or nonlinear systems excited by noise-like signals. System transfer functions can be determined from the power-density spectrum of the input signal and from the cross-power-density spectrum between input and output. These spectra can be computed directly from the time dependent input and output signals of the system without making the usual detour through correlation functions. The spectral approach to the system analysis problem is in many cases simpler, more accurate, and quicker to apply than the usual correlation techniques. An analogue computer which makes possible computation of the spectra directly from the time signals has been constructed and will be described. This computer and the techniques to be discussed have been applied extensively in the study of manual control system characteristics.

I. APPLICATION OF CROSS-SPECTRAL ANALYSIS

The type of problem that can be solved by cross-spectral analysis is illustrated in Fig. B-1. The unknown system may be linear or nonlinear and may contain internal sources of noise (or other signals not coherent with the input). Measurements can be made only on input, which is stochas-
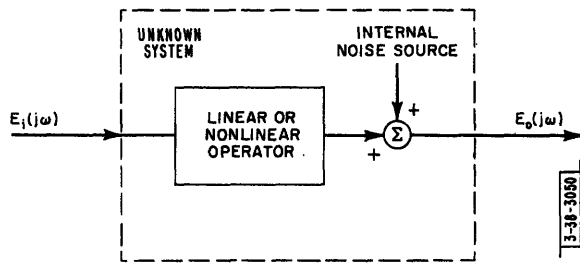
Fig. B-1. The type of unknown system whose characteristics can be determined by cross-spectral analysis.

tic, and on output. In the case of a linear system we want to determine the transfer function $H(j\omega)$ and the power-density spectrum of the noise $\Phi_{nn}(j\omega)$, which together describe the characteristics of the system. In the case of a nonlinear system we want to find the quasi-linear transfer function $H(j\omega)$ whose response to $E_i(j\omega)$ best approximates in the mean-square difference sense the system's response $E_o(j\omega)$. We can also determine a noise spectrum $\Phi_{nn}(j\omega)$, which includes the power introduced by internal signal sources and by system nonlinearities. For nonlinear systems, $H(j\omega)$ and $\Phi_{nn}(j\omega)$ will in general depend upon input-signal characteristics.

Because the noise is not linearly correlated with the input (for both linear and nonlinear systems) it can be shown that

$$\Phi_{io}(j\omega) = H(j\omega)\,\Phi_{ii}(j\omega) \quad , \tag{B-1}$$

and

$$\Phi_{oo}(j\omega) = |H(j\omega)|^2\,\Phi_{ii}(j\omega) + \Phi_{nn}(j\omega) \quad . \tag{B-2}$$

$\Phi_{ii}(j\omega)$, $\Phi_{io}(j\omega)$, etc. are the power-density spectra or cross-power-density spectra of the signals indicated by the subscripts. These equations determine $H(j\omega)$ and $\Phi_{nn}(j\omega)$. For linear systems, $H(j\omega)$ determined from (B-1) is equal to the transfer function of the linear operator of the unknown system (Fig. B-1). For nonlinear systems, $H(j\omega)$ is the quasi-linear transfer

function whose output is the best mean-square approximation to the system output, $E_o(j\omega)$. If the input is a gaussian process and if the nonlinear system is realizable, i.e., operates only on the past and present of input, the transfer function $H(j\omega)$ determined from (B-1) will be realizable.[27]

By using cross-power-density spectra, it is possible to resolve the system output into two components: one part that is linearly coherent with the input, and one part that is not linearly coherent. The input and the coherent part of the output are related by a linear transfer function. If there were a multiplicity of inputs and outputs, transfer functions could be determined relating each input to the part of each output which was linearly coherent with that input. Noise spectra representing the portions of each output that are not coherent with any input can also be found. The ability to perform this kind of resolution and to obtain a match between an input and part of one or of several outputs is useful for many problems of systems analysis.

It is also possible to describe the characteristics of the system of Fig. B-1 in terms of the correlation functions of input and output. The following equations describing input-output relations for the system of Fig. B-1 can be written[24]*

$$\phi_{io}(\tau) = \int_{-\infty}^{\infty} h(\sigma)\,\phi_{ii}(\tau - \sigma)\,d\sigma \quad , \tag{B-3}$$

and

$$\phi_{oo}(\tau) = \int_{-\infty}^{\infty} \int_{-\infty}^{\infty} [h(\sigma)\,h(a)\,\phi_{ii}(\tau + a - \sigma)]\,d\sigma\,da + \phi_{nn}(\tau) \quad , \tag{B-4}$$

where $\phi_{ii}(\tau)$, $\phi_{io}(\tau)$, etc. represent the correlation functions of the signals indicated by the subscripts.

These equations are the inverse Fourier transforms of the first set, (B-1) and (B-2), and therefore the description of the system in terms of the correlation functions is entirely equivalent to that in terms of the spectra. However, time domain solution for $h(t)$ and $\phi_{nn}(\tau)$ is extremely difficult and usually must be carried out in the frequency domain by taking the Fourier transforms of the time domain equations (B-3) and (B-4). This process of course results in the set of equations (B-1) and (B-2). Once the frequency domain equations have been obtained the solution is straightforward.

Since we usually have to get the equations in the frequency domain to obtain a solution, it seems worth while to try to eliminate the detour through the correlation functions and find the spectra directly from the time functions. To instrument this simplification is not difficult and there is considerable advantage in doing so. For most systems the spectra are more easily interpreted than the correlations; similarly, the transfer function $H(j\omega)$ is more convenient to use than the impulse response $h(t)$. Unless all the calculations are to be done with a digital computer, it is probably cheaper and quicker to find the spectra directly. It is difficult in practice to compute the correlation functions for τ great enough so that Gibbs phenomenon oscillations do not appear in the spectra when the correlations are transformed. These oscillations result from truncation

*Superscripts in bold face refer to references on p. 117.

of the correlation functions when they are computed out to only a finite value of τ. There are techniques for smoothing these oscillations, but they increase the complexity of transformation.[29]

There are, to be sure, certain advantages in using correlation functions to find the spectra. If the computations are done digitally, fewer operations are required when the spectra are computed in this way. Davenport, et al., have shown that for signals of long duration, correlation functions can be computed to a given accuracy in less time than can the spectra.[35] Such considerations may or may not be important, depending upon the analysis problem being solved.

The question of which method is superior remains unanswered in the general case. When there are many data to be analyzed so that a special purpose computer is justified, it may be more satisfactory to build a cross-spectrum computer than a correlator. The computer itself and the associated input and output equipment are likely to be simpler for spectral analysis method. For the study of manual control system characteristics, for which both correlational and spectral techniques were used, the spectral approach proved to be far superior.

II. DESCRIPTION OF THE CROSS-SPECTRUM COMPUTER*

The principle of operation of the cross-spectrum computer rests on the relation:[25]

$$\Phi_{ab}(j\omega) = \lim_{T \to \infty} \frac{1}{T} E_a^*(j\omega) E_b(j\omega) \quad , \tag{B-5}$$

in which the asterisk indicates the complex conjugate. This equation says that the cross-power-density spectrum at some frequency ω is equal to the product of the amplitudes of the ω components of each of the two signals, $e_a(t)$ and $e_b(t)$, and has a phase angle equal to the phase difference between the components of these two signals. The signals have duration T and are stationary random functions.

A spectrum computer that makes use of relation (B-5) has been constructed. A block diagram showing the essential features of this computer is given in Fig. B-2;[†] a photograph of the equipment is in Fig. B-3. Two signals $e_a(t)$ and $e_b(t)$ are fed to balanced modulators, each having the same carrier frequency. When the cross-spectrum at frequency f_m cps is desired, the carrier frequency is set at f_m+1500 cps. The outputs of the modulators contain frequency components equal to carrier frequency plus and minus the frequencies of all the components of the input signals. By passing the modulator outputs through identical, narrow, band-pass filters tuned to 1500 cps, signals at 1500 cps are obtained which have their amplitudes proportional to the amplitudes of the f_m components of e_a and e_b, respectively, and which have a relative phase angle that is the same as the phase difference of the f_m components of the original signals. The filter outputs are modulated again: The carrier frequency for $e_a(t)$ is 10 kcps; that for $e_b(t)$ is 12 kcps. The outputs of these two modulators are filtered at 8.5 and 10.5 kcps, respectively. In this process we have shifted the frequencies of the signals and added an arbitrary relative phase angle which is introduced by the 10- and 12-kcps carrier signals.

---

*Shortly after construction of this equipment was completed, the author's attention was directed to similar work being done at NACA, Langley Field, Virginia. NACA has independently constructed a computer that is similar in philosophy to that described here.[34]

†Detailed circuit diagrams of the computer are filed with the Lincoln Laboratory drafting room under basic file number 4841.
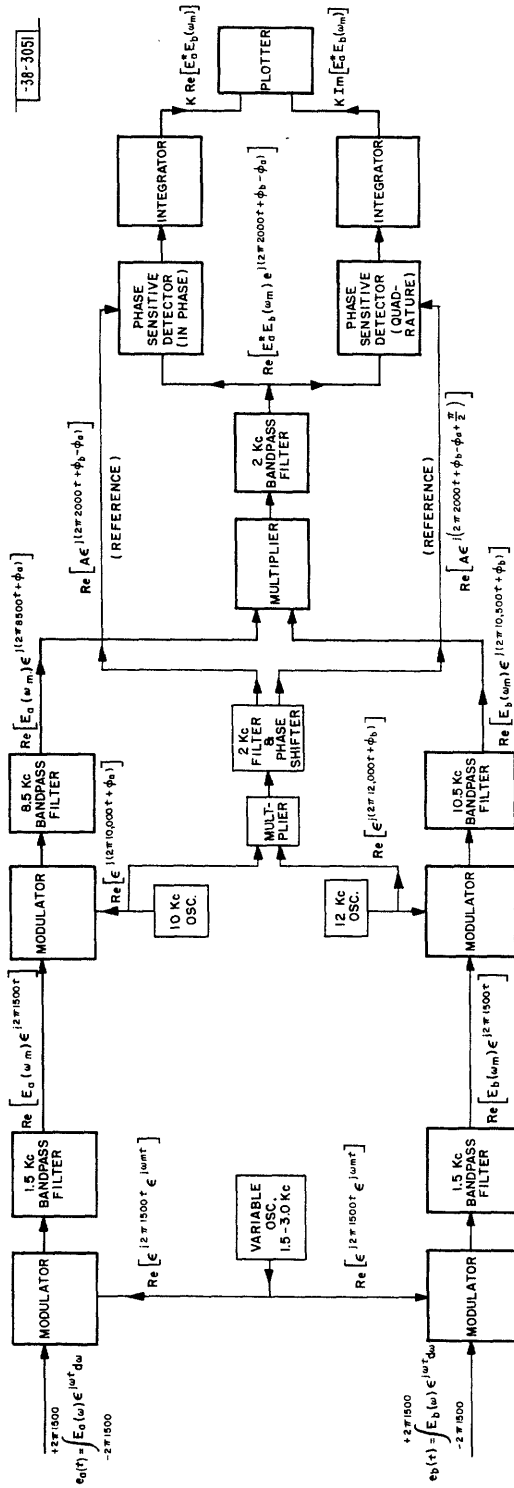
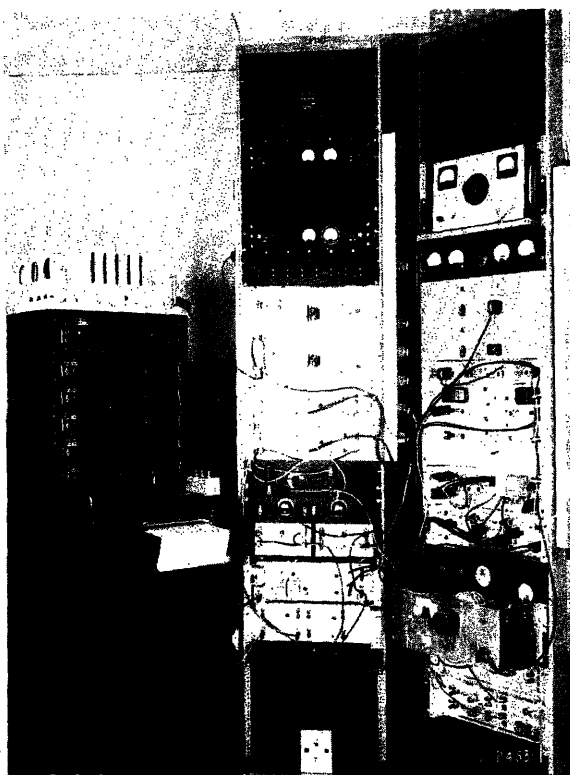Fig. B-2. Block diagram of cross-spectrum computer.

Fig.B-3. Photograph of cross-spectrum computer.

The 8.5- and 10.5-kcps signals are next fed to the signal multiplier whose output passes to a band-pass filter set at 2000 cps — the frequency difference between the two signals. The output of the 2000-cps filter is the cross-power spectrum shifted in frequency. It has an amplitude equal to the product of the amplitudes of the f_m components of e_a and e_b, and has a phase angle equal to the phase difference between these components of e_a and e_b plus an arbitrary phase angle added by the 10- and 12-kcps carrier signals. This arbitrary phase shift can be easily eliminated as follows: Derive a 2000-cps signal by multiplying the 10- and 12-kcps carrier signals together and by taking the difference-frequency signal resulting from this multiplication. This 2000-cps reference signal will have a phase angle that is equal to the phase shift introduced by the 10- and 12-kcps carrier signals. Use this 2000-cps reference signal as the reference signal to phase-sensitive-detect the signal-multiplier output. The integral of the output of the phase-sensitive-detector is proportional to the real part of the f_m components of the cross-power-density spectrum of e_a (t) and e_b (t). To find the imaginary part of the spectrum, phase-sensitive-detect the signal-multiplier output using the 2000-cps reference shifted by 90°.

The most critical components of the computer are the band-pass filters, particularly the filters which operate on the 1500-cps modulator output. The filter characteristics of each channel must be well matched so there will be no phase distortion of the signals relative to each other. The frequency resolution of the system depends upon the bandwidth and selectivity of the 1500-cps filters. By cascading two tuned LC filter sections and using positive feedback around them, a bandwidth of 3 to 5 cps can be easily obtained. Assuming that both e_a (t) and e_b (t) have flat spectra, 90 per cent of the filter output power lies within one bandwidth of the resonant frequency of the filters. Assuming an input frequency range of 0 to 1000 cps and band-pass filters of 5-cps bandwidth, 100 nearly independent points on a spectrum can be obtained.

In order to make effective use of the computer, a speed-up or slow-down in the time-scale of the data will often be necessary. For the data obtained in our tracking studies, which had a bandwidth of about 5 cps, a speed-up by a factor of about 200 was desirable. A data speed-change recording system (shown in the photograph of Fig. B-4) which was assembled from commercial and specially designed components, allowed a speed-up or slow-down of data by any multiple of 2, 4 or 8. The recording system has six channels for data and has both FM and
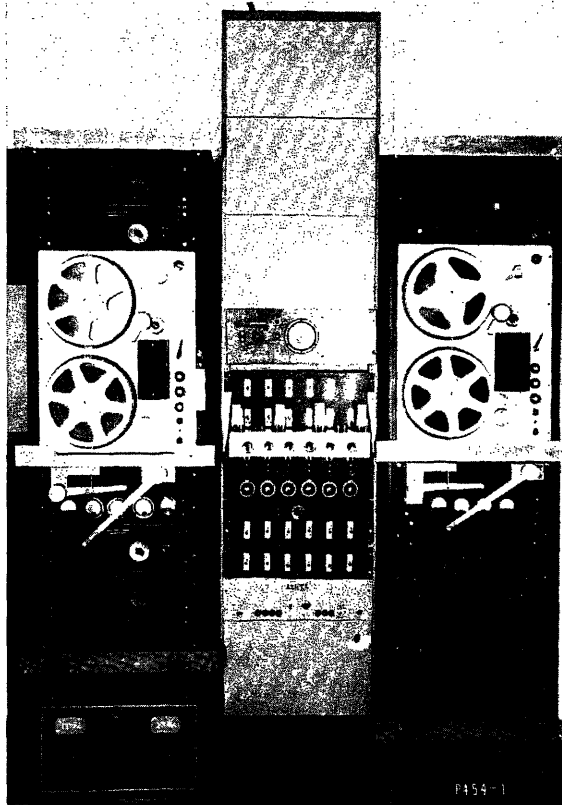
Fig. B-4. Photograph of data speed change recording system.

standard electronics which cover the frequency range of 0 to 75,000 cps. Together with the data speed-change recording system, the spectrum computer is a very flexible analysis tool which can handle a wide variety of analogue data.

III. PERFORMANCE

In brief, the performance specifications of the cross-spectrum computer are as follows: The bandwidth of the input signals which can be handled is from 0 to 1000 cps. The bandwidth of the filters is variable from about 3 to 20 cps. The system output is linear to within 5 per cent (of correct value) over a 60-db range of the output. Spectra can be determined to within an accuracy of about 3 to 4 per cent; the repeatability of the calculations is 2 to 3 per cent.

In Fig. B-5 are shown transfer functions for a high-pass RC filter. The crosses are magnitude and phase of the transfer function obtained with the spectrum computer when a one second sample of noise was used for the filter input. The solid lines are the theoretical values for the transfer functions. In Fig. B-6 are shown transfer functions for the human operator in a simple pursuit tracking task. All three sets of curves were computed from the same set of input response data which was obtained from one particular tracking run. The two sets of solid lines are the magnitudes and phases of transfer functions obtained using the computer. Curves A were computed first; curves B were computed several months later. Curves C, the dash-lines, are the results obtained using correlation functions to determine the spectra of input and response. The large differences in phase curves are probably a result of the fact that for these computations the spectrum computer band-pass filters had relatively wide skirts (bandwidth was 15 cps).

These two figures illustrate the accuracy and repeatability that can be expected of the computer when it is used to determine transfer functions. The performance as indicated by the figures was satisfactory for the problem for which it was intended. However, special components or circuits were not used in the computer to obtain more than ordinary linearity and stability. With more exacting design, much better performance could be readily achieved.
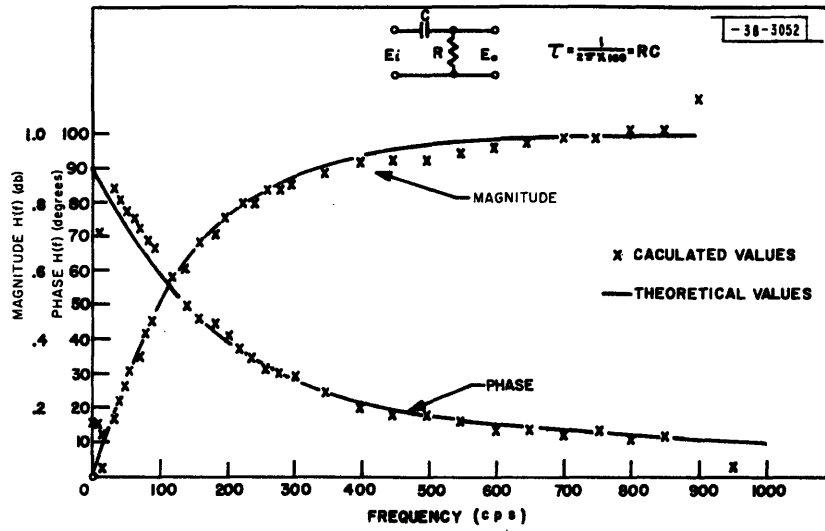
Fig.B-5. Magnitude and phase of transfer function for a high-pass filter. The calculated values were obtained using the cross-spectrum computer.
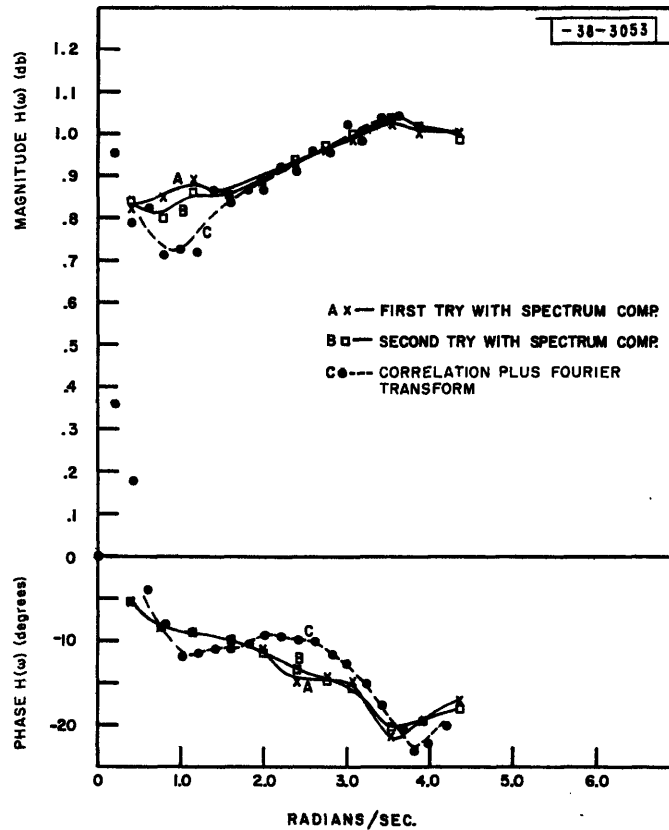

Fig.B-6. Comparison of human-operator transfer functions computed with the cross-spectrum computer and with a correlator.

137

APPENDIX C

INPUT SIGNAL CHARACTERISTICS

The input having the Continuous Spectrum was generated by passing a train of randomly spaced pulses through a low-frequency bandpass filter. The average pulse-repetition frequency was about 50 per second; the pulsewidth was about 4 milliseconds. Because the pulses were narrow, the input spectrum should assume the shape of the filter characteristics.

In Fig. C-1 are plotted the actual spectrum determined from measurements on the input and the nominal spectrum determined from knowledge of the filter characteristics.

The Rectangular, RC Filtered, and Selected Band Spectra were generated by summing a large number of sinusoids of arbitrary phase. Table C-I shows for each of these signals the spacing between adjacent frequencies and the number of components. The nominal and measured spectra for the Rectangular, RC Filtered, and Selected Band Spectra are shown in Figs. C-2, C-3 and C-4, respectively. In Figs. C-1 through C-4 the measured spectra are represented by the datum points and the nominal spectra by the solid lines.

TABLE C-I COMPOSITION OF INPUTS			
	Input	Spacing Δf (cps)	No. of Components
Rectangular Spectra	R .16	0.0025	64
	R .24	0.005	48
	R .40	0.01	40
	R .64	0.01	64
	R .96	0.02	48
	R 1.6	0.02	80
	R 2.4	0.05	48
	R 4.0	0.10	40
RC Filter Inputs	F 1	0.02	144
	F 2	0.02	144
	F 3	0.02	144
	F 4	0.005	48
Selected Band Spectra	B 1	0.01	96
	B 2	0.01	96
	B 3	0.01	96
	B 4	0.01	144
	B 5	0.01	144
	B 6	0.01	144
	B 7	0.01	48
	B 8	0.01	48
	B 9	0.01	48
	B 10	0.02	24

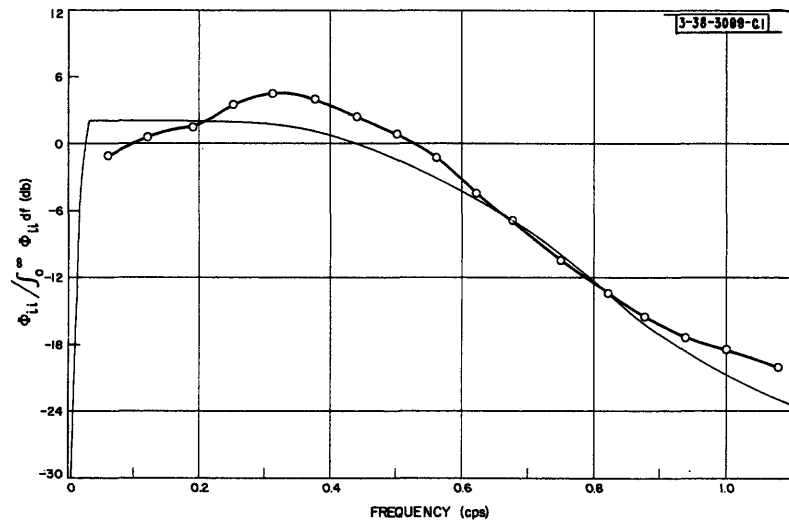Fig. C-1. Measured and nominal Continuous Spectra. This input was used for only the pursuit part of Experiment I — Variability.

TABLE C-II						
MOMENTS OF SPECTRA						
	Nominal			Measured		
Input	Mean Frequency $\frac{\alpha_1}{\alpha_0} = \bar{f}$ (cps)	Second Moment $\frac{\alpha_2}{\alpha_0}$ (cps)^2	Standard Deviation σ_f (cps)	Mean Frequency $\frac{\alpha_1}{\alpha_0} = \bar{f}$ (cps)	Second Moment $\frac{\alpha_2}{\alpha_0}$ (cps)^2	Standard Deviation σ_f (cps)
R .16	0.0800	0.00853	0.0462	0.0825	0.00975	0.0544
R .24	0.120	0.0192	0.0693	0.143	0.0268	0.0792
R .40	0.200	0.0532	0.115	0.223	0.0657	0.127
R .64	0.320	0.137	0.185	0.349	0.155	0.183
R .96	0.480	0.307	0.277	0.606	0.460	0.306
R 1.6	0.800	0.853	0.462	0.905	1.03	0.447
R 2.4	1.20	1.92	0.693	1.28	2.15	0.722
R 4.0	2.00	5.32	1.15	2.13	6.05	1.24
F 1	0.400	0.405	0.495	0.425	0.376	0.434
F 2	0.153	0.0516	0.168	0.173	0.0665	0.192
F 3	0.102	0.0191	0.0935	0.110	0.0216	0.0976
F 4	0.120	0.0192	0.0693	0.143	0.0268	0.0794
B 1	0.480	0.307	0.277	0.519	0.359	0.299
B 2	0.720	0.768	0.500	0.738	0.789	0.495
B 3	0.960	0.998	0.277	1.05	1.16	0.250
B 4	0.720	0.691	0.416	0.796	0.835	0.449
B 5	0.360	0.231	0.318	0.385	0.242	0.306
B 6	0.255	0.0953	0.174	0.305	0.127	0.186
B 7	0.240	0.0766	0.138	0.297	0.115	0.161
B 8	0.720	0.537	0.138	0.744	0.573	0.140
B 9	1.20	1.46	0.138	1.27	1.62	0.148
B 10	1.68	2.84	0.138	1.72	2.99	0.156

Table C-II shows nominal and measured moments of the spectra, i.e., the relative mean frequency $\bar{f}$, the relative second moment, α_2/α_0, and the relative standard deviation of the spectrum σ_f. These quantities have close relation to control system performance. They are defined by the following relations:

$$\bar{f} = \frac{\alpha_1}{\alpha_0} \quad ,$$

$$\sigma_f = \sqrt{\frac{\alpha_2}{\alpha_0} - \left(\frac{\alpha_1}{\alpha_0}\right)^2} \quad ,$$

(C-1)
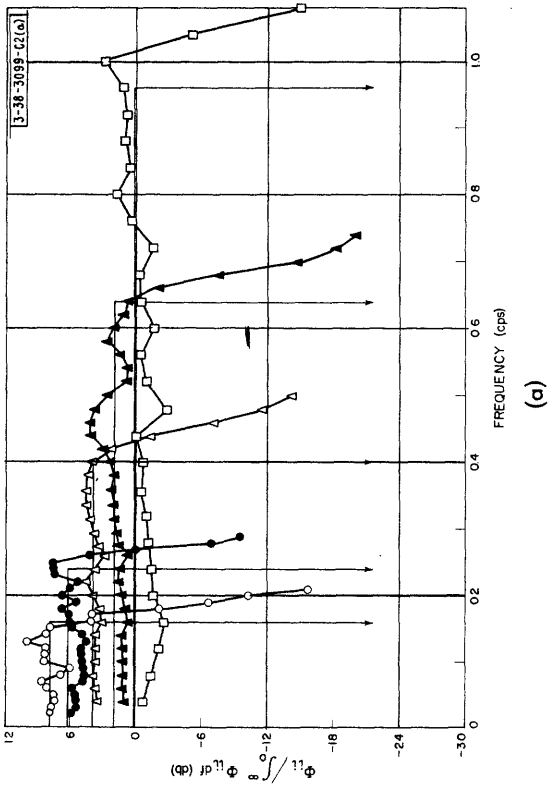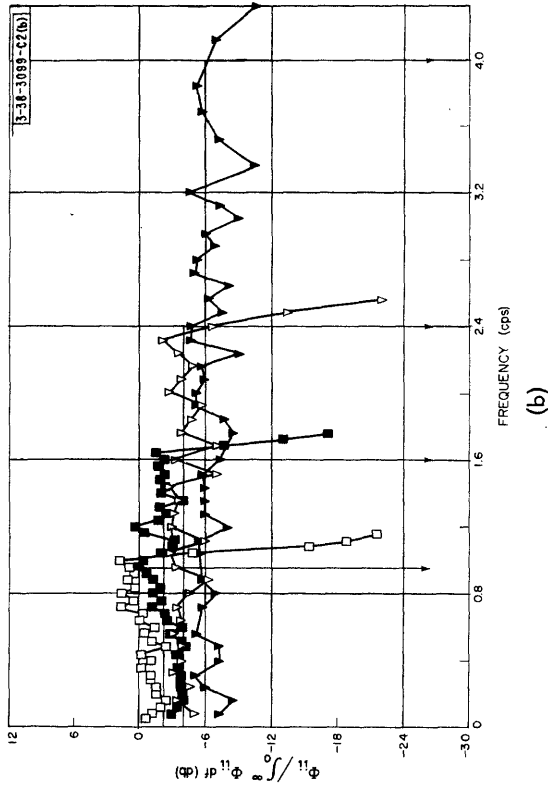
Fig. C-2. Measured and nominal Rectangular Spectra.

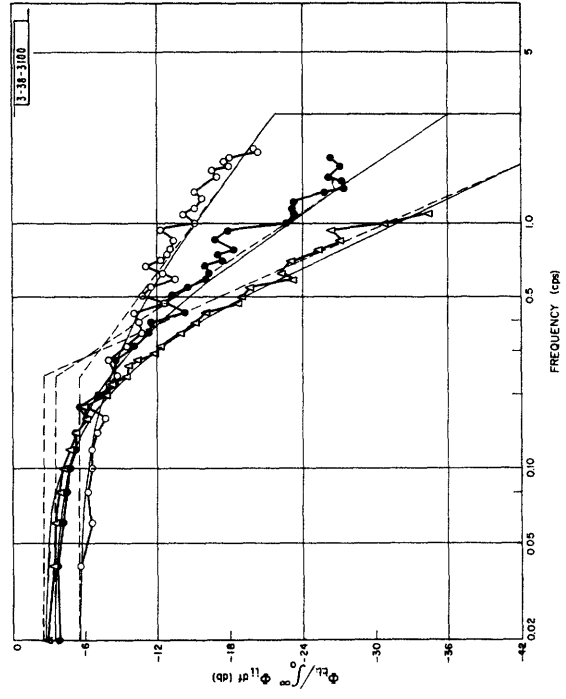R .16 (F1)
R .24 (F2)
R .40 (F3)
R .64
R .96
R1.6
R2.4
R4.0

Fig. C-3. Measured and nominal RC Filtered Spectra.

142

where

$$a_0 = \int_0^\infty \Phi_{ii}(f)\, df \quad,$$

$$a_1 = \int_0^\infty f\, \Phi_{ii}(f)\, df \quad, \tag{C-2}$$

$$a_2 = \int_0^\infty f^2\, \Phi_{ii}(f)\, df \quad.$$

Comparison of the measured and nominal spectra shows that almost always within the signal band the measured points lie within ± 3 db of the nominal. The deviations of the measured values probably result from inaccuracies in measurement of the spectra and from inaccuracies in the settings of the amplitudes of the sinusoidal components summed to make the signals. Large differences appear near frequencies at which the magnitude of the nominal spectra changes abruptly. The cross-spectrum computer (Appendix B) used for the measurements had filters of finite bandwidth, and therefore the measured spectra can not show infinitely sharp rate of cut-off. Corrections for the filter characteristics of the computer could have been made, but we have not done so. Another source of differences is the speed-up factor (128, 256, 512) that was used for analyzing the signals. The cross-spectrum computer was calibrated in multiples of 5 cps. When conversion was made from computer frequency to actual frequency, the computer frequencies were divided by 125, 250 or 500. The convenience of working with and plotting simple frequencies more than compensates for the 2.4 per cent error in the frequency scale of the final results. All the measured spectra and transfer functions are plotted against this slightly expanded frequency scale. Hence the cut-off frequencies of the measured spectra are somewhat higher than those of the nominal spectra.

The amplitude distribution of the sum of n randomly phased sinusoids approaches a normal distribution as n becomes large.[30] With one exception, B10, all signals had at least 40 components. Relative frequency and cumulative frequency distributions of amplitude were measured for one of the signals having 40 components; these are plotted in Fig. C-5. The measured functions were obtained from a 4-minute sample of the input. The amplitude, quantized to the nearest 0.1 inch (referred to the tracking display) was read every second. The smooth curves shown in Fig. C-5 are probability density and distribution functions of a normal distribution with mean and variance equal to the mean and variance of the sample. A test for the normality of the sample distribution, using the χ^2 of the difference between observed and expected frequencies in ten percentile intervals,[36] showed that the sample distribution was significantly different from normal at the 95 per cent level, but not at the 99 per cent level. It is not likely that the departure from normality exhibited by the sample is great enough to affect significantly human-operator characteristics.
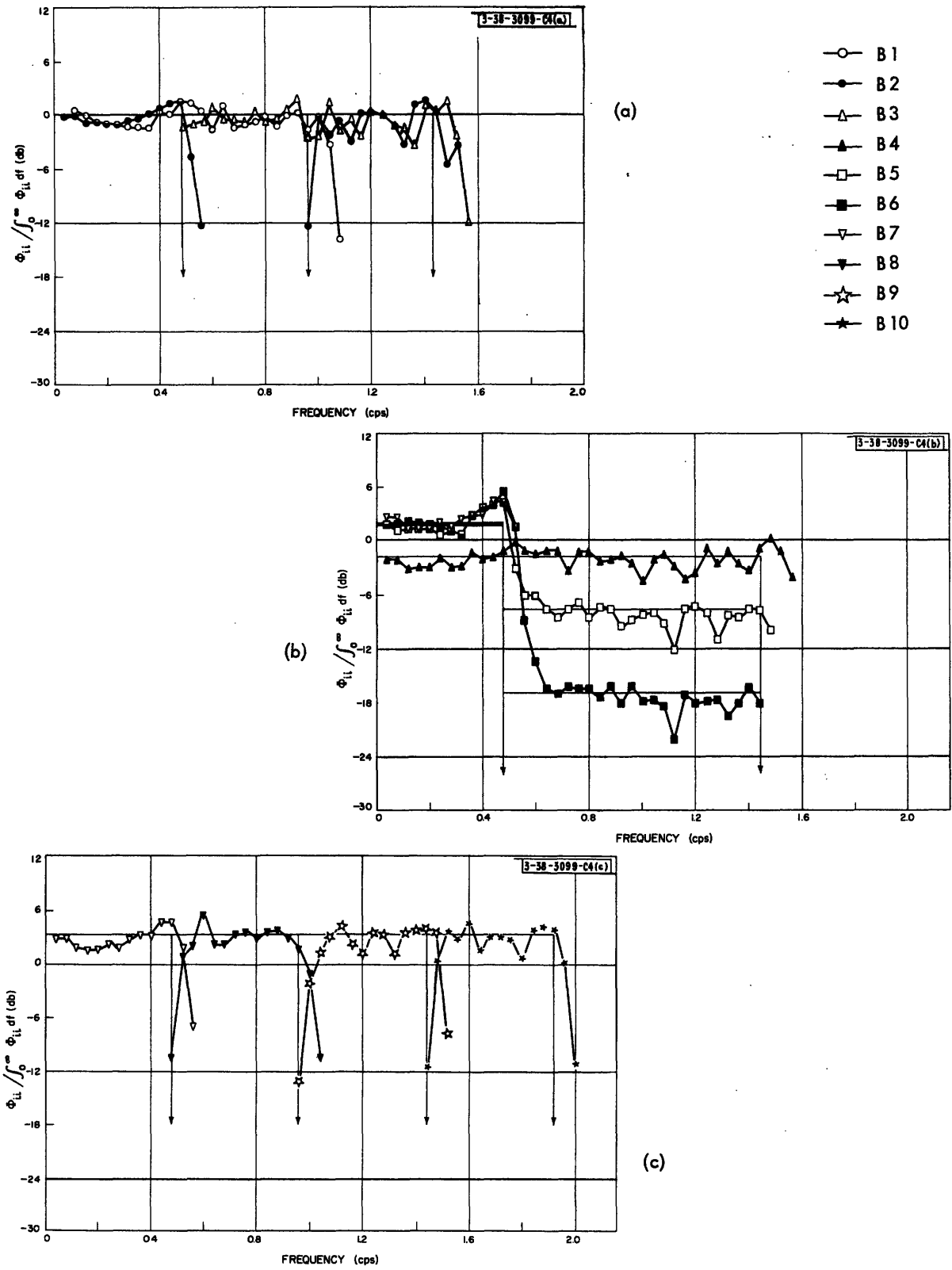
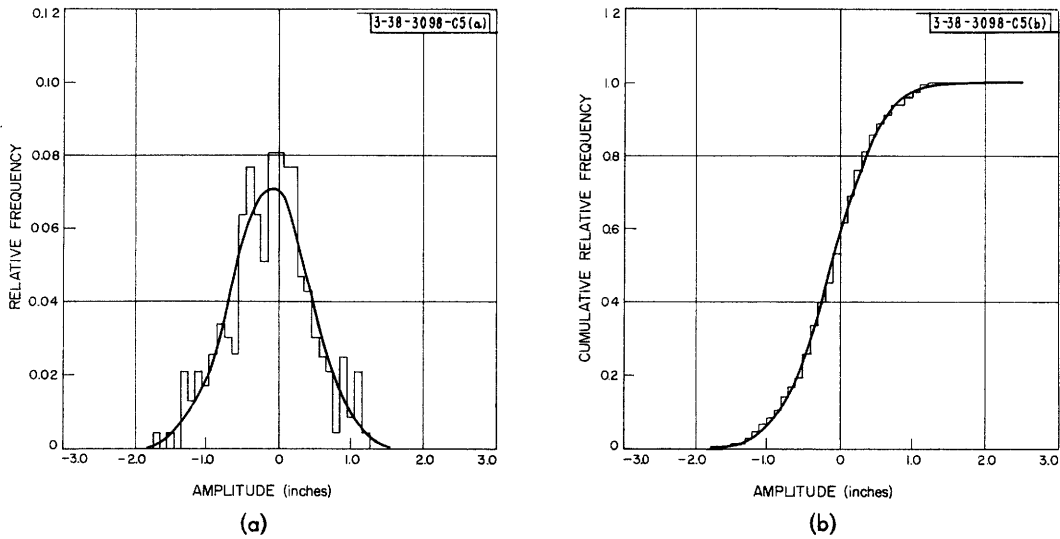Fig. C-4. Measured and nominal Selected Band Spectra.

144

Fig. C-5. Probability density (a) and distribution (b) functions of amplitude of Input R.40. This signal has only 40 sinusoidal components.

BIOGRAPHY

Jerome I. Elkind was born in New York, New York on August 30, 1929. He received the S. B. and S. M. degrees in electrical engineering from Massachusetts Institute of Technology in 1952. From 1952 to 1956 he has served as a Teaching Assistant and Research Assistant in the Electrical Engineering Department of M.I.T. and also as Staff Member of Lincoln Laboratory. His research activities have been in the fields of control systems, radar, and signal analysis.

Dr. Elkind is a member of Tau Beta Pi, Sigma Xi, Eta Kappa Nu, IRE, AIEE, and the Acoustical Society of America.